THE EFFECT OF AGGREGATION STATE ON THE DEGRADATION KINETICS IN SOLUTION OF AN OXIDIZABLE SULFIDE DICARBOXYLIC ACID DRUG

by

Miriam K. Franchini

A dissertation submitted in partial fulfillment of the requirements for the degree of

Doctor of Philosophy
(Pharmacy)

at the
UNIVERSITY OF WISCONSIN - MADISON
1995

A dissertation entitled

The Effect of Aggregation State on the Degradation Kinetics in Solution of an Oxidizable Sulfide Dicarboxylic Acid Drug

submitted to the Graduate School of the
University of Wisconsin-Madison
in partial fulfillment of the requirements for the
degree of Doctor of Philosophy

by

Miriam K. Franchini

Degree to be awarded: December 19___ May 19___ August 19 95

Approved by Dissertation Readers:

J. T. Carstensen — Major Professor

6/28/1995 — Date of Examination

Kenneth A. Connors

Ronald R. Benerito

Charles Read — Dean, Graduate School

FRANCHINI, MIRIAM K.

NAME

122 500 5832

Candidate for the degree of
Doctor of Philosophy

The Graduate School

Madison, June 28, *19* 95
(Date of examination)

To the Graduate Faculty:

We, the undersigned, report that as a committee we have examined

MIRIAM K. FRANCHINI
(student name)

upon the work done in the subjects named on the preceding page and upon the dissertation presented by the candidate we find

~~may not~~

that the candidate may properly be admitted to the degree of Doctor of Philosophy.

J. J. Carter

Kenneth A. Conn

Ronald R. Burton

George Zografi

R. Couch Woodall

I dissent from the foregoing report.

ACKNOWLEDGMENTS

M. K. Franchini received an Upjohn-Enz award in 1994, was a Pfizer Central Research fellow in 1992-93, and a Berlex fellow in 1991-92. Part of this work was also funded by Sandoz, Marion-Merrell-Dow, and Smith-Kline Beecham.

The author would also like to thank Abbott Labs and Bristol-Myers Squibb for the use of their surface tensiometers, Dr. Matt Sanders in the UW Chemistry department for the use of the cyclic voltammetry set-up, Dr. Ken Satyshur of the UW School of Pharmacy for the SYBYL representation of the molecular structure, Dr. Pasupati Mukerjee for helpful discussions regarding micellar theory (although this by no means is meant to imply he endorses *all* the ideas set forth in this thesis), and all the pharmaceutics faculty from whose courses the author gained a great deal knowledge, more than expected, and some of which has been, hopefully correctly, incorporated in this thesis.

Thanks also to all the professors within and outside of the UW School of Pharmacy who let me sit in on their classes, and lastly, great thanks are extended to my major professor, Jens Carstensen, without whose encouragement none of this would have been realized.

THE EFFECT OF AGGREGATION STATE ON THE DEGRADATION KINETICS IN SOLUTION OF AN OXIDIZABLE SULFIDE DICARBOXYLIC ACID DRUG

by Miriam K. Franchini

under the supervision of Jens T. Carstensen, Ph.D., Professor of Pharmaceutics

The degradation kinetics of a new synthetic leukotriene antagonist proposed for the treatment of asthma, 3(S)-(2-carboxy-ethylsulfanyl)-3-[2-(8-phenyloctyl)phenyl]propionic acid disodium salt, ($C_{26}H_{32}O_4S.2Na$), has been studied.

During the course of these kinetic studies it was observed that certain samples foamed; surface tensiometry revealed a cmc in water of 8.8 mM. Above 0.2 M, deviation from linearity was found in the log cmc versus log counterion concentration which was ascribed to salting out of the monomeric chains as proposed by Mukerjee in 1967; the data were found to fit to an *extended* Corrin-Harkins relation as proposed recently by Mukerjee and Chan.

Once the cmc data were obtained it became clear that the degradation of the compound above the cmc was zero order and below the cmc was (close to) first order when EDTA was present to control for trace metal catalysis. These data suggest that a submicellar aggregate is the decomposing species, namely the dimer. Above the cmc, the micelle serves as a depot for compound, so that when a dimer decomposes it will be replaced from the micelle.

Hence the decomposition appears zero order, because the concentration of the decomposing species remains constant.

Below the cmc, the concentration of dimer decreases with amount decomposed, so that an order of reaction other than zero (in fact close to first) dominates.

In the presence of trace metals, the kinetics are auto-catalytic at 60°C, first order at 93°C, and intermediate order at 75°C. The reason for this is that as temperature increases, both the oxidative and the non-oxidative reaction rate constants increase, but the oxygen partitioning (by Henry's law) make the oxygen concentrations in solution lower, so that the non-oxidative decomposition (which is first order) will predominate at the higher temperatures.

Neither the oxidative nor the non-oxidative reactions were buffer catalyzed by phosphate at pH 7 and 8, but both reactions were subject to a kinetic salt effect at these pH values.

Jens T. Carstensen, Ph.D.

TABLE OF CONTENTS

CHAPTER I. INTRODUCTION

Oxidation of sulfur-containing compounds has been extensively studied especially since the 1940's (Belen'Kii; Carstensen, 1990; Connors, 1986; Kharasch; Labuza; Lundberg; Monig; Stewart; Trost; Turney; Wallace), but if one examines closely the literature on these autooxidation reactions in solution, one finds that more often than not, the kinetics have not been reported beyond one half-life. In fact, only initial rates have been calculated because of the difficulty of assessing data which are neither first order nor second order over the entire course of the reaction (Lee; Sokoloski). The reaction has often mistakenly been taken to be zero-order or first-order (Kassem; Li, 1993[1]; Timmins) when in fact, had it been possible to follow the reaction to completion, the typical autooxidative sigmoidal curve might have resulted (Asker; Li, 1995[2]; Tan). In some cases, the reaction could not be followed to completion due to technical limitations, for example, poor solubility or volatility of a sulfide, or inhibition of the reaction by the degradation products (Bamford), leading to equilibrium conditions.

Similarly, the degradation kinetics of surfactants and other self-associating compounds has often not been followed beyond one half-life because of technical limitations, for example, the reaction

---

[1] Although initial rates are used to calculate first-order rate constants, the published kinetic profiles suggest the reaction reaches equilibrium after 1.5 half-lives, perhaps indicating an inhibitory effect by product.

[2] Published kinetic curves show that some reactions reached an equilibrium, while others demonstrate autooxidation, although the authors treat the data as zero or first-order.

medium may have gelled as the reaction proceeded due to polymerization side reactions (Amante; Barry; Kurz; Mitchell).

This thesis deals with a pharmaceutically active compound which not only degrades by an autooxidative route, but is also self-associating. Although many aspects of micellar catalysis of oxidation reactions have been documented (Hiemenz; Lim; Mittal; Pnigrahi; Romsted; Rosen), and drug decomposition in the presence of surfactants has been extensively studied, (Azaz; Daabis; Dawson; Hamid; Oliviera; Segal; Yasuhara) to the best of this author's knowledge, autooxidation of an optically active sulfide possessing a true critical micelle concentration (cmc) has never been reported. For, although many drugs are known to aggregate, it is uncommon to find one which possesses a true cmc (Mukerjee, 1974).

Some data have been reported on the decomposition of alkyl sulfates, surfactants such as sodium dodecyl sulfate which form true micelles, but these are prone to hydrolysis rather than autooxidation (Nogami[3]; Motsavage). In these cases, the rate of hydrolysis was significantly enhanced at surfactant concentrations above the cmc, but in all cases, the decomposition remained first order, or so it appeared because insufficient data may have been collected for the reasons cited above. Garnett reported, however, that at very high surfactant concentrations, the alkyl chain of the alkyl sulfates decomposed by autocatalysis. Autooxidation of the alkyl chains was

---

[3] One kinetic profile published in this article which showed decomposition beyond one half-life suggests autocatalysis, although the authors simply comment on the deviation from linearity in the first order plot.

also found for polysorbates, polyethylene glycols, polyoxyethylene fatty alcohol ethers, and cetomacrogol; in addition, the polysorbate esters were also found to degrade by hydrolysis (Donbrow).

In the case of decomposition of mono alkyl and aryl phosphates, hydrolysis was again first-order, but the rate was not affected by the state of molecular aggregation at pH values above the pK_a, or, was only slightly enhanced above the cmc at pH values below the pK_a (Seltzer).

Concentration effects on degradation kinetics of drugs have also been noted (Attwood and Florence; Darrington[4]; Lamy-Freund[5]; Meakin; Ong). In the case of insulin, which self-associates into an equilibrium mixture of monomers, dimers, tetramers and hexamers, depending on concentration, pH, and ionic composition, deamidation under acidic conditions occurred at a slower rate from the dimer than from the monomer.

As another example, penicillin G (Ong) was shown to be more stable to hydrolysis at high drug concentrations than low, with initial rates being determined from the first 5-10% of decomposition. This is a surface active compound which most likely stacks into small aggregates rather than forming true micelles. Generally, such compounds do not attain an aggregation number, n, greater than 20, and, while true micelle formers show negligible association in dilute

---

[4] Initial (<10% decomposition) or first-order (<50% decomposition) rates are reported.

[5] Although the authors refer to autooxidation, the published kinetic profiles appears to be first order, indicative of simple oxidation rather than autooxidation, which would have resulted in a sigmoidally shaped curve.

solution (e.g. only monomers, dimers, trimers, maybe tetramers) (Mukerjee, 1967; Atherton) molecules which self-associate without forming true micelles show extensive aggregation well below the apparent cmc (Attwood and Natarajan; Nikolov).

For example, although many authors refer to the micellization of promethazine HCl, close examination of the structure reveals a fused tricyclic ring, which most likely stacks into aggregates, rather than forming spherical or rod shaped micelles, as described above (Attwood, 1974, 1991). But this is the most relevant compound to the present work because it is a sulfide-containing compound which not only self-associates, but also undergoes oxidation. Degradation of promethazine HCl was followed at pH 4 (citrate buffer) with 0-0.2% ethylenediaminetetraacetic acid (EDTA) and low ionic strength (0.5) to at least one half-life, and nitrogen, oxygen, and air sparged reactions were compared. Apparent cmc values were determined by conductivity and refractometry from 25-70°C. Interestingly, the thermal degradation rate in the absence of light at 90°C was found to change from zero order at high drug concentrations to first order at lower drug concentrations (Meakin). It was purported that at intermediate concentrations the reaction order was first order from the monomer and fractional (half) order from the aggregate, with the two processes occurring simultaneously. The exception was for oxygen sparged systems; these did not show a simple kinetic profile except in the presence of EDTA, in which cases the rate was first order up to 70% degraded (at low drug concentrations).

The present thesis deals with autooxidation of a sulfide to a sulfoxide. The structure of the compound being studied is shown in Figures I-1 and I-2, and it will be referred to as Compound A in the following. The main differences between former studies and the present study are that in addition to being a different chemical entity, Compound A is believed to form true micelles, based on structure and cmc data, and in this thesis, high salt concentrations (up to 1 M), hence high ionic strengths (up to 2.2) were used.

Compound A, the S-enantiomer of a sulfide dicarboxylic acid salt, is an especially attractive compound to study because it is extremely water soluble (>350 mg/mL), is optically active, and is of low molecular weight (486.6) as compared to proteins. Compound A degrades very slowly in solution and the reaction medium does not gel as the reaction proceeds, allowing it to be very well characterized.

Since oxidation is a problem which plagues many pharmaceuticals (Carstensen, 1990; Connors, 1986) and since micelles have long been used as models for membranes and proteins, this work serves the dual purpose of characterizing the autooxidative kinetics of a pharmaceutically active compound, as well as providing a model for more complex compounds, namely proteins.

The original aim of this research was to study and model the observed kinetics of drug A in buffer solutions, which was to serve as a model compound for studying autooxidation by oxygen of a pharmaceutical in the absence of light and of additives such as peroxide, enzymes, solvents, or radical scavengers, using methionine as a model compound.

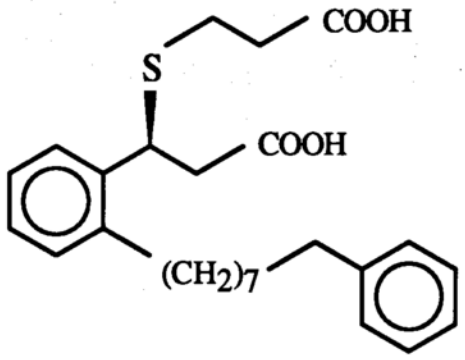

Compound A

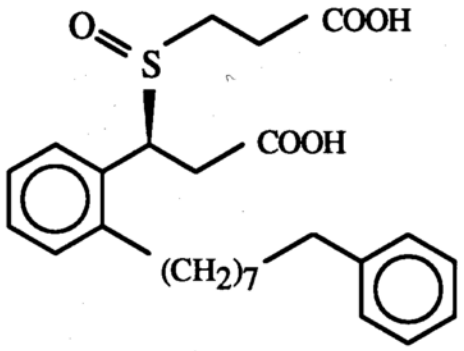

Sulfoxide analog (B)

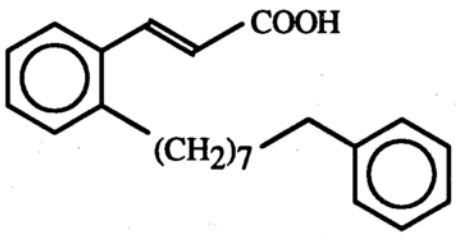

Cinnamate analog (C)

Figure I-1. Chemical structures of Compound A and its major degradation products

But, the oxidation of amino acids such as methionine and cysteine (Dixon) as well as the oxidation of lipids has been (Asker; Dupuis; Gehrke; Olatunji; Savige; Shechter) and still is (Li, 1993; Nguyen[6]) being extensively studied. Most recently it has been observed that the degradation of specific amino acids may result in alterations in biological activity or precipitation in protein formulations (Advant; Davio). Also, oxidation of lipids (Yamamoto) present as constituents of liposomes has been shown to be responsible for leakage of entrapped drug (Hunt). Since so much effort is already being expended in this area, the author decided instead to attempt to unravel the complexities of compound A itself, and to model the kinetics of the decomposition.

In the Master's Thesis (Franchini, 1992), the decomposition of A in solution was characterized by studying the kinetic salt effect, the buffer effect, the drug concentration effect, and the temperature effect at pH 7 in the presence of trace metals. However, when A was discovered to have a cmc in water of 8.8 mM, it became of interest to also determine the effect of buffer concentration on the cmc of A in those buffers used in the kinetic studies (0.05-1.0 M phosphate), and to determine whether the aggregation state of the drug could affect the kinetic rate.

This led to the development, in the present thesis, of schemes describing the observed kinetic behavior of A in the presence and absence of trace metals, and above and below the cmc as well. Also

---

[6] The published kinetic profile does not suggest autooxidation, but rather simple oxidation (first-order).

discussed is the non-linearity in the double-logarithmic Corrin-Harkins plot at high salt concentrations. Kinetic data reported in the Master's thesis have been reexamined in light of the new knowledge of the effect of buffer salts on the cmc of drug A.

By studying Compound A, which contains an oxidizable sulfur group, it was hoped some insight might be gained into the kinetics of oxidation of other sulfur-containing compounds. Since it is much easier and less expensive to work with a low molecular weight compound such as A rather than a protein, the results of this study may shed some light on the more complicated sulfur-containing amino-acid structures, as well as low molecular weight oxidizable compounds of pharmaceutical interest.

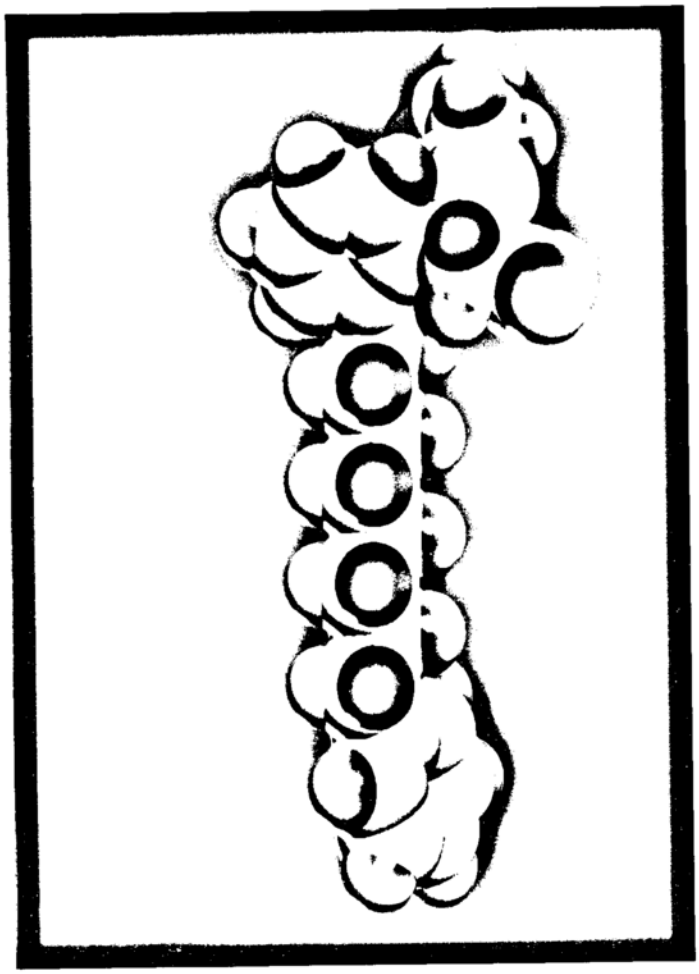

Figure I-2. Space-filling model of Compound A; SYBYL software, energy minimized structure. Sulfur is shown in yellow, oxygen in red, carbon in white, hydrogen in blue.

CHAPTER II. MATERIALS

II-A. Compound A

Compound A, the S-enantiomer of the disodium salt of a sulfide-dicarboxylic acid, 3(S)-(2-carboxy-ethylsulfanyl)-3-[2-(8-phenyl-octyl)-phenyl]propionic acid disodium salt, ($C_{26}H_{32}O_4S.2Na$), is a synthetic leukotriene antagonist proposed for the treatment of bronchial asthma. It has the structural formula shown in Figure I-1, which in part resembles naturally-occurring leukotrienes, "highly potent bronchoconstricting substances released primarily from mast cells and basophils on antigenic challenge." (Gleason)

The essential molecular features are that it is a disubstituted sulfide containing two carboxylic acids, and is represented, schematically by:

$$\begin{array}{l} R\text{-}CH\text{-}S\text{-}CH_2\text{-}CH_2\text{-}COO^-Na^+ \\ \quad / \\ CH_2COO^-Na^+ \end{array} \qquad (1)$$

and has been shown to degrade primarily to a sulfoxide and a cinnamic acid analog. The compound is quite stable at 25°C and the kinetic studies reported here have been carried out at rather high temperatures in order to obtain degradation within a reasonable

time frame. It has the following physical and chemical characteristics (SKB Draft Product Reference Guide):

Molecular weight:	486.6 (disodium salt); 442.6 (acid)
Appearance:	white to off-white powder
pK_a Values:	5.4 and 6.7
Solubility:	poorly water-soluble (free acid)
	>350 mg/mL in aqueous base or water (disodium salt)
	5.84 mg/mL in ethanol (disodium salt)
Specific Rotation:	-12.6 (1% in water at 25°C)

Compound A has been supplied by a pharmaceutical company, Smith-Kline Beecham. The method of analysis in this work is by way of high pressure liquid chromatography (HPLC); an HPLC chromatogram of A monitored at 215 nm showed 99.8% of the total area under a single peak.

II-B. Chemicals and Supplies

Chemicals used were reagent grade, except acetonitrile (Burdick and Jackson), which was HPLC grade. Trifluoroacetic acid was obtained from Pierce (Rockford, IL) as an ampuled solution, 1 g/mL of water; 1 N KOH volumetric standard solution was obtained from Aldrich (Milwaukee, WI), concentrated H_3PO_4 from Baker (Baker Chemicals, Phillipsburg, NJ), EDTA disodium salt was from Sigma (St. Louis, MO), and hydroquinone was from Aldrich

(Milwaukee, WI). Water was distilled, deionized (Milli^{Q} Water Apparatus, Millipore Corp., Milford, MA). The buffer salts KH_2PO_4, K_2HPO_4, and the KCl were roasted at 110°C at least 5 hours and allowed to cool in a desiccator prior to use. Buffers were prepared from reagent grade chemicals and filtered through a Rainin (Emoryville, CA) Nylon-66 0.2 micron membrane to remove particulates. Some solutions were filtered through a Rainin (Emoryville, CA) Nylon-66 0.2 micron membrane housed in a disposable 13 mm Swinnex filter holder (Gelman) fitted to a syringe before the final dilution step. Teflon-faced stoppers (20 mm 4416/50 gray butyl) and Type-1 flint glass 10-mL vials were obtained from West. For sparging, a mini bubbler with coarse frit (Cat. 7531-04, 30-mL bottle 24140 with 24/40 stopper Cat. no. 7532-06) and a rotameter (Tube #32; float 1/8 inch glass) were obtained from Ace Glass, Vineland, NJ 08360. Needles used for sparging were 22 gauge 3" Luer hub stainless steel (ID/OD 0.016 x 0.028; Spectrum S/N 1481845F, available through Fisher Cat. No. 185310), and for venting, 23 G, 1 inch disposable (Becton-Dickinson, Rutherford, NJ).

CHAPTER III. INSTRUMENTATION

III-A. High Pressure Liquid Chromatography (HPLC)

The chromatographic system consisted of a Waters (Millipore Corp., Milford, MA) 484 Tunable Absorbance Detector, a Waters WISP 712 Autosampler, a Waters 501 HPLC solvent delivery system, and FIAtron (Oconomowac, WI) CH-30 column heater with TC-50 controller. Data acquisition and processing was accomplished through the Rainin Dynamax Method Manager Software on a Macintosh SE Computer (Apple Computer Inc., Cupertino, CA).

III-B. Surface Tensiometers

Surface tensions were determined using the Wilhelmy plate technique on two separate instruments, a Cahn electrobalance C-2000 housed in a vibration-free enclosure (Abbott Labs, Abbott Park, IL), and a Kruss K10 tensiometer (Bristol-Myers Squibb, Syracuse, NY). The circular sample cell was made of Teflon (Cahn) or glass (Kruss) and of similar dimensions, such that 10.0 mL of sample pipetted to the sample cell filled it to approximately one-third of its depth. A circulating thermostatically-controlled water-bath was used to maintain temperature in the sample cell, which was monitored with a temperature probe. To minimize evaporation during measurement, a sample cell cover was made for the Kruss instrument by cutting off the bottom one fourth of a 100-mL

polypropylene water bottle, and cutting a slit in it such that the cover could be slipped over the sample cell without disturbing the Pt plate.

III-C. Cyclic Voltammetry

The set up used was a laboratory-fabricated apparatus in the UW Chemistry department electronics laboratory consisting of an xy recorder (x=y=0.1V/inch; 0.5 sec/inch), waveform (sweep) generator (1 Hz; 10-70 Kohms resistance), digital multimeter (Range 2 DCV function), and Pt wire electrodes.

III-D. Differential Scanning Calorimeter (DSC)

The DSC used was a SEIKO (Elk Grove Village, Illinois) DSC 220C with Automatic Cooling (liquid N_2), and Model SSC 5200H Disk Station with Optional Software Series "DSCINTEG", "DSCSUB", "DSCPURITY", v. 1.0 (Area Partitioning Integration Software, Data Subtraction Software, and Purity Calculation Software); Seiko solid sample pans (aluminum, crimped); standard: indium, run at same heating rate as sample (2°C/min).

III-E. pH Meter

The pH meter used was an Orion (Cambridge, MA) Research Digital Ionalyzer/501 pH meter calibrated at two points with appropriate buffers.

III-F. Sample Dilutor

Samples and standards were diluted in the same proportions using an ICN Biomedicals, Inc. (Horsham, PA) Digiflex Dilutor. Using the dilutor allowed rapid and precise dilution of samples with minimum waste of sample, glassware, and diluent. The dilutor accuracy was checked by filling volumetric ware with multiple dispensions from the same setting, e.g. by filling a 10-mL volumetric flask with water using 200 μL increments.

III-G. Ovens and Baths

Ovens were used for 75 and 93°C studies (Stable Therm Gravity Oven, and Model OV12, Blue M Electric Co., Chicago, IL; Hotpack oven, Philadelphia, PA), a thermostatically-controlled circulating water-bath was used for 60°C studies (Lauda, Germany), and silicon oil baths were used for the majority of the 93°C studies. The oil bath temperature was regulated using a heating mantle/ rheostat Precision instruments regulator.

III-H. Software

Data analysis was aided by the use of the following software for Macintosh: CricketGraph (Computer Associates International, v. 1.3 and III 1.5 f), Statworks (v. 1.2), Student MATLAB (The Mathworks Inc., Prentice-Hall, Englewood Cliffs, NJ 07632, 1992, v. S3.5), SYSTAT (SYSTAT, Inc. FPU version 5.2.1), and Microsoft word (Microsoft Corporation, v. 5.1a); and for PC: SCIENTIST (MicroMath Scientific Software, Salt Lake City, Utah 84121, 1993). Programs were written in MATLAB or SCIENTIST, utilizing the numerical integration routines available within the programs to analyze kinetic schemes. It should be noted that whenever rate constants have been reported which were obtained by numerical integration, the full number without regard to significant figures has been reported in order that the kinetic curve may be reproduced if necessary. SYBYL software was used to generate the space-filling model of Compound A.

CHAPTER IV EXPERIMENTAL METHODS

IV-A. Decomposition of the Sulfide

IV-A-1. Sample Preparation

Sample solutions of 100 mL were prepared by dissolving an appropriate amount of drug in ca. 90 mL of buffer in a volumetric flask and adjusting the pH before the volume was brought to the mark. Two-mL aliquots were then distributed to 10-mL vials using the dispenser/dilutor which had been sparged with sample solution. Vials were stoppered and sealed. One-third each of the samples were then sparged with argon, oxygen, or stored as is, i.e. air headspace, at the experimental temperature. During sparging, the pull-tab on the aluminum seal was bent back to allow penetration of the sparge and vent needles.

IV-A-2. Analysis for Oxygen by Cyclic Voltammetry

The length of sparge-time required was determined by running separate experiments using cyclic voltammetry as follows. The instrument was zeroed, and a baseline scan in the range -0.8 to +0.08 volts was taken on ca. 12 mL of 0.5N H_2SO_4, H_20, or buffer, which is in great excess over the two mL sample size. Sparging with N_2 was started (ca. 0.75 cc/min.) and scans taken at timed intervals until the

shape of the curve remained constant (the reaction monitored is the conversion of O_2 to peroxide).

To quantitate the disappearance of oxygen from the solution, the height of the signal at +0.015 or +0.025 V was measured and compared to the baseline scan; this is where the greatest positive change was observed in the signal. For example, before sparging, the signal was 0.37 V, and when sparging was complete, the signal was reduced to 0.16 V (it is not expected to reach zero). The normalized response is the ratio of these two voltages.

As can be seen from Figure IV-1 and IV-2, a sparge time of less that 2 minutes at a flow rate of ca. 0.75 cc/min was deemed appropriate to sparge 12-mL of buffer; therefore 15 minutes was deemed to be more than sufficient to sparge 2-mL in a 10-mL vial with a slightly lower bubble speed to allow for foaming.

IV-A-3. Method of Sparging with Argon or Oxygen

Cylinder gas was passed through a mini-bubbler filled with water to saturate the gas and minimize evaporation of the sample during sparging. The gas stream was then fed into stoppered 10-mL vials, approximately 10 connected in series by Tygon tubing and glass tees, through 22 gauge 3-inch Luer hub steel needles, and a rotameter at the end monitored gas flow. Stoppers were self-sealing Teflon-faced. The sparge needle sat below the surface of the solution (2 mL) in the vials, and the vials were vented with a second needle

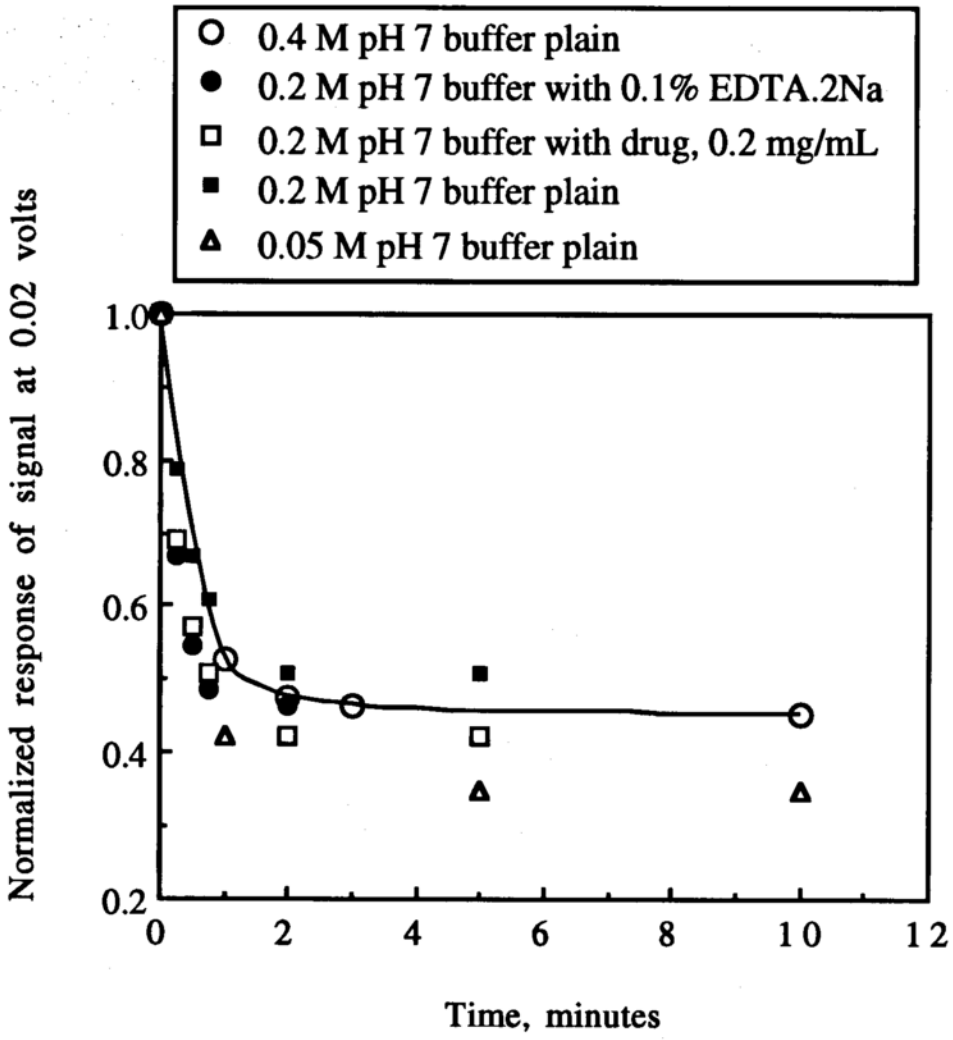

Figure IV-1 Relative change in O_2 concentration in solution in buffers bubbled with N_2 as monitored by cyclic voltammetry; normalized response. After approximately two minutes, the normalized response levels off, indicating the reaction is complete, and the oxygen concentration in solution is nil.

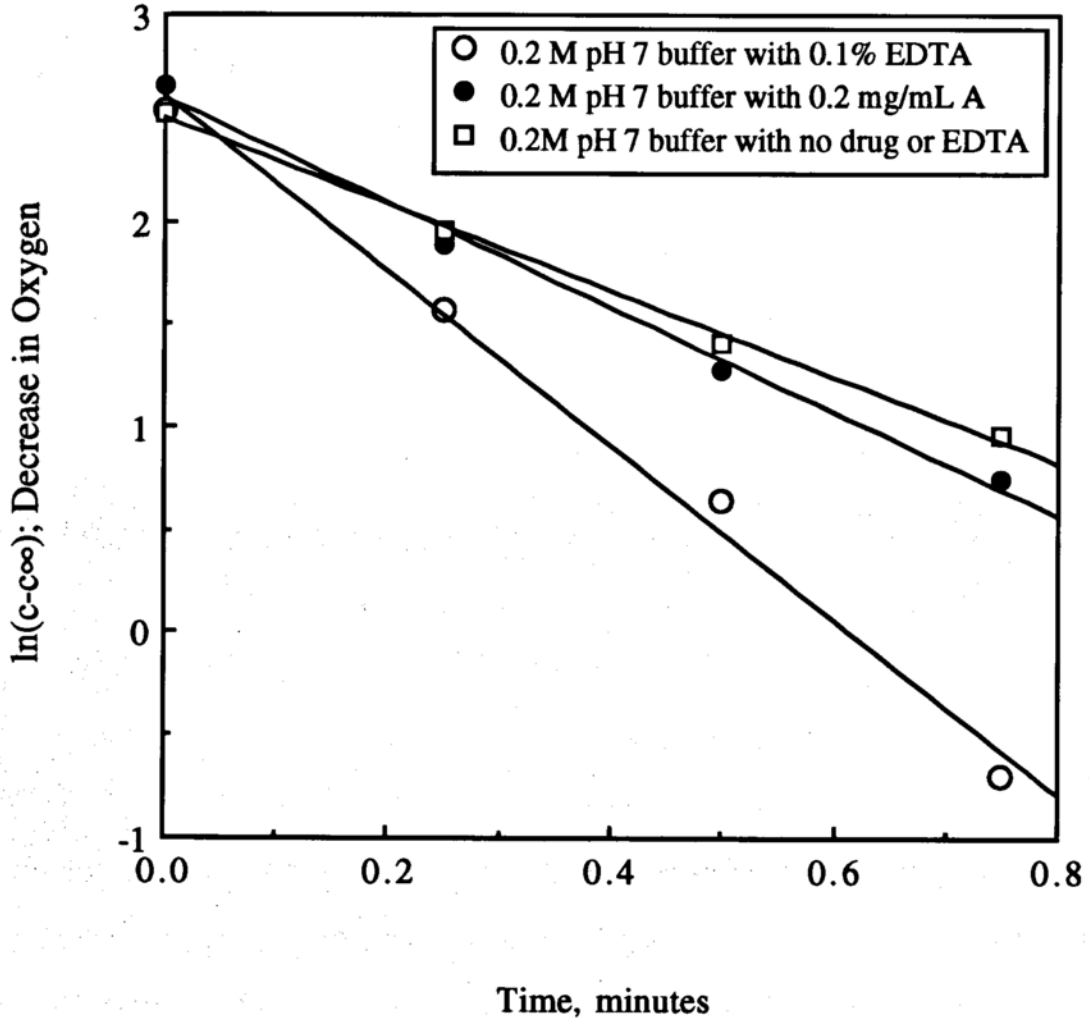

Figure IV-2 Relative change in O_2 concentration in solution in KH_2/PO_4 buffers bubbled with N_2 as monitored by cyclic voltammetry; data from Figure IV-1 treated as a sigma minus plot. The linear regression equations are:

0.2 M buffer with EDTA:	$y = 2.50 - 2.09x$	$r^2 = 0.998$
0.2 M buffer with drug:	$y = 2.59 - 2.54x$	$r^2 = 0.993$
0.2 M buffer plain:	$y = 2.60 - 4.24x$	$r^2 = 0.992$

(one inch disposable) which did not touch the solution. The large headspace ensured an excess of sparge gas in the vial.

The rate of bubbling had to be slower than that used in the cyclic voltametry experiments (ca. 0.75 cc/min), as the solutions at drug concentrations in excess of the cmc foamed considerably. After sparging 15 minutes with argon or O_2, the vent needle was removed from the vials. When bubbling stopped, the sparge needle was raised above the level of the solution and gently removed. An initial assay value was determined by HPLC analysis (described below) of two each of the vials prepared with air headspace, or argon-sparged or oxygen-sparged (Appendix C, Table C-1). Statistical analysis showed these not to be significantly different at the 99% confidence level (Appendix C, Table C-2); therefore, for a given buffer molarity, temperature, and initial drug concentration, the average results from the three treatments were used as the initial assay value (T_0) in the subsequent tables in Appendix C.

As a control, buffer without drug and a 1 mg/mL hydroquinone solution were sparged and stored in the same manner as the samples. Hydroquinone is very sensitive to oxygen and turns brown as it is oxidized, and thus served as a control for leakage in the argon sparged systems. At 93°C and at 4°C, little or no discoloration was noted in the hydroquinone samples. The efficiency of sparging was also confirmed by the fact that argon-sparged samples at 93°C remained clear and colorless for the duration of the experiments, that is, there was no sulfoxide formed, which is yellow, as would be expected in the presence of oxygen. At 75°C, some discoloration was

occasionally noted in samples stored in an oven, and was attributed to seal deformation rather than inefficiency of sparging.

IV-A-4. HPLC method

Samples were assayed by HPLC (SKB Pharmaceutical Analysis Test Method) using a Waters Reverse Phase 125 Å 10μm μBondapack™ Phenyl column at 40°C, and a mobile phase consisting of 50:50 CH_3CN:H_20 with 0.1% Trifluoroacetic Acid (Pierce), vacuum-filtered through a Rainin Nylon-66 0.45 micron membrane. Generally, the HPLC system was allowed to equilibrate for at least 20 minutes prior to beginning a run, and initially at least 3 standard injections preceded the run as a check on baseline stability and system reproducibility. Generally, the standard deviation of multiple injections was well under 2% within a run.

For analysis, 100 or 200-μL of appropriately-diluted sample (initial drug concentration = 25 or 0.05 mg/mL, respectively) were injected onto the column. Detection was at 215 nm and the flow rate was 2.0 mL/minute. Standards were injected at regular intervals throughout the run and at the end of the run. Standard curves were prepared by injecting 25, 50, 75, and 100 μL of two separately weighed standard stock solutions prepared in mobile phase, or by injecting 100 μL of an appropriately diluted stock solution. Both methods yielded equivalent results; this served as a check on the autosampler and dilutor precision.

Typical chromatograms are shown in Figures IV-3 and 4; typical elution ranges are 6-8 minutes for the sulfoxide, 8-12 minutes for the parent, and 13-16 minutes for the cinnamate.

IV-A-4-a. Sample Dilution for HPLC: General Comments

As the decomposition progressed, it was observed that although solutions were clear and colorless or yellow at elevated temperatures, the cinnamate, formed as a degradation product, precipitated upon cooling. In the Master's Thesis, samples were filtered in order to remove the insoluble cinnamic acid analog and then diluted appropriately with water and analyzed by HPLC. This made it difficult to assess this decomposition product.

Therefore, in the present work, dilutions were made with mobile phase as this was found to solubilize the cinnamate analog, as evidenced by the mass balance. In some cases, insolubles remained which were usually yellow or off-white/light brown in color. These solutions were filtered after the first dilution and before the second and final dilution, and at this step it was always the case that the filtrate was clear and colorless.

Prior to any dilution, the pH of the sample was taken at room temperature. Failure to dilute sufficiently, especially the high molarity and high ionic strength solutions, resulted in split peaks in the chromatography.

Figure IV-3 Typical HPLC chromatograms. Top: Drug stored in 0.4 M pH 8 buffer (with EDTA.2Na) after 10 days at 93°C, oxygen-purged, 91.1% A retained. Bottom: Drug stored in 0.2 Mμ pH 8 buffer (with EDTA.Na) after 150 days at 93°C, air headspace, 19.6% A retained.

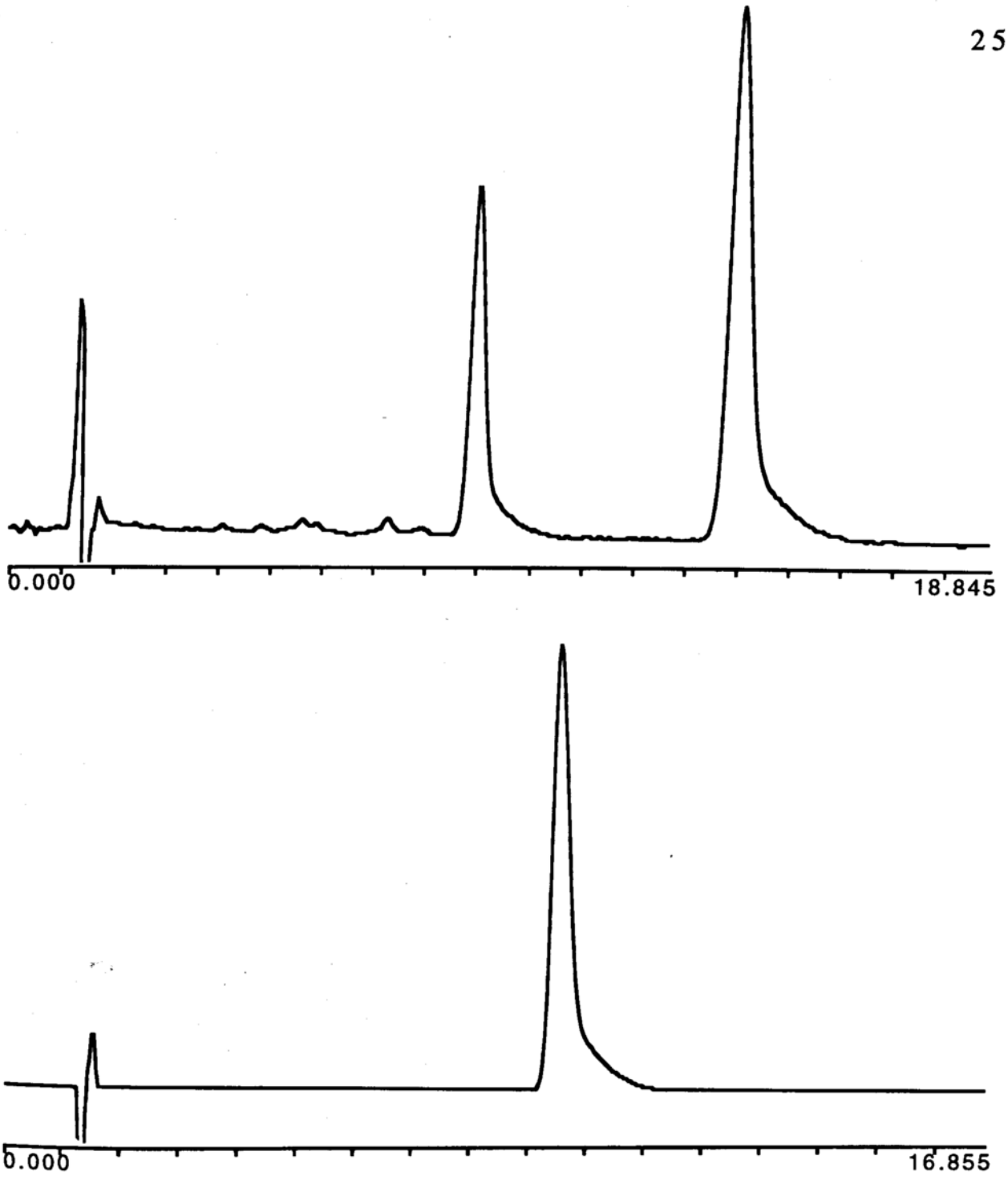

Figure IV-4 Typical HPLC chromatograms from oxygen-purged samples. Top: Drug stored in 0.2 Mμ pH 8 buffer (with EDTA.2Na) for 122 days at 93°C, 9.7% A retained. Bottom: Drug stored in water in the refrigerator (ca. 4°C) for four years, 0.25 mg/mL, air headspace.

IV-A-4-b. Sample Dilution for HPLC for Samples with an Initial Drug Concentration of 25 mg/mL (above the cmc)

It shall be seen in the following that 25 mg/mL is above the cmc under the experimental conditions used. In these cases, the entire 2-mL vial contents was washed out and diluted to 100 mL in a volumetric flask with mobile phase. 100 μL of this solution was then further diluted with the Digiflex dilutor with 8900 μL of mobile phase, and 100 μL injected for analysis by HPLC.

In cases where the contents of the volumetric flask was turbid or contained insolubles, a portion was first filtered through a Rainin Nylon-66 0.2 micron filter. In all cases, the resulting filtrate was clear and colorless, even though the mixture may have been white or yellow. Since the sulfoxide is yellow, it appears as though this filtration process removed the sulfoxide, as was also evident from the chromatography. Therefore, only the appearance of cinnamate was followed quantitatively, and this was done by assuming the cinnamate had the same response factor as the parent compound.

IV-A-4-c. Sample Dilution for HPLC for Samples with an Initial Drug Concentration of 0.05 mg/mL (below the cmc)

It shall be seen in the following that 0.05 mg/mL is below the cmc under the experimental conditions used. In these cases, the 2-mL samples were diluted to 10 mL with mobile phase directly in the vial using the dilutor; in all cases there were no insolubles at this

step. 500 μL of this dilution was further diluted with 3500 μL of mobile phase using the dilutor, and 200 μL injected for analysis by HPLC.

IV-B. Determination of the Critical Micelle Concentration of A

With the Kruss K10 instrument, before the first run of each day, the plate was burned, but between samples, including calibration samples with water, the plate was not burned. Rather, the old sample was suctioned or pipetted out of the cell, and the cell rinsed with three volumes of water or buffer, each time dipping the plate completely in the rinsing solution.

Using this rinsing procedure, the surface tension of water was recovered even after the most concentrated drug solution had been the previous sample, indicating no contamination by the previous sample. After the new sample was pipetted to the cell, the plate was dipped several times to wet it. The platform was then raised very slowly until the solution "grabbed" the plate. The surface tension was measured when it reached a constant value, usually after an equilibration time of 2-4 minutes for the high temperatures, and longer (up to 45 minutes) at low temperatures. Longer times could not be used at high temperatures due to evaporation, thus the same length of equilibration time was allowed at a given temperature before the surface tension reading was recorded.

The published (CRC) surface tension of water was used to calibrate the instrument at the temperature being studied.

The surface tension of the buffer without drug at a given temperature was also determined as a control to check for surface tension lowering contaminants, and to allow for calculation of surface pressure, π :

$$\pi = \gamma_o - \gamma \qquad \text{(IV-1)}$$

where γ_o is the surface tension of buffer without drug, and γ is surface tension with drug (Rosen).

The surface excess, Γ, in moles/m^2, was calculated from the slope of the plot of surface tension, γ, vs (log C) according to the Gibbs adsorption equation for a 1:1 ionic surfactant in the presence of swamping electrolyte (Rosen)

$$\Gamma = -\frac{1}{2.303RT}\left(\frac{d\gamma}{d(\log C)}\right) \qquad \text{(IV-2)}$$

From this, the area per molecule at the interface, in $Å^2$, was calculated (Rosen)

$$A_m = \frac{10^{20}}{N_{Av}\Gamma} \qquad \text{(IV-3)}$$

Ionic strength was calculated according to

$$\mu = \frac{1}{2}\Sigma(c_i z_i^2) \qquad \text{(IV-4)}$$

where c_i is the concentration of each type of ion and z is its charge. The concentration of each type of ion was determined iteratively using the Henderson-Hasselbach equation

$$pH = pK_a + \log\frac{[base]}{[acid]} \qquad \text{(IV-5)}$$

at each iteration, correcting the pK_a for ionic strength assuming the Davies equation

$$pK_{a(true)} = pK_a \pm \frac{(2n-1)(0.507\sqrt{\mu})}{1+1.6\sqrt{\mu}} \qquad \text{(IV-6)}$$

to hold, where n = 2 for phosphate as described in Perrin and Dempsey. For certain buffers, the actual quantities added were used to determine the ionic strength, and to check the calculation.

CHAPTER V. EXPERIMENTAL DESIGNS

V-A. Decomposition of the sulfide

V-A-1. Summary of Studies in the Master's Thesis

In the study, 0.2 mg/mL solutions (4×10^{-4} M) of the drug were prepared in various concentrations of pH 7.0 potassium phosphate buffer ranging from 0.01 to 1.0 M, with and without ionic strength adjustment with KCl to a common value of 2.2, ampuled under air (i.e. ca. 22% oxygen), stored, protected from light, at 60, 75, and 93°C, and assayed by HPLC after different storage times. In all cases the number of moles of oxygen in the system was in great excess over that of the compound.

Such a wide range of concentrations was used because some form of complex formation (Connors, 1965, 1966, 1969; Mollica) was suspected as being the cause of the unusual kinetic behavior noticed in preliminary investigations. The ionic strength of 2.2 was chosen because it represents the calculated ionic strength of the highest molarity buffer used in the studies (i.e., 1.0 M pH 7). The drug concentration of 0.2 mg/mL was chosen arbitrarily, but the effect of drug concentration was assessed by preparing samples at four other drug concentrations ranging from 0.05 to 0.5 mg/mL in both low and high ionic strength buffers, and stressing these at 75°C and 93°C. Kinetics at initial drug concentrations between 1 and 10 mg/mL in H_20 with and without EDTA.2Na at 93°C were also investigated. In

quite a few cases, the drug concentration data were ambiguous, the reason for which did not become clear until the present work was undertaken.

The main conclusions to be drawn from the Master's study were that

a) a kinetic salt effect, but not buffer catalysis, was operative in the pH 7 phosphate buffer system

b) kinetic profiles generated at 60, 75, and 93°C were different, that is, at 93°C, most of the data appeared first-order, i.e. obeyed the equation

$$\ln (A/A_o)=-kt \qquad (V-1)$$

while at 60°C, some data, especially that generated at high buffer concentrations, displayed auto-oxidative behavior which could be fit to the equation

$$\ln(A/(1-A)) = -kt \qquad (V-2)$$

where A is parent drug concentration;

c) the compound was surface active and possessed a cmc in water of 4.3 mg/mL (8.6×10^{-3} M) at 22°C; and

d) preliminary studies suggested that the unusually high levels of KCl and buffer salts used contained sufficient quantities of unidentified trace metals to catalyze the degradation reaction, and this catalysis could be reduced by the addition of EDTA.2Na (Figure V-1).

V-A-2. Present Work

In the present study, initial drug concentrations of 25 and 0.05 mg/mL were chosen for study. These were deemed to be sufficiently above and below the cmc so as to avoid the transition concentration of the cmc over several half-lives of the degradation reaction, allowing one to check for micellar catalysis/protection. This is in contrast to the studies in the Master's thesis, where the drug concentration in many cases crossed the cmc as the decomposition progressed.

The degradation was studied at 60, 75, 93°C, and at three buffer concentrations, 0.1, 0.2, 0.4 M phosphate containing 0.2% EDTA.2Na, with and without ionic strength adjustment with KCl to a common value of 0.89 or 1.22, and adjusted to either pH 7 or 8. The ionic strengths of 0.89 and 1.22 represent the calculated ionic strength of the 0.4 M pH 7 and 8 buffers, respectively.

Although phosphate is not as efficient a buffer at pH 8 as at 7, it was felt that at the high molarities used the buffer capacity would be sufficient. This allowed direct comparison without introducing another buffer type. As decomposition progressed, however, the pH, especially of oxygen-sparged samples, was found to drop slightly,

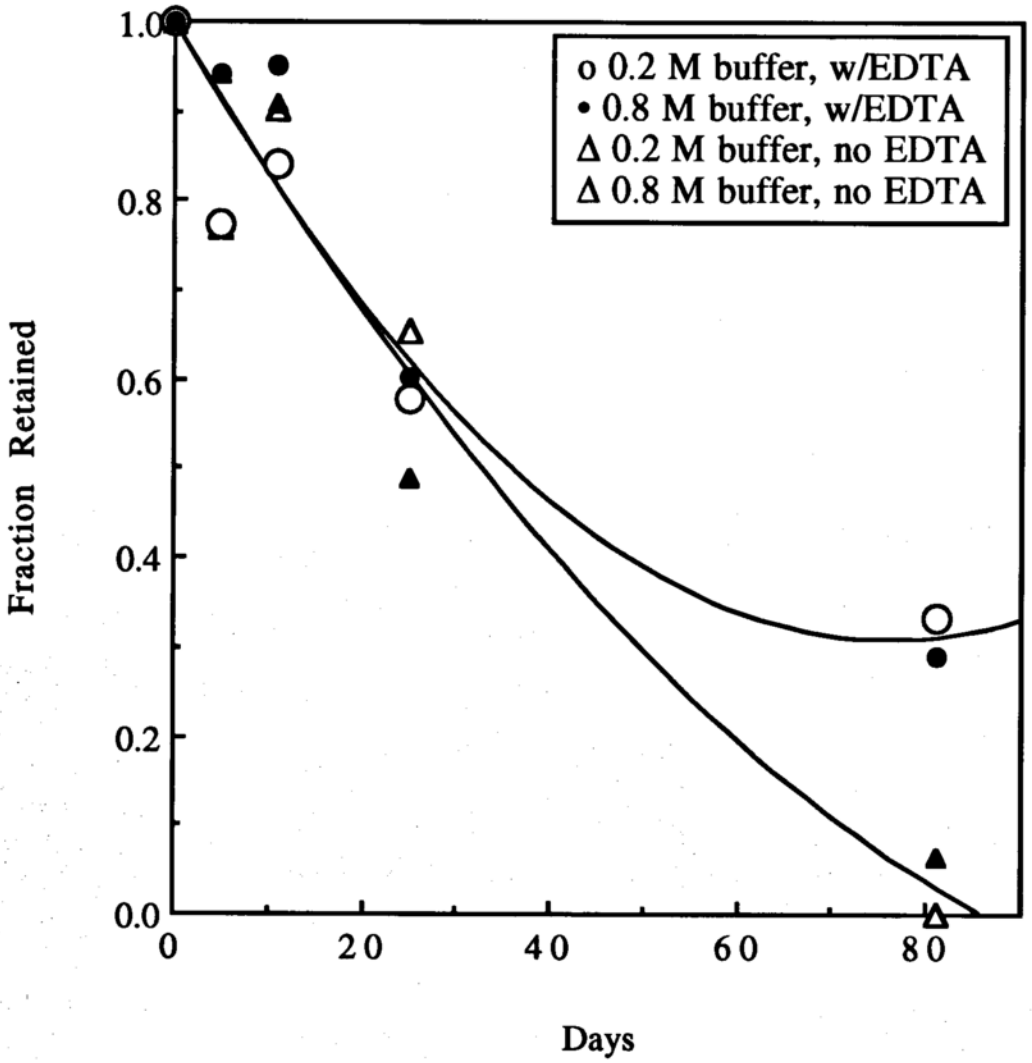

Figure V-1 Data from Master's Thesis showing the effect on the decomposition of A at 75°C by adding 0.1% EDTA.2Na to 0.2 M and 0.8 M pH 7 phosphate buffers (KH_2PO_4/KOH). The polynomial fit through the data is to guide the eye. Initial drug concentration = 0.2 mg/mL

and these later time points were not necessarily used in data analysis. In addition, in some very degraded samples (greater than 2 half-lives), a shoulder appeared on the parent peak in the chromatography, so these data were not used in the data analysis, although they are reported parenthetically in the Tables in Appendix C

All experiments were conducted in the presence of 0.2% EDTA.2Na (0.005M) to prevent trace metal catalysis, since preliminary work in the Master's Thesis showed that 0.1% slowed the reaction considerably (Figure V-1). The vials or ampuls were protected from light by covering the baths with aluminum foil. At least one vial was pulled per time point, and eight or more time points were analyzed per kinetic curve for disappearance of A and appearance of the cinnamate analog. For selected time points, multiple vials were assayed in order to determine the standard deviation. Buffers without drug served as controls for chromatographic interferences, precipitate formation, discoloration etc.

V-B. Critical Micelle Concentration

The cmc values of compound A were determined at pH 7 and pH 10 in phosphate buffers, ranging from 0.05 M to 1.0 M, similar to those used in the kinetic studies. Most of the cmc values at 22°C were determined using the Cahn instrument, while all the cmc values

at higher temperatures were determined using the Kruss K10 instrument.

For the cmc determinations, geometric dilutions of a stock solution of A in a given buffer were made with the same buffer such that the surface tension of at least eight concentrations of A per buffer per temperature were determined. The raw surface tension vs concentration data are presented in Appendix C. The cmc values were determined by the intersection of the linear portions of the plots of surface tension vs log concentration, by setting equal the equations of the two linear regression lines and solving for $x = \log C$. Representative plots of the raw data are shown in Figures V-1 and V-2.

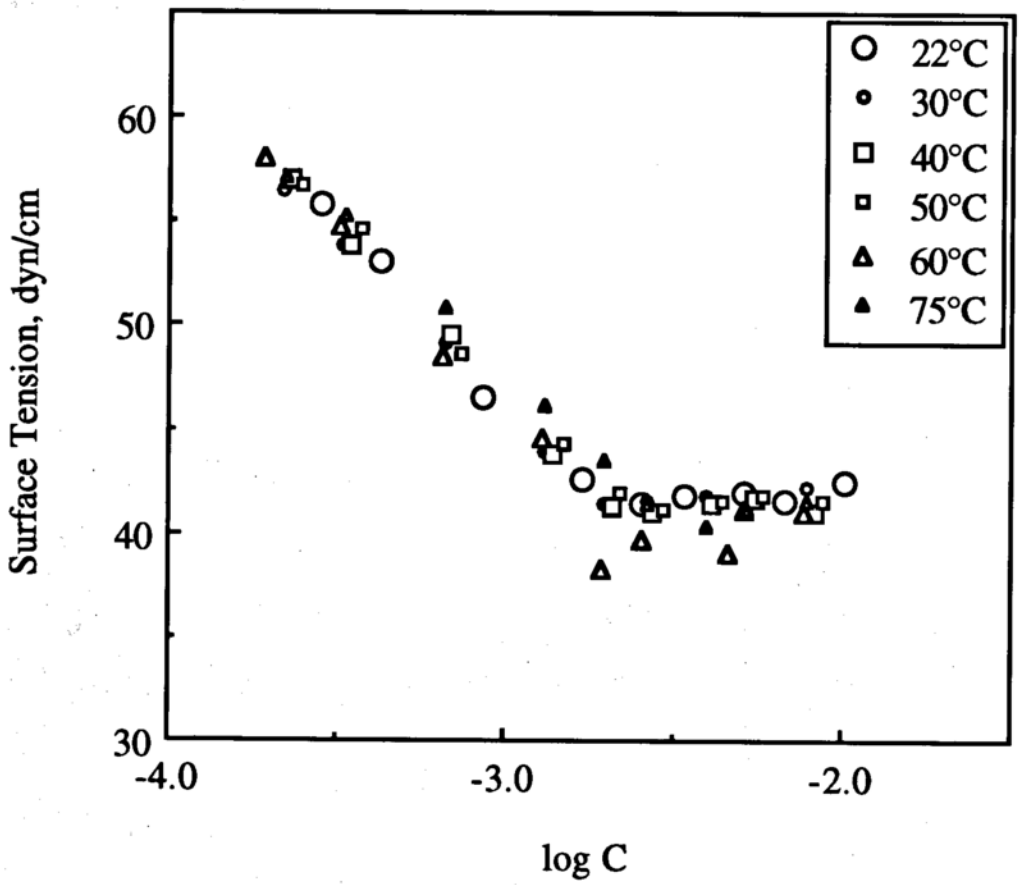

Figure V-1 Surface tension vs log(molar concentration of A) determined in 0.1 M pH 7 phosphate buffer at indicated temperatures; at all but 22°C, the buffers also contained 0.2% or 0.005 M EDTA.2Na.

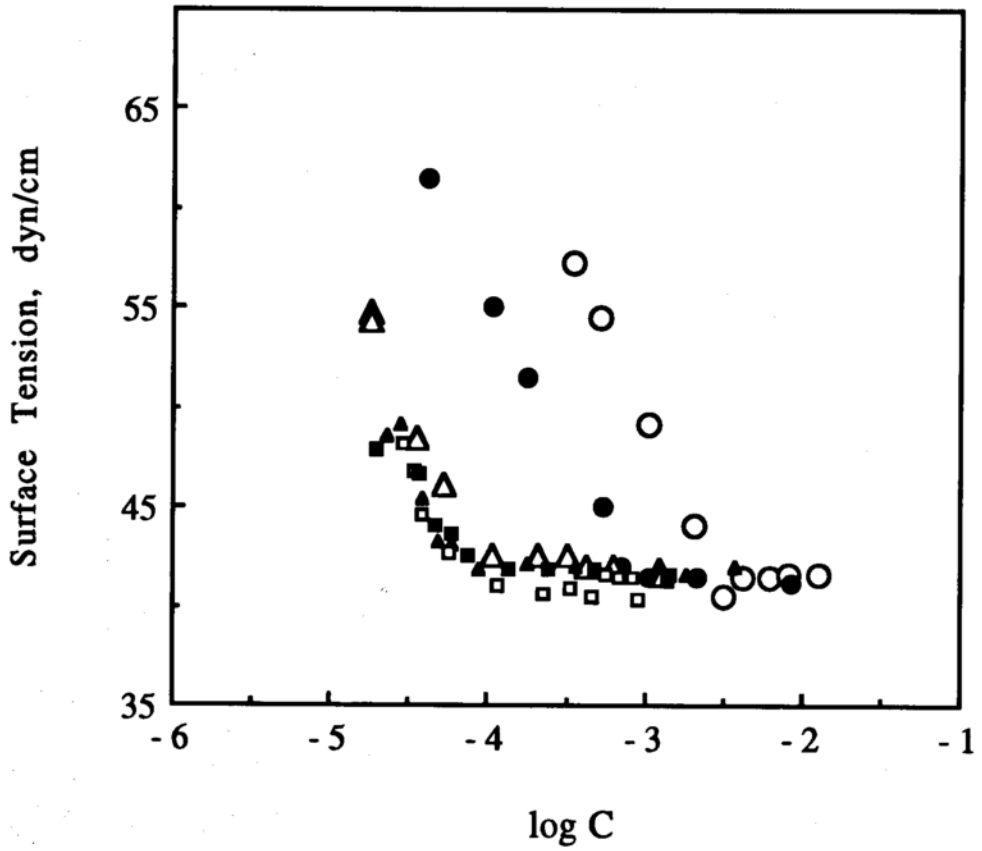

Figure V-2 Surface tension vs log(molar concentration of A) determined at 22°C with Cahn (C) or Kruss (K) tensiometers in pH 7 phosphate buffers of indicated molarity; where indicated, the ionic strength has been adjusted by the addition of KCl: open circle, 0.05 M (K); filled circle, 0.2 M (C); open triangle, 1.0 M (K); filled triangle, 0.2 M μ = 2.2 (C); open square, 0.4 M μ = 2.2 (K); filled square, 0.8 M μ = 2.2 (C).

CHAPTER VI. RESULTS AND DISCUSSION: CRITICAL MICELLE STUDIES OF THE MODEL COMPOUND.

VI-A. Reason for the Work

As may be seen in the molecular model shown in Figure I-2, the basic features of A are that it consists of a polar head group, containing one sulfur and two carboxyl groups, and a nonpolar hydrocarbon tail.

Although it might be expected that such a molecule would self-associate in solution, it is by no means certain that this would be in the form of micelles, and in fact in the initial phases of the Master's Thesis, the idea that the drug could assemble into true micelles was dismissed. That the drug was very surface active was evident by the ease with which an aqueous solution foamed. Also, certain solution stability samples were observed in the early stages of storage to foam upon shaking but to lose their foaming capability as decomposition progressed. Finally, at the author's request, the surface tension of the drug was monitored as a function of drug concentration, and these preliminary data collected by the manufacturer suggested a cmc in H_20 of 4.3 mg/mL ($8.6x10^{-3}$ M) at 22°C.

But because cmc values are a function of both temperature and salt concentration, and since a kinetic study would, by necessity, be one where both would be variables, more extensive surface tensiometry studies were undertaken by the author in order to assess the surface activity of the molecule in the presence of buffers

and other salts similar to those used in the kinetic studies (Franchini, *ACS Abstracts of Meetings*, 1994).

These additional studies were not initiated with the intent to probe micellar theory, but rather were carried out with the expectation of providing an explanation for aberrances observed in the solution degradation kinetic studies of the Master's Thesis. Specifically, at both 93°C and 75°C, kinetic data obtained at drug concentrations between 0.05 and 0.5 mg/mL were superimposable when the study was conducted in dilute buffer, but not in concentrated buffer as demonstrated in Figure VI-1.

VI-B. Critical Micelle Concentrations--Results

Results from the surface tensiometry studies of Compound A are summarized in Table VI-1, and it appears that cmc values determined in buffers of the same ionic strength are nearly the same. Although an ionic strength effect is suggested, it is well-documented that the cmc of an ionic surfactant is sensitive to the concentration of ions of opposite charge, and, as Table VI-1 shows, slight differences in the cmc values are consistent with slight differences in counterion concentration, $[K^+]$. In this study, buffers have been adjusted to constant ionic strength rather than constant $[K^+]$ because the objective was not to study the counterion effect, but rather to determine the cmc of Compound A in buffers to be used for solution kinetic studies.

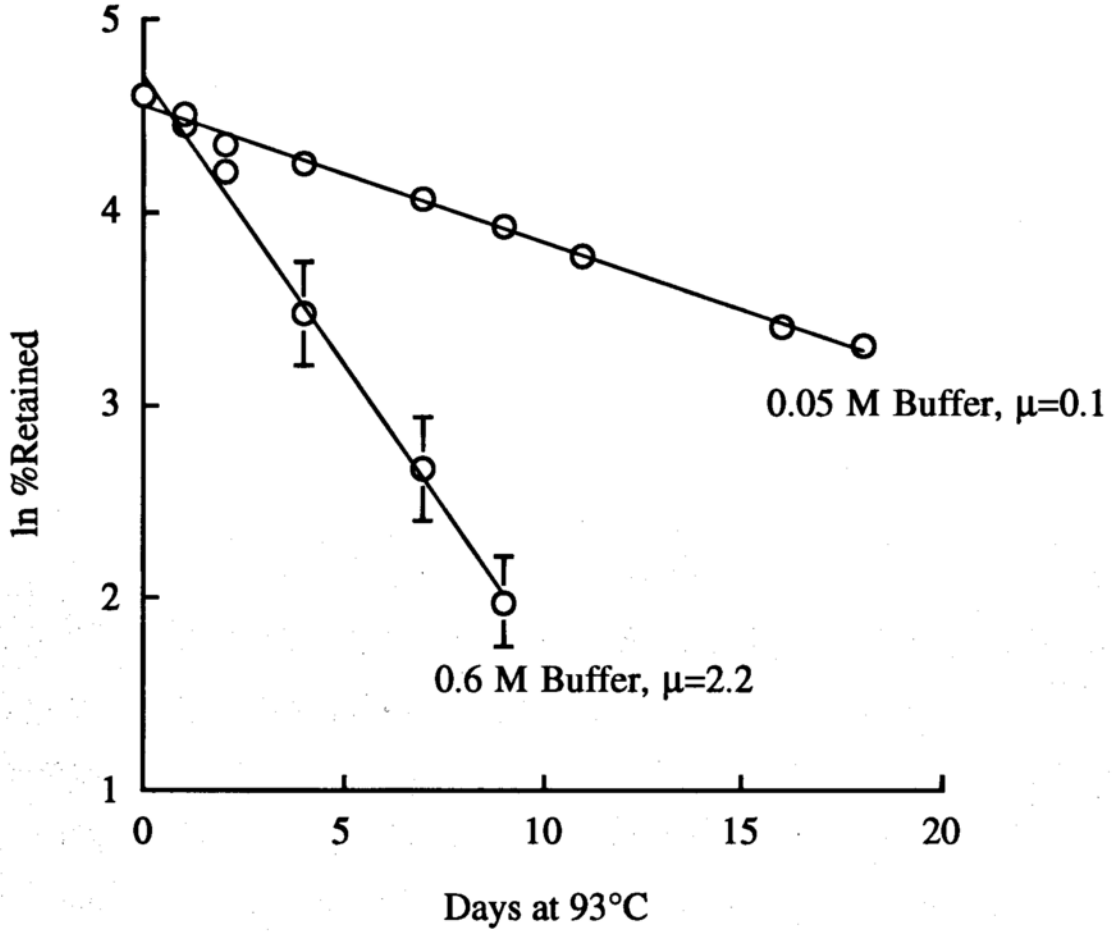

Figure VI-1 Solution kinetics at 93°C in pH 7 phosphate buffers; mean of 4 drug concentrations: 0.05, 0.1, 0.2, 0.5 mg/mL. The 0.6 M buffer has been adjusted to an ionic strength of 2.2 with KCl. These equations describe the data:

0.05 M buffer: $y = 4.55 - 0.071x$ $r^2 = 0.995$

0.6 M buffer: $y = 4.70 - 0.30\ x$ $r^2 = 0.995$

Table VI-1 Cmc values (mM) of A in determined in buffers of indicated molarity

Buffer[a]	μ	[K^+]	22°C	30°C	40°C	50°C	60°C	75°C
0.05 M, pH 7	0.11	0.08	3.2	--	--	3.7	4.1	--
0.1 M, pH 7	0.22	0.16	1.9	1.9	2.0	2.4	2.4	3.2
0.2 M, pH 7	0.45	0.32	0.82	1.1	1.1	1.3	1.2	1.6
			0.86[c]	--	--	--	--	--
0.4 M, pH 7	0.89	0.65	0.46	0.46	0.64	0.72	0.64	0.91
0.6 M, pH 7	1.2	0.97	0.25	--	--	0.37	0.42	--
0.8 M, pH 7	1.5	1.29	0.15	--	--	--	--	--
1.0 M, pH 7	2.23	1.62	0.077	--	--	--	--	--
0.2 M, pH 7	2.23[b]	2.11	0.064	--	--	--	--	--
0.4 M, pH 7	2.23[b]	1.99	0.070	--	--	--	--	--
0.8 M, pH 7	2.23[b]	1.86	0.088	--	--	--	--	--
0.1 M, pH 7	0.89[b]	0.83	--	--	0.46	0.58	0.58	0.86
0.2 M, pH 7	0.89[b]	0.77	--	--	0.52	0.60	0.62	--
0.1 M, pH 10	0.3	0.2	--	--	3.2	--	--	3.4
0.2 M, pH 10	0.6	0.4	--	--	1.4	--	--	2.2
0.4 M, pH 10	1.2	0.8	--	--	0.62	--	--	1.0
0.2% EDTA, pH 7	0.06	0.015	--	--	--	7.2	--	--
H_2O	--	--	8.8	--	--	--	--	--

[a] Molarity of KH_2PO_4 (in pH 7 KH_2PO_4/KOH), or K_2HPO_4 (in pH 10 K_2HPO_4/KOH)
[b] ionic strength adjusted with KCl
[c] contains 0.005 M (0.2%) EDTA.2Na; all others at 22°C do not, however all buffers at higher temperatures do

With this in mind, the main finding will be addressed, which is the deviation from linearity observed in the Corrin-Harkins plot at high counterion concentration.

VI-C. Deviation in the Corrin-Harkins Relation

The Corrin-Harkins equation states that for ionic surfactants

$$\log \text{cmc} = a - b \log(C_s + \text{cmc}) \qquad \text{(VI-1)}$$

where C_s represents the counterion concentration from the electrolyte or buffer salt (Mukerjee, 1967; Hiemenz). This relation has been verified for a large number of ionic surfactants in dilute salt solutions (Rosen), and suggests that a plot of log(cmc) vs log (total counterion concentration) should be linear.

The data at 22°C from Table VI-1 are plotted in this fashion in Figure VI-2, using $[K^+]$ values for C_s, and using twice the cmc in the parenthetical expression of Eq. [VI-1], owing to this being a dicarboxylic acid salt.

It is noted that significant deviation occurs at buffer concentrations above ca. 0.2 M. Deviation from linearity in the Corrin-Harkins relation at high salt concentration was first documented by Mysels, and subsequently explained by Mukerjee in 1967 to be due to salting out of the hydrophobic monomer chains.

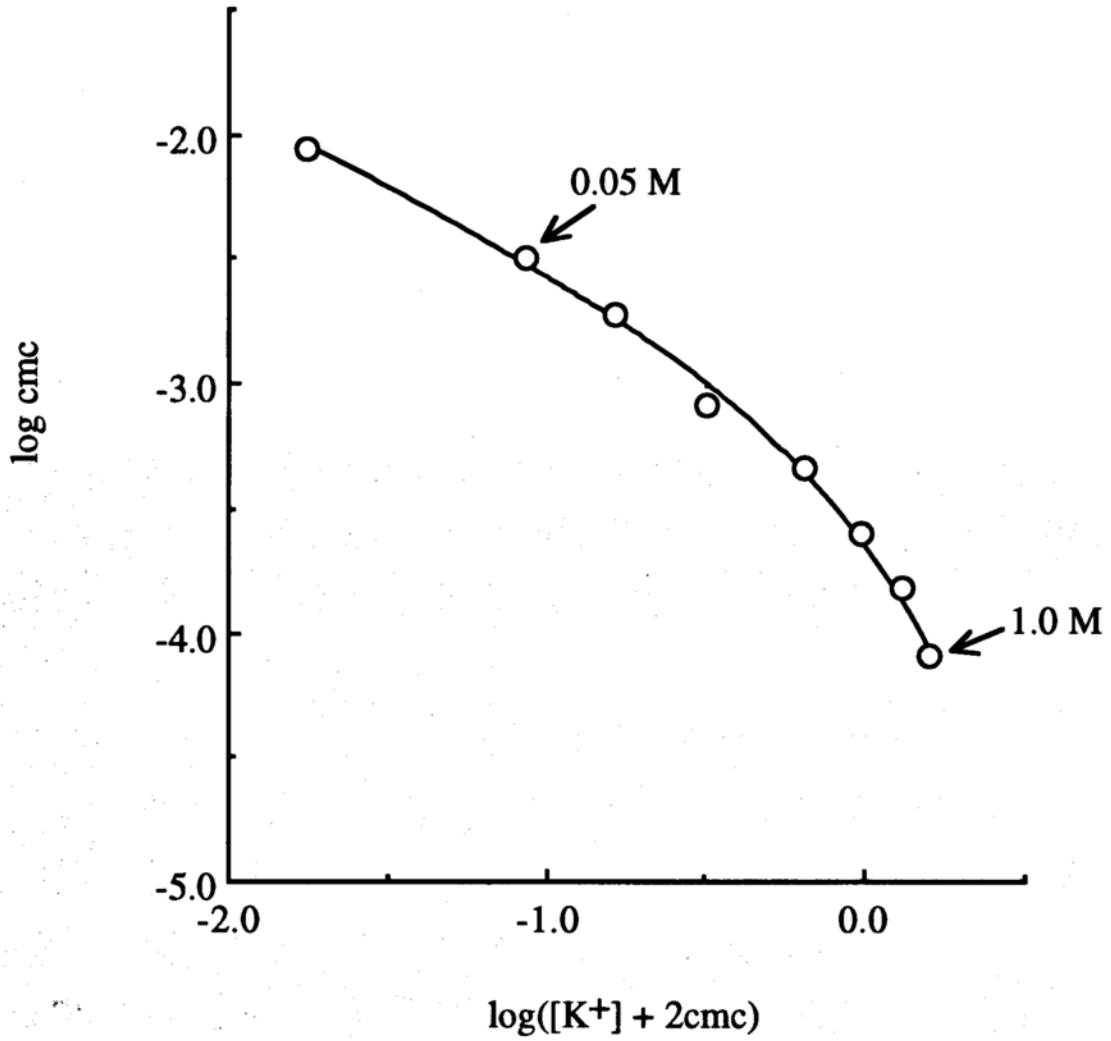

Figure VI-2 Corrin-Harkins double logarithmic plot of Compound A in 0.05 - 1.0 M pH 7 phosphate buffers, 22°C; data from Table VI-1. The fit is to Eq. [VI-3]. In all cases, solutions were clear and colorless to the naked eye.

This is because the added electrolytes increase the internal pressure of the solution by electrostriction of water. In turn, this increases the activity coefficient of the hydrophobic chains in a manner analogous to that found for nonpolar molecules in aqueous salt solutions, e.g. benzene in NaCl (McDevit and Long)

$$\log f = k_S C_S \qquad \text{(VI-2)}$$

where k_S is a salting-out coefficient, and C_S is concentration of added salt. Mukerjee (1993) and Chan (1993) have recently shown that when the salting-out term is added to the Corrin-Harkins relation, Eq. [VI-1] for ionic surfactants becomes

$$\log cmc = a - b \log(C_S + cmc) - k_S(C_S + cmc) \qquad \text{(VI-3)}$$

Again, it is noted that the parenthetical expressions represent total counterion concentration, so that in the case of a dicarboxylic acid salt, the term cmc is multiplied by 2, although this represents a very minor contribution at higher salt concentrations, where C_S is much greater than the cmc. Taking this into account, the data in Figure VI-2 have been fitted to Eq. [VI-3]; the fit is shown as the solid curve, and it is quite good.[7] The non-linear curve-fit parameter

---

[7] It is also noted that plotting log cmc against the square root of salt ionic strength was found to fairly well linearize this and some literature data (see Appendix A). This however, is an empirical observation; it is fairly well-established that the total counterion concentration rather than the salt ionic strength is responsible for changes in cmc by salt concentration. It is also noted that DeVijlder (1989) describes an equation for neutral surfactants whereby concentration is replaced by activity raised to some factor n, where n

estimates (SYSTAT) were found to be -3.2 for a, 0.64 for b and 0.48 for k_s, the salting-out coefficient; 95% confidence limits are -3.34 to -2.99 for a; 0.50 to 0.78 for b and 0.32 to 0.64 for k_s.

VI-D. Reasonableness of Parameter Estimates obtained for extended Corrin-Harkins relation

In order to judge the reasonableness of the parameter estimates obtained from curve fitting the data to Eq. [VI-3], an estimate of 0.67 for k_s was obtained independently using the group additivity rule for salting-out coefficients (Chan, 1985; Mukerjee, 1965) as shown in Table VI-2. Being able to obtain a k_s value which is even of the same order of magnitude as that predicted by the group additivity principle is satisfying. It should be noted that in none of these samples was any clouding or precipitation noticeable to the naked eye.

Along the same lines, the reasonableness of the parameter estimate obtained for b may be judged by comparing it with literature values obtained for the slope in Eq. [VI-1]. As has been shown (Mukerjee, 1967; Hiemenz) the value of b, according to the mass-action model of micelle formation in ionic surfactants, represents the fraction of counterions which are bound to the micelles. This value has been found to range from ca. 0.2 for bile salts which form small aggregates to 0.6-0.9 for anionic surfactants, such as sodium dodecyl sulfate, which are known to form micelles

---

is 1/2 for univalent electrolytes. This equation does not always linearize the data, but rather breaks the data into two discrete segments as shown in DeVijlder (1990; 1991).

Table VI-2 Estimate of salting-out coefficient by group contribution

	k_s	x	No. groups in A	
benzene/KCl	0.166		2	= 0.332
CH_2/KCl[a]	≈0.026		13	= 0.338
				TOTAL k_s = 0.67

[a]assuming that ($k_{s,\ KCl}$ /$k_{s,\ NaCl}$) = 0.82, as per Masterton and Lee; McDevit and Long; and Morrison.

(Mukerjee, 1967; Rosen). The value of b obtained for A, namely 0.64, supports the idea that the drug compound associates as micelles rather than as small oligomers. The structure of the molecule also supports this hypothesis since it is not planar or rigid. The actual size of the micelle could be obtained by light scattering, but that would be the subject of a separate dissertation owing to the difficulties of such measurements.

It should be noted that the fit in Figure VI-2 was done on 8 data points, from 0 to 1.0 M buffer. In Figure A-1 of Appendix A, three additional points are shown, which represent the data obtained in 0.2, 0.4, and 0.8 M pH 7 buffers adjusted to a common ionic strength of 2.2 with KCl, which is the calculated ionic strength of the 1.0 M buffer (Table VI-1).; it may be seen from this figure that the three additional points fall close to the curve. In fact, when these three additional points are included in the curve-fitting, the parameter estimates become -3.3 for a, 0.72 for b and 0.35 for k_s, which fall within the 95% confidence bounds. This suggests that the system does not discern between $[K^+]$ contributed from KH_2PO_4 *vs* KCl, it only senses the *total* counterion concentration.

VI-E. Other Examples of Non-Linearity in the Corrin-Harkins Relation

A limited number of studies have been documented which report similar nonlinear behavior for ionic surfactants in the presence of high salt (Chan,1993; Ozeki and Ikeda; Tanaka and Ikeda), the first in the literature being that of Mysels and Mysels.

The fact that this nonlinearity has not been more widely reported is because most of the data in literature have been generated at low salt concentrations.

That the nonlinearity is not an artifact is best realized by examining data reported for dodecyl dimethyl ammonium chloride (DDAC) by Ozeki and Ikeda (1981), which have been reproduced in Figure VI-3. Four completely different ways of obtaining cmc values all resulted in curvature in the Corrin-Harkins plot at ca. 0.2 M NaCl. These studies are especially credible since a simple 1:1 electrolyte was used, rather than the more complicated phosphate buffer used in this dissertation; the dependence of the ionization of phosphate on pH and ionic strength makes it more difficult to quantitate the counterion concentration in these buffer preparations.

By light scattering, Ikeda (1991) also reported a structural change in the micelles (sphere-to-rod transition) coincident with the deviation in the Corrin-Harkins plot observed for DDAC. It may well be that such a transition is real, and it may be that A undergoes a similar structural change. This change may be induced by the salting out of the monomeric chains. In order to test this, data reported by Ikeda and his colleagues as well as other reliable literature data have been fitted to Eq. [VI-3] and the results shown in Table VI-3. In all cases, the parameter estimate obtained for k_s is of the same order of magnitude as that calculated from group contributions.

The fit for the combined data for DDAC is shown in Figure VI-3 and one can see that it is quite good. The parameter estimates for the combined data were found to be -2.8 for a, 0.55 for b and 0.18

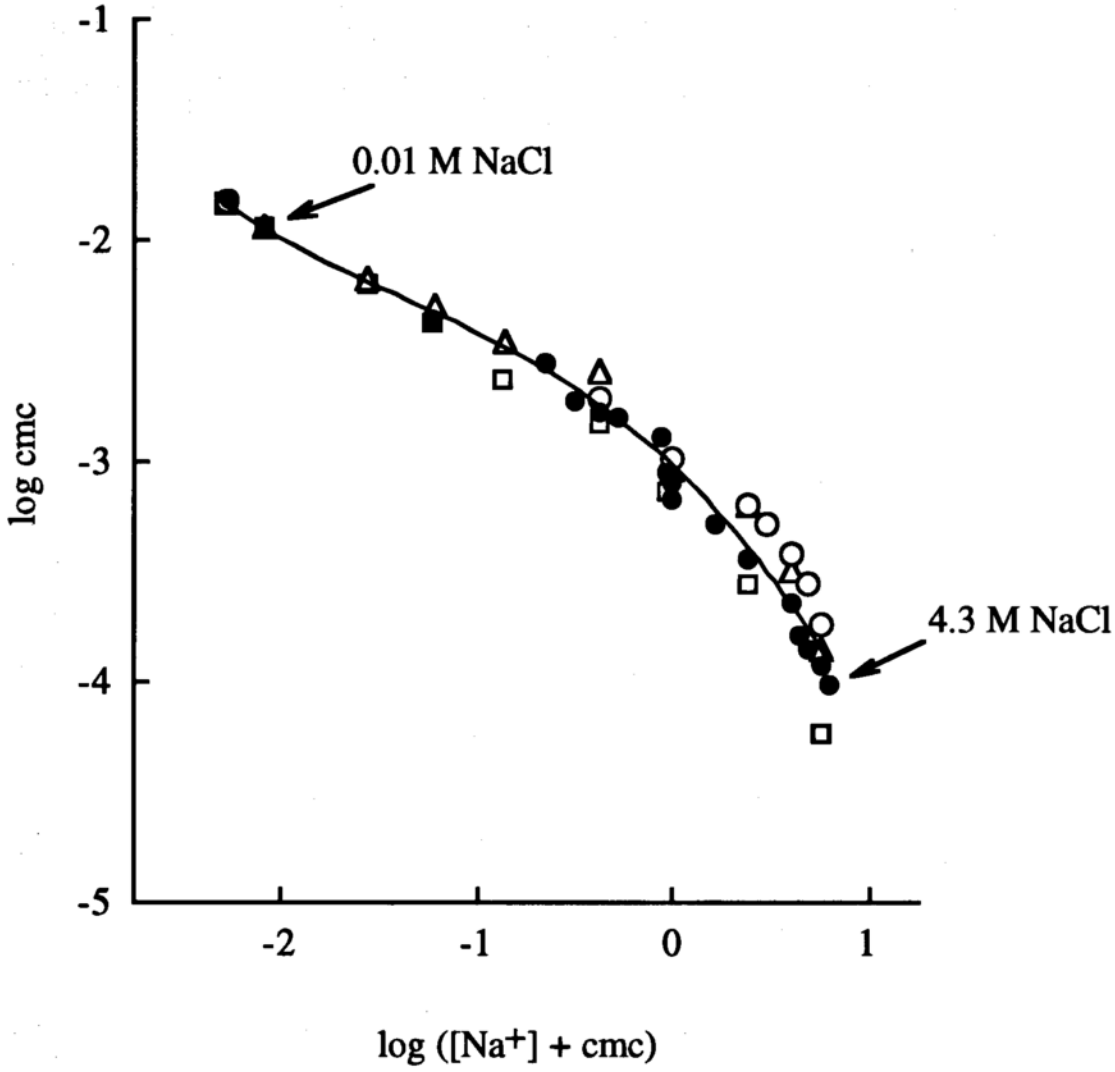

Figure VI-3 Corrin-Harkins plot for dodecyl dimethyl ammonium chloride (DDAC). Cmc values determined by Sudan Red B solubilization (open circle), viscosity (filled circle), light scattering (triangle), surface tensiometry (square). The fit is to Eq. [VI-3]. Data from Ozeki (1981).

Table VI-3 Parameter estimates for literature data fitted to Eq. [VI-3]. Method refers to method for determining the cmc; k_s* refers to an approximate k_s calculated by group contribution, assuming each methyl group contributes 0.032 when NaCl is used; DTAB is dodecyl trimethyl ammonium bromide; DDAC is dodecyldimethylammonium chloride.

	a	b	k_s	k_s*
DTAB in NaBr; drop weight method (Tanaka and Ikeda, 1991)	-3.0	0.64	0.1	0.4
DDAC in NaCl by Sudan Red B solubilization; uv (Ozeki and Ikeda, 1985)	-2.9	0.58	0.2	0.4
DDAC in NaCl by Light Scattering (Ikeda, 1984)	-2.7	0.48	0.2	0.4
DDAC in NaCl by Viscosity (Ozeki and Ikeda, 1985)	-2.8	0.52	0.1	0.4
DDAC in NaCl by Surface Tensiometry (Ozeki and Ikeda, 1980)	-2.9	0.58	0.2	0.4
12,12,12-trifluorododecyltrimethyl ammonium fluoride in KF by FMR (Muller, 1972)	-1.8	0.39	0.3	0.4

for k_s, which are reasonable; the theoretical value for k_s is 0.4 when calculated from the group additivity principle.

It should also be mentioned that Chan (1993) and Mukerjee (1993) have proposed an additional term to Eq. [VI-3] to account for interfacial free energy effects which may or may not be significant, depending on the system under study. Evaluation of the Chan-Mukerjee extended model, however, requires estimates for area per monomer at the micellar interface, which is not readily obtained, and βM, which represents the amount by which the interfacial tension of the micelle-aqueous electrolyte changes as the molarity, M, of the electrolyte solution changes. Evaluating the model using estimates for area and β of 100 $Å^2$ and 3, respectively, did not have a significant effect on k_s in the case of Compound A.

A few other findings from this study are summarized below.

VI-F. Area Per Molecule at the Interface

The area per molecule at the air/aqueous interface, from Eq. [IV-3], was found to be more sensitive to changes in pH than to changes in temperature or buffer concentration/ionic strength (Table VI-4). Experimentally, the mean A_m, averaged over all temperatures and buffer concentrations studied, was found to be 62.4±9 $Å^2$ (N=38) at pH 7, and 88.3±13 $Å^2$ (N=6) at pH 10. For comparison, the area per molecule of sodium decyl sulfate is 75.5 $Å^2$ (Chan, 1985).

Table VI-4 Area per molecule at the interface, in $Å^2$/molecule, for Compound A

Buffer[a]	μ	$[K^+]^c$	22°C	30°C	40°C	50°C	60°C	75°C
0.05 M, pH 7	0.11	0.08	54	--	--	53	68	--
0.1 M, pH 7	0.22	0.16	72	60	59	76	56	71
0.2 M, pH 7	0.44	0.32	62	56	62	63	55	64
			58[d]	--	--	--	--	--
0.4 M, pH 7	0.89	0.65	67	60	68	71	63	78
0.6 M, pH 7	1.2	0.97	64	--	--	68	62	--
0.8 M, pH 7	1.5	1.29	66	--	--	--	--	--
1.0 M, pH 7	2.23	1.62	51	--	--	--	--	--
0.2 M, pH 7	2.23[b]	2.11	58	--	--	--	--	--
0.4 M, pH 7	2.23[b]	1.99	52	--	--	--	--	--
0.8 M, pH 7	2.23[b]	1.86	99	--	--	--	--	--
0.1 M, pH 7	0.89[b]	0.83	--	--	65	65	55	77
0.2 M, pH 7	0.89[b]	0.77	--	--	62	66	73	--
0.1 M, pH 10	0.3	0.2	--	--	75	--	--	88
0.2 M, pH 10	0.6	0.4	--	--	74	--	--	96
0.4 M, pH 10	1.2	0.8	--	--	91	--	--	106
0.2% EDTA, pH 7	0.06	0.015	--	--	--	63	--	--

[a] Molarity of KH_2PO_4 (in pH 7 KH_2PO_4/KOH), or K_2HPO_4 (in pH 10 K_2HPO_4/KOH)
[b] ionic strength adjusted with KCl
[c] counterion concentration
[d] contains 0.005 M (0.2%) EDTA; all others at 22°C do not, however all buffers at higher temperatures do

The expected area of the fully extended drug molecule A may be approximated (Rosen) by adding areas occupied by CH_2 groups (nine at ca. 7Å^2 each), phenyl groups (two at ca. 25 Å^2 each) and a branch point (+20%); doing so results in a value of 136 Å^2. That this number is larger than the A_m found experimentally at either pH 7 or pH 10 suggests the drug molecule at these pH's is not lying flat at the interface, but rather, that portions of it extend into the aqueous or air environment. It should be noted that the area per molecule at the air/solution interface is not necessarily the same as the area per molecule at the micellar interface.

The A_m values are of expected and reasonable magnitudes, since at pH 7 the compound is not as fully ionized as at pH 10; this would result in more molecules of A crowding the air/solution interface at pH 7, hence a lower area per molecule than at pH 10. This is in accord with the surface pressure measurements.

VI-G. Surface Pressure

The surface pressure measurements, calculated from Eq. [IV-1], indicate that the compound has a greater ability to lower the surface tension of the buffer (i.e. is more surface active) at pH 7 than at pH 10 (Figure VI-4) since it is ionized to a lesser extent at pH 7.

Although not very sensitive to changes in temperature, the surface pressure was more sensitive to changes in temperature at pH 7 than at 10 owing to the fact that the pK_a, and hence the degree of

ionization, changes with temperature (Figure VI-5), and these changes will be greater at a pH near the pK_a.

VI-H. Effect of Temperature on the cmc

The effect of temperature on the cmc in the presence of a given buffer was found to be small, although an upward trend with increasing temperature was noted in all cases, as may be seen in Figure VI-6. Although for some surfactants in water, the cmc vs temperature plot exhibits a broad minimum, it is not uncommon to observe only an increasing trend as found herein.

VI-I. Effect of EDTA on the cmc Value

Cmc values determined in a 0.2 M pH 7 phosphate buffer with and without 0.2% EDTA disodium salt were only slightly different, 0.86 vs 0.82 mM as may be seen from Table VI-1; and, in a control solution of EDTA (without phosphate buffer), the cmc of A was found to be of the same order of magnitude as the cmc determined in water: in an unbuffered 0.2% EDTA solution (adjusted to pH 7 with KOH) at 50°C, the cmc was found to be 7.2 mM, compared to 8.8 mM in water at 22°C. This again reflects the fact that the counterion concentration is that which affect the cmc, and this is very low in a pH 7 0.2% EDTA.2Na solution (ca. 0.015, Table VI-1).

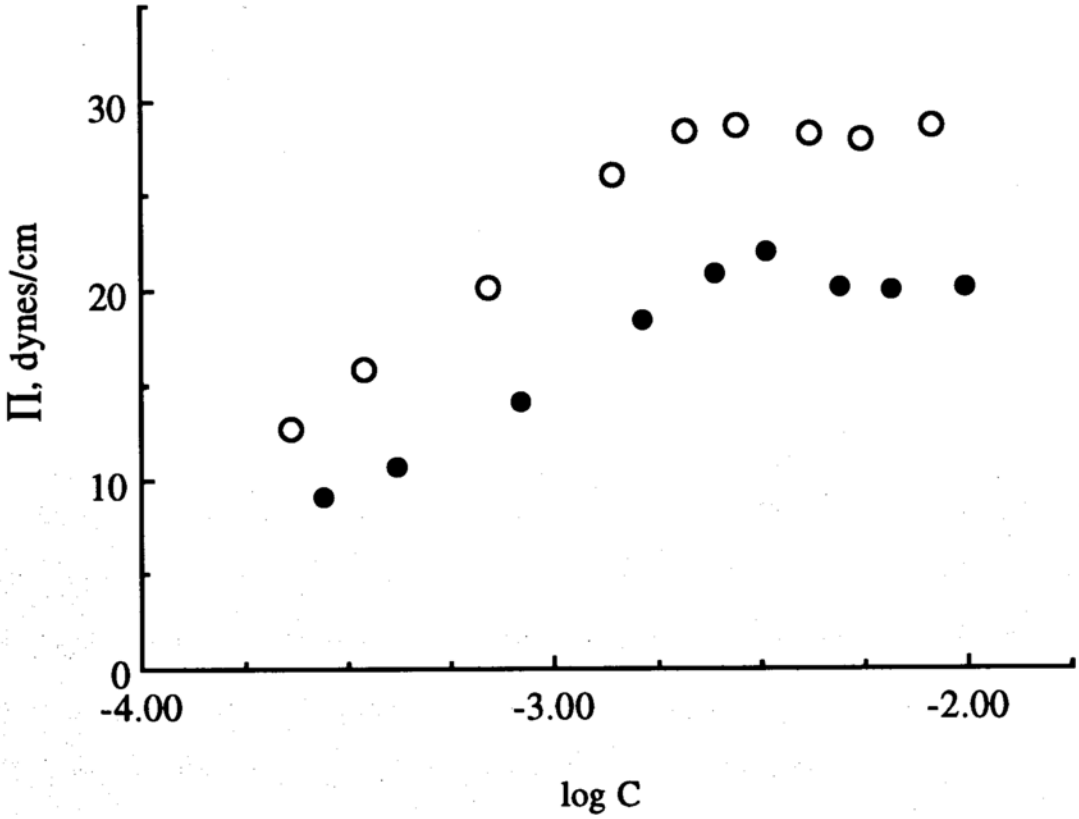

Figure VI-4 Surface Pressure*vs* log(molar concentration of A) in 0.1 M pH 7 KH_2PO_4/KOH (open circle) and 0.1 M pH 10 K_2HPO_4/KOH (filled circle) at 40°C.

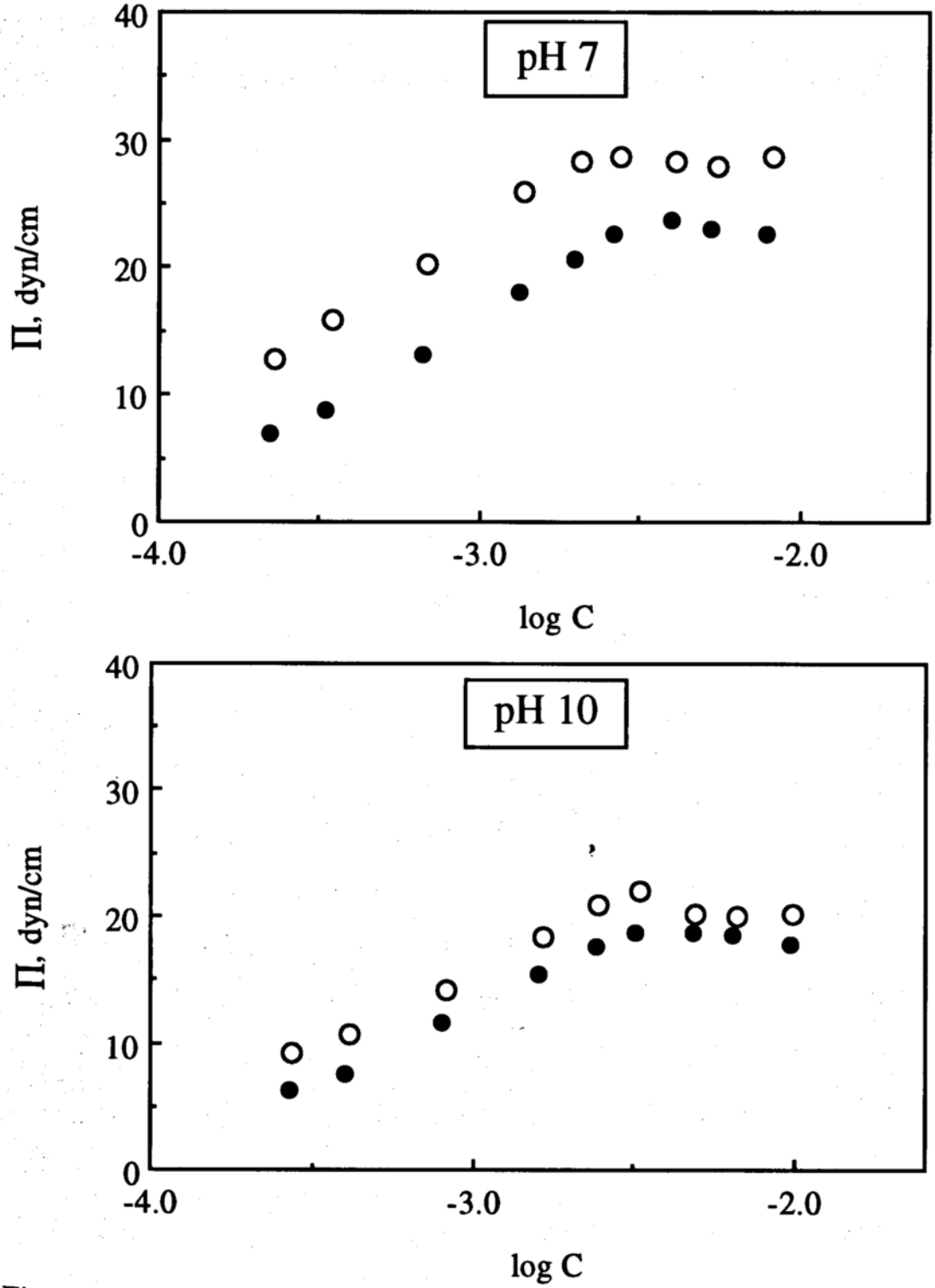

Figure VI-5 Surface Pressure *vs* log(molar concentration of A) in 0.1 M pH 7 KH_2PO_4/KOH and 0.1 M pH 10 K_2HPO_4/KOH at 40°C (open circle) and 75°C (filled circle).

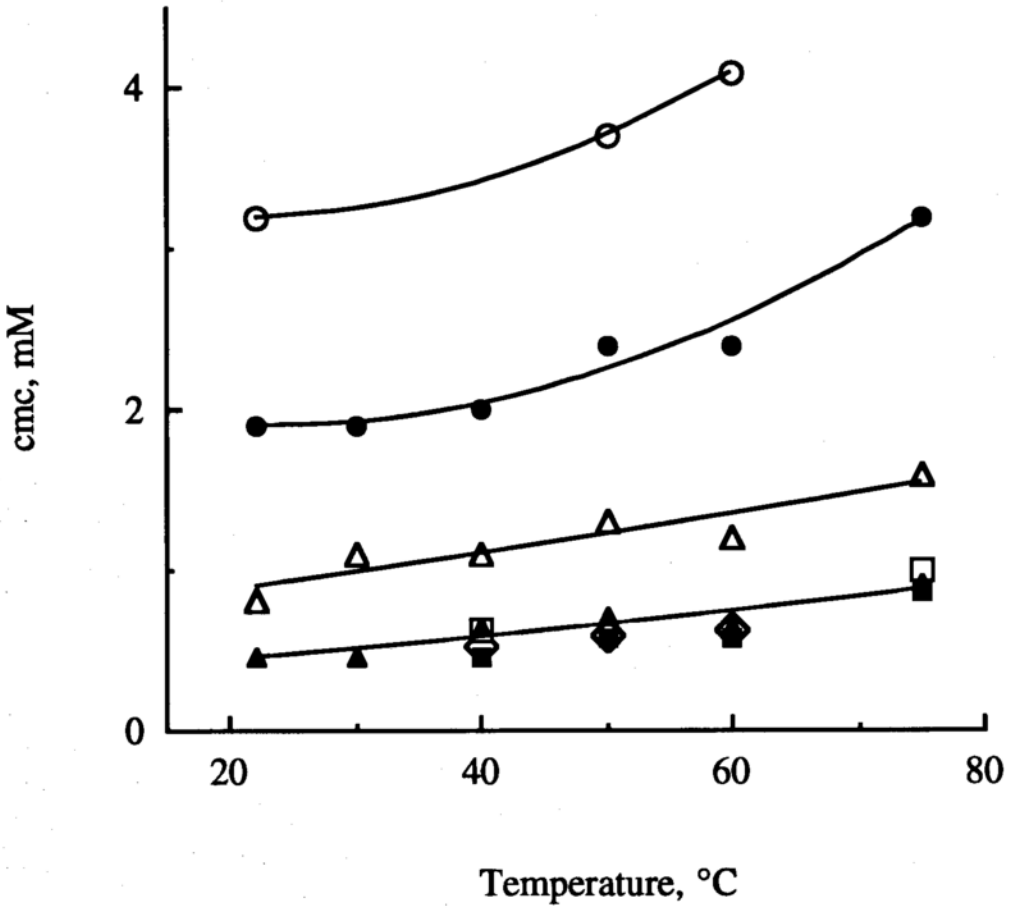

Figure VI-6 Cmc of A as a function of temperature in phosphate buffers of indicated molarity; data from Table VI-1. Except at 22°C, the buffers are also 0.005 M in EDTA disodium salt (0.2%). Curves are drawn to guide the eye.

0.05 M pH 7 (open circle); 0.1 M pH 7 (filled circle); 0.2 M pH 7 (open triangle); 0.4 M pH 7 (filled triangle); 0.4 M pH 10 (open square); 0.1 M pH 7, μ = 0.89 with KCl (filled square); 0.2 M pH 7, μ = 0.89 with KCl (diamond).

VI-J. Surface Tension of Buffers Without Drug

The surface tensions of the buffers used were determined in order to calculate surface pressure, but also to ensure that they did not contain any surface tension lowering contaminants. These surface tensions were found to be only slightly higher than that of water at the same temperature, and to follow the same trends as those in water, that is, to decrease in a linear fashion with temperature (Figure VI-7). In fact, when the published (CRC) surface tension (ST) data for water at 20, 30, 40, 50, and 60°C are treated by linear regression, the equation for the line is

$$ST = 76.06 - 0.16T \qquad r^2 = 0.999 \qquad \text{(VI-6)}$$

where T is absolute temperature. This compares well with the equation obtained by regressing the mean of the buffer data at each temperature on temperature:

$$ST = 76.40 - 0.15T \qquad r^2 = 0.990 \qquad \text{(VI-7)}$$

All the data shown in Figure VI-7 fall within 2% of this mean regression line.

The surface tension of the buffers was also found to increase in a linear fashion with buffer molarity, hence, counterion concentration, which is self-consistent (Figure VI-8). Similar trends have been reported for other salts (Gurovich, Jasper).

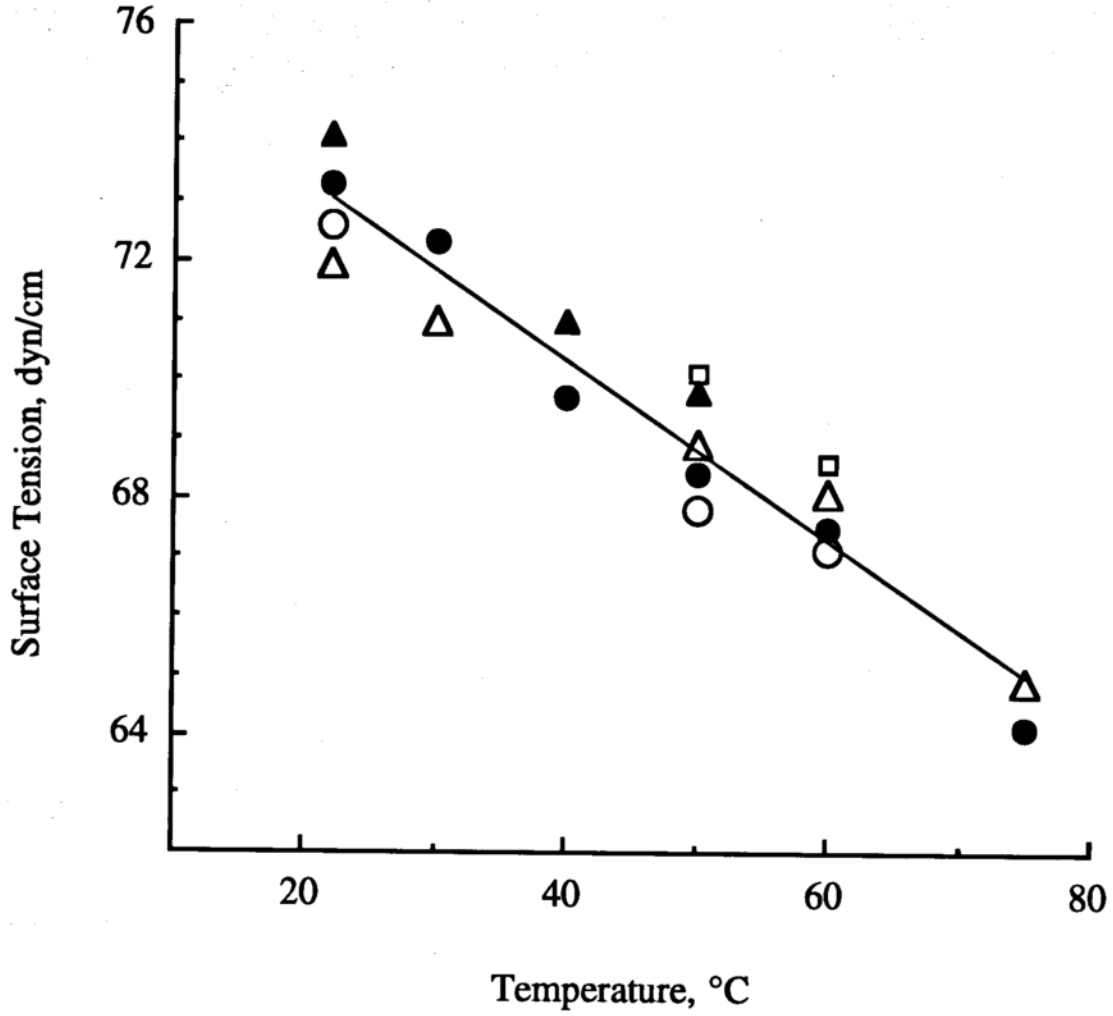

Figure VI-7 Surface tension, γ_o, of pH 7 KH_2PO_4/KOH phosphate buffers (no drug added) as a function of temperature: 0.05 M (open circle), 0.1 M (filled circle), 0.2 M (open triangle), 0.4 M (filled triangle), 0.6 M (open square). The regression line is drawn through the mean of the data at each temperature.

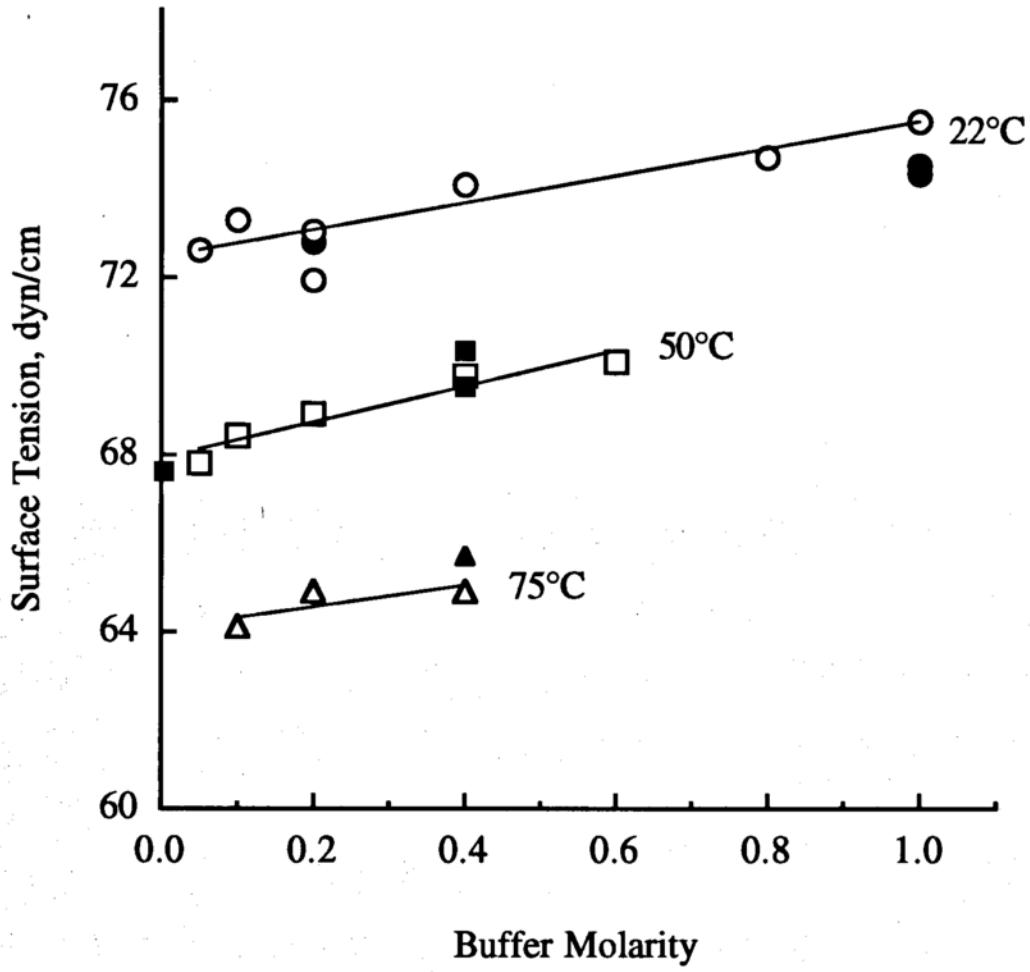

Figure VI-8 Surface tension, γ_o, of pH 7 phosphate buffers (no drug added) as a function of buffer molarity at indicated temperatures. Filled symbols represent surface tensions of buffers of different molarity adjusted to the same ionic strength as the nominal buffers, 0.4 or 1.0 M buffer; except the filled square near 0 buffer molarity which represents the surface tension of a pH 7 0.2% EDTA.2Na solution (0.005 M) at 50°C. For the corresponding $[K^+]$, see Table VI-1. Except at 22°C, the buffers are also 0.005 M in EDTA.2Na (0.2%). The slope of the line at 22°C is 3.04, which is an approximation for β in βM (see Section VI-E).

VI-K. Effect of Ionic Strength

As mentioned above, cmc values determined in buffers of different molarity but adjusted to the same ionic strength with KCl were found to be nearly the same. Although this appears to be an ionic strength effect, it is well-documented that the cmc of an ionic surfactant is sensitive to the concentration of ions of opposite charge, and, as Table V1-1 shows, buffers adjusted to the same ionic strength are similar in counterion concentration, so that, for the most part, slight differences in the cmc values are consistent with slight differences in counterion concentration (Figures V-2, VI-6).

VI-L. Is there a structural change in the micelle? A geometrical argument.

According to Israelachvili, it is possible, based on geometrical considerations, to predict whether or not a structure will assemble into spherical vs non-spherical micelles, or into vesicles, bilayers or inverted structures. The method outlined in his text is applied here to the drug A.

First, a critical length, l_c, is calculated, which represents a maximum effective length that a chain can assume, which is less than the fully extended length, l_{max}:

$$l_c \leq l_{max} \approx (0.154 + 0.1265x) \text{ nm} \qquad \text{(VI-8)}$$

where x is the number of carbon atoms in a saturated hydrocarbon chain. For drug A, the longest chain of continuous carbon atoms (equating sulfur to carbon) will be taken as x, and the reader can verify from Figure I-1, that it is 21 (6 from the benzene ring, 8 from the alkyl chain, 2 from the benzene ring, 5 from the thiocarboxy chain). This gives an l_c value of 2.8105 nm. The volume occupied by a chain of 21 carbons is given by

$$v \approx (27.4 + 26.9x) \times 10^{-3} \text{ nm}^3 \qquad \text{(VI-9)}$$

which solves to 0.5923 nm^3. As mentioned in the text, the ratio of v/l_c is constant, and is equal to 0.21. The shape of the aggregate will depend on the magnitude of the ratio $\frac{v}{A_m l_c}$, as follows:

$$\frac{v}{A_m l_c} < \frac{1}{3}, \text{ or, for drug A: } A_m > 63 \text{ Å}^2 \quad \text{spherical} \qquad \text{(VI-10)}$$

$$\frac{1}{3} < \frac{v}{A_m l_c} < \frac{1}{2}, \text{ or, } \quad 42 \text{ Å}^2 < A_m < 63 \text{ Å}^2 \quad \text{non-spherical} \qquad \text{(VI-11)}$$

$$\frac{1}{2} < \frac{v}{A_m l_c} < 1, \text{ or, } \quad 21 \text{ Å}^2 < A_m < 42 \text{ Å}^2 \quad \text{vesicles or bilayers} \qquad \text{(VI-12)}$$

$$\frac{v}{A_m l_c} > 1, \text{ or, } \quad A_m < 21 \text{ Å}^2 \quad \text{inverted} \qquad \text{(VI-13)}$$

where A_m is the area per molecule at the interface, from section

VI-F.

Accordingly, then, for drug A, at pH 7, where A_m was found to be 62.4±9 $Å^2$, it is possible that under certain conditions of temperature and counterion concentration (Table VI-4)[8], a sphere-to-rod transition may occur; at pH 10 on the other hand, where A_m was found to be 88.3±13, it is more likely that the drug aggregates into spherical micelles. Such a structural change may well account for the differences observed in the kinetics between pH 7 and 8, if one considers that the decomposing species somehow interacts with the micelle or the Stern layer surrounding the micelle (the double layer is sometimes referred to as the reaction volume in micellar catalysis reactions; for example, a higher charge density of H^+ would be found in the Stern layer than in the bulk, leading to catalysis if H^+ is involved in the reaction). A non-spherical micelle may structurally hinder or help a reaction, depending on what it the reaction is. A worm-like micelle with a tertiary structure may structurally "bury" some of the reacting species, either the dimer or the H^+, leading to a decrease in rate, analogous to proteins with buried amino acids which are not prone to reaction.

Also according to the Israelachvili text, an aggregation number may be calculated from geometrical considerations as follows. The radius, R, of the micelle may be calculated as

---

[8] Please note that due to the technical difficulties associated with obtaining surface tension data at high temperatures, the scatter and lack of obvious trends (other than pH) in the A_m values in Table VI-4 is most likely due to experimental error rather than a lack of a trend, say, with increasing counterion concentration or temperature; such trends have been reported (Rosen).

$$R = \frac{3v}{A_m} \qquad \text{(VI-14)}$$

and the aggregation number, N, may be calculated as

$$N = \frac{4\Pi R^2}{A_m} \qquad \text{(VI-15)}$$

The standard deviation, σ, for N is usually between $\sqrt{N}$ and $2\sqrt{N}$. From these equations, then, one obtains an R of 2.848 nm at pH 7 and 2.012 nm at pH 10, resulting in an aggregation number of 163 ± 26 at pH 7 but only 58 ± 15 at pH 10 (taking $\sigma/\sqrt{N}$ as 2, the worst case).

From geometrical considerations, in order for a sphere to form, R must be less than l_c, and one can see that this is not the case at pH 7, only at pH 10, consistent with the argument above. Because the cmc values are not greatly affected by pH or temperature, the cmc alone is insufficient as a predictor of whether or not the kinetics may be affected. One must also consider the surface pressure as well as the size and shape of the micelle; these are significantly affected by pH and temperature, and, the size and shape of the micelle may be affected by the salt concentration. Thus the kinetics may be different depending how far above the cmc one is. The higher one is above the cmc, the more nonspherical the micelle assembly may become, although some surfactants are known to maintain sphericity even at high salt or surfactant concentration.

Of course the previous argument rests on the assumption that $x = 21$. As a comparison, for sodium dodecyl sulfate, with $x = 12$, N is found experimentally to be 74. The volume is then 0.3502 nm^3, A_m is 57 $Å^2$, R is 1.84, and l_c is 1.67 nm, resulting in a ratio $\frac{v}{A_m l_c}$ of 0.37 which suggests non-spherical micelles.

VI-M. General Comments About the Study

At pH 10, the surface tension values above the cmc were slightly higher than at pH 7, and, plots of surface tension vs log C showed a slight minimum at the cmc (plots not shown; data from Appendix B). At pH 7, a minimum was occasionally observed, but no pattern was noticed as to its occurrence. In water and in 0.2% EDTA at pH 7 a slight minimum was also observed. In those cases where a minimum was present, the intersection of lines about the minimum was taken as the cmc.

Ionization effects or a trace basic impurity may be responsible for the observed minimum; the drug was not recrystallized, however, because it was desired to study the compound in the same form as in the kinetic studies which had been previously done. Furthermore, the drug was the S-enantiomer, and the drug company supplying the compound had not revealed details as to its isolation, only that great care had been taken to avoid the presence of trace metals; HPLC analysis showed 99.8% of the area under a single peak at 215 nm, suggesting that the drug as received was of very high purity.

VI-N. Error Analysis for cmc Measurements

Owing to the logarithmic nature of the x-axis, the error in the cmc cannot be stated as being for example ±2% of the cmc, because it is calculated from the intersection of two lines, one being nearly parallel to the logarithmic x-axis, the other running as a negative slope. For example, to say that the cmc is 6.16 mM ± 2% would imply a range of 6.04 - 6.28 mM, or 2.94 - 3.06 mg/mL; if instead, one assumes, more appropriately, that the error is ±2% of *log* cmc, these ranges widen considerably to 5.57-6.82 mM, or 2.71-3.32 mg/mL.

Therefore in Table VI-4 the 1, 2, 3, and 5% error in estimating log C at the intersection of the linear portions of the ST vs log c plots is determined and converted to concentration in order to get an idea of the magnitude of the error involved in cmc determinations. Of course, it is noted that the cmc does not occur at a discrete concentration but over a range.

Table VI-4 Estimate of error in cmc determinations.

Let the cmc be 3, 0.3, or 0.03 mg/mL, or 6.16, 0.616, or 0.0616 mM. On a log scale, these molar concentrations would be -2.21, -3.21, and -4.21; a ±2% error in the cmc would be -2.21 ±0.044, -3.21 ± 0.064, and -4.21 ±0.084, respectively. For comparison, the cmc range is calculated below if instead the range is determined at ± 1, 2, 3, and 5% of log cmc. Results are given in mg/mL; to convert to mM of A, divide by 486.6, the molecular weight.

	cmc		
Error	3 mg/mL	0.3 mg/mL	0.03 mg/mL
1%	2.8-3.2	0.28-0.32	0.027-0.033
2%	2.7-3.3	0.26-0.35	0.025-0.036
3%	2.6-3.5	0.24-0.37	0.022-0.040
5%	2.3-3.9	0.21-0.43	0.018-0.049

CHAPTER VII. RESULTS AND DISCUSSION: OXIDATION STUDIES OF THE MODEL COMPOUND IN THE PRESENCE OF TRACE METALS

VII-A. General Discussion

The structures of A and its major degradation products, the sulfoxide, B, and the cinnamate, C, are shown in Figure I-1. In the general discussion below, B and C and other compounds in the degradation will be referred to simply as Products.

For oxygen sensitive drugs such as A it is nearly impossible to rationally assess kinetic parameters without knowledge of the effect of electrolytes (and other solutes) on the solubility (partitioning) of oxygen in water. Published literature results (Khomutov) suggest that oxygen solubility is sensitive to both electrolyte identity and molarity. At high ionic strengths, some kinetic effects also tend to be specific to the electrolyte concerned (Lewis). These effects may be pronounced at elevated temperatures.

What complicates the present picture is that the solubility of oxygen may be enhanced by the presence of drug micelles, but presumably, any oxygen solubilized by the hydrophobic core of the micelle would be unavailable for reaction with the sulfur group, since the sulfur is associated with the head of the monomer and would lie at the periphery or interface of the micelle. Therefore, in the presence of micelles, the oxygen in solution available for reaction

would be in equilibrium with oxygen solubilized in the hydrocarbon core of the micelle:

$$[O_2]_{micelle} \rightleftharpoons [O_2]_{soln} \qquad \text{(VII-1)}$$

and

$$[O_2]_{soln} = K_{free}[O_2]_{micelle} \qquad \text{(VII-2)}$$

Now, the concentration of oxygen dissolved in *dilute* solution is governed by Henry's Law,

$$[O_2]_{soln} = K_H P_{O_2} \qquad \text{(VII-3)}$$

where K_H is the Henry's law constant, and P_{O_2} is oxygen pressure over the solution. Assuming that atomic rather than molecular oxygen is the reactive species, the concentration in dilute solution available for reaction would be

$$[O]_{soln} = (K_H P_{O_2})^{0.5} \qquad \text{(VII-4)}$$

That is, although the total amount of oxygen dissolved may be greater in solutions containing micelles, ultimately, the amount available for reaction remains the same as in a solution without micelles, because, in dilute solution, the non-solubilized amount is governed solely by the Henry's law constant. Thus the equilibrium constant K_{free} may be ignored. It is possible that the oxygen solubilized by the micelle might interact with the hydrocarbon chains

to form alkene products, but such reactions usually require more vigorous conditions (Trost).

If salt such as buffer is present, then the concentration of oxygen in solution is further changed as predicted by the Setchenow equation (Setchenow),

$$\log \frac{[O_{2,H_2O}]}{[O_{2,H_20+salt}]} = k_s C_s \qquad \text{(VII-5)}$$

where the solubility of gas in *electrolyte* solutions is governed by the temperature-dependent salting out coefficient, k_s, and the molar concentration of salt, C_s.

It is recalled that the compound in solution is prone to oxidation by the following (stoichiometric) scheme:

$$A + O_{2(soln)} \longrightarrow Products \qquad \text{(VII-6)}$$

and may be prone to non-oxidative decomposition to not necessarily the same products by a scheme such as:

$$A + H_2O \longrightarrow Products \qquad \text{(VII-7)}$$

or simply

$$A \longrightarrow Products \qquad \text{(VII-8)}$$

In the case of argon sparging, it would be scheme VII-7 or 8 which would apply, and it is noted that these samples stay colorless and develop a strong rotten egg odor, most likely due to a volatile sulfur-containing product, other than sulfoxide, formed in addition to the cinnamic acid analog, since the cinnamate is sulfur-free. On the other hand, samples exposed to oxygen or air discolor but do not develop such a strong smell until the reaction is well advanced, if at all.

In Eq. [VII-6] it is not known (and has not been elucidated) whether it is atomic or molecular oxygen which is included in the prime oxidation step. Assuming the former, and knowing that the oxygen concentration in solution is affected by salt as described above, the overall rate equation in dilute solution describing the rate of the disappearance of A with time is given by

$$dA / dt = -k_1[A]\sqrt{(K_H P_{O_2})} \qquad \text{(VII-9)}$$

and in salt solution

$$dA / dt = -k_1[A]\sqrt{[O]^2{}_{H_2O} - k_s C_s} \qquad \text{(VII-10)}$$

or

$$dA / dt = -k_1[A]\sqrt{K_H P_{O_2} - k_s C_s} \qquad \text{(VII-11)}$$

or more simply

$$dA / dt = \psi[A] \qquad \text{(VII-12)}$$

where now ψ is a pseudo-first order reaction rate constant, assuming excess oxygen is present, and intentionally ignoring intermediate steps, such as proton abstraction and radical formation (e.g. hydroxyl, peroxy, superoxy, or S···S radicals).

Keeping in mind that neither the Henry's law constant nor the salting-out constant may adhere to an Arrhenius type of relation (Franchini, 1993), as illustrated in Figure VII-1 redrawn from the Master's Thesis, the question becomes, what is the temperature dependence of ψ? Qualitatively, a drug in solution in an ampul, which is a totally closed system, may experience two opposite effects as temperature is raised:

(a) The observed rate constant for the reaction would increase, presumably by an Arrhenius relation.

(b) The oxygen in solution would decrease based on the temperature dependence of the Henry's law constant and the salting-out constant.

(c) There may be a diffusional component that would affect the oxidation.

If Eq. [VII-6] were obeyed, then, quantitatively, in aqueous solution,

$$\ln \psi = -\ln k_1 + \ln[O_2] = -\ln k_1 + \ln(KP_{O_2}) = \frac{E_a}{RT} + \ln(\phi(T)) - \alpha \qquad \text{(VII-13)}$$

where $[P_{O_2}]$ is experimentally determinable and a part of α, and the temperature-dependent K = ø(T). Under given conditions, α can be placed in the first term of the equation. In salt solution Eq. [VII-13] would become

$$\ln \psi = -\ln k_1 + \ln[O_2] \qquad \text{(VII-14)}$$

$$= -\ln[k_1] + \frac{1}{2}\left(\frac{\ln(K_H P_{O_2} - k_s C_s)}{2.303}\right) \qquad \text{(VII-15)}$$

$$= \frac{E_a}{RT} + \frac{\ln([\phi(T)]P_{O_2} - [\phi_2(T)]C_s)}{4.303} - \alpha \qquad \text{(VII-16)}$$

where $k_s = \phi_2(T)$.

Total oxygen concentration in solution may be estimated from the data shown in Figure VII-1 (Franchini, 1993), however, caution should be exercised when extrapolating beyond the 0-30°C experimental range in the figure. It is not guaranteed that the trends in Figure VII-1 will be obeyed at higher temperatures, or in salts other than NaCl. The limited data which have been published regarding oxygen concentration in salt solutions at temperatures above 30°C indicate that the nature of the salt as well as the temperature affect the solubility of gases, and for instance, with Li salts, a gas may be salted in at higher temperatures, rather than being salted out, as discussed in the Master's Thesis.

Since the studies reported herein were not done manometrically, nor at temperatures for which either K_H or k_s are

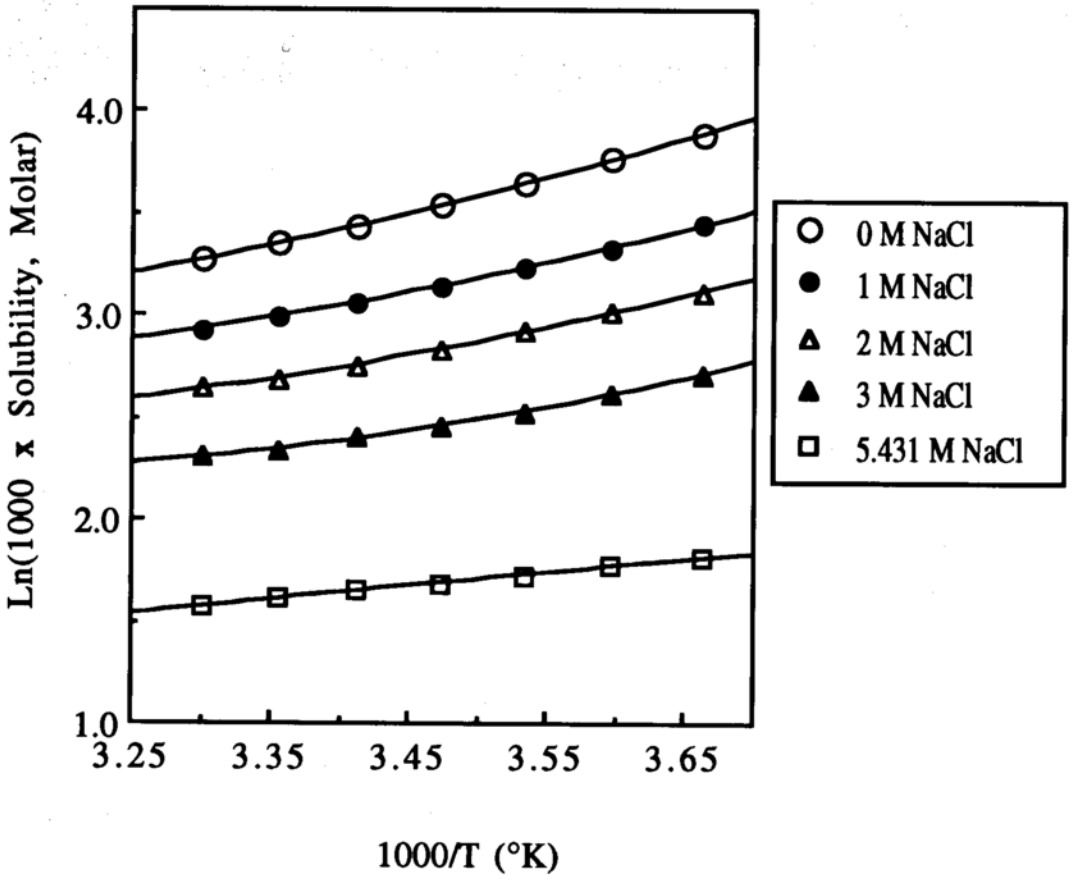

Figure VII-1 Solubility of oxygen in H_20 and salt solutions between 0 and 30°C (in volume of gas reduced to 0°C and 1 atm., dissolved in one volume of solution when the partial gas pressure is 1 atm.); data from International Critical Tables.

known, no attempt has been made to solve for ψ, but the discussion is presented for further consideration. Even if these studies had been done manometrically, one would still have to conduct separate experiments in the presence and absence of drug at various concentrations of drug in order to determine the solubilizing effect of drug on oxygen concentration in solution, in addition to the effects of salt and temperature, but, as noted in the Master's Thesis, oxygen has not been found to be appreciably solubilized by detergent micelles.

Because it is technically extremely difficult to accurately determine oxygen concentration in solution between room temperature and boiling, rather than determining the actual oxygen concentration or using manometry to determine oxygen consumption, the reaction was monitored by measuring the disappearance of A in samples sparged with argon (ca. 0% O_2), or oxygen (ca. 100% O_2), or, stored with an air headspace (ca. 22% O_2). This allowed the reaction to be run in separate vials for each time point, which is more a pharmaceutical application.

As will be demonstrated below, in the simplest case, the observed rate constants from samples sparged with oxygen or stored with air headspace should theoretically be a sum of the oxidation rate constant $k_1[O]$ and the elimination rate constant k_2. Since k_2 is obtained directly from the slope of the first-order plots of argon-sparged systems, $k_1[O]$ should be obtained by difference.

VII-B. The Autooxidation in Solution in the Presence of Trace Metals

The studies was carried out in the presence and in the absence of metal ions. The former case will be discussed first. Much of the text is from Franchini and Carstensen, *Int. J. Pharm.* **111**(1994)153-158.

Oxidation reactions are often affected by the presence of heavy metals, such as iron, which may act as catalysts; and, it has been suggested that phosphate buffers bind Fe(III) (Cher). Although the drug was manufactured in such a manner as to control for heavy metal contamination, the reagent grade buffers used in the kinetic studies were not so controlled, as generally one uses such dilute buffers (less than 0.2 M) that this is not of concern. Therefore, although trace metals were not intentionally introduced into the systems under study, the high concentration of buffer salts and KCl used in these kinetic studies may have been a source of trace metal, as evidenced by the fact that adding EDTA.2Na to buffers slowed the reaction considerably (Figure V-1). Without free trace metals the autooxidation reaction was inhibited or could not be initiated in the absence of light or chemical additives such as peroxide.

Generally, if less than 1% metal ions are in the system, then the catalytic effect is proportional to the concentration of metal ion, but with concentrations over 2%, the efficacy of the additive falls off, and the autooxidation rate becomes independent of metal concentration (Waters). Based on label specifications, it is conceivable that the concentration of trace metals present in the phosphate buffers used

was less than 1%, such that an increase in buffer molarity was accompanied by an increase in trace metal concentration, hence an increase in rate at pH 7.

The kinetics of oxidation of A in solution were investigated in buffers without EDTA.2Na in the Master's Thesis and are herein reinterpreted and a simple decomposition scheme proposed to which most of the data generated could be fitted. The fact that data generated at some buffer concentrations were not as well described by the scheme reflects the fact that in some samples, as decomposition progressed, the drug concentration shifted from being above the cmc to being below the cmc, and that there were different amounts of trace metal present depending on buffer concentration; in some buffers there was insufficient trace metal to effect the autocatalytic oxidation reaction. These subjects are dealt with in greater depth in subsequent sections.

VII-B-1. The Scheme

Characteristic decomposition curves generated from data reported in the Master's thesis are shown in Figure VII-2. It is noted that at 93°C the reaction pattern appears to be first order, whereas at lower temperatures the decomposition profile is a typical autooxidative S-shaped curve. Several conventional oxidation schemes were tried on the data, and the following scheme is one to which much, but not all, of the data fit:

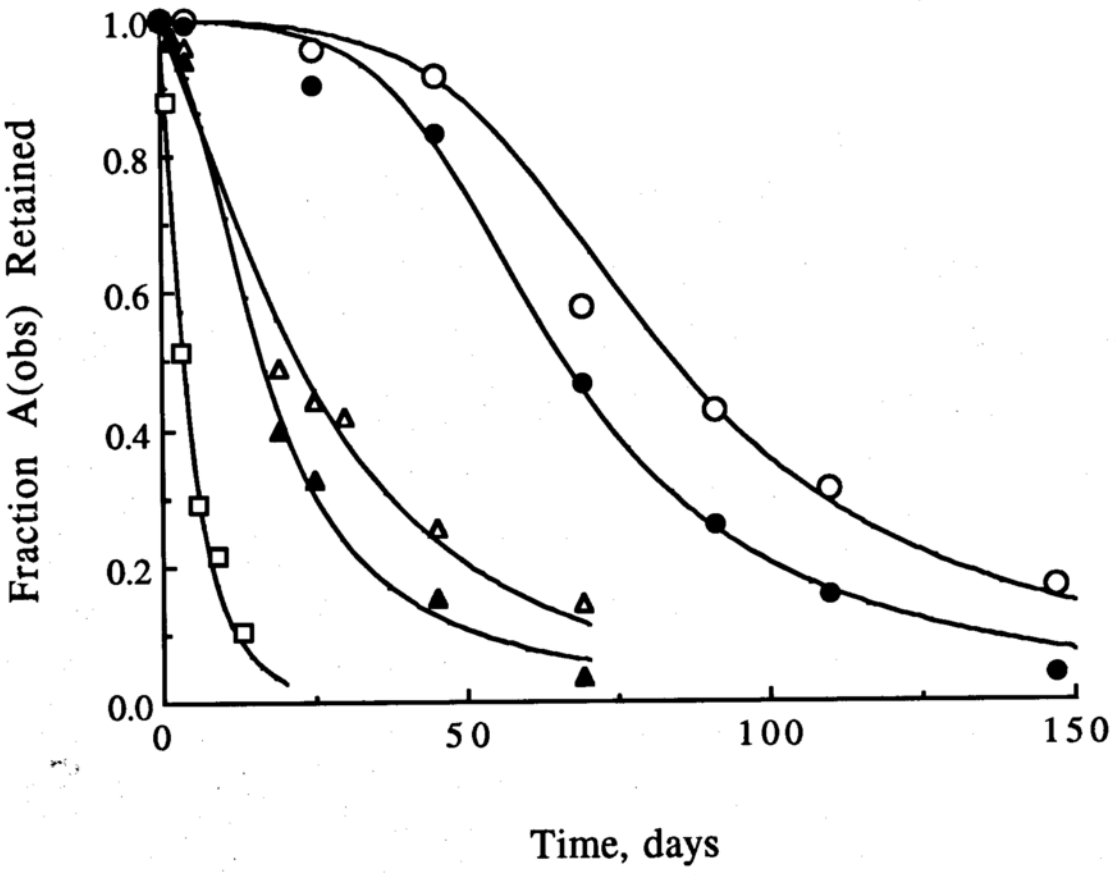

Figure VII-2 Decomposition data of a 0.2 mg/mL solution of A in pH 7 phosphate buffers of indicated molarity not adjusted for ionic strength (μ), and without EDTA: 60°C: 0.6 M (open circles), 0.8 M (filled circles); 75°C: 0.8 M (open triangles), 1.0 M (filled triangles); 93°C: 0.4 M (squares). Symbols: experimental data, i.e. $[A]_{obs}$ by HPLC; curves: numerical integration of Eq. [VII-33] using parameters given in Table VII-3a.

$$A + A \rightleftharpoons A_2 \qquad K = \frac{k_f}{k_r} = \frac{[A_2]}{[A]^2} \qquad \text{(VII-17)}$$

$$A_2 + O_2 \xrightarrow{k_1} B \qquad k_1' = k_1''[O_2] \qquad \text{(VII-18)}$$

$$A \xrightarrow{k_2} C \qquad \text{(VII-19)}$$

where A_2 is the dimer, K is the equilibrium (dimerization) constant, k_f and k_r are the forward and reverse rate constants, B represents the sulfoxide analog, C the cinnamic acid analog, k_1" is the autooxidation rate constant, k_2 is the elimination rate constant, and where it is assumed that $[O_2]$ is constant. The products B and C can undergo further reaction.

The scheme resembles those proposed for micellar catalysis in which the pseudo-phase model is invoked, as it has been shown to adequately describe the observed kinetics, in spite of the admitted thermodynamic inconsistencies in the pseudo-phase model. In the case reported here, the drug itself is both substrate and surface active agent. Rather than considering two phases, monomer and micelle, the scheme relies on a dimerization which has been shown to explain other anamolous behavior involving surface-active agents (Mukerjee, 1967). If the dimer is further in equilibrium with higher aggregates, this is ignored for the time being, but is dealt with in Chapter VIII. Trace metal catalysis is not explicitly listed in the scheme, nor are other intermediate steps such as hydrogen abstraction and free radical formation.

The shape of the time vs. concentration curve at a given temperature at pH 7 may reflect the competition between reactions VII-18 and 19, which will be influenced by the position of the equilibrium in VII-17. For example, at 93°C the predominant reaction is assumed to be degradation to the cinnamate, hence a first-order reaction, whereas at 60°C, the autooxidation is assumed to predominate, giving rise to the S-shaped curves. At a range of temperatures in between the decomposition is a combination of the two.

The change from the oxidation being the predominant reaction to being a secondary reaction is due to the decrease in oxygen concentration in solution at higher temperatures (Connors, 1986; Franchini, 1993) being more significant than the increase in the oxidation rate constant. That is, at higher temperatures the Henry's law equilibrium oxygen concentration decreases, and the term $k_1'=k_1''[O_2]$ may decrease since the decrease in $[O_2]$ may overpower the increase in k_1'. This dual behavior makes Arrhenius plots nonlinear over the entire temperature range, rather than showing a break in the curve where there is an isokinetic temperature (Ericksen). This precludes any type of Arrhenius extrapolation.

Ordinarily, it might not be surprising that extrapolation on occasion is not valid (as in the case of parallel reactions), but as has been hinted at elsewhere (Asker; Bamford; Brown; Carstensen, 1990; Connors, 1986; Kassem; Schroeter; Ventura) a series of factors affect the concentration/time profile of oxidation reactions in solution, and these change with temperature as is apparent in the present studies.

Note that in all cases in pH 7 phosphate buffers, as buffer molarity increases, so does ionic strength, as shown in Table VII-2. At pH 7, as buffer molarity hence ionic strength was increased, so too did the rate of decomposition. These buffers did not contain a metal chelating agent, such that the observed effect may have been due in part to trace metal catalysis. The fact remains however, that at pH 8, in most cases, a *decrease* in rate was observed as buffer concentration was increased. In the studies at pH 8, sufficient EDTA was added so that trace metal catalysis was not an issue. In both cases, adjusting the ionic strength to a common value negated the buffer effect in both cases. These points will be addressed again in the section on kinetic salt effects.

VII-B-2. Proof of the Non-Oxidative (Elimination) Pathway: Solid State Decomposition by DSC, and Anaerobic Solution Decomposition

The elimination (non-oxidative) pathway Eq. [VII-19] was subsequently proven to exist by two separate experiments, one by solid state degradation by DSC, and the other by solution degradation in argon-sparged systems.

Degradation in the solid state by DSC was accomplished by heating 9.76 mg of drug in a crimped aluminum solid sample pan from 25 to 280°C at 2°C, 5°C, or 10°C/min, followed by cooling to 25 at 40°C/min (Figure VII-3). The pan was then opened; the solid in pan was an off white-colored crystalline material with an odor of rotten egg. The solid could be immediately solubilized by mobile

Table VII-2 Calculated ionic strength, μ, of pH 7 phosphate buffers, KH_2PO_4/KOH without EDTA.2Na; and, observed rate constants obtained from the slopes of the first-order plots of kinetic data reported in the Master's Thesis which were generated at 93°C in these buffers. In the last four entries, the ionic strength, μ, has been adjusted to 2.2 with KCl.

Buffer Molarity	Calculated μ	k_{obs}, day^{-1}
0.01	0.02	0.088
0.05	0.11	0.096
0.05	0.11	0.068
0.10	0.22	0.107
0.20	0.45	0.112
0.40	0.89	0.153
0.40	0.89	0.174
0.60	1.3	0.220
0.60	1.3	0.243
0.80	1.8	0.307
1.0	2.2 (no KCl)	0.278
0.01	2.2	0.285
0.40	2.2	0.198
0.60	2.2	0.178
0.80	2.2	0.205

phase, which was then analyzed by HPLC. The chromatogram (Figure VII-4) revealed three main peaks, with most of the area under the peak corresponding to the cinnamate: intact drug, 10.7 area %; cinnamate, 87.0 area %; and an unknown peak eluting between the two, 2.3 area %. A peak corresponding to sulfoxide was absent in the chromatogram, as was the characteristic yellow color, suggesting that a direct degradation to the cinnamate was occurring.

It would seem evident that if the sulfoxide was formed but degraded immediately to the cinnamate, this may explain the absence of sulfoxide in the chromatogram. However, solution kinetic studies suggested that this transformation should occur very slowly.

In order to confirm this, anoxic samples were prepared (argon sparged) and monitored as a function of time. Unlike air or oxygen-containing samples, at 93°C in no case was a yellow color ever detected in the argon-sparged samples, nor a peak corresponding to sulfoxide. In addition, the argon-sparged samples developed a rotten egg odor identical to that of the DSC sample, suggesting formation of a volatile sulfide, perhaps that formed when the molecule is cleaved in two to form the cinnamate. By mass balance, this could be $SH\text{-}CH_2\text{-}CH_2\text{-}COOH$; or H_2S gas plus $CH_3\text{-}CH_2COOH$, or a mixture of SH-R products or disulfides[9], but no attempts were made to prove this. Rather, the cinnamate was monitored since it had an identifiable peak by HPLC. HPLC traces from samples sparged with

---

[9] If this were the case, then toxicity may be an issue should a company decide to stabilize the solution by excluding oxygen.

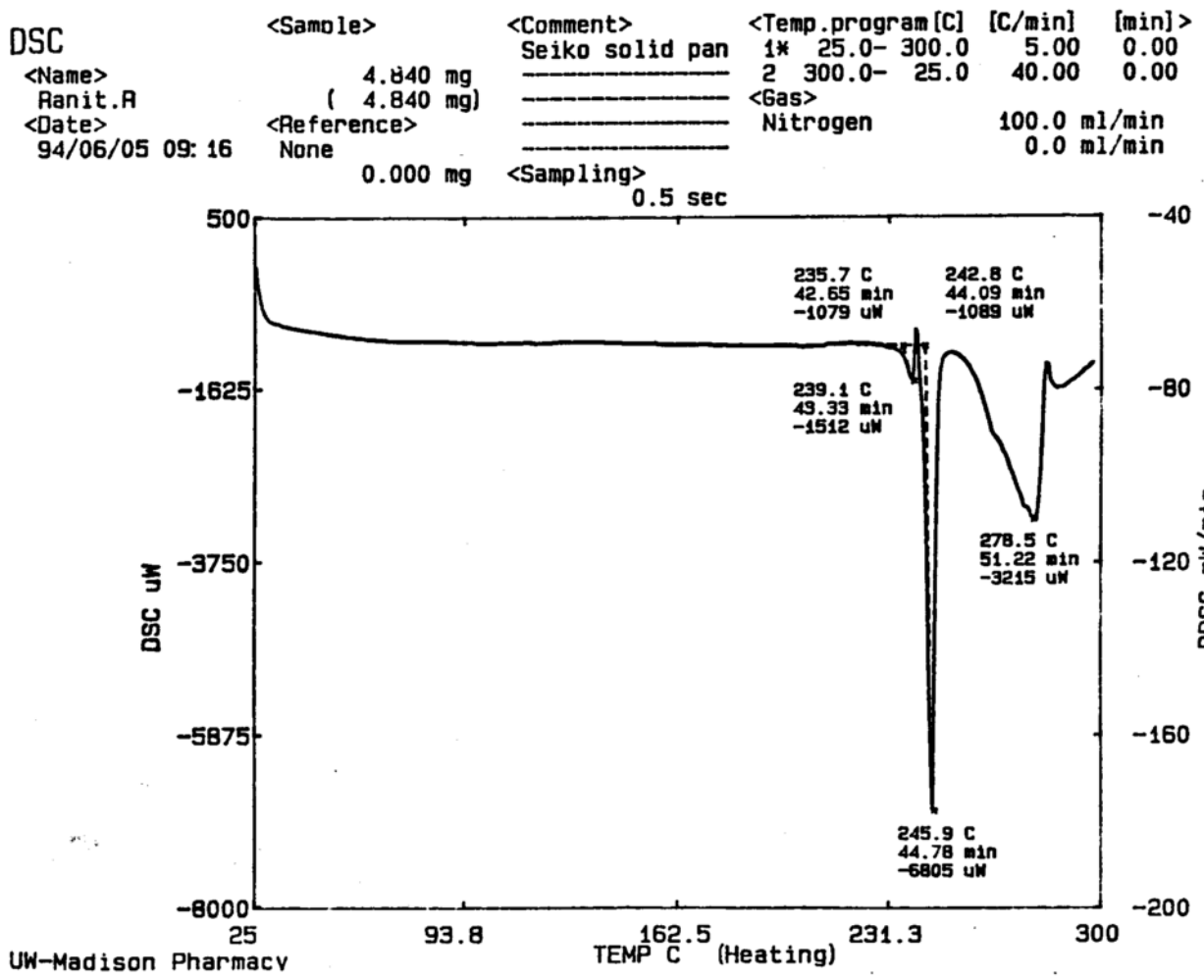

Figure VII-3 a) DSC thermogram of 9.76 mg of A heated in a crimped aluminum solid sample pan from 25 to 280°C at 5°C/min, followed by cooling to 25 at 40°C/min (cooling curve not shown).

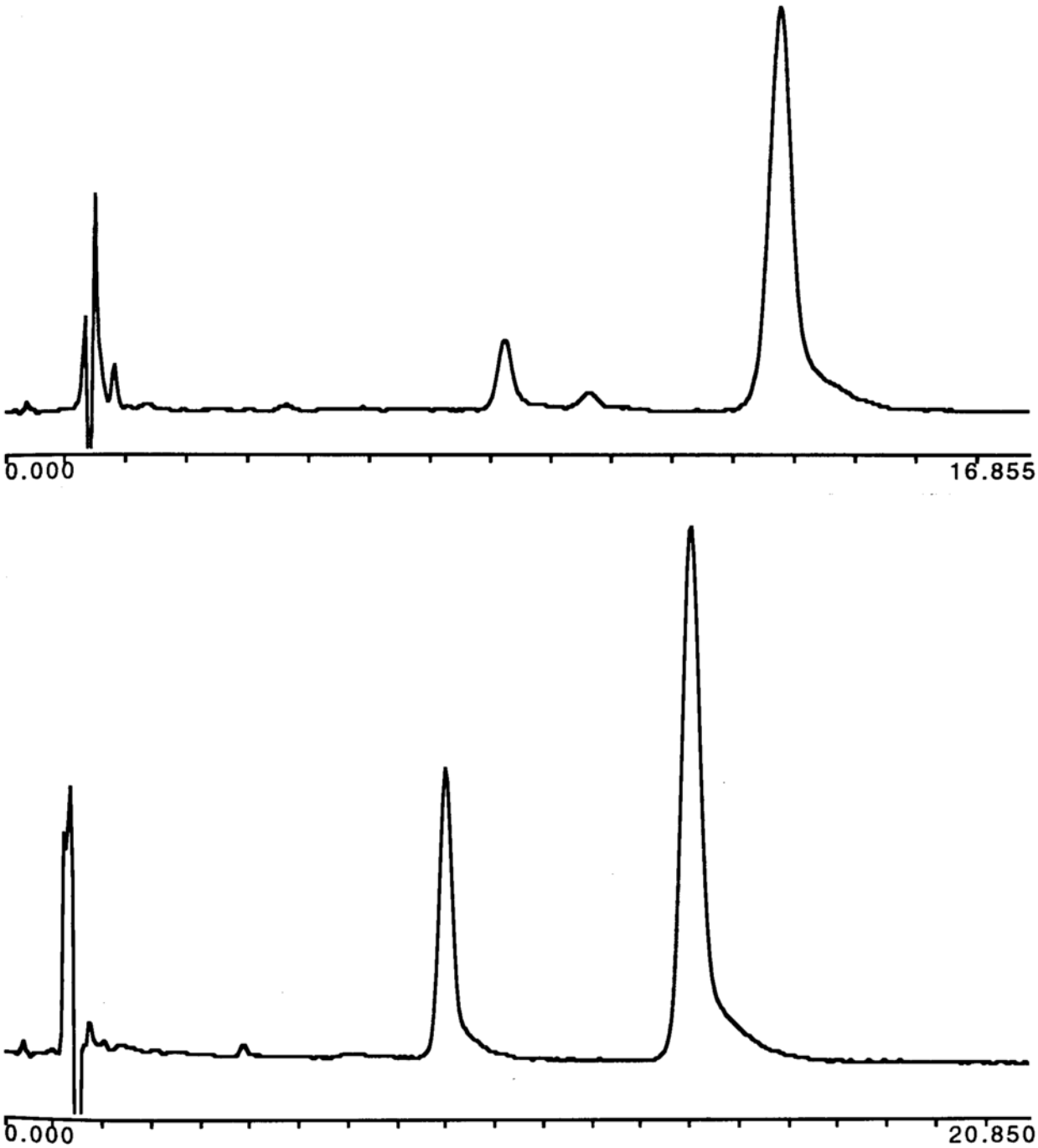

Figure VII-4 Top: HPLC chromatogram of solid A heated by DSC, as described in Figure VII-3. Bottom: Drug stored in 0.4 Mμ pH 7 buffer (with EDTA.2Na) for 162 days at 93°C, argon-sparged, 25.7% A retained. In both chromatograms, the two largest peaks after the void volume correspond to the parent and cinnamate analog. The unknown peak eluting between the two in the top trace was noticeably absent from most sample chromatograms.

argon, O_2, or stored with air headspace are shown in Figures VII-4, IV-3 and 4.

It should be noted that these two experiments were carried out at a time subsequent to when the scheme was proposed; they were carried out to test the validity of the scheme, and the results obtained were quite satisfying, as they confirmed the possibility of direct decomposition to the cinnamic acid analog. The results from the argon-sparged samples are further discussed in subsequent sections.

VII-B-3. Equations Describing the Scheme for Decomposition of A in the Presence of Trace Metals

The quantity monitored by HPLC is

$$[A]_{obs} = [A] + 2[A_2] \qquad \text{(VII-20)}$$

$$= [A] + 2K[A]^2 \qquad \text{(VII-21)}$$

and the rate equation describing the change in $[A_{obs}]$ with time is

$$d[A]_{obs}/dt = d[A]/dt + 2\ d[A_2]/dt. \qquad \text{(VII-22)}$$

where the rate equation for the disappearance of monomeric A is:

$$d[A]/dt = -k_f[A]^2 + k_r[A_2] - k_2[A] \qquad \text{(VII-23)}$$

and that describing the rate of disappearance of dimer is

$$d[A_2]/dt = k_f[A]^2 - k_r[A_2] - k_1'[A_2] \qquad \text{(VII-24)}$$

Inserting Eq. [VII-23] and [VII-24] into [VII-22], and rearranging gives

$$d[A]_{obs}/dt = k_f[A]^2 - k_2[A] - [A_2](k_r + 2k_1') \qquad \text{(VII-25)}$$

Since $A_2 = K[A]^2$ and $K=k_f/k_r$,

$$d[A]_{obs}/dt = -2Kk_1'[A]^2 - k_2[A] \qquad \text{(VII-26)}$$

It is often assumed in autooxidations that the oxidation rate constant is proportional to the amount decomposed[10] (Atkins; Carstensen,1990)

$$k_1' = k_1[\text{Decomposed}] \qquad \text{(VII-27)}$$

The amount decomposed may be represented by

---

10 For simplicity it is assumed that all decomposition products affect the reaction, since it is not possible to distinguish between them.

$$[\text{Decomposed}] = [A]_o - [A]_{obs} \qquad \text{(VII-28)}$$

$$= [A]_o - ([A] + 2K[A]^2) \qquad \text{(VII-29)}$$

Then, Eq. [VII-27] and [VII-29] inserted into equation [VII-26] give, after rearrangement

$$d[A]_{obs}/dt = 2KM[A]^4 + M[A]^3 - M[A]_o[A]^2 - k_2[A] \qquad \text{(VII-30)}$$

where

$$M = 2Kk_1 \qquad \text{(VII-31)}$$

In order to integrate Eq. [VII-30], both sides must be expressed in terms of $[A]_{obs}$; in order to achieve this, we at this point assume

$$[A]_{obs} \approx [A], \qquad \text{(VII-32)}$$

which is true when $(1/16K^2 + A_{obs}/2K) >> [A]_{obs}^2$, with $[A]_{obs}$ expressed in terms of fractions from 0 to 1 (see Appendix to this chapter). Thus, Eq. [VII-30] becomes

$$d[A]_{obs}/dt = 2KM[A]_{obs}^4 + M[A]_{obs}^3 - M[A]_o[A]_{obs}^2 - k_2[A]_{obs} \qquad \text{(VII-33)}$$

VII-B-4. Numerical Integration

Because it is not possible to solve Eq. [VII-33] in closed form, it was integrated numerically (Atkins) using SCIENTIST, and the constants shown in Table VII-3a were obtained as parameter estimates. These estimates were used to simulate the profiles shown in Figure VII-2 (solid curves) using the numerical integration routine in Student MATLAB, and one can see that the fits agree reasonably well with the experimental data (symbols). Simulating the profiles with software different from that used to obtain the parameter estimates serves as a cross-validation of the softwares.

The reader may verify from Table VII-3a that approximation A-3 in the Appendix to this chapter is valid for these sets of parameters. Tables VII-3b, c, and d give the parameter estimates obtained from the numerical integration of Eq. [VII-33] for data reported in the Master's Thesis generated at 60, 75, and 93°C.

VII-B-5. Reasonableness of Parameter Estimates Obtained from Numerical Integration of Eq. [VII-33]: Energy of Activation of the Non-Oxidative Pathway

One of the drawbacks of not being able to solve a differential equation in closed form is that one cannot obtain explicit equations for the rate constants. One must then rely on those obtained from the numerical integration, which may be suspect, owing to the

Table VII-3a Parameter values obtained by numerical integration of Eq. [VII-33] as shown in Figure VII-2. The values have not been rounded in order that the reader may exactly reproduce by simulation the kinetic profiles shown.

	0.4 M/93°C	0.8 M/75°C	1.0 M/75°C	0.6 M/60°C	0.8 M/60°C
$k_{1,\ day^{-1}}$	357.82	16.494	13.844	0.311	0.327
$k_{2,\ day^{-1}}$	0.1355	0.0226	0.01601	9.32×10^{-3}	0.0133
K, M^{-1}	4.84×10^{-4}	1.49×10^{-3}	6.62×10^{-3}	0.0855	0.100

Table VII-3b Data at 60°C from the Master's Thesis analyzed by Eq. [VII-33], plots not shown. Buffers do not contain EDTA.2Na. Where indicated by the symbol μ, ionic strength has been adjusted with KCl to 2.2. Note that the results obtained for 0.6 and 0.8 M buffers do not agree with those in Table VII-3a, pointing to the existence of multiple solutions. Both sets of parameters give reasonable fits to the experimental data. The values have not been rounded in order that the reader may exactly reproduce by simulation the kinetic profiles obtained.

Buffer	k_1, day^{-1}	k_2, day^{-1}	K, M^{-1}
0.2 M pH 7	0.0026904	0.0070351	0.59077
0.4 M pH 7	2.632	0.0017455	0.010383
0.6 M pH 7	4.0107	0.0017098	0.0089675
0.8 M pH 7	0.048737	0.021415	0.32846
1.0 M pH 7	0.11126	0.023267	0.22722
0.2 Mμ pH 7	0.011845	0.017022	0.55812
0.8 Mμ pH 7	0.95990	0.0051503	0.017312

Table VII-3c Data at 75°C from the Master's Thesis analyzed by Eq. [VII-33], plots not shown. Buffers do not contain EDTA.2Na. Where indicated by the symbol μ, ionic strength has been adjusted with KCl to 2.2. Note that the results obtained for the 0.8 M and 1.0 M buffer do not agree with that in Table VII-3a, pointing to the existence of multiple solutions. Both sets of parameters give reasonable fits to the experimental data. The fits to the data are quite good. Multiple solutions to the same data are shown for data generated in 0.2 M and 1.0 M buffers. The first set was used to determine E_a. The values have not been rounded in order that the reader may exactly reproduce by simulation the kinetic profiles obtained.

Buffer	k_1, day^{-1}	k_2, day^{-1}	K, M^{-1}
0.2 M pH 7	0.030654	0.015447	0.09295
0.2 M pH 7	14.30	0.013810	2.7178×10^{-4}
0.4 M pH 7	1.89×10^{-16}	0.015145	5.39×10^{-17}
0.6 M pH 7	1.89×10^{-16}	0.020775	5.39×10^{-17}
0.8 M pH 7	6.2885	0.024162	0.0031775
1.0 M pH 7	0.30408	0.0091961	0.073608
1.0 M pH 7	1.6269	0.026879	0.044322

Table VII-3d Data at 93°C from the Master's Thesis analyzed by Eq. [VII-33], plots not shown. Buffers do not contain EDTA.2Na. Where indicated by the symbol μ, ionic strength has been adjusted with KCl to 2.2. Note that the results obtained for the 0.4 M buffer does not agree with that in Table VII-3a, pointing to the existence of multiple solutions. Both sets of parameters give reasonable fits to the experimental data. The data generated in 0.8 M buffer indicate significant autocatalysis (Figure VII-6), whereas in the other buffers, the rate is nearly first order. This may be because only at a buffer concentration of 0.8 M is sufficient trace metal present to catalyze the reaction. The addition of KCl to adjust the ionic strength may somehow quench this, as may be seen by the lack of autocatalysis in the data generated in 0.2 Mμ and 0.8 Mμ buffers. The fits to the data are quite good. The values have not been rounded in order that the reader may exactly reproduce by simulation the kinetic profiles obtained.

Buffer	k_1, day^{-1}	k_2, day^{-1}	K, M^{-1}
0.4 M pH 7	1.89×10^{-16}	0.19202	5.39×10^{-17}
0.6 M pH 7	1.89×10^{-16}	0.28273	1.14×10^{-15}
0.8 M pH 7	82.896	0.094803	0.0082156
0.4 Mμ pH 7	1.34×10^{-10}	0.20613	5.39×10^{-17}
0.8 Mμ pH 7	1.89×10^{-16}	0.21951	5.39×10^{-17}

existence of multiple solutions. It was desired, then to determine the reasonableness of the parameter estimates obtained by calculating the energy of activation, E_a, for the non-oxidative pathway, and this was done in two ways.

The first was to assume that, at 93°C, the reaction is essentially first-order, that is, the non-oxidative (elimination) degradation to the cinnamate predominates, and the rate of this reaction may be obtained directly from the slope of the ln concentration vs time plot. One can now obtain an energy of activation for the non-oxidative reaction from an Arrhenius plot, using the experimental k_{obs} at 93°C, and the k_2 values determined from numerical integration at 60, 75°C, and 93°C (Table VII-3b, c, and d).

Such a plot is shown in Figure VII-5 for data generated in a 0.4 M buffer; from the slope, one obtains a value for E_a of 34.1 kcal/mole for the non-oxidative reaction in 0.4 M pH 7 buffer. This is not unreasonable, considering that E_a values for most reactions of pharmaceutical interest (i.e. organic compounds in solution) lie between 18 and 22 kcal/mol. The E_a is obtained by multiplying the slope of the Arrhenius plot by 1.98×10^{-3} kcal/°K/mol.

The results for other data treated in this fashion are summarized in Table VII-4a, from which it appears that at pH 7 and at drug concentrations below the cmc, the E_a is lower than that obtained near or above the cmc. For convenience, the actual rate constants used from Table VII-3 and the Master's Thesis are reproduced in Table VII-4b. In these experiments, there was no control for trace metal catalysis, and the initial drug concentration

Table VII-4a. Results from plotting data generated at 60, 75, and 93°C in the Master's Thesis by the Arrhenius relation (initial drug concentration, 0.2 mg/mL). The rate constants used are given in Table VII-4b. Due to autocatalysis in the 0.8 M buffer at 93°C (Figure VII-6), the last entry is a more reasonable estimate of E_a in this buffer than the penultimate entry.

	y-int.	-slope	r^2	E_a	cmc, mg/mL[c]
0.2 M pH 7:	25.73	1.028×10^4	0.953	20.4	0.6-0.8
0.4 M pH 7:	45.35	1.722×10^4	0.999	34.1	0.4-0.5
0.6 M pH 7:	48.67	1.832×10^4	0.998	36.2	0.2-0.3
0.8 M pH 7:	25.28	9943.2	0.829	(19.7)[a]	<0.2
0.8 M pH 7:	17.45	7298	0.946	14.4[b]	<0.2

---

[a] includes k_{obs} at 93°C

[b] a better estimate than [a]; does not include k_{obs} at 93°C, but only rate constants obtained at 60, 75, and 93°C by numerical integration.

c estimated range between 60°C and 93°C from data in Table VI-1.

Table VII-4b. Rate constants ($days^{-1}$) used to obtain data in Table VII-4a. Rate constants either obtained by numerical integration (n.i.) of Eq. [VII-33], from Table VII-3, or, from the slope of the first-order plot (k_{obs}) of data from the Master's Thesis. They are reproduced here for convenience. In the case of the 0.8 M buffer, the k_{obs} value is not as reliable as k_2 obtained by numerical integration, because in this buffer at 93°C, the kinetics are not first-order, but rather autocatalytic, and in fact the fit to Eq. [VII-33] is quite good as shown in Figure VII-6.

	60°C (n.i.)	75°C (n.i.)	93°C (n.i.)	93°C (k_{obs})
0.2 M pH 7	0.00704	0.01545	n.d.	0.112
0.4 M pH 7	0.00175	0.01514	0.192	0.174
0.6 M pH 7	0.00171	0.02077	0.28273	0.220
0.8 M pH 7	0.0133	0.0226	0.0948	(0.307)

n.d. not determined due to insufficient data (N=3).

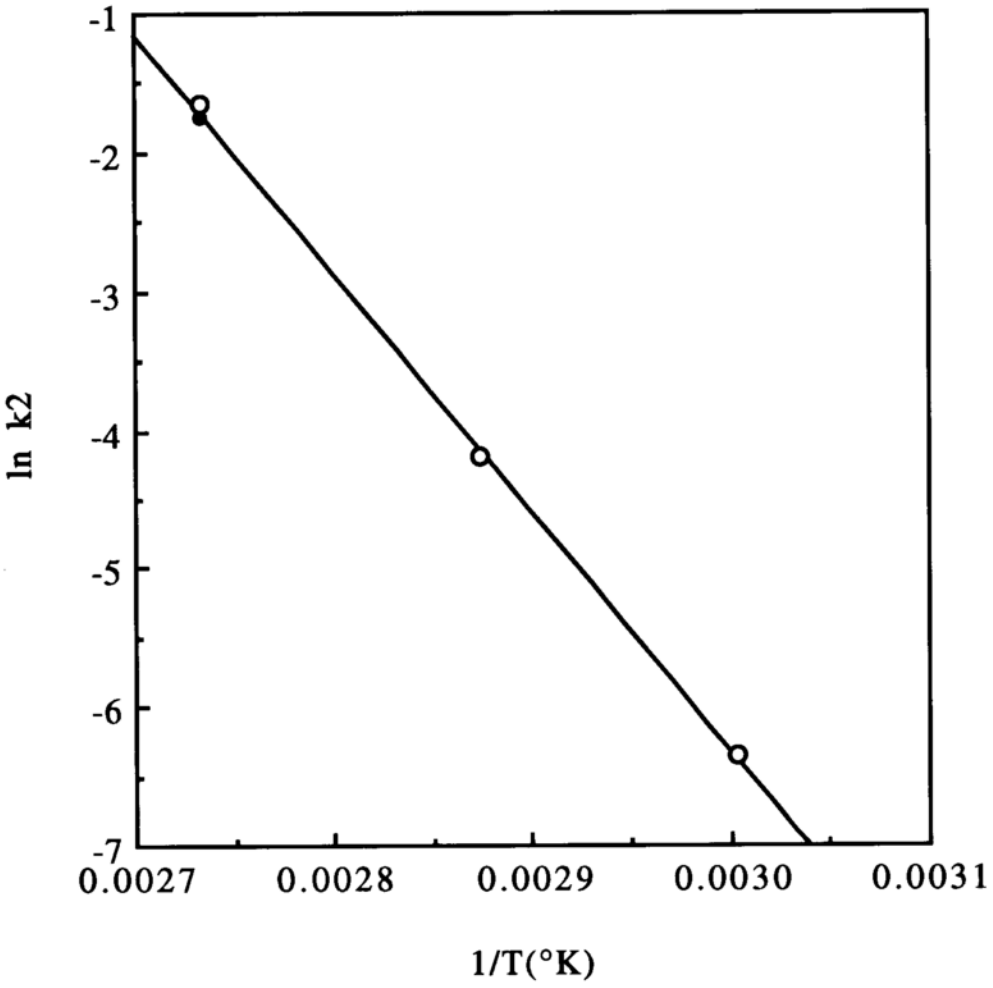

Figure VII-5 Arrhenius plot of elimination (non-oxidative) rate constants obtained in 0.4 M pH 7 phosphate buffers at 93°C (filled circle), from slope of first-order plot of data in the Master's Thesis, and at 60, 75°C and 93°C (open circles), obtained as parameter estimates from numerical integration of the data by Eq. [VII-33]. The equation for the line is

$$y = 45.35 - 1.723 \times 10^4 x \qquad r^2 = 0.999$$

From the slope, one obtains an E_a of 34.1 kcal/mol.

was 0.2 mg/mL, such that the drug concentration may have crossed the cmc during the course of the reaction. Thus the fit to Eq. [VII-33] may not have been perfect in some cases, leading to poor estimates for the rate constants, and a low correlation coefficient in Table VII-4a.

For example, in Table VII-4a, in the case of the 0.8 M buffer, both entries are generated from the same data set, except that the last entry only uses the results from numerical integration, and does not include the k_{obs} at 93°C. Because the data generated at 93°C in the 0.8 M buffer indicate autocatalysis (Figure VII-6), treating it as first-order yields an erroneous value of k_{obs}, making the estimate of E_a of 14.4 a more reliable estimate than 19.7 which was obtained by including k_{obs}.

A second means of obtaining E_a was from Arrhenius plots of data generated at 60, 75, and 93°C at pH 8 and in the presence of EDTA.2Na; sparging samples with argon blocked the autooxidative pathway, allowing one to obtain an estimate of the energy of activation for the non-oxidative pathway.

As may be seen in Table VII-5 and Figures VII-7 and 8, the energy of activation for the non-oxidative pathway at pH 8 was slightly higher at concentrations above the cmc (21.3 kcal/mol) than below (19.8 kcal/mol). This observation is consistent, whether one looks at oxygen or argon-sparged samples, or those with air headspace, or if one plots ln k_{ox} (discussed in Chapters VIII and IX) vs 1/T, bearing in mind that in the case of drug concentrations above the cmc, the ordinate is ln(zero-order rate constant), while at

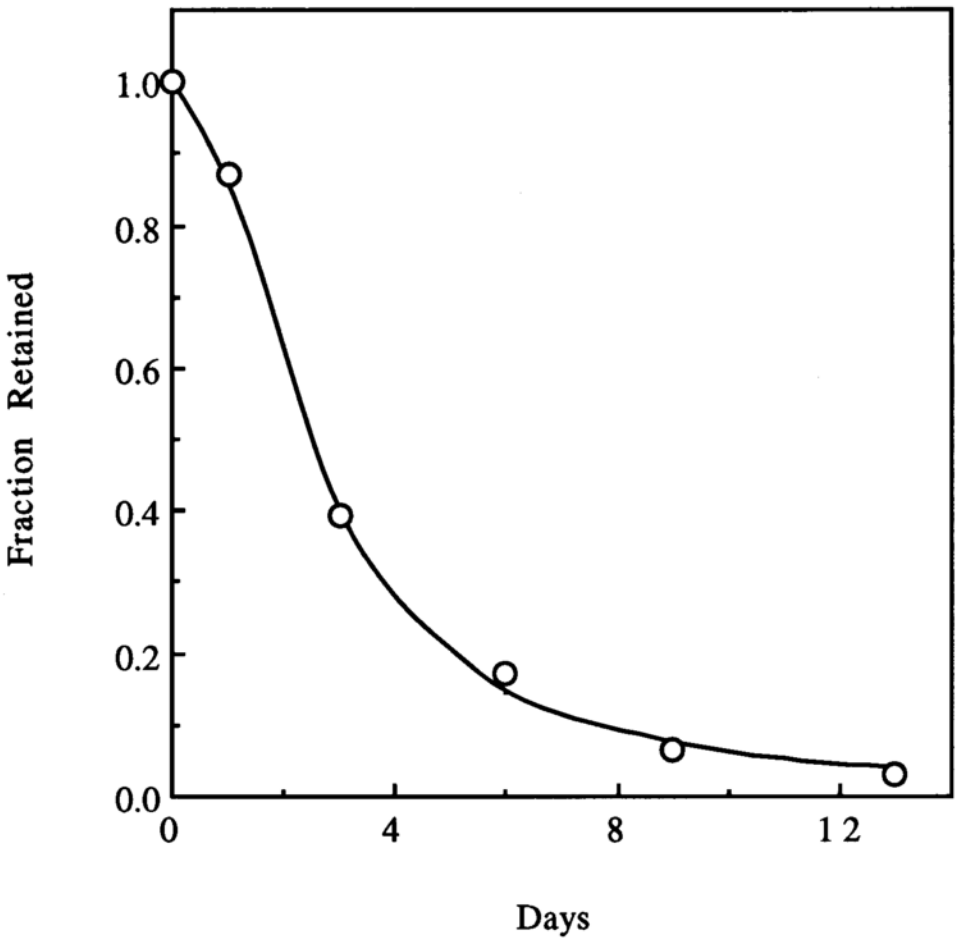

Figure VII-6 Data generated at 93°C with air headspace in 0.8 M pH 7 phosphate buffer. This buffer concentration was high enough such that trace metals from the buffer salts catalyzed the reaction. The symbols are experimental data, and the fit shown is by numerical integration of Eq. [VII-33]. Parameter estimates for k_1, k_2, and K are 82.896, 0.094803, and 0.0082156 (Table VII-3d). At lower buffer molarities or in buffers containing KCl to adjust the ionic strength, the reaction at 93°C was nearly first order, allowing a value for k_2 to be obtained as k_{obs} from the first order plot.

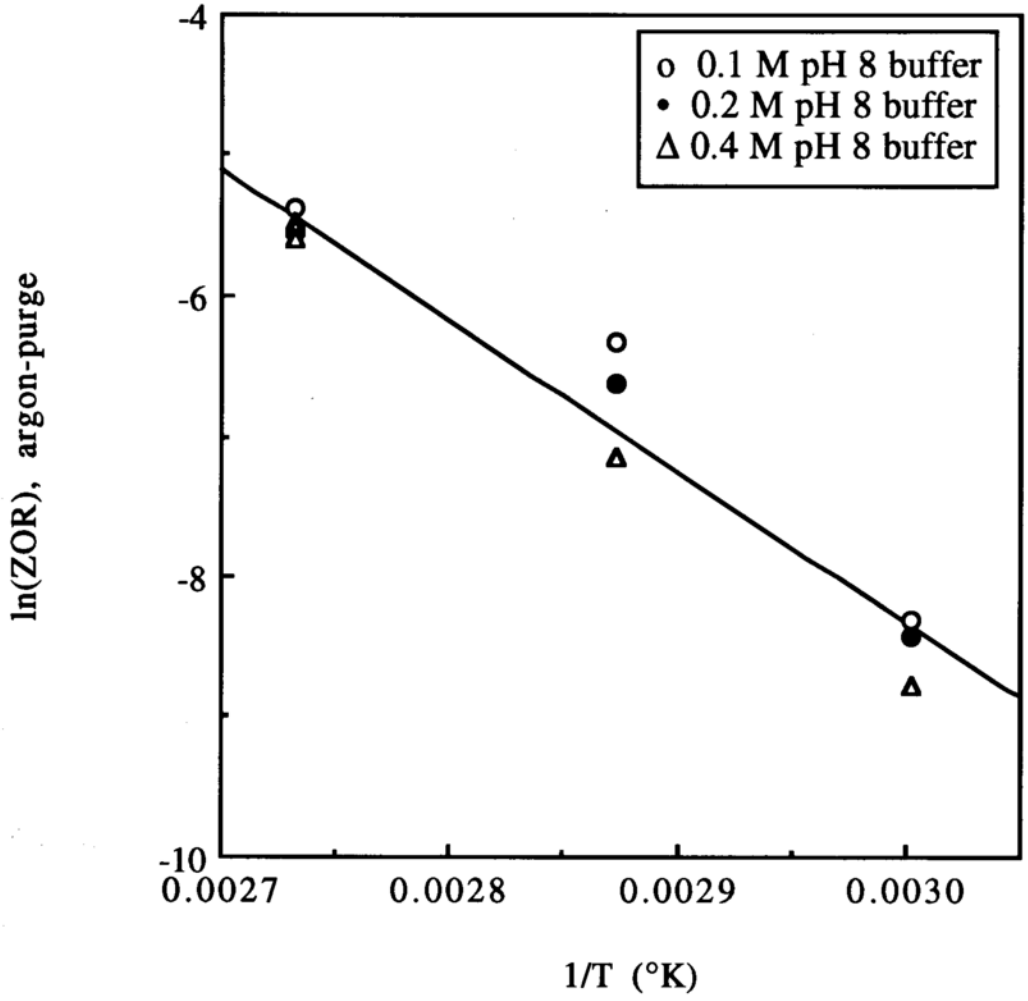

Figure VII-7 Arrhenius plot for elimination (non-oxidative) pathway decomposition of A (argon-sparged samples) at initial drug concentration = 25 mg/mL (above the cmc); data from Table VII-5.

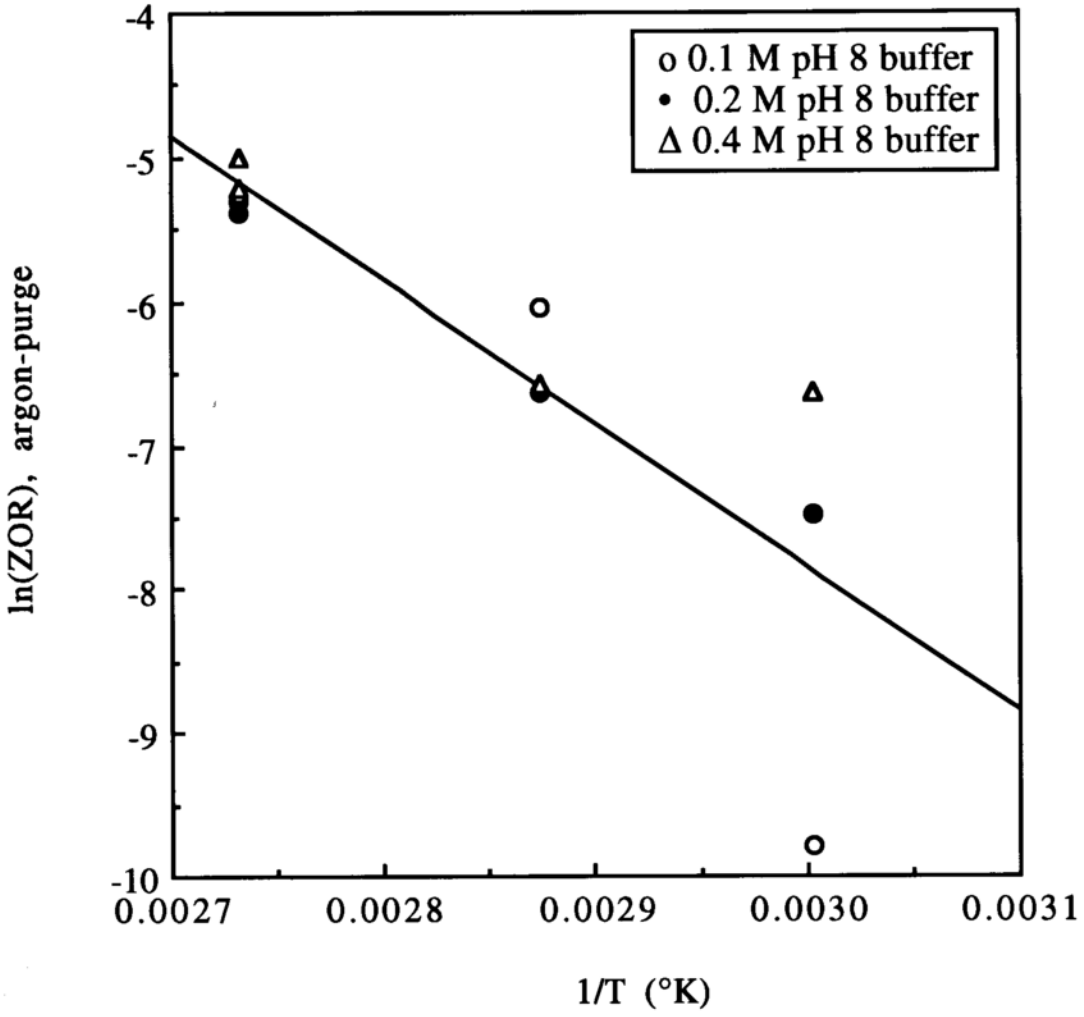

Figure VII-8 Arrhenius plot for the elimination (non-oxidative) pathway (argon-sparged samples) at initial drug concentration = 0.05 mg/mL (<cmc); data from Table VII-5. The E_a is for the pooled data is 19.8 kcal/mol; eliminating the outlier gives 13.9 kcal/mol.

Table VII-5 Results of Arrhenius plots of data from Appendix C. The 0.1M μ and 0.2M μ data have been combined with the 0.4 M data since they are at a common ionic strength. The symbol < signifies less than and > signifies greater than.

	y-int.	-slope	r^2	E_a, kcal/mol
ARGON SPARGE >cmc				
0.1M	24.14	10740	0.951	21.3
0.2M	33.50	10580	0.973	20.9
0.4M	26.87	11860	0.998	23.5
pooled data	23.91	10750	0.957	21.3
ARGON SPARGE <cmc				
0.1M	39.98	16386	0.851	32.4
0.2M	15.84	7783.2	0.994	15.4
0.4M	11.54	6136.7	0.865	12.2
pooled data	22.08	9975.1	0.798	19.8
AIR Headspace >cmc				
0.1M	29.44	12560	0.999	24.9
0.2M	25.06	11121	0.982	22.0
0.4M	28.02	12141	0.998	24.0
pooled data	27.28	11865	0.988	23.5
AIR Headspace <cmc				
0.1M	17.31	8244.1	0.998	16.3
0.2M	19.30	8987.1	0.996	17.8
0.4M	23.44	10471	0.995	20.7
pooled data	20.22	9303.2	0.980	18.4
O_2 SPARGE >cmc				
0.1M	21.92	9702.3	0.982	19.2
0.2M	20.64	9346.9	0.991	18.5
0.4M	23.09	1024.2	0.991	20.3
pooled data	21.42	9608.4	0.970	19.0
O_2 SPARGE <cmc				
0.1M	16.02	7530.1	0.995	14.9
0.2M	19.74	8913.7	0.999	17.6
0.4M	24.44	10585	0.978	21.0
pooled data	20.40	9121.2	0.957	18.0
k_{ox}, O_2 sparge >cmc				
0.1M	18.94	8898.3	0.999	17.6
0.2M	16.60	8199.0	1.000	16.2
0.4M	19.17	9084.8	0.963	18.0
pooled data	18.03	8656.3	0.963	17.1
k_{ox}, O_2 sparge <cmc (note: scatter and curvature in these plots)				
0.1M	8.99	5271.7	0.878	10.4
0.2M	14.03	7083.4	0.939	14.0
0.4M	23.59	1.0567	0.860	20.9
pooled data	15.83	7739.6	0.776	15.3

concentrations below the cmc, the ordinate is ln(first-order rate constant) as will be discussed below. Statistically this observation is confirmed by a paired t-test of the 12 pairs of E_a data generated above and below the cmc in Table VII-5 (excluding the pooled results). This gives a t-statistic of 1.613, and a significance of 0.135 (Statworks), indicating that the E_a above the cmc is different from the E_a below the cmc, with 86.5% confidence.

VII-B-6. General Comments Regarding the Scheme, and a Re-Examination of Data Generated in the Master's Thesis

It should be recognized that the solution presented here is *a* solution and the intent is to show that a model, such as proposed, will give the correct profile. Although the energy of activation results were quite reasonable, the values obtained for K by numerical integration were rather low; in contrast, the formation constant for lauryl sulfate dimers has been experimentally determined to be 100-350 $mole^{-1}$, while the association constants for the ion pairs of $(CH_3)_4N^+$, $(C_2H_5)_4N^+$, and $(n\text{-}(C_3H_7)_4N^+$ lauryl sulfates were found to be to be 13, 19, and 21 $mole^{-1}$ (Mukerjee, 1967). The dimerization is a simplified view: bearing in mind that temperature and total ion concentration affect the cmc (Hiemenz; Mukerjee and Mysels), the intermediate species could well be a higher aggregate, and in effect could be the sums of such aggregates; the term A_2 should be viewed in this light. It may be that the dimer conformation facilitates the autocatalysis, so that in most cases, the dimerization product (A_2)

reacts to a much greater extent than other n-mers, even if present, such that the reactions with other species may be neglected. This concept is further explored in following chapters.

It should be kept in mind that the kinetic studies reported in the Master's Thesis were carried out without knowledge of the cmc, and in the presence of varying amounts of trace metal. Re-examining these kinetic data, it appears that data generated at 75°C and 93°C in a buffer of high molarity showed much more scatter than those generated in buffer of low molarity, as mentioned earlier (see Figure VI-1). It is recalled that in each case, the results have been averaged over four initial drug concentrations, 0.05, 0.1, 0.2, and 0.5 mg/mL.

To further illustrate this point, the actual profiles generated at each drug concentration are shown in Figures VII-9 through 12; the discrepancies are much more evident at 75°C, and in fact it appears as though the actual shape of the kinetic profile is affected at different drug concentrations in the 0.6 M buffer. This is similar to data reported by Motsavage and Kostenbauder regarding the hydrolysis of sodium dodecyl sulfate and Meakin, Stevens, and Davies regarding the decomposition of promethazine HCl at drug concentrations above and below the cmc or apparent cmc.

With knowledge of the cmc in these buffers, it is now possible to reinterpret these data, and in so doing one finds, that the observed scatter in the data reflects the change in aggregation state of the

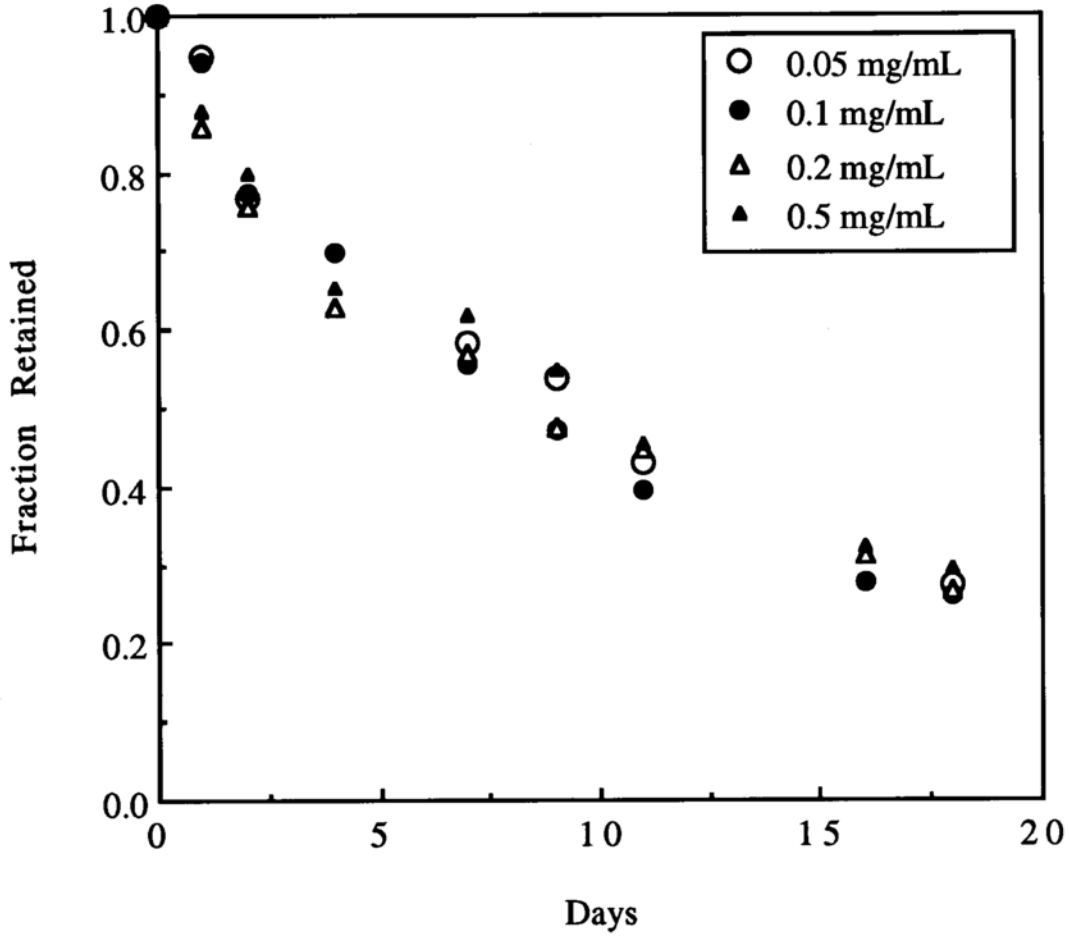

Figure VII-9 Kinetic data generated at 93°C in 0.05 M pH 7 KH_2PO_4/KOH buffer; effect of drug concentration is nil at initial drug concentrations below the cmc.

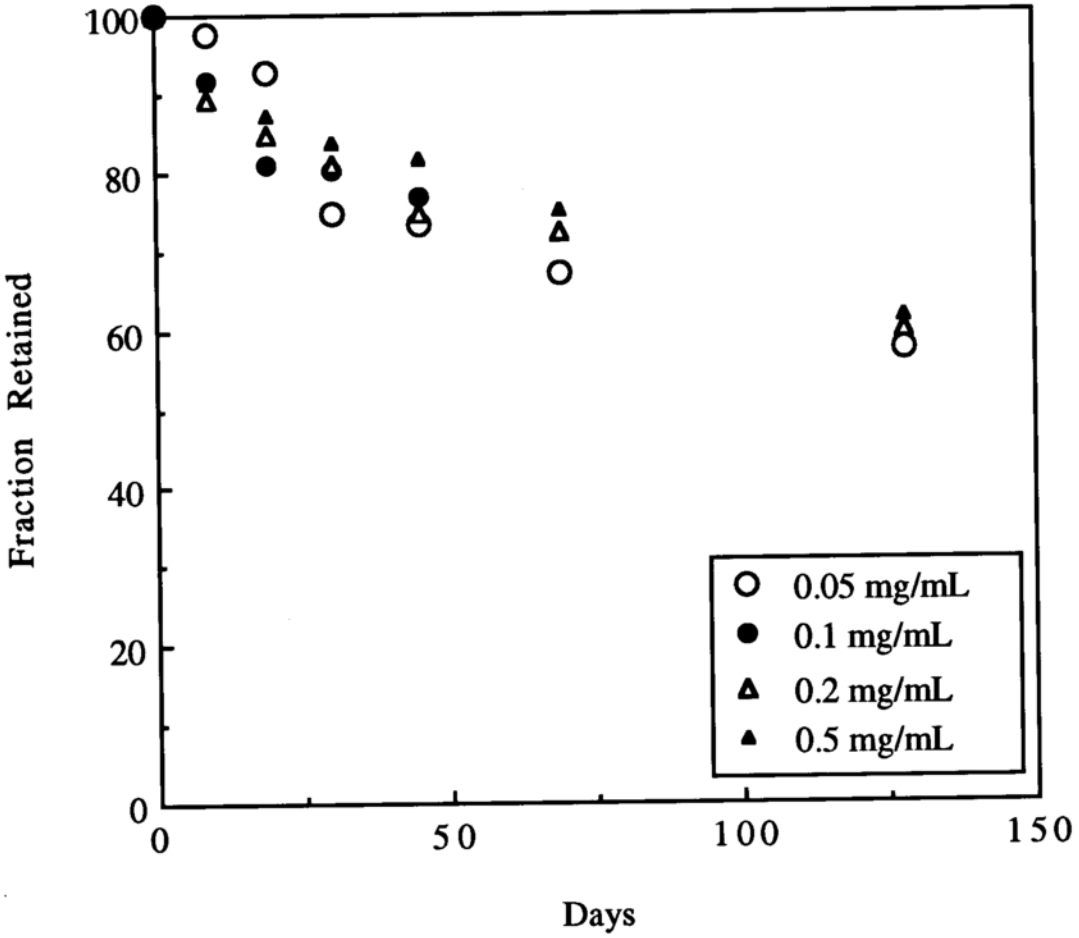

Figure VII-10 Kinetic data generated at 75°C in 0.05 M pH 7 KH_2PO_4/KOH buffer; effect of drug concentration is nil at initial drug concentrations below the cmc.

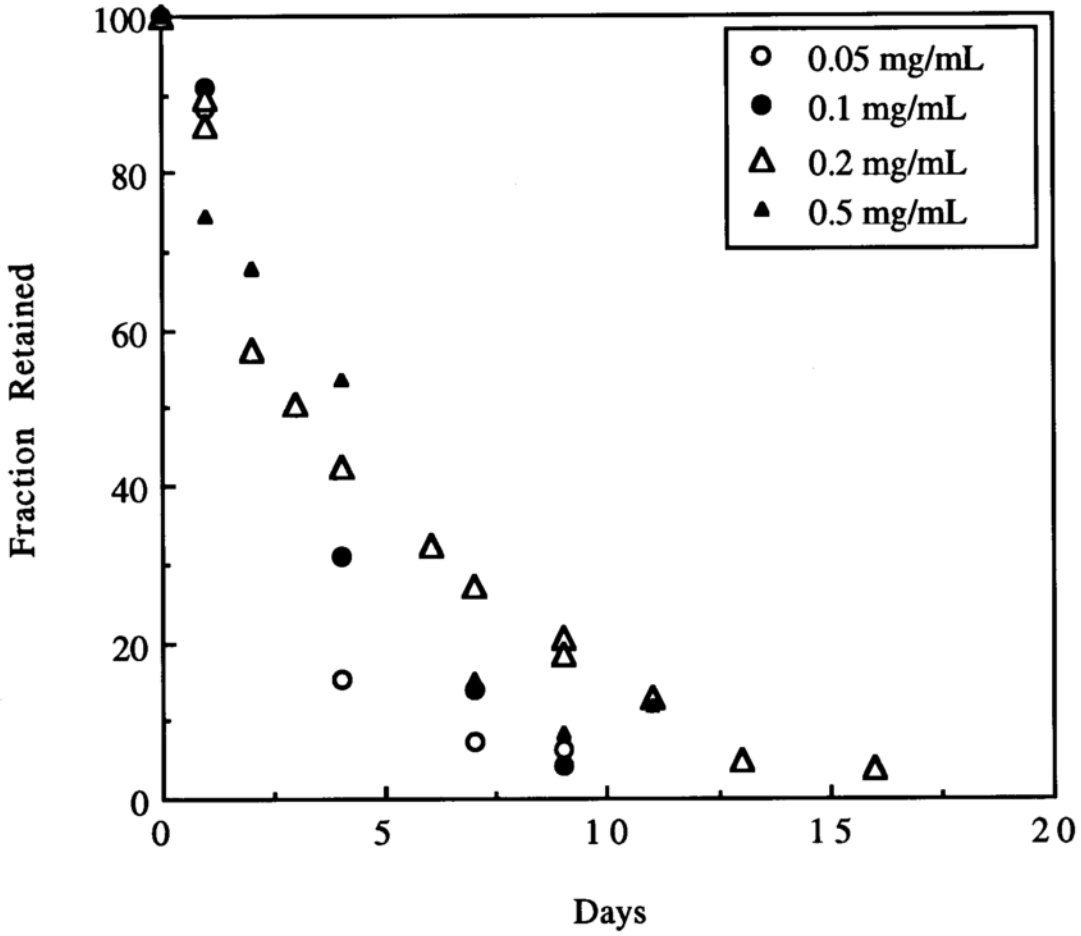

Figure VII-11 Kinetic data generated at 93°C in 0.6 M pH 7 KH_2PO_4/KOH buffer adjusted to an ionic strength of 2.2 with KCl; a drug concentration effect is evident

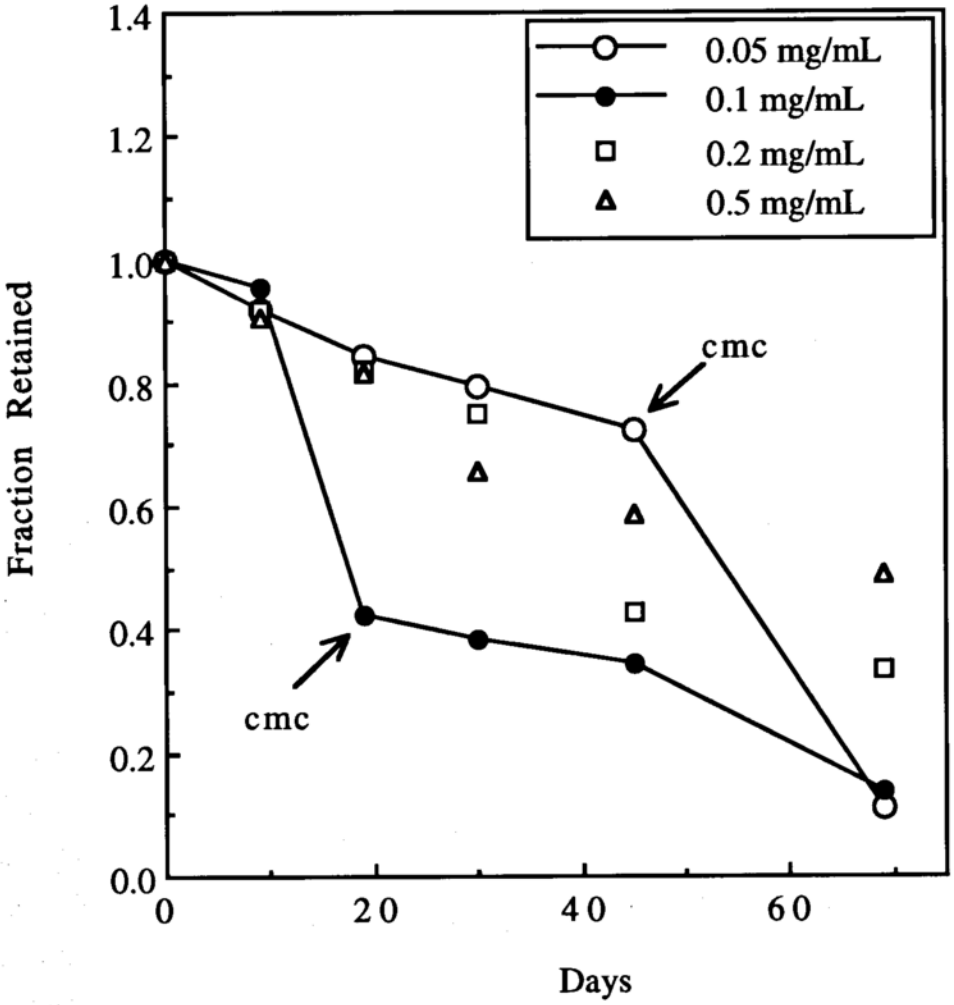

Figure VII-12 Kinetic data generated at 75°C in 0.6 M pH 7 KH_2PO_4/KOH buffer adjusted to an ionic strength of 2.2 with KCl; a drug concentration effect is evident, as is autooxidation (this buffer does not contain EDTA).

molecule throughout the course of the reaction: in the case of the 0.05 M buffer, the initial drug concentrations were well below the observed cmc in that buffer (ca. 1.6 mg/mL) and good precision was observed in the kinetic profile, whereas in the case of the 0.6 M buffer, the initial drug concentrations were near or above the cmc in that buffer (ca. 0.04 mg/mL) such that as decomposition progressed, the concentration of drug in solution eventually fell below the cmc. It is noted that in this case, the precision of the mean data suffered greatly. The same trend was noted at 75°C, in fact the kink in the curves (Figure VII-12) coincide roughly with the cmc, suggesting that the rate of degradation of the compound is affected by its self-associative behavior. As may also be seen in Figure VII-12, the kinetic profiles at 75°C are further complicated by autooxidation, making interpretation difficult. The reader is referred to Figure 1 of Motsavage and Kostenbauder for comparison.

VII-B-7. Kinetic Salt Effect vs Buffer Catalysis

The correlation between buffer molarity and ionic strength is shown in Table VII-2; any change noted in kinetic rate as one altered the buffer molarity could either be attributed to buffer catalysis or to a kinetic salt effect.

A series of experiments reported in the Master's Thesis showed that when preparations in these buffers were adjusted to a common ionic strength of 0.9 or 2.2 with KCl, then the kinetic profiles at the same ionic strength, and both at 75 and 93°C, became identical,

implying a kinetic salt effect rather than buffer catalysis at pH 7 by phosphate.

A kinetic salt effect can also be demonstrated by plotting, as in Figure VII-13, kinetic rates by the Debye-Huckel equation

$$\log k = \log k_o + \frac{2Q(Z_A Z_B)\sqrt{\mu}}{1+\sqrt{\mu}} \qquad \text{(VII-42)}$$

where Z represents the positive or negative charges on the reacting species A and B, and

$$Q = 1.825x10^6 (\frac{\rho}{\varepsilon^3 T^3})^{0.5} \qquad \text{(VII-43)}$$

where ρ is density, ε is dielectric constant, and T is absolute temperature.

The least squares fit of the data in Figure VII-13 is

$$\log k_{obs} = -1.32 + 1.17(\frac{\sqrt{\mu}}{1+\sqrt{\mu}}) \qquad r^2 = 0.807 \qquad \text{(VII-44)}$$

In water at 90°C, 2Q has been estimated to be 1.17 (Carstensen, 1970), such that the slope obtained in Figure VII-13 not only indicates a positive kinetic salt effect, but also is of reasonable magnitude.[11]

---

[11] That the slope was found to be exactly 1.17 is at best fortuitous.

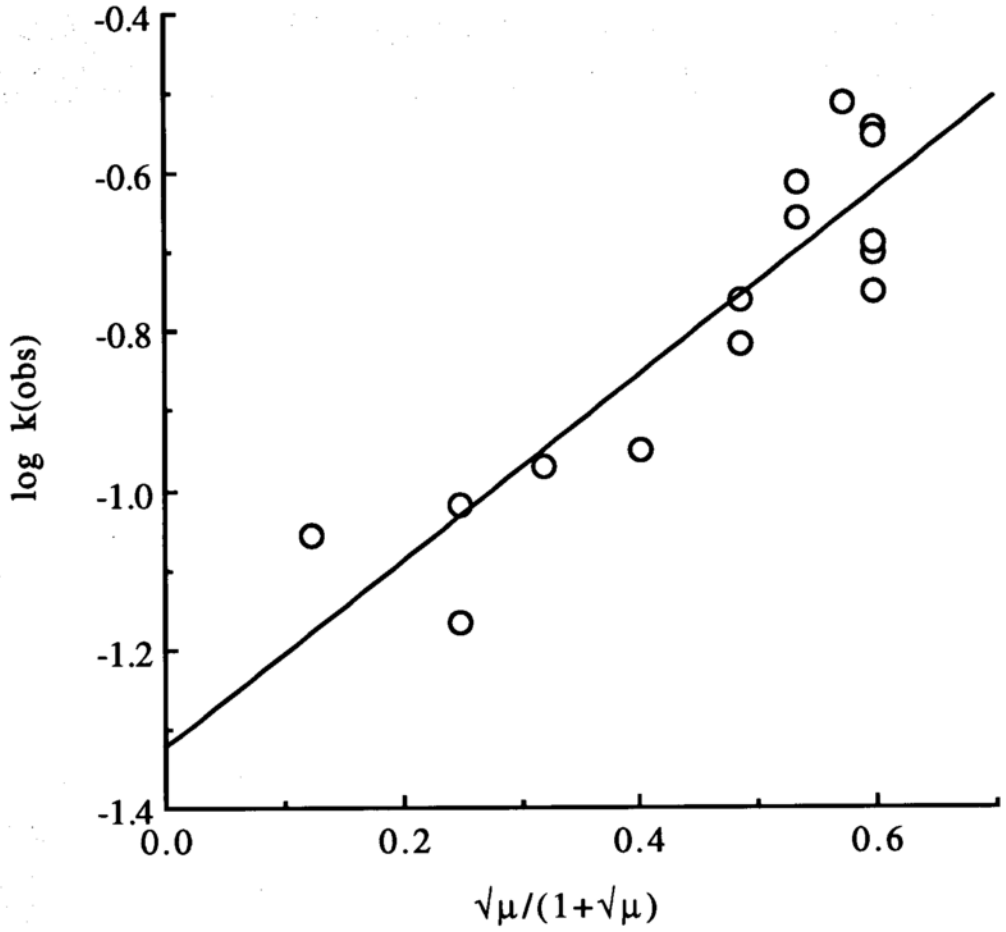

Figure VII-13 Positive kinetic salt effect. Data from Master's Thesis, generated at 93°C in pH 7 phosphate buffers ranging from 0.05 to 1.0 M at 75°C and 60°C, with air headspace. The k_{obs} have been obtained by treating as first order the data reported in the Master's Thesis, which are tabulated in Table VII-2.

One might argue that this plot is biphasic, in which case there appears to be a break at an ionic strength corresponding to a buffer concentration of 0.2 M, but the fact that there is a positive kinetic salt effect is indisputable. The scatter in the data most likely reflects the fact that these may not be purely first-order reactions, as in all cases, the initial drug concentration was 0.2 mg/mL, and no precaution was taken to exclude trace metals, that is, these buffers did not contain EDTA.2Na. This is further elaborated upon below, but what is important was that a *positive* kinetic salt effect was observed under these conditions.

Likewise, in the present set of experiments, pH 8 buffers adjusted to a common ionic strength of 1.2, which corresponds to the calculated ionic strength of the pH 8 0.4 M buffer containing 0.2% EDTA.2Na, the kinetic curves at 93°C were also superimposable, again implying a kinetic salt effect. Considering that changing the buffer molarity also changes the counterion concentration, hence the cmc, the observed kinetic salt effect also reflects the aggregation state of the system.

Interestingly however, in these present sets of experiments at initial drug concentrations above the cmc, a *negative* kinetic salt effect was observed at 60 and 75°C, as may be seen in Figures VII-14 and 15. That is, an increase in the buffer ionic strength was accompanied by a *decrease* in the rate of reaction; at 60°C, there are insufficient data to see the effect as dramatically. The only exception at 60°C is in argon-sparged samples at initial drug concentration below the cmc (0.05 mg/mL); in these samples the kinetics in 0.4 M

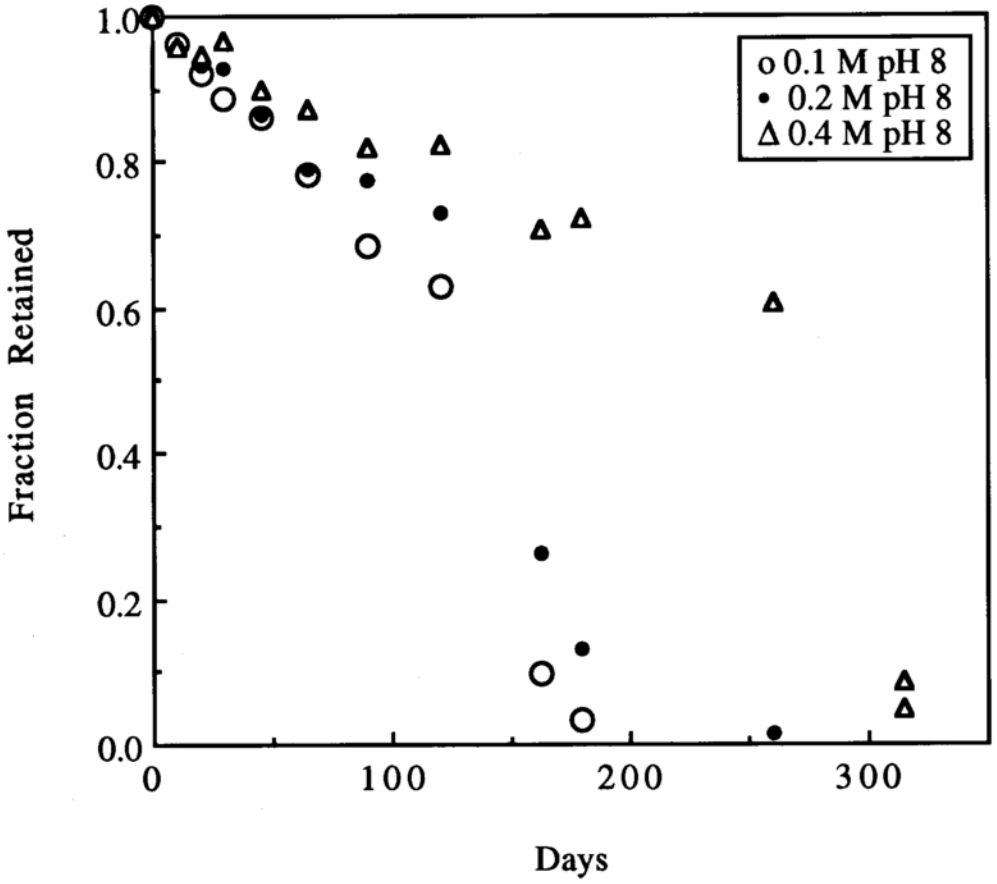

Figure VII-14 Negative kinetic salt effect at 75°C; oxygen sparge. Initial drug concentration above the cmc, 25 mg/mL, in pH 8 buffer with 0.2% EDTA.2Na. Note the profile indicative of autocatalysis.

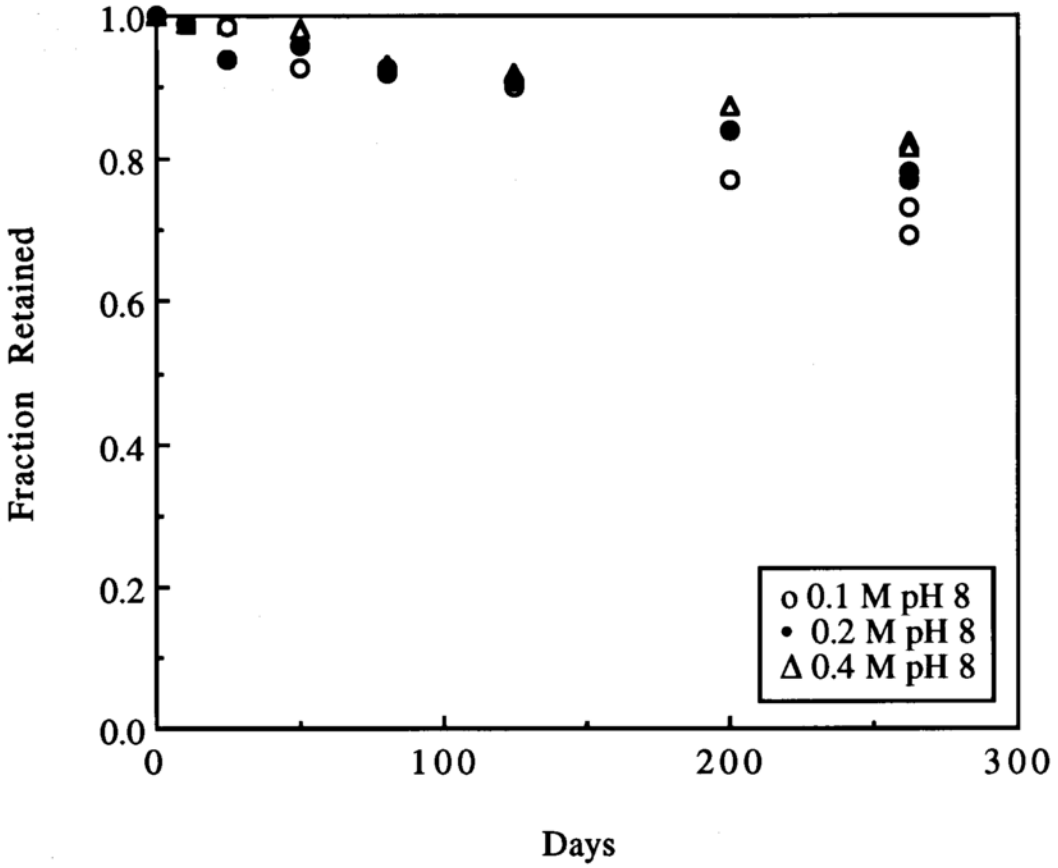

Figure VII-15 Negative kinetic salt effect at 60°C in pH 8 buffer with 0.2% EDTA.2Na; oxygen-sparged samples (insufficient data to observe autocatalysis, if any). Initial drug concentration below the cmc, 0.05 mg/mL. The same trend was observed at initial drug concentrations above the cmc (argon and oxygen-sparged samples, and samples with air headspace), and below the cmc, air headspace.

buffer were faster than in 0.1 and 0.2 M buffers and may imply a different mechanism at this temperature. The results generated in the 0.1 and 0.2 M buffers were indistinguishable after 262 days. But, in the studies at 60°C, less than 10% of the parent had decomposed during the time frame of the experiment, which was terminated due to lack of time.

At 93°C the effect is not as evident, but it appears there is a *positive* (argon-sparged) or *no* (oxygen containing samples) kinetic salt effect at initial drug concentrations below the cmc, and a *negative* kinetic salt effect at initial drug concentrations above the cmc, as may be seen in Figures VII-16 through 19. Argon-sparged samples show more scatter. These data may be anamolous, or may reflect a structural change in the micelle, as suggested by the surface tensiometry studies. In fact, if one examines Figure VI-2 one sees that the deviation from linearity occurs at a counterion concentration corresponding to ca. 0.2 M.

Some interpret a negative kinetic salt effect to imply that the decomposition involves a positively and a negatively charged species, such that the product $Z_A Z_B$ would be negative, yielding a negative slope from Eq. [VII-42], whereas a positive kinetic salt effect implies either both positively charged or both negatively charged reacting species, and absence of a kinetic salt effect (zero slope) implies at least one neutral reacting species.

According to this argument, then, one may conclude that in the presence of trace metal catalysis and at pH 7, the reaction mechanism is different than in the absence of trace metal catalysis at

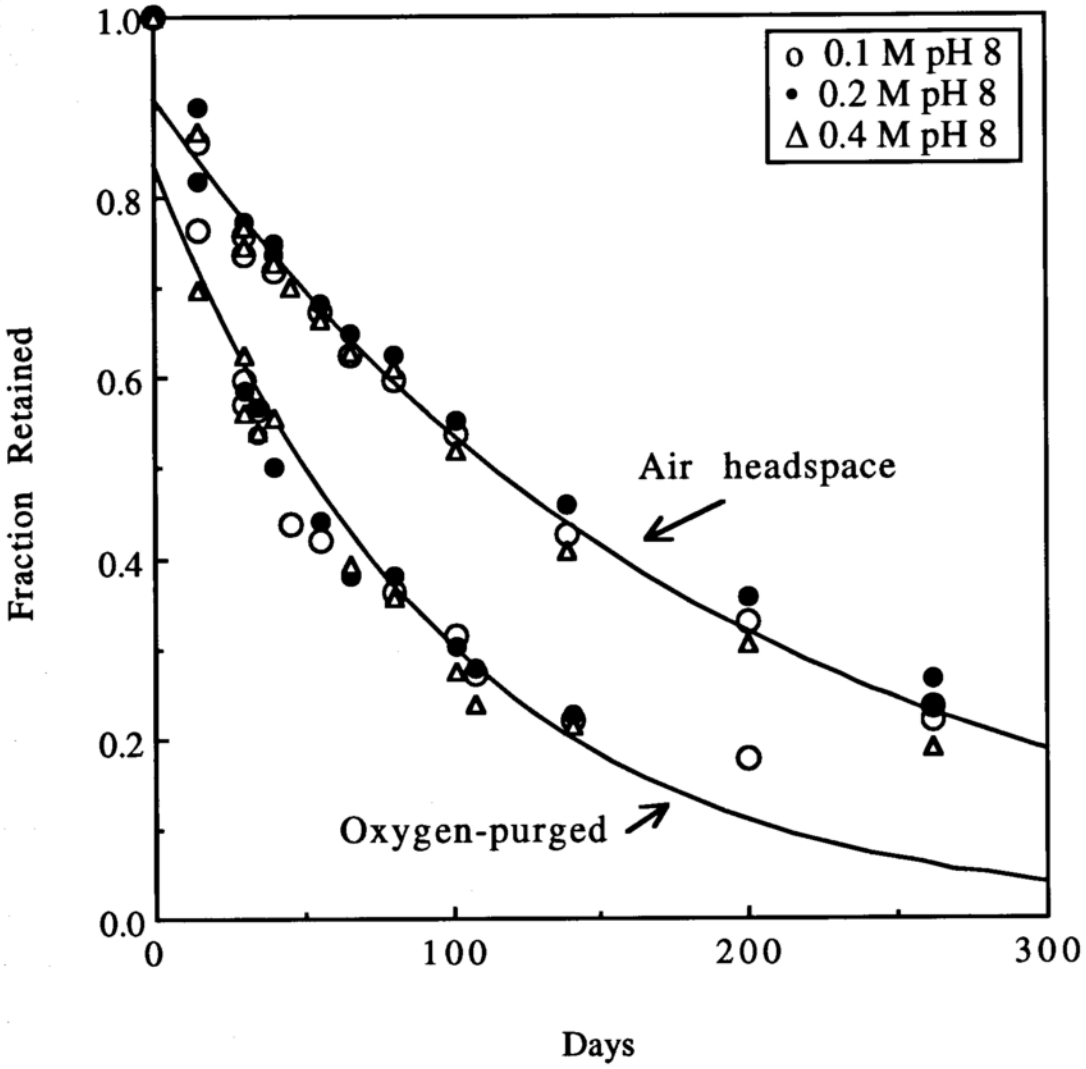

Figure VII-16 Kinetic salt effect, or lack of, at 93°C at initial drug concentration below the cmc, 0.05 mg/mL, in pH 8 buffers. First-order plots yield the following:

$y = -0.179 - 0.010x$	$r^2 = 0.955$	Oxygen-sparged
$y = -0.081 - 0.0053x$	$r^2 = 0.983$	Air headspace

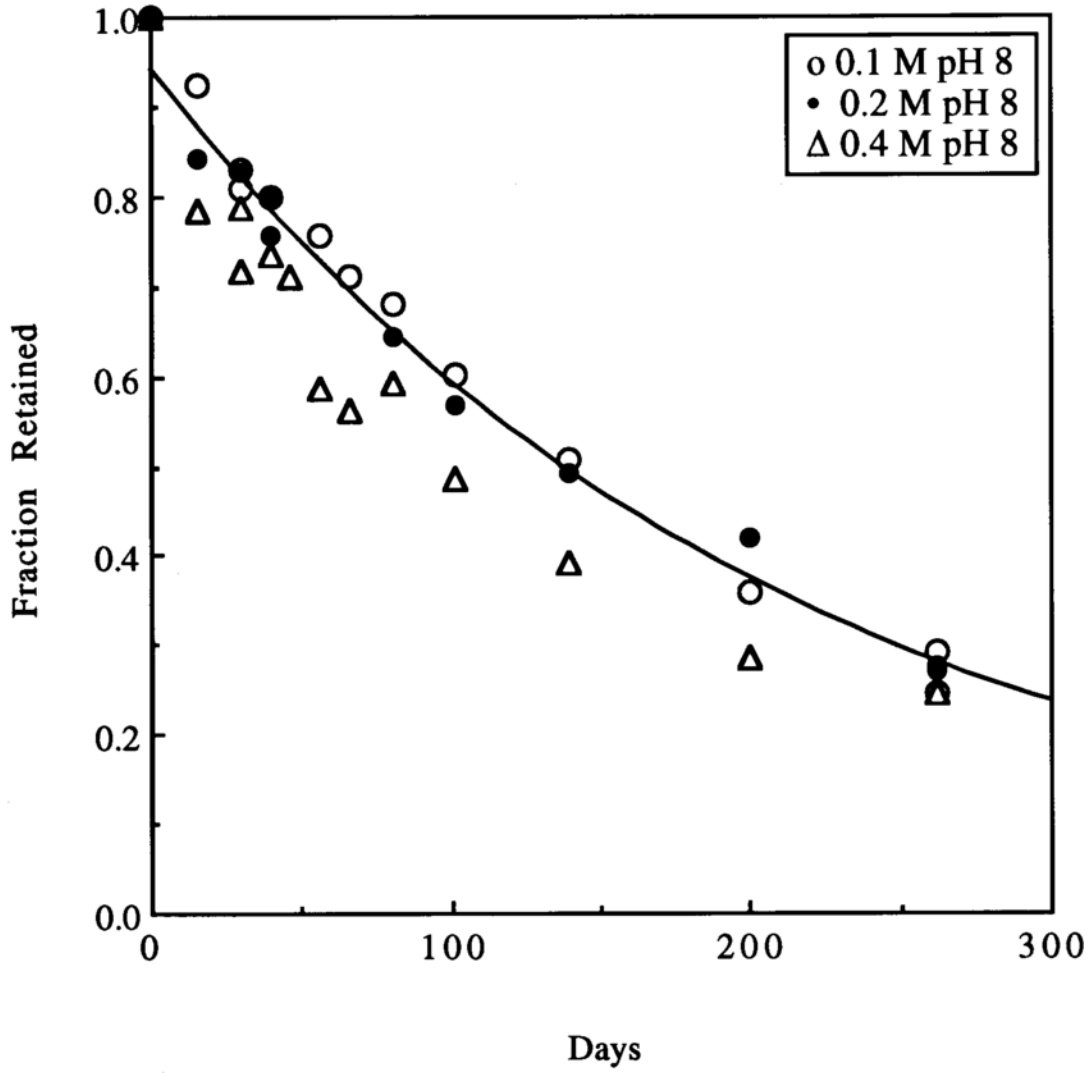

Figure VII-17 Positive kinetic salt effect at 93°C in pH 8 buffer; samples sparged with argon. Initial drug concentration below the cmc, 0.05 mg/mL.

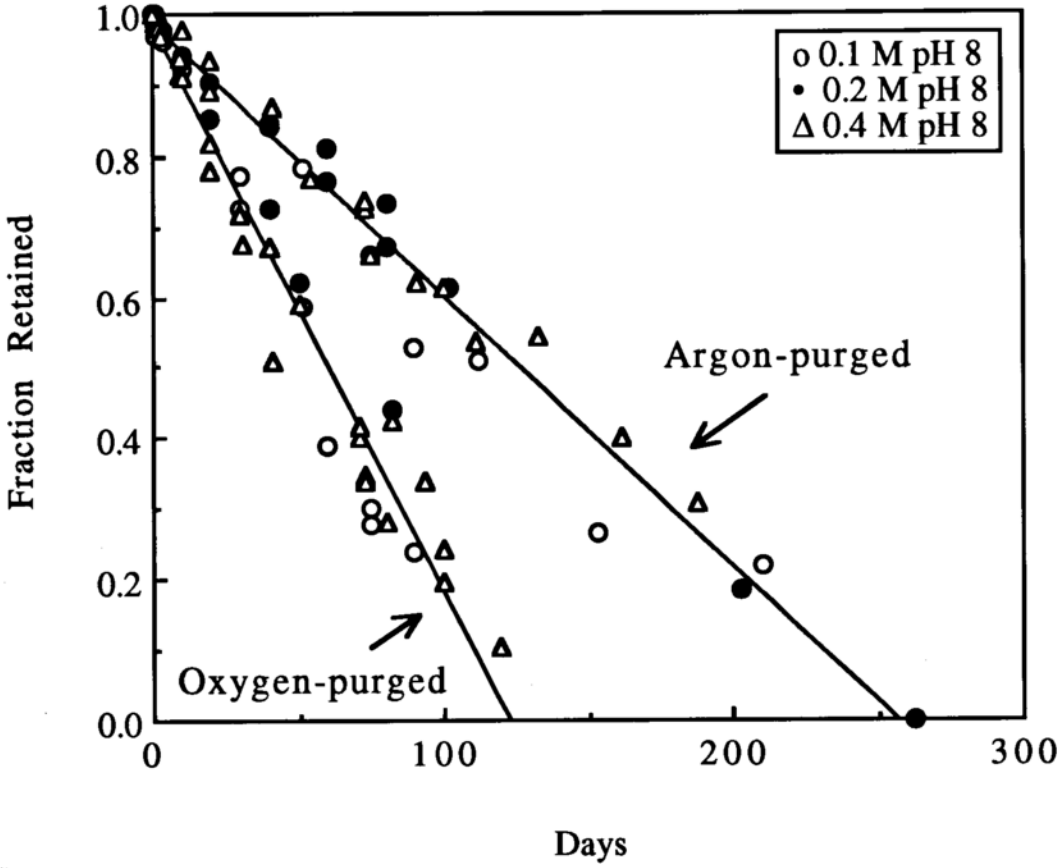

Figure VII-18 Negative or no kinetic salt effect at 93°C in pH 8 buffer. Initial drug concentration above the cmc, 25 mg/mL. Linear regression gives

$y = 0.987 - 0.0038x$	$r^2 = 0.976$	Argon-sparged
$y = 0.986 - 0.0080x$	$r^2 = 0.966$	Oxygen-sparged

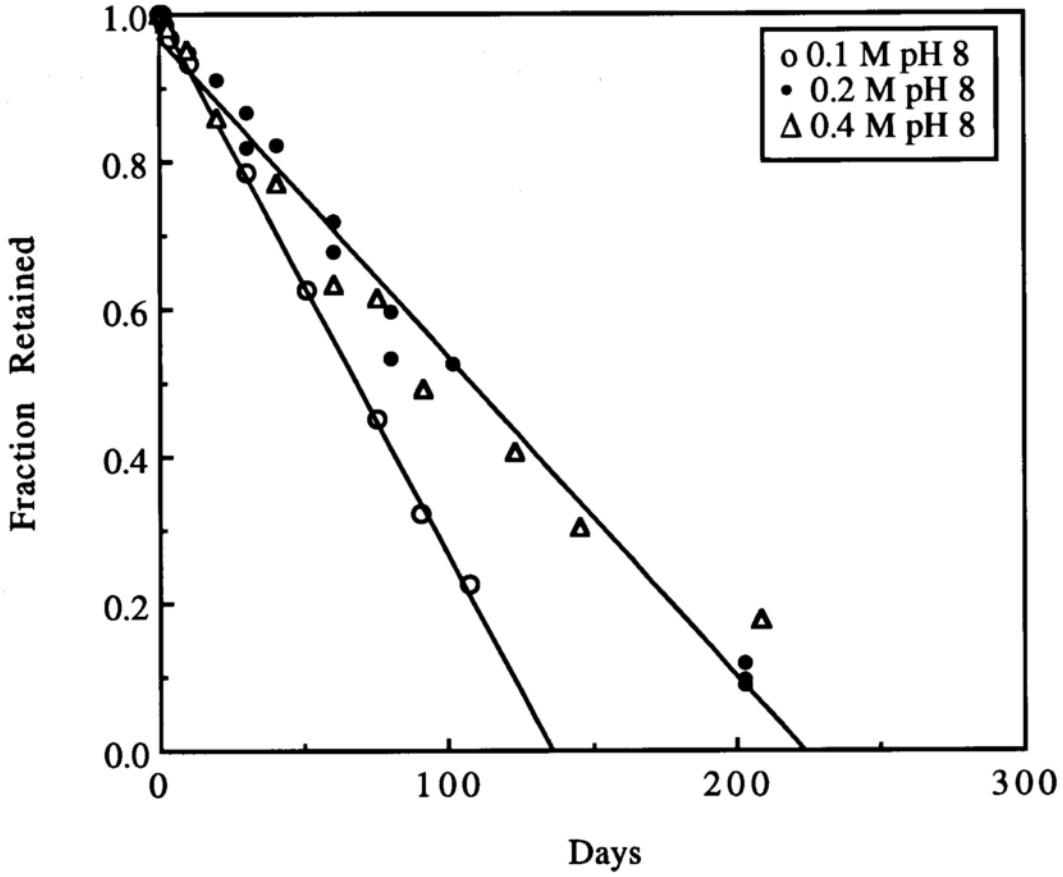

Figure VII-19 Negative kinetic salt effect at 93°C in pH 8 buffer; air headspace. Initial drug concentration above the cmc, 25 mg/mL.

pH 8, since a positive kinetic salt effect is observed without EDTA at pH 7, and for the most part a negative kinetic salt effect is observed at pH 8 in samples also containing EDTA.

Unfortunately, there are insufficient data to conclude whether the change in mechanism is due to the effect of trace metals or the effect of pH, but consistently, the data indicate that the mechanism at pH 7 is different from that at pH 8, and that at pH 8 the mechanism above and below the cmc may be different, and that argon vs oxygen-containing samples may degrade by a different mechanism. The latter was of course proven to be the case, as mentioned earlier.

The fact that a different mechanism operates under oxygen vs argon sparged systems at 93°C at pH 8 may also be deduced from the mass balance. In most cases in air headspace and argon-sparged systems, the area under the parent and cinnamate peaks sum to 100% of the initial drug concentration (Figures VII-20 and 21, Table VII-1), indicating that under these conditions, the cinnamate is the main decomposition product.

However, with oxygen-sparged samples, there is much more variability in the mass balance, and in many cases, the mass balance falls short of 100%, beyond experimental error (Table VII-1). In these samples, the cinnamate reaches a maximum level then levels off and perhaps starts to decline, as shown in Figure VII-22. This suggests that there is a third or other degradation product which is important in the oxygen-containing systems. It may well be that the cinnamate itself undergoes autooxidation by homolytic abstraction of the hydrogen at the carbon alpha to the double bond as has been

Table VII-1 Mass balance: cinnamate + parent peak areas. Pooled data from Appendix C.

	AIR HEADSPACE					ARGON PURGED					OXYGEN PURGED				
	N	mean	sem	sd	cv	N	mean	sem	sd	cv	N	mean	sem	sd	cv
93°C>cmc															
0.1M	8	0.997	0.009	0.027	2.7	9	1.008	0.016	0.049	4.8	10	0.888	0.054	0.171	19.3
0.2M	14	1.010	0.010	0.039	3.9	12	0.999	0.016	0.057	5.7	11	0.847	0.060	0.199	23.5
0.2M											8	0.947	0.026	0.073	7.7
0.4M	10	0.998	0.010	0.031	3.1	12	1.019	0.018	0.061	6.0	12	0.968	0.014	0.050	5.2
0.1Mμ	13	0.980	0.012	0.042	4.3	12	1.009	0.013	0.044	4.4	11	0.956	0.034	0.112	11.7
0.2Mμ	11	1.020	0.014	0.047	4.6	10	1.048	0.020	0.064	6.1	11	0.893	0.050	0.166	18.6
0.4MpH7	7	1.048	0.014	0.037	3.6	6	1.057	0.018	0.044	4.2	7	0.970	0.038	0.100	10.3
0.4MpH8	6	1.013	0.007	0.017	1.6	6	1.018	0.009	0.022	2.1	7	1.001	0.006	0.017	1.7
93°C<cmc															
0.1M	10	1.020	0.007	0.023	2.2	10	1.022	0.006	0.012	1.9	12	0.895	0.026	0.089	10.0
0.2M	10	1.034	0.008	0.025	2.5	10	0.962	0.022	0.070	7.3	12	0.918	0.019	0.067	7.3
0.4M	11	1.026	0.008	0.026	2.5	13	0.934	0.022	0.078	8.4	11	0.912	0.016	0.054	5.9
0.1Mμ	12	1.040	0.008	0.029	2.8	12	0.936	0.025	0.087	9.3	13	0.881	0.033	0.118	13.4
0.2Mμ	12	1.097	0.012	0.041	3.8	12	1.007	0.033	0.114	11.3	13	0.925	0.028	0.101	10.9
0.2Mμ						11	1.036	0.016	0.052	5.0					
0.4MpH7	7	0.839	0.039	0.104	12.4	6	0.838	0.056	0.135	16.1	7	0.772	0.068	0.180	23.3
0.4MpH8	7	0.912	0.022	0.057	6.3	8	0.853	0.031	0.087	10.2	7	0.770	0.066	0.175	22.7
75°C>cmc															
0.1M	12	0.971	0.006	0.021	2.2	10	0.983	0.006	0.018	1.8	8	0.966	0.006	0.017	1.8
0.2M	12	0.983	0.008	0.030	3.0	9	0.994	0.010	0.030	3.0	8	0.990	0.006	0.018	1.8
0.4M	12	0.984	0.005	0.016	1.7	8	0.988	0.004	0.012	1.2	11	0.990	0.010	0.032	3.2
60°C>cmc															
0.1M	9	0.990	0.004	0.011	1.1	9	0.977	0.004	0.011	1.1	9	0.997	0.009	0.026	2.6
0.2M	9	0.994	0.003	0.008	0.8	9	0.985	0.004	0.013	1.4	9	0.995	0.002	0.006	0.6
0.4M	9	0.998	0.003	0.009	0.9	9	0.995	0.002	0.007	0.7	8	0.990	0.006	0.018	1.8
60°C<cmc															
0.1M	9	0.993	0.007	0.021	2.2	8	1.005	0.006	0.018	1.8	9	0.984	0.009	0.026	2.7
0.2M	9	0.996	0.004	0.012	1.2	9	0.998	0.004	0.011	1.1	9	0.980	0.008	0.024	2.5
0.4M	9	0.997	0.004	0.012	1.2	9	0.954	0.013	0.039	4.1	9	0.996	0.004	0.013	1.3
OVERALL	23	0.997	0.002	0.048	4.9	23	0.984	0.011	0.052	5.3	23	0.935	0.014	0.067	7.2

sem=standard error of the mean=sd/√N; sd=standard deviation (n-1); cv=coefficient of variation=(sd/mean)*100%

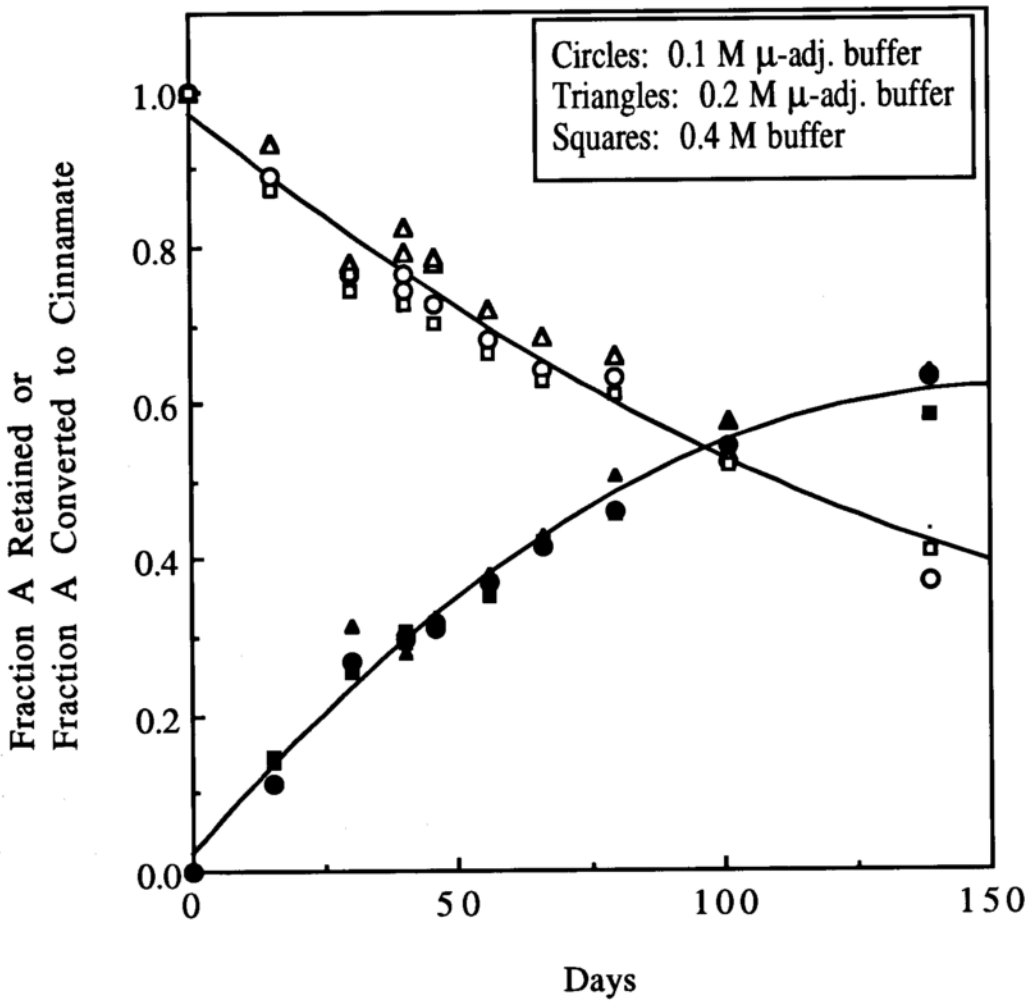

Figure VII-20 Mass balance for samples prepared in pH 8 buffers (μ=1.2) containing 0.2% EDTA.2Na and stored at 93°C with an air headspace. The initial drug concentration was 0.05 mg/mL. Where indicated, the ionic strength has been adjusted with KCl. Data from Appendix C. Curves drawn to guide the eye.

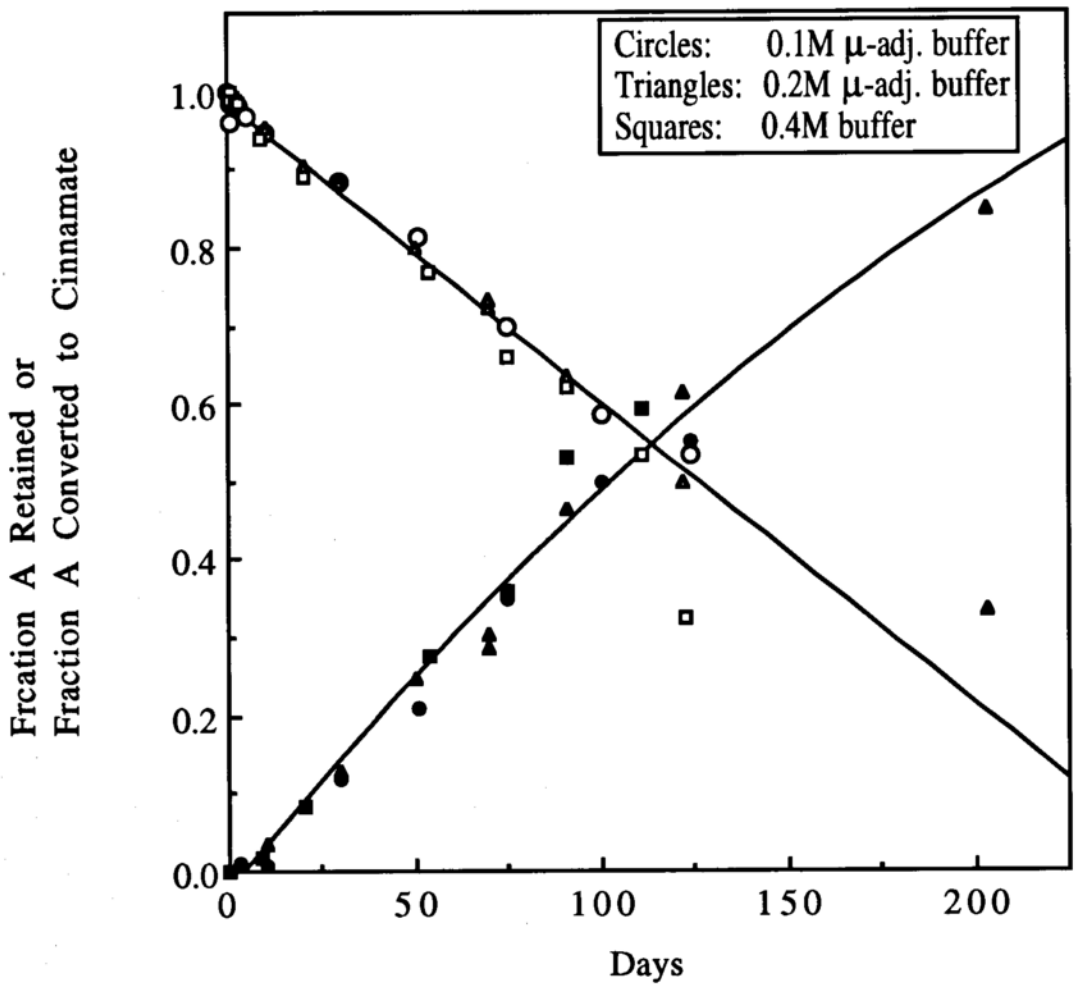

Figure VII-21 Mass balance for samples prepared in pH 8 buffers (μ=1.2) containing 0.2% EDTA.2Na, sparged with argon, and stored at 93°C. The initial drug concentration was 25 mg/mL. Where indicated, the ionic strength has been adjusted with KCl. Data from Appendix C. Curves drawn to guide the eye.

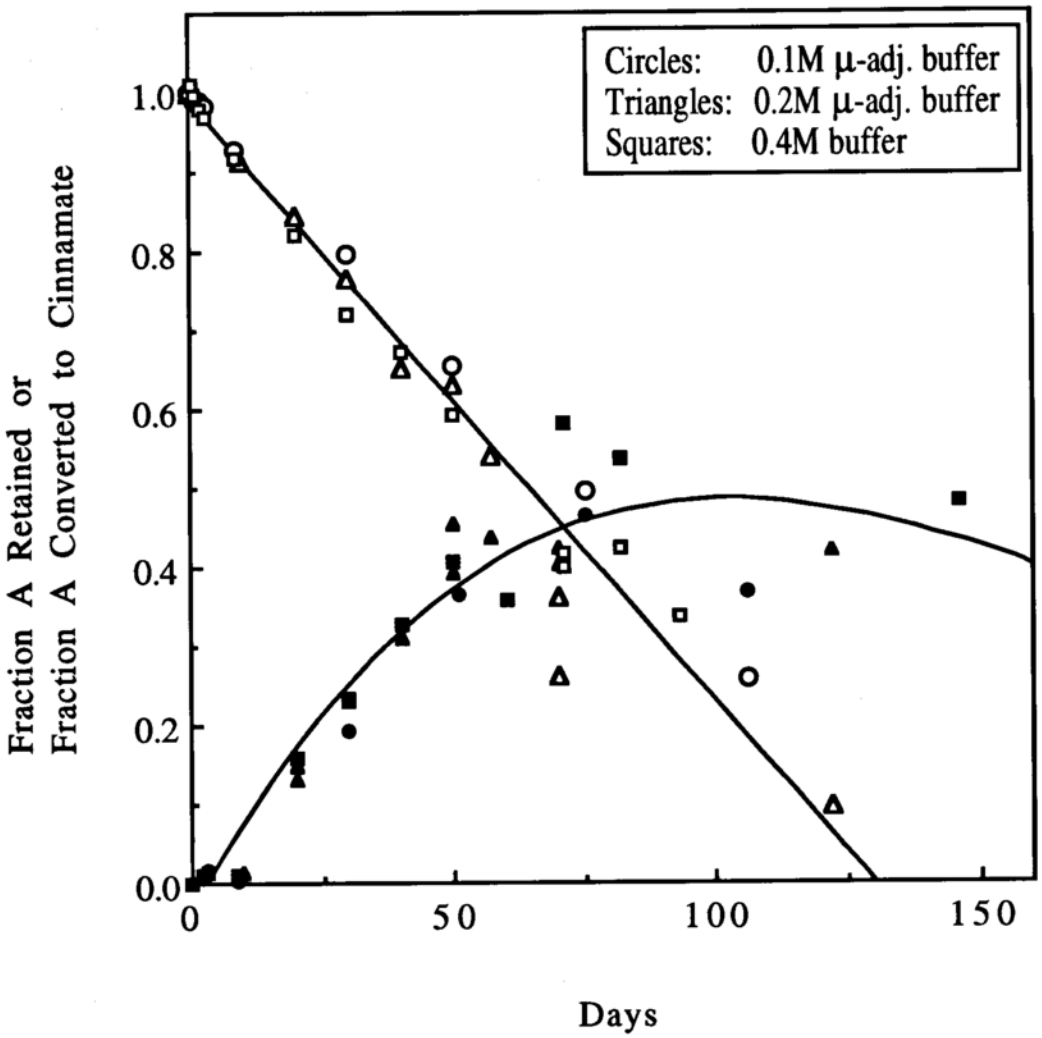

Figure VII-22 Mass balance for samples prepared in pH 8 buffers (μ=1.2) containing 0.2% EDTA.2Na, sparged with oxygen, and stored at 93°C. The initial drug concentration was 25 mg/mL. Where indicated, the ionic strength has been adjusted with KCl. Data from Appendix C. Curves drawn to guide the eye.

demonstrated for the linoleates, or "drying oils", or, by forming copolymers with oxygen by homolytic abstraction of one of the vinylic hydrogens, as demonstrated for styrene (Turney, Waters).

The chromatograms of samples sparged with oxygen were in fact "noisier", with more peaks eluting in or near the void volume, and many small peaks eluting at various retention times. No attempt was made however to identify these peaks, as this was beyond the scope of the study, and proper instrumentation was not at hand. There could possibly be sulfone formation, or the cinnamate could further degrade, as evidenced by a maximum in the concentration vs time profile for cinnamate (Figure VII-22). It should be kept in mind also, that the cinnamate was quantitated by assuming it had the same response factor as the parent drug, for lack of a standard. A sulfoxide peak was not prominent in any samples containing EDTA, and if present, was difficult to positively identify because several small peaks eluted nearby, and a standard was not available to confirm retention time.

The fact that argon sparged samples do not discolor (i.e., as one might assume, do not oxidize) and yet have decomposition rates of the same order of magnitude (albeit slower) than when oxygen is present would indicate that the rate-controlling reaction is one other than the oxidation step. It could, for instance be at pH 7, in light of the positive kinetic salt effect, that the reaction should more properly be written:

$$A^{=} + A_m^{2m-} \rightarrow A_{m+1}^{2(m+1)-} \longrightarrow \text{decomposes} \qquad \text{(VII-45)}$$

or,

$$A^{=} + A^{=} \rightarrow A_2^{4-} \longrightarrow \text{decomposes} \qquad \text{(VII-46)}$$

This is not unreasonable since the pH-values in the study are above the second pK of compound A. At pH 8 in the cases where a negative kinetic salt effect is observed, the decomposition reaction should include both a positive and a negative species.

The fact that argon-sparged samples did not discolor is also an indication of the efficiency of the sparging, and suggests that the decomposition of $A^{=}$ could well be a hydrolysis followed by oxidation rather than the opposite sequence.

Appendix to Chapter VII

From Eq. [VII-20] and [21] it is seen that

$$[A]^2 + [A]/2K - [A]_{obs}/2K = 0 \qquad \text{(VII-A-1)}$$

Solving using the quadratic formula (taking the positive root) gives

$$[A] = -1/4K + ((1/4K)^2 + [A]_{obs}/2K)^{0.5} \qquad \text{(VII-A-2)}$$

If

$$((1/4K)^2 + [A]_{obs}/2K) >> [A]_{obs}^2 \qquad \text{(VII-A-3)}$$

then

$$[A] \approx -1/4K + ((1/4K)^2 + [A]_{obs}/2K + ([A]_{obs})^2)^{0.5} \qquad \text{(VII-A-4)}$$

$$[A] \approx -1/4K + ((1/16K^2 + [A]_{obs})^2)^{0.5}, \text{ or} \qquad \text{(VII-A-5)}$$

$$[A] \approx [A]_{obs} \qquad \text{(VII-A-6)}$$

CHAPTER VIII. OXIDATION STUDIES IN THE PRESENCE OF EDTA.2NA AT DRUG CONCENTRATIONS IN EXCESS OF THE CMC

In the previous data treatment for studies done in pH 7 phosphate buffers without EDTA, a scheme was espoused whereby the molecule dimerized, and an autocatalytic decomposition of the dimer competed with an elimination (non-oxidative) decomposition of the monomer. This scheme proved to be quite satisfactory for much of the data generated at pH 7; a few anamolous data sets were ascribed to experimental error.

However, as mentioned above, the fact that the dimer could be in equilibrium with higher aggregates was not taken into account in the modeling, as was not the fact that the rates could be different above and below the cmc. The main reason these points were not addressed was because at that point, the values of the cmc had not been determined. Once these were defined, it became apparent that heretofore ascribed experimental error was in fact an indication that the aggregation state of the molecule was affecting the kinetic profile, and that modification of the scheme presented in Chapter VII might be appropriate. Such a modification might include an additional (higher) equilibrium.

In order to further explore this effect, as part of this thesis the kinetics were reexamined at lower buffer molarities (0.1, 0.2, 0.4 M) at pH 7 and 8 such that the initial drug concentration was either below the cmc or well above the cmc throughout at least four half-lives of the reaction. These further studies were done in the

presence of 0.2% EDTA.2Na in order to remove the complication of trace metal catalysis. In addition, by studying the kinetics under argon sparge, it was possible to eliminate the oxidation reaction pathway in order to determine the true elimination rate constant, k_2.

VIII-A. Species in the System, Meaning of A_{obs}

In dealing with self-associating systems, the situation is complicated by the multiple stepwise equilibria associated with micelle formation. The stepwise formation is as follows:

$$A + A \leftrightharpoons A_2 \qquad K_2 = [A_2]/[A]^2 \qquad [A_2] = K_2[A]^2 \qquad \text{(VIII-1)}$$

$$A_2 + A \leftrightharpoons A_3 \qquad K_3 = [A_3]/[A_2][A] \qquad [A_3] = K_3[A_2][A] = K_3K_2[A]^2 \qquad \text{(VIII-2)}$$

$$A_3 + A \leftrightharpoons A_4 \qquad K_4 = [A_4]/[A_3][A] \qquad [A_4] = K_4[A_3][A] = K_4K_3K_2[A]^4 \qquad \text{(VIII-3)}$$

$$\vdots \qquad\qquad \vdots \qquad\qquad \vdots$$

$$A_{(q-1)} + A \leftrightharpoons A_q \qquad K_q = [A_q]/A_{(q-1)}][A] \qquad A_q = K_q[A_{(q-1)}][A] \qquad \text{(VIII-4)}$$

$$\vdots \qquad\qquad \vdots \qquad\qquad \vdots$$

$$A_{(n-1)} + A \leftrightharpoons A_n \qquad K_n = [A_n]/[A_{(n-1)}][A] \qquad A_n = K_n[A_{(n-1)}][A] \qquad \text{(VIII-5)}$$

$$= (\prod_{(2\text{-->}n)} K_n)[A]^n \qquad \text{(VIII-6)}$$

where n is the aggregation number, and the K values represent the stepwise equilibrium constants.

For real micellar systems, K_q must gradually increase with q for values of low q, followed by an uncertain region when the sphere/rod transition is encountered, around q = 50-200, followed by a constant K_q at high values of q. That is, cooperative followed by anticooperative association phenomena are believed to be at play in

the formation of giant micelles, and the stepwise equilibrium constants are not equal (Mukerjee, 1977). This is difficult to model and the actual K_q values very difficult to determine (Muller) therefore, the following is used (Mukerjee, 1974)

$$K_2' < K_3 = K_4 ... = K_n = K \qquad \text{(VIII-7)}$$

which represents a step function in an approximate manner. K_2' is hypothetical and taken to be much less than the actual dimerization constant, and all equilibrium constants other than K_2' are consolidated into one constant K_m distinct from K_2'; that is

$$K_m = \prod K_3 K_4 ... K_n \qquad \text{(VIII-8)}$$

Values for n and K_m for a series of alkyl sulfates are given in Table VIII-1. From the summation as illustrated above, one obtains the following expression:

$$\frac{[A_{obs}]-[A]}{[A]} = \left(\frac{K_2'}{K}\right)\left(\frac{X}{1-X}\right) \qquad \text{(VIII-9)}$$

where X = K[A], that is,

$$[A_{obs}] = \frac{[A]^2 K_2'}{1-K[A]} + [A] \qquad \text{(VIII-10)}$$

Table VIII-1 Values for K_m and n for a series of sodium alkyl sulfates at 25°C (Aniansson).

	n	$K_m \approx$ n/cmc (M/l)
NaC_6SO_4	17	41
NaC_7SO_4	22	100
NaC_8SO_4	27	208
NaC_9SO_4	33	548
$NaC_{10}SO_4$	41	1227
$NaC_{11}SO_4$	52	3171
$NaC_{12}SO_4$	64	7273
$NaC_{14}SO_4$	80	39167
$NaC_{16}SO_4$	100	216667

Unfortunately, it is impossible to isolate A from this expression, so a simplification is used which treats all stepwise constants as equal. This is generally believed to be the case for molecules which form small aggregates (n<20), for example by stacking (dyes, purines and pyrimidines) rather than forming micelles. If there are j species in total, then

$$[A_{obs}] = [A] + [A_2] + [A_3] + \ldots\ldots [A_j] \qquad \text{(VIII-11)}$$

Assuming all the stepwise equilibrium constants to be equal,

$$= [A]\{1 + K[A] + K^2[A]^2 \ldots\ldots K^{j-1}[A]^{j-1}\} \qquad \text{(VIII-12)}$$

$$= [A]\{1 + X + X^2 \ldots X^q \ldots\ldots\} \qquad \text{(VIII-13)}$$

This latter is a geometric series and, assuming $X < 1$, has the sum:

$$[A_{obs}] = \frac{[A]}{1 - K[A]} \qquad \text{(VIII-14)}$$

or:

$$[A] = \frac{[A_{obs}]}{1 - K[A_{obs}]} \qquad \text{(VIII-15)}$$

It is noted that the final expressions for A_{obs} become identical when $K_2' = K$.

VIII-B. Order of the Reaction at Drug Concentrations in Excess of the cmc

The view put forth in the following argument is that even above the cmc there are going to be several non-micellar species (denoted A, A_2, ... A_m) in addition to the micellar species, A_n, but only one of the submicellar aggregates, A_m, decomposes and the others and the micelle do not:

$$A_m + O \rightarrow AO + A_{m-1} \qquad \text{(VIII-16)}$$

or in the anaerobic case:

$$A_m \rightarrow B + A_{m-1} \qquad \text{(VIII-17)}$$

where B is a decomposition product(s). Every time an A_m decomposes, the non-micellar species equilibrium must be reestablished by the loss of a monomer from the micelle, A_n:

$$A_n \rightarrow A_{n-1} + A \qquad \text{(VIII-18)}$$

$$A + A_{m-1} \rightarrow A_m \qquad \text{(VIII-19)}$$

This is a bit akin to the pseudo-zero order decomposition of suspensions where, in many cases, molecules in solution, when they decompose, are immediately replaced by a dissolving molecule.

For this thesis, a large series of experiments were carried out (Appendix C), and although one could graph each one, it would be preferable to place these in one graph so that the order of the reaction might be established.

To accomplish this, the following approach has been taken. If the data, instead of being plotted as a fraction retained as a function of time t, is plotted against a reduced time, $t/t_{0.5}$, where $t_{0.5}$ is the half life of the reaction, then all the data should fall into one plot. To demonstrate this, the decomposition data at concentrations above the critical micelle concentration in 0.1 M pH 8 buffer and in the presence of air are shown in Figure VIII-1. It is noted that the equation for the line is:

$$y = 1.0009 - 0.0073434x \qquad \text{(VIII-20)}$$

with $r^2 = 0.999$. More than justifiable significant figures have been included, for reasons that shall become apparent. The half life ($t_{0.5}$) can be calculated as:

$$0.5/0.0073434 = 68._1 \text{ days} \qquad \text{(VIII-21)}$$

where now the correct number of significant figures have been included.

The data in Figure VIII-1 can now be plotted as a function of $t_{0.5}$ as shown in Figure VIII-2.

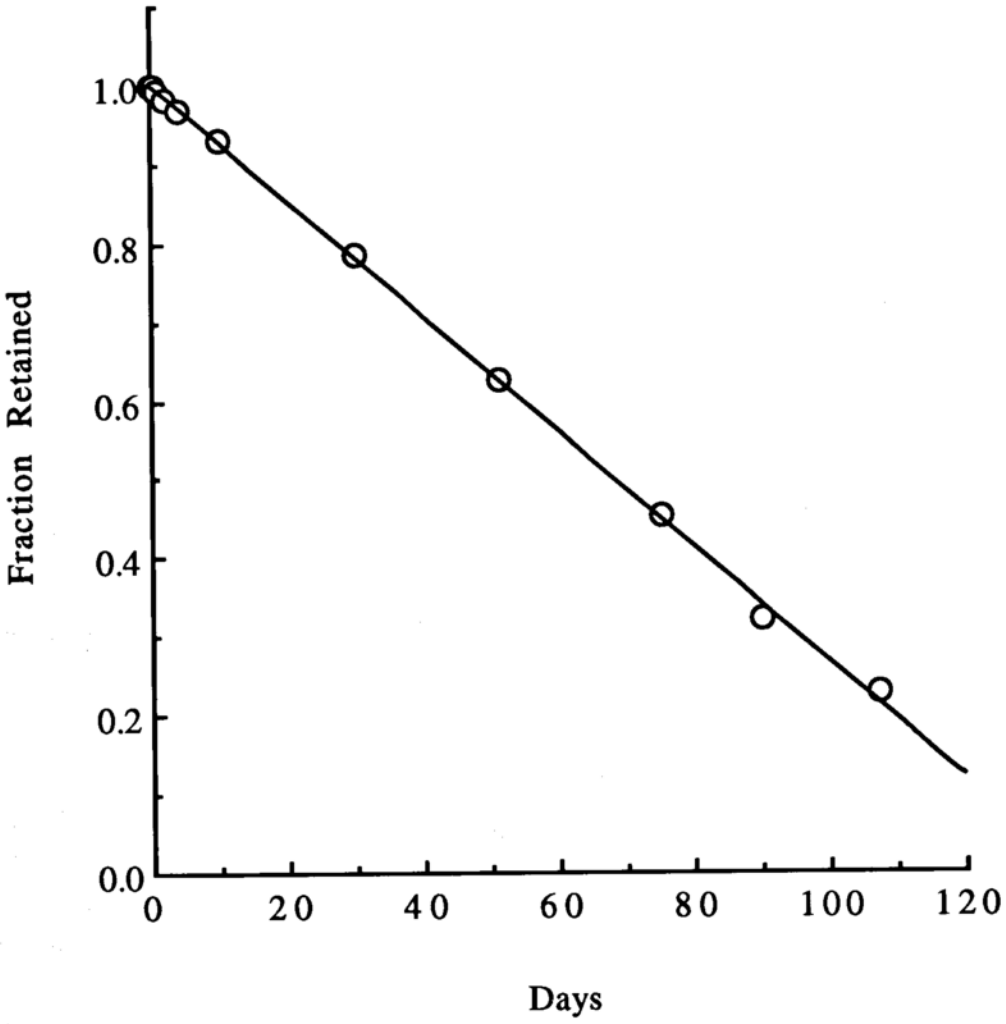

Figure VIII-1 Decomposition of A at 93°C in 0.1 M pH 8 phosphate buffer; air headspace. Initial drug concentration, 25 mg/mL.

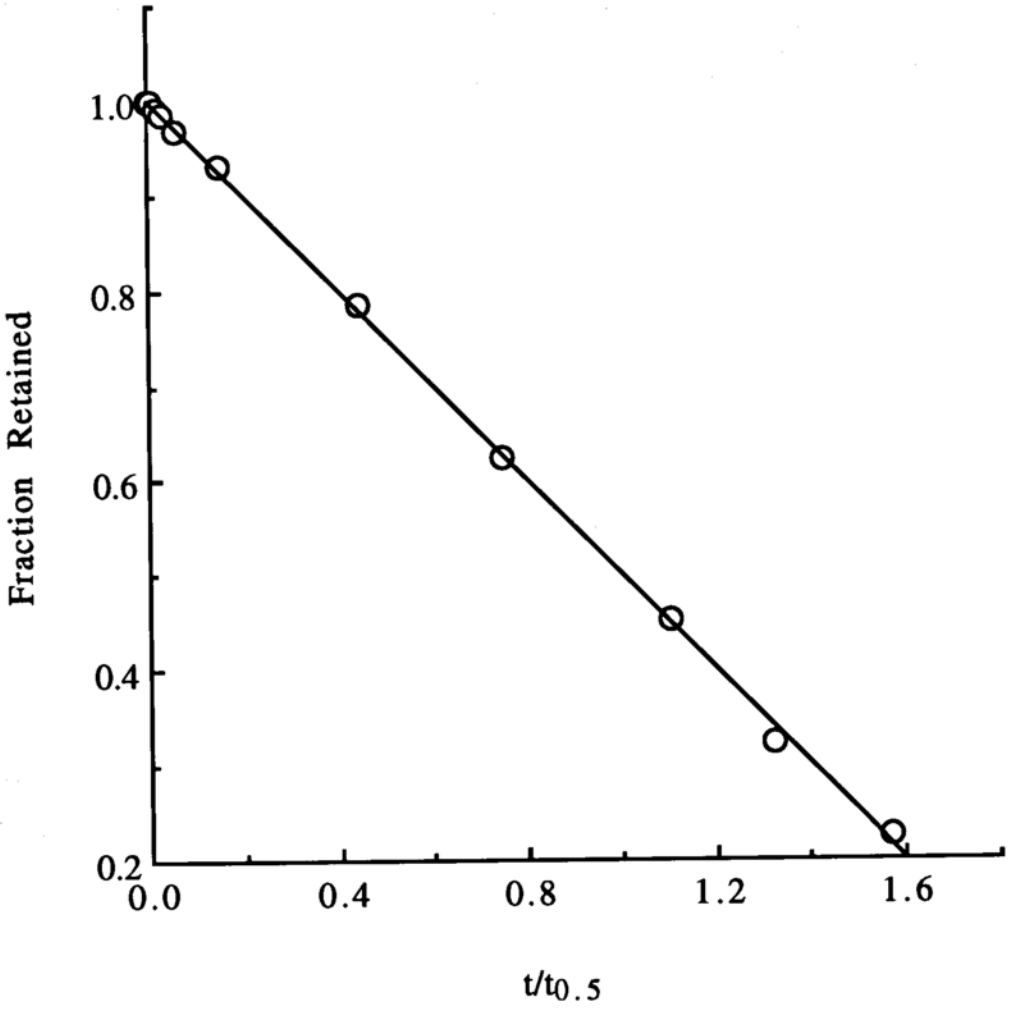

Figure VIII-2. Figure VIII-1 plotted against reduced time, where $t_{0.5}$ is $0.5/k_{obs}$.

The equation for the line in Figure VIII-2 is

$$y = 1.00 - 0.5x \qquad \text{(VIII-22)}$$

as it should be, i.e. the slope is 0.5, since $t/t_{0.5}$ is used as abscissa.

This data treatment allows data from all relevant experiments to be compared, and the Durbin-Watson test for curvature, which requires more than 20 data points, to be performed. Accordingly, all observed zero-order rate constants and half-lives for each condition at initial drug concentrations of 25 mg/mL have been calculated from the data in Appendix C and are reported in Table VIII-2. The reduced data are plotted in Figures VIII-3 and VIII-4. The data are obviously zero order and this lends credence to the model espoused above.

Now that the order of the reaction has been established at concentrations in excess of the cmc, the following two schemes are presented as possible mechanisms leading to such zero-order behavior in addition to the more general approach presented above.

VIII-C. Scheme I: Decomposition from the monomer

The simplest case would be if the aggregation number were 3 and the decomposing species were A, decomposing by parallel competing pathways to the sulfoxide, B, by an oxidation reaction via k_1, and to the cinnamate C, by an elimination or hydrolytic pathway via k_2:

Table VIII-2 Observed zero order rate constants (-slope) and half-lives of data generated in buffers of indicated molarity at an initial drug concentration of 25 mg/mL (above the cmc). Samples sparged with argon or O_2, or stored with an air headspace. Raw data, Appendix C. Buffers contain 0.2% EDTA.2Na to control for trace metal catalysis. μ indicates that the ionic strength has been adjusted with KCl to 1.2, the ionic strength of the 0.4 M pH 8 buffer with EDTA.2Na. At 93°C, pH 8, the mean represents the average of the data generated in buffers of the same ionic strength, namely, 0.4M, 0.1Mμ and 0.2Mμ; at all other conditions, data generated in 0.1 M, 0.2M and 0.4 M buffers have been averaged. r^2 = coefficient of correlation

Condition	Intercept	-10^3xSlope[a]	r^2	$t_{0.5}$	N	$k_{ox}x10^3$[b]
pH 8, 93°C (phosphate buffer with 0.2% EDTA.2Na)						
0.1 M Argon	0.983	4.60	0.982	108.7	11	--
0.2 M Argon	1.003	3.91	0.989	127.9	11	--
0.4 M Argon	0.991	4.18	0.996	119.6	11	--
0.4 M Argon	1.007	3.70	0.997	135.0	9	--
0.1 Mμ Argon	0.987	3.75	0.993	133.3	10	--
0.2 Mμ Argon	0.998	4.00	0.996	125.0	9	--
Mean		3.9±0.2		128.2±7.2		
0.1 M Air	1.000	7.34	0.999	68.1	11	2.74
0.2 M Air	0.973	4.37	0.989	114.4	14	(0.46)
0.4 M Air	0.996	5.53	0.991	90.4	11	1.35
0.4 M Air	0.998	6.09	0.997	82.1	9	2.39
0.1 Mμ Air	1.000	5.60	0.999	89.3	12	1.85
0.2 Mμ Air	1.004	6.10	0.995	82.0	9	2.10
Mean		5.8±0.3		86.0±4.5		1.9±0.4
0.1 M O_2	1.004	9.17	0.989	54.5	12	4.57
0.2 M O_2	0.996	6.94	0.995	72.0	6	3.03
0.4 M O_2	0.997	8.32	0.997	60.1	12	4.14
0.1 Mμ O_2	1.000	6.91	0.999	72.4	10	3.16
0.2 Mμ O_2	0.997	7.90	0.989	63.3	7	3.90
Mean		7.7±0.7		65±6		3.7±0.5
pH 7, 93°C (phosphate buffer with 0.2% EDTA.2Na, adjusted with KCl to the ionic strength of the 0.4 M pH 8 buffer)						
0.4Mμ Argon	0.995	5.09	0.996	98.2	8	--
0.4Mμ Air	0.982	9.61	0.974	52.0	7	4.52
0.4Mμ O_2	1.006	14.1	0.998	35.4	5	9.01

Table VIII-2 (continued)

Condition	Intercept	-10^3xSlope[(a)]	r^2	$t_{0.5}$	N	$k_{ox}x10^3$[(b)]
pH 8, 75°C (phosphate buffer with 0.2% EDTA.2Na)						
0.1M Argon	0.992	1.77	0.987	282.5	10	--
0.2M Argon	0.987	1.32	0.986	378.8	8	--
0.4M Argon	0.983	0.788	0.975	634.5	8	--
Mean		1.3±0.5		432±182		
0.1M Air	0.995	1.38	0.987	362.3	11	(-0.39)
0.2M Air	1.004	1.28	0.981	390.6	12	(-0.04)
0.4M Air	0.993	0.942	0.976	531.3	12	0.154
Mean		1.2±0.2		428±90		
0.1M O_2	0.991	3.15	0.990	158.7	8	1.38
0.2M O_2	0.981	2.28	0.953	219.3	8	0.96
0.4M O_2	0.982	1.49	0.973	335.6	11	0.70
Mean		2.3±0.8		238±90		1.0±0.3
pH 8, 60°C (phosphate buffer with 0.2% EDTA.2Na)						
0.1M Argon	0.985	0.247	0.882	2024	9	--
0.2M Argon	0.995	0.220	0.960	2273	8	--
0.4M Argon	0.998	0.153	0.824	3268	8	--
Mean		0.21±0.05		2522±658		
0.1M Air	0.989	0.244	0.896	2049	9	(-0.003)
0.2M Air	0.992	0.213	0.952	2347	9	(-0.01)
0.4M Air	0.999	0.226	0.926	2212	9	0.07
Mean		0.23±0.02		2203±149		
0.1M O_2	0.985	0.657	0.980	761.0	9	0.41
0.2M O_2	0.991	0.549	0.988	910.7	9	0.33
0.4M O_2	0.994	0.510	0.953	980.4	8	0.36
Mean		0.57±0.08		884±112		0.37±0.04

(a) k_{obs}

(b) $k_{ox} = k_{obs}$, oxygen or air *minus* k_{obs}, argon

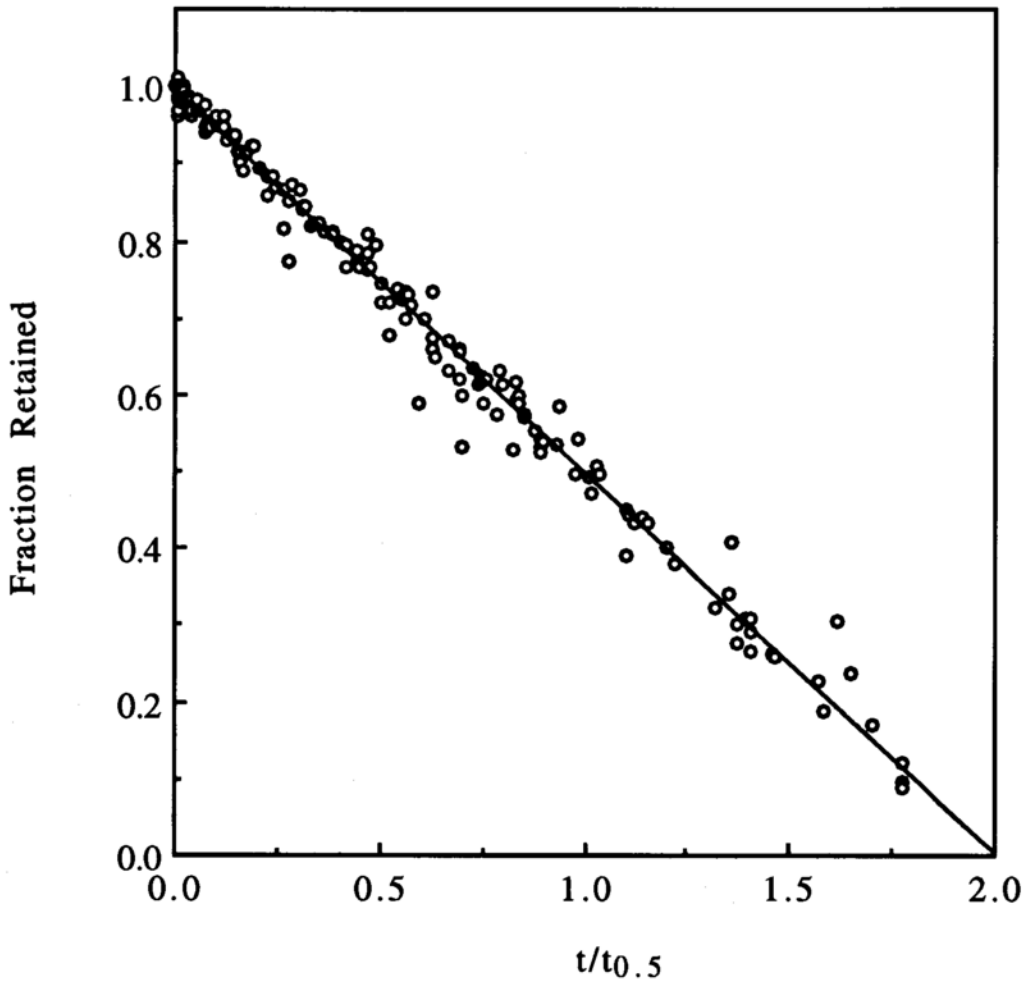

Figure VIII-3 All data at 93°C plotted against reduced time, where $t_{0.5} = 0.5/k_{obs}$. The linear regression equation is

$$y = 0.995 - 0.496x \qquad r^2 = 0.990$$

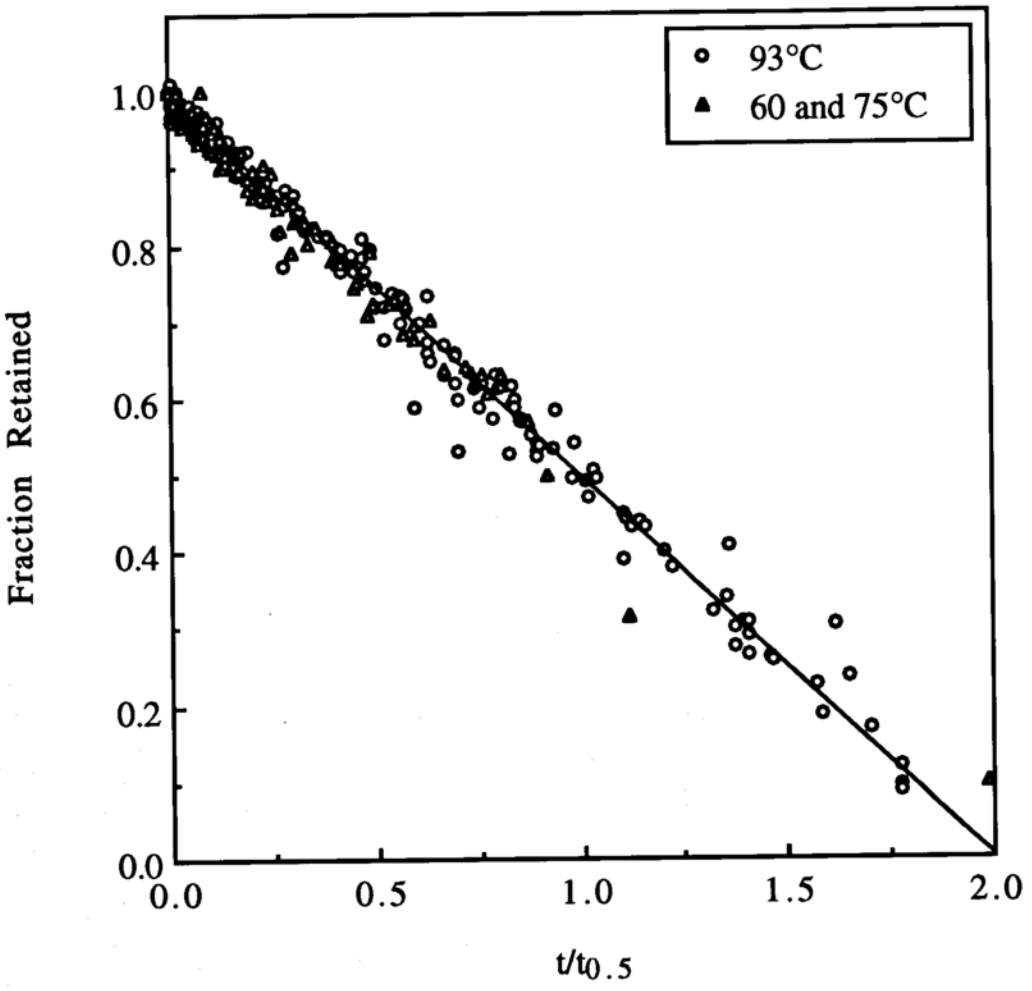

Figure VIII-4 Data at 60°C (oxygen sparge only) and 75°C superimposed on data at 93°C from Figure VIII-3. The linear regression for the two lower temperatures is

$$y = 0.988 - 0.490x \qquad r^2 = 0.977$$

and for the combined data

$$y = 0.992 - 0.493x \qquad r^2 = 0.988$$

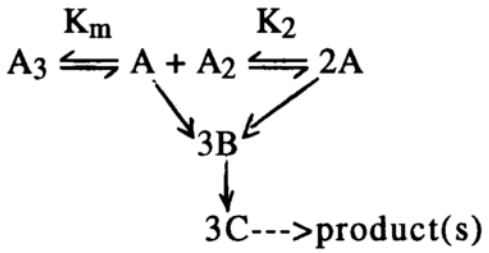

The stepwise reactions are then

$$2A \rightleftharpoons A_2 \qquad K_2 = \frac{k_f}{k_r} = \frac{[A_2]}{[A]^2} \qquad [A_2] = K_2[A]^2 \qquad \text{(VIII-23)}$$

$$A_2 + A \rightleftharpoons A_3 \qquad K_m = \frac{k'_f}{k'_r} = \frac{[A_3]}{[A_2][A]} \qquad [A_3] = K_m K_2 [A]^3 \qquad \text{(VIII-24)}$$

$$A \xrightarrow{k'_1} B \qquad \text{via } k_1[O], \text{ or } k_1' \qquad \text{(VIII-25)}$$

$$A \xrightarrow{k_2} C \qquad \text{via } k_2 \qquad \text{(VIII-26)}$$

$$A + A_2 = \text{cmc} \qquad \text{(VIII-27)}$$

$$A_3 = A_{obs} - \text{cmc} \qquad \text{(VIII-28)}$$

such that the net reaction is A_3+3A -->3B + 3C; f and r refer to forward and reverse rates of formation of higher aggregates. The differential equation describing the rate of disappearance of monomer is

$$\frac{d[A]}{dt} = -3k_1'[A] - 3k_2[A] - k_f[A]^2 + k_r[A_2] - k_f'[A_2][A] + k_r'[A_3] \quad \text{(VIII-29)}$$

Substituting for [A] and [A_3], and since $k_f/K_2 = k_r$, and $k_r' K_m = k_f'$

$$\frac{d[A]}{dt} = -3\sqrt{\frac{[A_2]}{K_2}}(k_1' + k_2) \quad \text{(VIII-30)}$$

As shown above, the concentration of A_2 remains essentially at steady state, such that the term $-3\sqrt{\frac{[A_2]}{K_2}}$ may be lumped into one constant ζ. Integration yields a *pseudo-zero-order* rate equation for kinetics done at concentrations above the cmc:

$$[A] - [A]_0 = -(k_1' + k_2)\zeta t \quad \text{(VIII-31)}$$

Because $[A] = [A_{obs}]/(1 - K[A_{obs}]A)$, it is difficult to evaluate this properly without knowledge of K. But, if one assumes

$$d[A_{obs}]/dt = d[A]/dt + d[A_2]/dt + d[A_3]/dt \quad \text{(VIII-32)}$$

and that $d[A_2]/dt$ is at steady state, i.e. is equal to 0 and that $d[A_3]/dt$ is negligible compared to d[A]/dt because we are working at very high drug concentrations (i.e., since A_3 is the highest species it

will have the smallest molar concentration, and the loss is assumed negligible, at least in the first half life of decomposition) then,

$$d[A_{obs}]/dt = d[A]/dt \qquad \text{(VIII-33)}$$

and the equation may be solved

$$[A_{obs}] - [A_{obs}]_0 = -3\zeta(k_1' + k_2)t \qquad \text{(VIII-34)}$$

$$= -3\zeta(k_o)t \qquad \text{(VIII-35)}$$

$$= k_{obs}t \qquad \text{(VIII-36)}$$

where $\zeta^2 = A_2/K_2$

For example, for the data set generated in 0.2 Mμ pH 8 with O_2 sparge at 93°C, this model gives $k_o = 0.30356$, and $\zeta = 0.0090729$, when the differential equation is solved numerically. The slopes of the zero-order plots are given in Table VIII-2, which, according to this scheme, either represent $-3\zeta(k_1' + k_2)$, in the case of oxygen sparge and air headspace, or $-3\zeta(k_2)$ in the case of argon sparge.

In the event of autocatalysis, the input function

$$k'' = k_1'[1 - A_{obs}] \qquad \text{(VIII-37)}$$

replaces k_1' although no evidence of autocatalysis was observed at drug concentrations above the cmc, at 93°C, in the presence of EDTA.2Na, even in oxygen-sparged samples. At 75°C, some

autocatalysis was evident as shown in Figure VII-14; at 60°C the reaction was only followed to less than one half-life due to time and sample constraints, so that autocatalysis, if present, was not evident.

By subtracting from the slope of the oxygen-containing samples the slope obtained from the argon-sparged samples, i.e., k_{ox}, one obtains, according to this scheme, $-3\zeta k_1'$. Since 3ζ is a constant, the *ratio* of the slopes $k_{ox}/k_{obs,\ argon}$ (Table VIII-3) gives the relative proportion of oxidative and non-oxidative and rates, which may be seen is close to 1 at 93°C at pH 8 when comparing oxygen and argon-sparged treatments. The slower rate in air reflects the fact that the rate constant k_1' is a product of the true rate constant and the oxygen concentration in solution; in a pure oxygen environment [O] in solution will be higher, albeit a constant.

VIII-D. Scheme II: Decomposition from the Dimer

Suppose it is the dimer, rather than the monomer which decomposes, and the aggregation number is again 3:

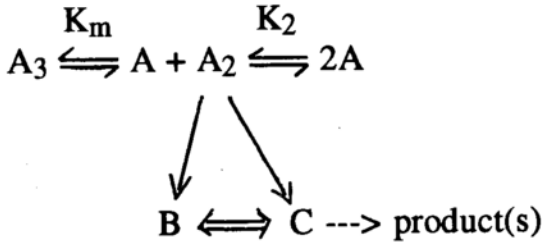

The governing equations are:

$2A \rightleftharpoons A_2$ $\quad K_2 = \frac{k_f}{k_r} = \frac{[A_2]}{[A]^2}$ $\quad [A] = \sqrt{\frac{[A_2]}{K_2}}$ (VIII-38)

$A_2 + A \rightleftharpoons A_3$ $\quad K_m = \frac{k'_f}{k'_r} = \frac{[A_3]}{[A_2][A]}$ $\quad [A_3] = K_m K_2 [A]^3$ (VIII-39)

$A_2 \xrightarrow{k'_1} B$ $\quad$ via $k_1[O] = k'_1$ (VIII-40)

$A_2 \xrightarrow{k'_2} C$ $\quad$ via k_2 (VIII-41)

Now, $[A_3] = (A_{obs} - cmc)$ (VIII-42)

and $cmc = [A_2] + [A]$ (VIII-43)

The differential equation describing the rate of disappearance of A_2 with time is

$$\frac{d[A_2]}{dT} = k_f[A]^2 - k_r[A_2] - k'_f[A_2][A] + k'_r[A_3] - k'_1[A_2] - k_2[A_2] \quad \text{(VIII-44)}$$

Substituting for $[A_3]$, K_2, and $[A]$, one obtains Eq. [VIII-45]

$$\frac{d[A_2]}{dT} = \frac{k_f[A_2]}{K_2} - k_r[A_2] - k'_f[A_2]\sqrt{\frac{[A_2]}{K_2}} + k'_r K_m [A_2]\sqrt{\frac{[A_2]}{K_2}} - k'_1[A_2] - k_2[A_2]$$

Realizing $k_f/K_2 = k_r$ and $k'_r K_m = k'_f$, one obtains

$$\frac{d[A_2]}{dT} = [A_2](-k_1' - k_2) \qquad \text{(VIII-46)}$$

Because[A_2] remains constant, this again represents a pseudo-zero order situation, and the solution is, in terms of fractions,

$$[A_2] = 1 - \zeta(k_1' + k_2)t \qquad \text{(VIII-47)}$$

where $\zeta = [A_2]$. The question remains, how is A_2 related to A_{obs}. If it is the mth species which decomposes, then

$$[A_m] = K^{m-1}[A] = K^{m-1}(A_{obs}/\{1-KA_{obs}\}) \qquad \text{(VIII-48)}$$

or

$$A_2 = K[A] = K(A_{obs}/(1-KA_{obs})) \qquad \text{(VIII-49)}$$

so that the integrated form of Eq. [VIII-46] is

$$A_{obs} = (1-\zeta k_1't-\zeta k_2t)(1-KA_{obs})/K \qquad \text{(VIII-50)}$$

By nonlinear curve fitting it *may* be possible to solve for ζ, k_1', k_2, and K, although the author could not do so successfully, or, one may assume as above that

$$d[A_{obs}]/dt = d[A]/dt + d[A_2]/dt + d[A_3]/dt \qquad \text{(VIII-51)}$$

and that K_2 is large such that the compound prefers to exist as a dimer (which is not an unreasonable assumption considering the shape of the molecule and the fact that many surfactants are known to exist as dimers or trimers rather than as monomers) (Mukerjee, 1967); and that $d[A_3]/dt$ is small compared to $d[A_2]/dt$, such that $d[A_{obs}]/dt$ is a good approximation for $d[A_2]/dt$. With these simplifications, the reaction is pseudo-zero order with a slope corresponding to $-\zeta(k_1'+k_2)$ where $\zeta = [A_2]$. In Scheme I, $\zeta=3\sqrt{(A_2/K_2)}$. From plots of cinnamate formed (Figures VII-20 through 22), one may see that oxygen-containing samples the cinnamate appears to decompose to another product although this will in no way affect the rate constant for the disappearance of the parent species.

VIII-E. Comments About Data Generated Above the Cmc

In Table VIII-3, the reader may confirm that including the 0.1 and 0.2 M buffer results at 93°C does not affect the average significantly, but increases the standard deviation (n-1) since the rate generated in the 0.1 M buffer is consistently higher than in 0.2 or 0.4 M pH 8 buffers. This reflects the negative kinetic salt affect as discussed earlier, which is most evident at 75°C, where an increase in buffer molarity is accompanied by a decrease in rate, resulting in a high standard deviation in the mean.

The fact that in all cases at pH 8, the compound appears to be more stable in the 0.4 M buffer than in lower buffer molarities

suggests a different reaction mechanism than at pH 7, where a positive kinetic salt effect was observed. This may be due to a structural change in the micelle (Esch) at high salt and/or drug concentrations (i.e. sphere to rod or to wormlike). Generally, a sphere-to-rod transition is thought to be induced by high salt or high surfactant concentration (Anacker; Corti; Mittal; Mukerjee, 1974). At pH 8, such a structural change may make certain portions of the molecule sterically hindered, thus slowing decomposition. This coincides with the observation that at high salt concentrations (above 0.2 M) there is deviation in the Corrin-Harkins plot.

In all cases at 93°C, samples sparged with argon remained clear and colorless, whereas samples containing oxygen turned yellow, indicative of sulfoxide formation. Thus, the slope obtained from the zero-order plot of data generated under argon-sparge reflects the non-oxidative (elimination) rate constant, whereas the slope obtained from data generated from oxygen-containing samples reflects contributions from both the non-oxidative and the oxidative degradation. Accordingly, the final column in Table VIII-2, k_{ox}, is the difference of the two, and reflects the oxidation rate constant (although it is not the true rate constant, as discussed under Schemes I and II).

By taking the ratio of k_{ox} and the slope obtained from the argon-sparged samples, one may get a feel for which pathway predominates under a given set of conditions. These data are calculated in Table VIII-3. As may be seen, at pH 8 at 93°C under oxygen sparge, the ratio suggest that the non-oxidative (elimination)

Table VIII-3 Ratio of k_{ox} to $k_{obs,\ argon}$, where k_{ox} is $k_{obs,\ Oxygen\ or\ air}$ *minus* $k_{obs,\ argon}$. Data from Table VIII-2.

	$(k_{ox}/k_{obs,\ argon})$			
	pH 8.93°C	pH 7.93°C	pH 8.75°C	pH 8.60°C
0.1 M Air	0.60	---	---	---
0.2 M Air	(0.12)	---	---	---
0.4 M Air	0.32	0.89	0.20	0.46
0.4 M Air	0.64	---	---	---
0.1 M μ Air	0.49	---	---	---
0.2 M μ Air	0.52	---	---	---
Mean	0.51±0.12			
0.1 M O_2	0.99	---	0.78	1.66
0.2 M O_2	0.78	---	0.73	1.50
0.4 M O_2	0.99	1.77	0.89	2.35
0.1 M μ O_2	0.84	---	---	---
0.2 M μ O_2	0.98	---	---	---
Mean	0.92±0.10		0.80±0.08	1.84±0.45

rate is of the same order of magnitude as the oxidation rate ($k_{ox}/k_{obs,\ argon}$ ca. 1), while at pH 7, it appears that oxidation predominates over elimination. This supports the theory that different mechanisms are at play at pH 7 vs pH 8, as also suggested by the opposing kinetic salt effects at these two pH's.

As expected, the oxidation rate predominates over the elimination rate at 60°C, where there is more oxygen in solution available for reaction. Similarly, the oxidation rate is higher in oxygen-sparged samples than in samples with air headspace, again reflecting the greater concentration of oxygen in solution in these samples, and the fact that the oxidation rate constant depends on the concentration of oxygen *in solution.*

At 75°C, some later time points (above 160 days) were omitted in the calculation of the k_{obs} for argon-sparged samples in Table VIII-2 due to formation of yellow color in these samples. This may be due to leaks in the system; these samples were stored in an oven as opposed to a silicone oil bath, and the stoppers tended to dry out and deform and lose the seal beyond ca. 160 days. Air-sparged samples at 75°C appeared to be more stable; here the seals were not punctured.

At 60°C, only ca. 10 - 20% degradation was achieved after 300 days in air/argon and oxygen-sparged samples, respectively, so the study was terminated due to lack of time and sample. At 60°C, the rates appear to be similar, but this may reflect the fact that the rate constant has been obtained from initial rates. When <10% decomposition is achieved it is impossible to distinguish between

zero and first order, therefore, only the oxygen-sparged sample data, which were at least 20% degraded, are shown in Figures VIII-3 and 4. The oxygen-sparged samples do appear to be zero order through 20% degradation. As observed at 75°C, it appears as though the compound is more stable in 0.4 M buffer than at lower buffer concentrations.

CHAPTER IX. OXIDATION STUDIES IN THE PRESENCE OF EDTA.2NA AT DRUG CONCENTRATIONS BELOW THE CRITICAL MICELLE CONCENTRATION.

Data from 93°C decomposition of the compound at drug concentrations below the critical micelle concentration are shown in an untransformed plot in Figure IX-1. It is difficult to judge whether these data are first, zero or some intermediate order. It is more desirable to place them on a common graph, and this has been done in the same manner as employed in the treatment of the data generated above the critical micelle concentration, as discussed in Chapter VIII. The half life for each curve in Figure IX-1 has been obtained by treating the data as first order, and dividing ln 0.5 by the slope; results are tabulated in Table IX-1. When the data in Figure IX-1 are plotted against reduced time, $t/t_{0.5}$, then Figure IX-2 results.

The data in Figure IX-2 are not linear, and this is much more evident from this figure than from Figure IX-1. With the larger number in the common set, the data can be treated by Durbin Watson statistics and show distinct curvature on the 99% confidence level.

Plotting the data generated below the cmc (Appendix C, initial drug concentration, 0.05 mg/mL) as first-order against reduced time (Table IX-1) allows comparison across treatments on a common graph, as shown in Figure IX-3.

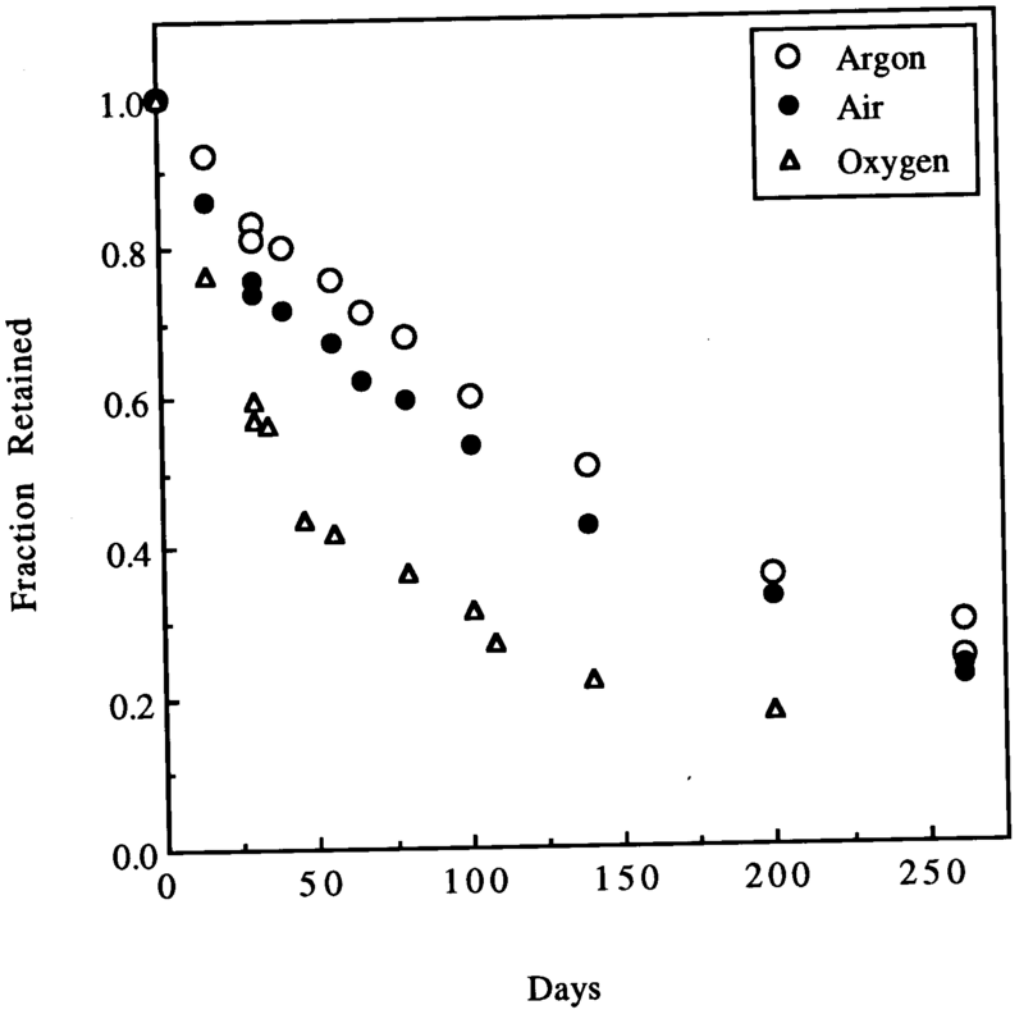

Figure IX-1 Data from 93°C below the cmc generated in 0.1 M pH 8 phosphate buffer with 0.2% EDTA.2Na (data from Appendix C).

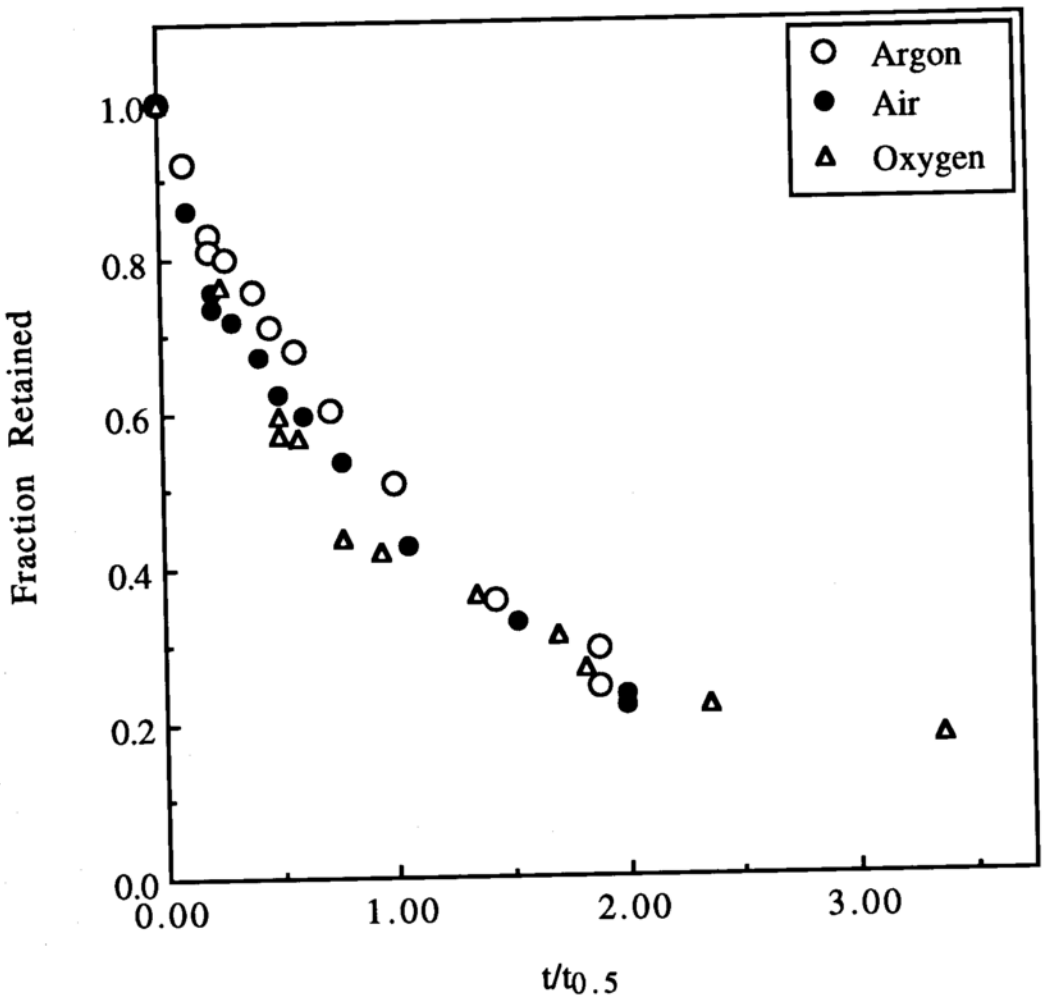

Figure IX-2 Data at 93°C generated in 0.1 M pH 8 phosphate buffer; initial drug concentration below the cmc (0.05 mg/mL); data from Appendix C and Table IX-1.

Table IX-1 First-order rate constants (-slope) from kinetic data generated at drug concentrations below the cmc, in pH 7 and 8 phosphate buffers of indicated molarity, containing 0.2% EDTA.2Na, in argon or oxygen sparged samples, or samples stored with an air headspace. Raw data from Appendix C.

Condition	10^2xInt.	-10^3xSlope	$r^{2(a)}$	$t_{0.5}^{(b)}$	N	$10^3 x k_{ox}$
pH 8, 93°C						
0.1M Argon	-1.57	4.96	0.991	139.7	13	--
0.2M Argon	-5.85	4.62	0.988	150.0	11	--
0.4M Argon	-13.7	5.29	0.965	131.0	13	--
0.1Mμ Arg.	-5.05	6.74	0.894	102.8	13	--
0.2Mμ Arg.	-0.758	5.45	0.983	127.2	10	--
Mean		5.83±0.80		120.3±15.3		
0.1M Air	-9.41	5.27	0.993	131.5	13	0.31
0.2M Air	-7.42	5.00	0.992	138.6	13	0.38
0.4M Air	-6.04	5.96	0.993	116.3	13	0.67
0.1Mμ Air	-4.08	6.01	0.978	115.3	13	(-0.73)
0.2Mμ Air	-10.7	5.43	0.986	127.6	13	(-0.02)
Mean		5.80±0.32		119.7±6.8		0.45±0.19
0.1M O_2	-19.1	10.1	0.951	68.6	11	5.14
0.2M O_2	-17.8	10.2	0.949	67.9	12	5.58
0.4M O_2	-17.0	10.8	0.967	64.2	11	4.84
0.1Mμ O_2	-10.1	13.2	0.946	52.5	13	6.46
0.2Mμ O_2	-10.7	11.9	0.933	58.2	13	6.45
Mean		12.0±1.2		58.3±5.8		5.69±0.74
pH 7, 93°C						
0.4Mμ Arg.	-2.49	9.53	0.969	72.7	9	--
0.4Mμ Air	-12.7	10.1	0.986	68.8	11	0.57
0.4Mμ O_2	-57.7	26.4	0.995	26.2	8	16.9
pH 8, 75°C (from initial rates, ignoring any autocatalysis)						
0.1 M Argon	1.25	2.39	0.961	290	10	--
0.2 M Argon	-1.69	1.33	0.983	521	9	--
0.4 M Argon	0.125	1.39	0.766	499	12	--
Mean		1.70±0.59		437±127		
0.1 M Air	0.925	1.79	0.978	387	13	(-0.60)
0.2 M Air	1.55	1.60	0.985	433	12	0.27
0.4 M Air	-0.041	1.13	0.971	613	12	(-0.26)
Mean		1.51±0.34		478±119		

Table IX-1 (continued)

Condition	10^2xInt.	-10^3xSlope	$r^{2(a)}$	$t_{0.5}{}^{(b)}$	N	$10^3 x k_{ox}$
pH 8, 75°C (from initial rates, ignoring any autocatalysis), continued						
0.1 M O_2	0.318	3.94	0.992	176	8	1.55
0.2 M O_2	320	2.68	0.970	259	8	1.35
0.4 M O_2	-0.805	1.87	0.979	371	11	0.48
Mean		2.83±1.04		269±98		1.13±0.57
pH 8, 60°C						
0.1M Arg	-0.831	0.056	0.148	12309	9	--
0.2M Arg	-0.802	0.083	0.256	8329	9	--
0.4M Arg	-2.87	0.296	0.416	2341	9	--
Mean		0.145±0.131		7660±5018		
0.1M Air	-0.156	0.564	0.984	1229	9	0.51
0.2M Air	0.565	0.437	0.936	1586	9	0.35
0.4M Air	0.895	0.357	0.946	1941	9	0.06
Mean		0.453±0.104		1585±356		0.31±0.23
0.1M O_2	-1.13	1.31	0.968	529	9	1.25
0.2M O_2	-0.515	0.915	0.971	757	9	0.83
0.4M O_2	0.354	0.759	0.986	913	9	0.46
Mean		0.995±0.284		733±193		0.85±0.40

(a) coefficient of correlation

(b) $0.693/k$

k_{ox} = (k_{obs}, oxygen or air) - (k_{obs},argon)

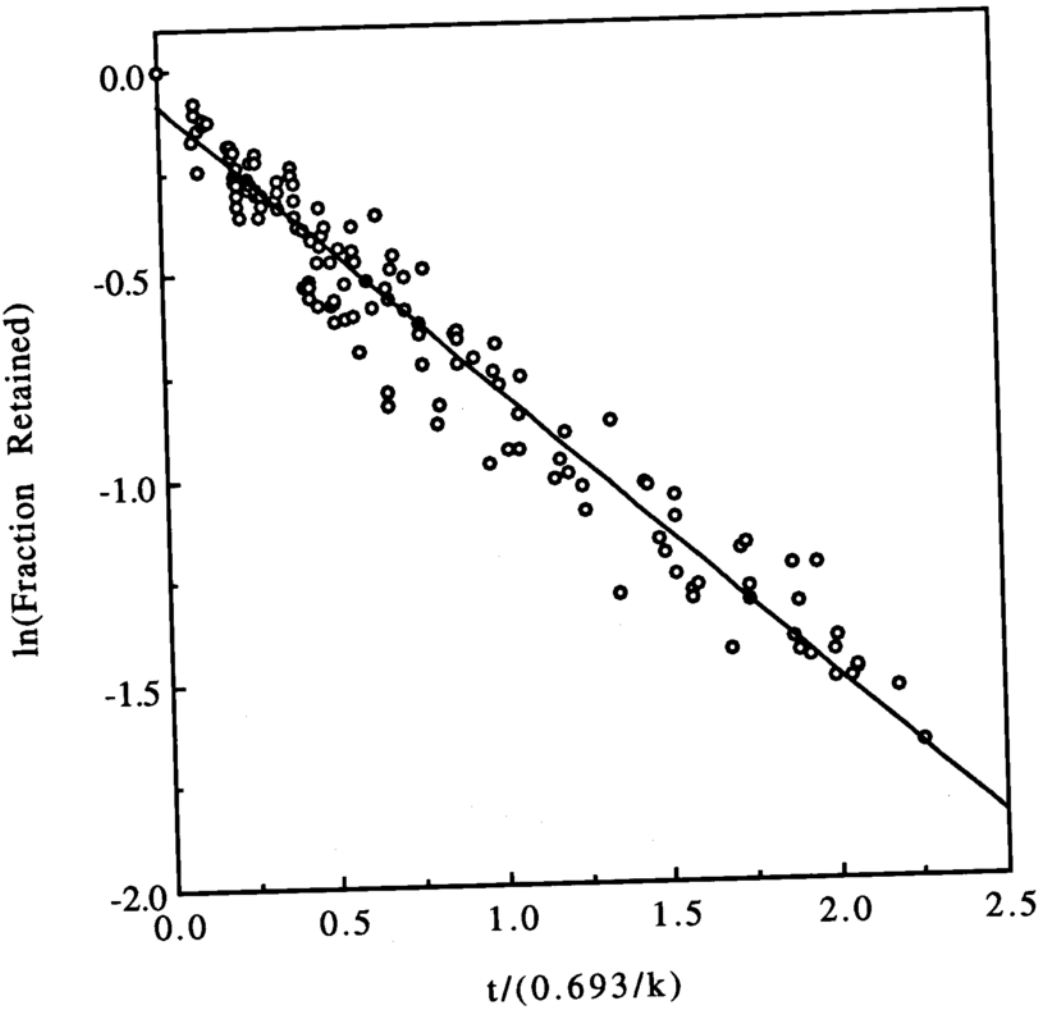

Figure IX-3 Data from Table IX-1 and Appendix C plotted against reduced time.

The linear regression for the pooled data in Figure IX-3 is

$$y = -0.0874 \ -0.704 \qquad r^2=0.956 \qquad \text{(IX-1)}$$

Theoretically the intercept should be 0 and the slope 0.693; it is seen the results agree well with theoretical, however there is considerable scatter about the line.

The fit may be improved by considering the following scenario. Below the cmc there will, again, be equilibria of the type:

$$A + A \rightleftharpoons A_2 \qquad \text{(IX-2)}$$

$$A + A_2 \rightleftharpoons A_3 \qquad \text{(IX-3)}$$

$$\vdots$$

$$A + A_x \rightleftharpoons A_{x+1} \qquad \text{(IX-4)}$$

As before, in the simplest point of view one might consider only one of the species, A_m, as decomposing. If the sum of concentrations other than A_m is denoted A_Σ then

$$[A_{obs}]=[A_m]+[A_\Sigma] \qquad \text{(IX-5)}$$

$$\frac{d[A_{obs}]}{dt}=\frac{d[A_m]}{dt}+\frac{d[A_\Sigma]}{dt} \qquad \text{(IX-6)}$$

If A_Σ were constant (actually, A_Σ diminishes as the overall concentration of A_{obs} decreases, but will be assumed constant at this point) then Eq. [IX-5] becomes:

$$\frac{d[A_{obs}]}{dt} = \frac{d[A_m]}{dt} = -k[A_m] = -k([A_{obs}] - [A_\Sigma]) \qquad \text{(IX-7)}$$

so that

$$\ln([A_{obs}] - [A_\Sigma]) = -kt + \ln([A_{obs}]_o - [A_\Sigma]) \qquad \text{(IX-8)}$$

where $[A_{obs}]$ is the fraction, F, retained and $[A_{obs}]_o$ is the initial concentration, which is 1 in terms of fractions.

If it is assumed that, in Eq. [IX-8], $A_\Sigma = 0.2$, then the least squares parameter values of each of the conditions shown in Table IX-2 below are obtained. Of course, the half-life would occur when A=0.5 of A_o; therefore the equation from which a half-life may be obtained would be

$$\ln\frac{(0.5-0.2)}{(1-0.2)} = kt_{0.5} \qquad \text{(IX-9)}$$

or,
$$t_{0.5} = 0.981/k \qquad \text{(IX-10)}$$

If all the data in Figure IX-1 are plotted as first-order versus this new reduced time, then the trace in Figure IX-4 is obtained.

Table IX-2 ln[Fraction - 0.2] versus time. Data at 93°C below the cmc from Appendix C (initial drug concentration = 0.05 mg/mL).

Condition	Intercept	-Slope$\times 10^3$	r^2	N	$t_{0.5}$[(a)]
pH 8, 93°C					
0.1 M Argon	-0.171	8.10	0.989	12	121.1
0.2 M Argon	-0.295	6.41	0.985	9	153.0
0.4 M Argon	-0.245	10.7	0.988	13	91.7
0.1 Mμ Argon	-0.215	10.5	0.956	12	93.4
0.2 Mμ Argon	-0.164	8.74	0.978	12	112.2
0.1 M Air	-0.282	8.64	0.992	11	113.5
0.2 M Air	-0.268	7.89	0.995	11	124.3
0.4 M Air	-0.233	9.71	0.989	12	101.0
0.1 Mμ Air	-0.258	8.28	0.974	11	118.5
0.2 Mμ Air	-0.172	8.63	0.986	13	113.7
0.1 M O_2	-0.201	23.3	0.962	11	42.1
0.2 M O_2	-0.203	22.4	0.976	12	43.8
0.4 M O_2	-0.271	21.5	0.979	9	45.6
0.1 Mμ O_2	-0.264	22.2	0.895	11	44.2
0.2 Mμ O_2[(b)]	-0.410	15.6	0.866	11	62.9
pH 7, 93°C					
0.4 Mμ Argon	-0.270	10.7	0.963	7	91.7
0.4 Mμ Air	-0.258	18.7	0.989	8	52.4
0.4 Mμ O_2	-0.178	42.0	0.963	5	23.4
pH 8, 60°C					
0.1 M O_2	-0.206	1.72	0.965	9	570.3
0.2 M O_2	-0.228	1.19	0.970	9	582.4
0.4 M O_2	-0.218	0.975	0.985	9	710.8

(a) 0.981/k

(b) aberrant data, not used

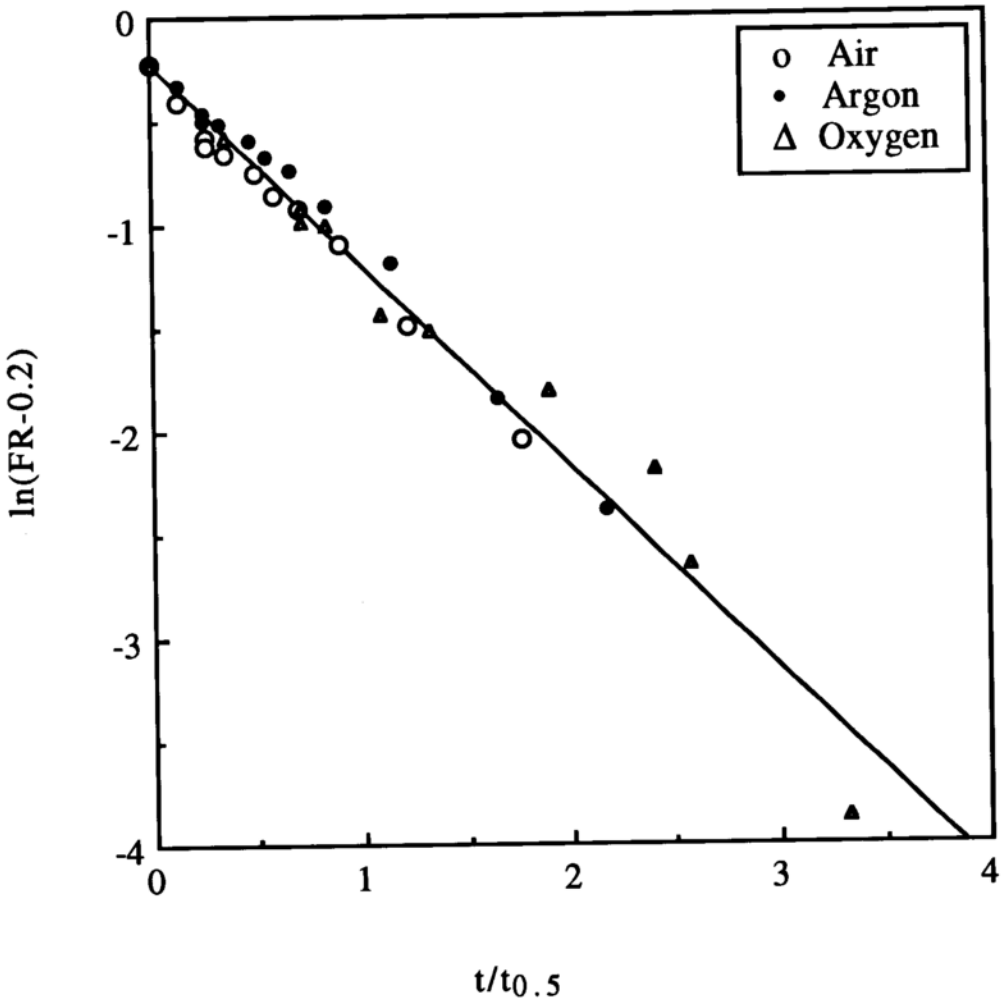

Figure IX-4 Data generated in pH 8 0.1 M buffer at 93°C; Figure IX-1, plotted against reduced time, where $t_{0.5} = 0.981/k$.

The least squares fit for the line in Figure IX-4 is

$$\ln[F-0.2] = -0.224 - 0.973\frac{t}{t_{0.5}} \qquad \text{(IX-11)}$$

with a correlation coefficient of 0.974. Data from all treatments are shown in Figure IX-5 and it is apparent that the trend is first order for the reaction below the cmc in pH 8 phosphate buffers at 93°C.

The linear regression for the pooled data in Figure IX-5 is

$$y = -0.232 - 0.980x \qquad r^2 = 0.977 \qquad \text{(IX-12)}$$

For both Figures IX-4 and 5, the intercept should be ln 0.8 = -0.223 which agrees well with the results obtained. It is not to be expected that the system is sufficiently well behaved to allow a single treatment past two half-lives, and in fact, in some cases, the last one or two time-points were omitted from Table IX-2 and in Figure IX-5; this is reflected by the difference in the value of N between the Tables IX-1 and 2.

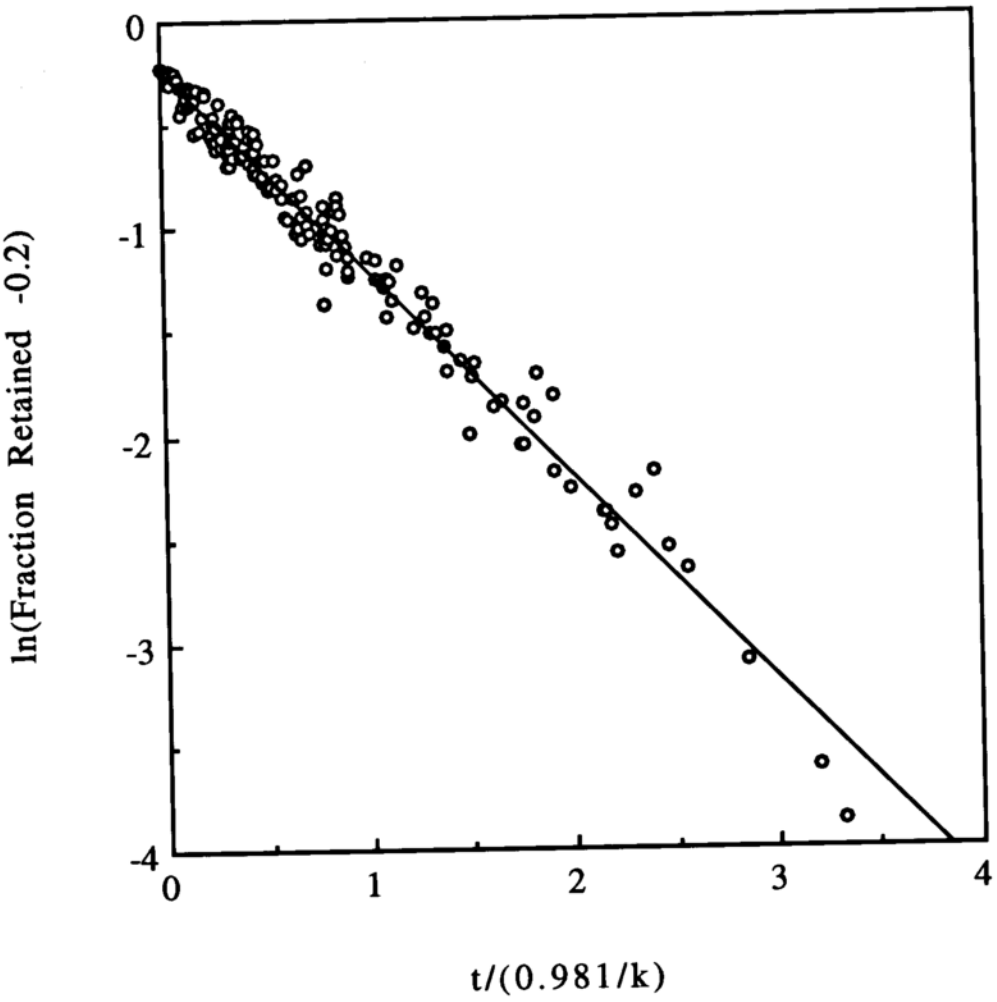

Figure IX-5 All data from Table IX-2 plotted against reduced time.

If necessary, the data can be refined by using values of A_Σ different from 0.2. The best presentation mode would be rewrite Eq. [IX-7] as:

$$\ln \frac{[A_{obs}]-[A_\Sigma]}{[A_{obs}]_o-[A_\Sigma]} = -kt \qquad \text{(IX-13)}$$

and impose the restriction that the intercept be zero, but this serves no purpose because, as mentioned, A_Σ is not constant.

To arrive at an expression more in line with actuality, reference is made to Eq. [VIII-48] and [IX-4], repeated here for convenience:

$$[A_m] = K^{m-1}[A] = K^{m-1}\left(\frac{[A_{obs}]}{1-K[A_{obs}]}\right) \qquad \text{(VIII-48)}$$

$$\frac{d[A_{obs}]}{dt} = \frac{d[A_m]}{dt} = -k[A_m] = -k([A_{obs}]-[A_\Sigma]) \qquad \text{(IX-6)}$$

Inserting the former in the latter now gives:

$$\frac{d[A_{obs}]}{dt} = -\frac{kK^{m-1}[A_{obs}]}{1-K[A_{obs}]} \qquad \text{(IX-14)}$$

$$\frac{d[A_{obs}]}{dt} = \frac{Q[A_{obs}]}{1-K[A_{obs}]} \qquad \text{(IX-15)}$$

where

$$Q = -kK^{m-1} \qquad \text{(IX-16)}$$

Eq. [IX-14] can now be written:

$$(1 - K[A_{obs}])\frac{d[A_{obs}]}{[A_{obs}]} = d[\ln[A_{obs}] - Kd[A_{obs}] = Qdt \qquad \text{(IX-17)}$$

which integrates to:

$$\ln[A_{obs}] - K[A_{obs}] = Qt + \ln[A_o] - K[A_o] \qquad \text{(IX-18)}$$

$$\ln[F] - KF = Qt - K \qquad \text{(IX-19)}$$

where F is fraction retained (based on A_{obs}) and where A_o is the original observed concentration of drug substance.

It should then be possible, by iterating K, to find the value of K which gives the best fit. Plots could then be made of (ln[F] - KF) vs t, from which r^2 may be determined.

When the correlation coefficients are plotted versus the iterant as in Figure IX-6, an optimum value of K should become apparent. But it should be pointed out, again, that such iteration in general has shown only that the term KA is sufficiently small so as not to make a difference in whether the data are plotted as Eq. [IX-20] or simply as first order

$$\ln[F] = -Qt \qquad \text{(IX-20)}$$

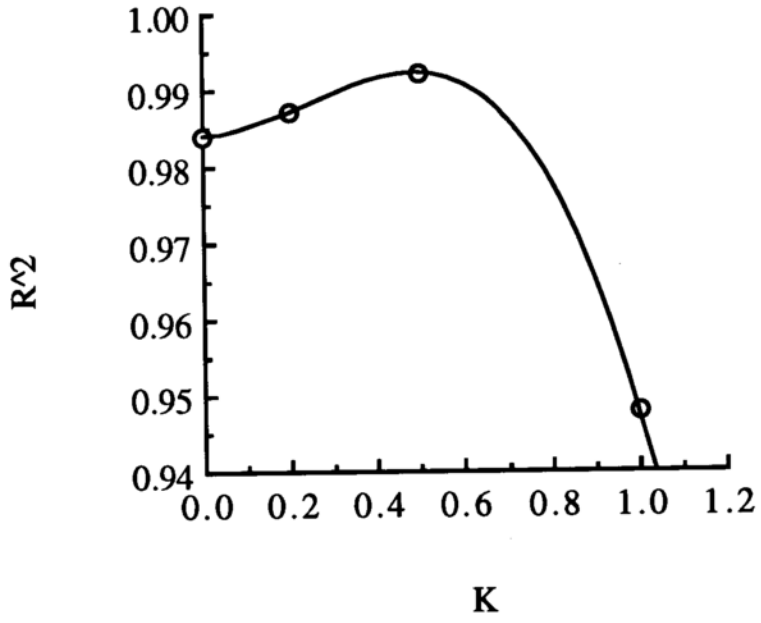

Figure IX-6 Example of Correlation Coefficients plotted as a function of the iterant, K.

Now that it has been established that the reaction is first order at drug concentrations below the cmc, the following schemes are presented which could account for such an observation, in addition to the general model discussed above.

IX-A. Scheme I: Simultaneous Decomposition from the Monomer and the Dimer

In the simplest case in the absence of autocatalysis, if n=3, then below the cmc, no A_3 will be present; only the dimerization will be important. The scheme could be the same as that developed for degradation in the presence of trace metals at pH 7. The relevant differential equation is Eq. [VII-26]:

$$\frac{d[A_{obs}]}{dT} = -2Kk_1'[A]^2 - k_2[A]$$

Even if one assumes that [A] = [A_{obs}], this still remains a nonlinear differential equation, and must be solved numerically.

IX-B. Scheme II: Parallel Decomposition From The Monomer

At pH 8, below the cmc, the scheme might be:

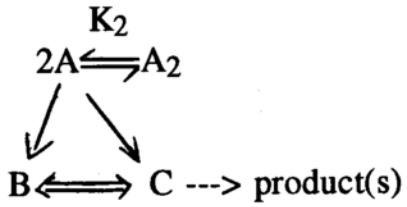

The relevant stepwise reactions are

$$2A \rightleftharpoons A_2 \qquad K_2 = \frac{k_f}{k_r} = \frac{[A_2]}{[A]^2} \qquad [A_2] = K_2[A]^2 \qquad \text{(IX-21)}$$

$$2A \xrightarrow{k_1'} B \qquad \text{via } k_1[O] = k_1' \qquad \text{(IX-22)}$$

$$2A \xrightarrow{k_2} C \qquad \text{via } k_2 \qquad \text{(IX-23)}$$

The differential equation describing the rate of disappearance of A would be

$$\frac{d[A]}{dT} = k_r[A_2] - k_f[A]^2 - k_1'[A]^2 - k_2[A]^2 \qquad \text{(IX-24)}$$

Substituting for $[A_2]$ and realizing that $k_rK_2 = k_f$, one obtains

$$\frac{d[A]}{dT} = 2[A](-k_1' - k_2) \qquad \text{(IX-25)}$$

The reader can verify that if one started with the expression

$$\frac{d[A_{obs}]}{dT} = \frac{d[A]}{dT} + 2\frac{d[A_2]}{dT} \qquad \text{(IX-26)}$$

one would, after simplification , also obtain Eq. [IX-25] except the left hand side would be $\frac{d[A_{obs}]}{dT}$. Eq. [IX-25] integrates to a first-order expression. The problem is equating [A] with $[A_{obs}]$.

$$[A_{obs}] = [A] + 2[A_2] = [A] + 2K_2[A]^2 \qquad \text{(IX-27)}$$

[A] can be expressed in terms of $[A_{obs}]$ by solving the quadratic equation, and $[A_2]$ can be expressed in terms of $[A_{obs}]$. Inserting these into Eq. [IX-24] would give the desired kinetic equation. However, it is simpler to proceed as follows.

IX-C. Scheme III: Parallel Decomposition From The Dimer

A parallel pathway such as the following fits much of the data generated below the cmc at pH 8, although such a scheme does not fit as well the data generated at pH 7. This further supports the notion that different mechanisms are at play at pH 7 in the presence of trace metals and at pH 8 in the presence of the metal chelating agent EDTA.2Na. The scheme for decomposition from the dimer would be

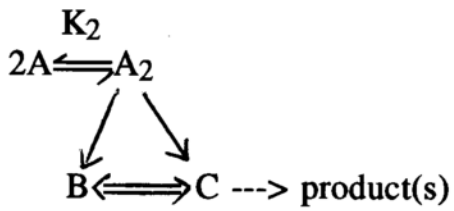

The relevant stepwise reactions are then

$$2A \rightleftharpoons A_2 \qquad K_2 = \frac{k_f}{k_r} = \frac{[A_2]}{[A]^2} \quad [A_2] = K_2[A]^2 \qquad \text{(IX-28)}$$

$$A_2 \xrightarrow{k_1'} B \qquad \text{via } k_1[O] = k_1' \qquad \text{(IX-29)}$$

$$A_2 \xrightarrow{k_2} C \qquad \text{via } k_2 \qquad \text{(IX-30)}$$

The differential equation describing the rate of disappearance of $[A_2]$ would be, after simplification:

$$\frac{d[A_2]}{dT} = -k_1'[A_2] - k_2[A_2] \qquad \text{(IX-31)}$$

Integrating again provides a first-order expression for kinetics below the cmc, which is what is observed experimentally in the absence of autocatalysis.

$$[A_{obs}] = A + 2A_2 \qquad \text{(IX-32)}$$

$$[A_{obs}] = \sqrt{\frac{[A_2]}{K_2}} + 2[A_2] \qquad \text{(IX-33)}$$

In this case, if K_2 is assumed to be very large, implying that the molecule exists preferentially as a dimer, which is not unreasonable (Mukerjee, 1967)[12], then

$$[A_2] = \frac{[A_{obs}]}{2} \qquad \text{(IX-34)}$$

allowing Eq. [IX-30] to be solved:

$$\ln \frac{[A_{obs}]}{[A_{obs}]_o} = -(k_1' + k_2)t = -k_{obs}t \qquad \text{(IX-35)}$$

At 93°C, the plots are first order, indicative of no autooxidation. The values for k_2 may be obtained directly from the slopes of the first-order plots (ln fraction A_{obs} retained vs time) of data generated under argon-sparge. By difference, one may obtain k_1' in the air and oxygen-sparged system, that is

---

12 Such a dimer might be

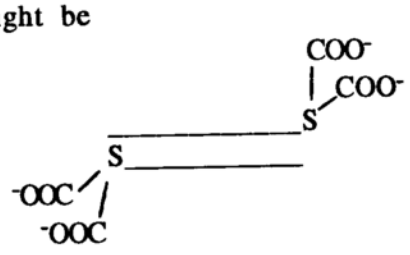

$$k_{obs} = k_1' + k_2 \qquad \text{(IX-36)}$$

These values and values of the ratio $k_{ox}/k_{obs,\ argon}$ are found in Table IX-3. In the presence of autooxidation, the input function

$$k_1''=k_1'(1-[A_{obs}]) \qquad \text{(IX-37)}$$

would replace k_1'

The differential equation simplifies to

$$d[A_{obs}]/dt = -k_1'[A_{obs}] + k_1'[A_{obs}]^2 - k_2(A_{obs}) \qquad \text{(IX-38)}$$

which cannot be solved in closed form because it is nonlinear, but can be solved numerically. Data generated at 60°C under oxygen sparge have been fitted to this equation in Figures IX-7 and IX-8.

IX-D. Comments About Data Generated at Drug Concentrations Below the cmc

It is obvious from this data treatment in Table IX-3 that oxidation becomes much more important at lower temperatures relative to the elimination rate, as was found at drug concentrations above the cmc. It is also interesting to note that the oxidation rate decreases relative to the elimination (non-oxidative) rate as the buffer molarity is increased at 60°C, but remains fairly constant at 93°C.

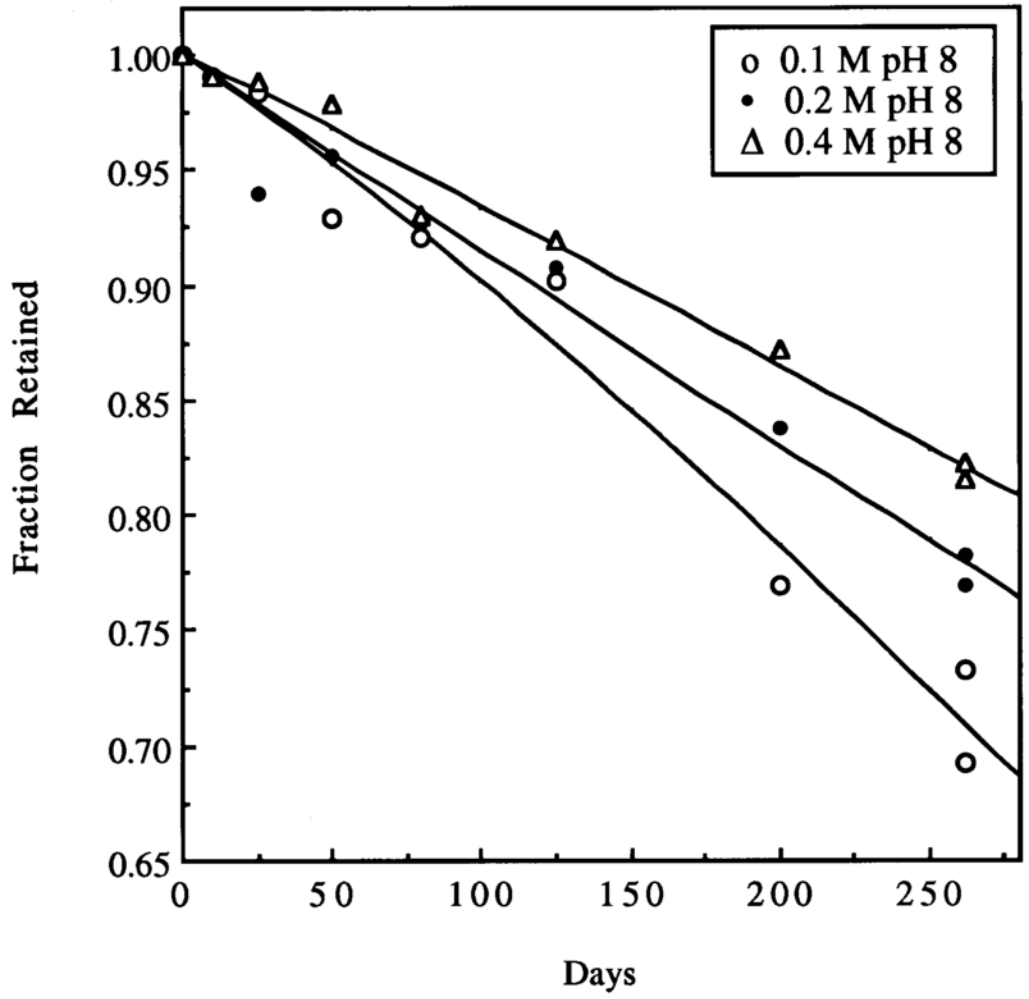

Figure IX-7 Data generated at initial drug concentration below the cmc (0.05 mg/mL) at 60°C with oxygen sparge (from Appendix C). The fit shown is by numerical integration of Eq. [IX-38]; the parameter estimates obtained are given in Table IX-4.

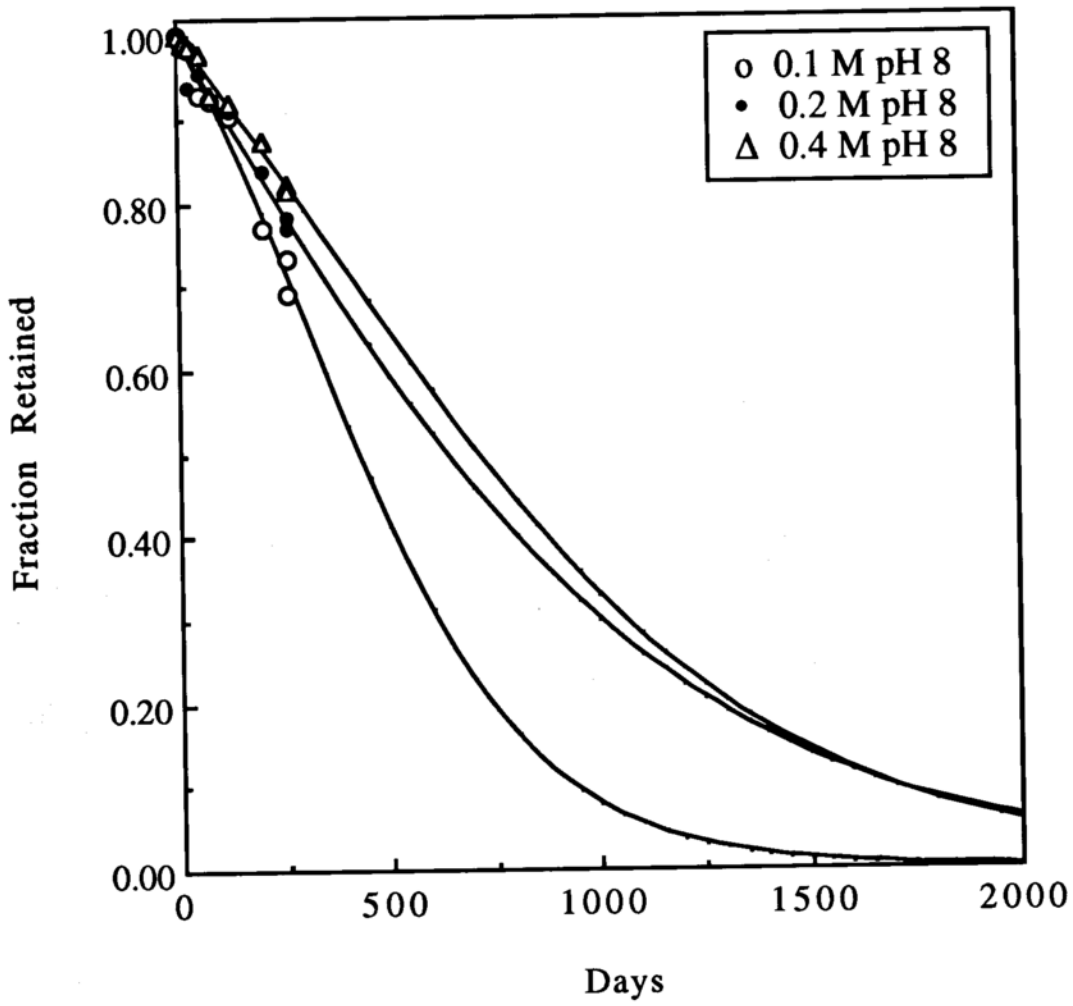

Figure IX-8 Simulation of Eq. [IX-38] to 2000 days using the parameter estimates given in Table IX-4. At later time points, the autooxidation should manifest itself. Symbols are experimental data (from Figure IX-7) obtained at 60°C with oxygen sparge. Extended time points used to show complete theoretical profile.

Table IX-3 Ratio of $k_{ox}/k_{obs,argon}$ for data generated at drug concentrations below the cmc.

$k_{ox} = k_{obs,\ oxygen\text{-}sparge\ or\ air\ headspace} - k_{obs,\ argon\text{-}sparged}$, from Table IX-1.

	$(k_{ox}/k_{obs,argon})$		
	pH 8.93°C	pH 7.93°C	pH 8.60°C
0.1 M Air	0.06	---	9.06
0.2 M Air	0.08	---	4.21
0.4 M Air	0.13	0.06	0.20
Mean	0.09±0.04		4.49±4.44
0.1 M O_2	1.04	---	22.2
0.2 M O_2	1.21	---	9.98
0.4 M O_2	0.92	1.77	1.55
0.1 M μ O_2	0.96	---	---
0.2 M μ O_2	1.18	---	---
Mean	1.06±0.13		11.2±10.4

Table IX-4 Estimates of k_1' and k_2 obtained by numerical integration of Eq. [IX-38]. The data generated in argon sparge contain too much scatter to allow direct comparison with the numerically integrated estimates for k_2, but they are presented in Table IX-1 for reference.

	$k_1' \times 10^4$	$k_2 \times 10^4$
0.1 M pH 8	30.939	8.8636
0.2 M pH 8	8.9938	8.5247
0.4 M pH 8	13.565	6.3683

At 60°C, under air and argon, less than 20% degradation was monitored. Since these are insufficient to distinguish between zero and first order these data have not been treated further, thus are missing from Table IX-2 and Figures IX-3 and IX-5. Under oxygen sparge, up to ca. 30% degradation was monitored, and these data, which have been treated as first order, have been included in the data treatment.

IX-E. Analogy with Suspension

In a suspension, the concentration in solution is the drug's equilibrium solubility, which is a constant at a given temperature. This concentration remains constant as long as there are suspended particles which serve as a reservoir of solid drug, resulting in a pseudo-zero order process, as demonstrated below.

For $$C \xrightarrow{k_1} Product \qquad \text{(IX-39)}$$

$$\frac{dC}{dt} = -k_1 C \qquad \text{(IX-40)}$$

For decomposition from a suspension:

$$\frac{dC}{dt} = -k_o(Solubility) \qquad \text{(IX-41)}$$

where $$k_o = k_1 S \qquad \text{(IX-42)}$$

Solubility is constant at a given temperature, so the reaction is pseudo-zero-order (Martin):

$$C = C_o - k_o t \qquad \text{(IX-43)}$$

When all the suspended particles are dissolved, the system changes to a first-order reaction. Similarly, the drug studied in this thesis was shown to degrade by a zero-order process as long as micelles were present, and by a first-order process below the cmc. This could only be the case as long as the decomposition did not occur from the micelle, but rather from a sub-micellar aggregate, for which the concentration remains constant as discussed in Chapter VIII.

It was also observed for the drug studied in this thesis, that the energy of activation obtained from an Arrhenius plot of data generated at drug concentrations above the cmc was higher than that below the cmc, as shown in Figure IX-9. Again, this is analogous to what is found with suspensions, that is, the energy of activation from a suspension is higher than from solution because it includes the heat of solution of the drug, as illustrated below:

From Eq. [IX-42]: $$\log k_o = \log k_1 + \log S \qquad \text{(IX-44)}$$

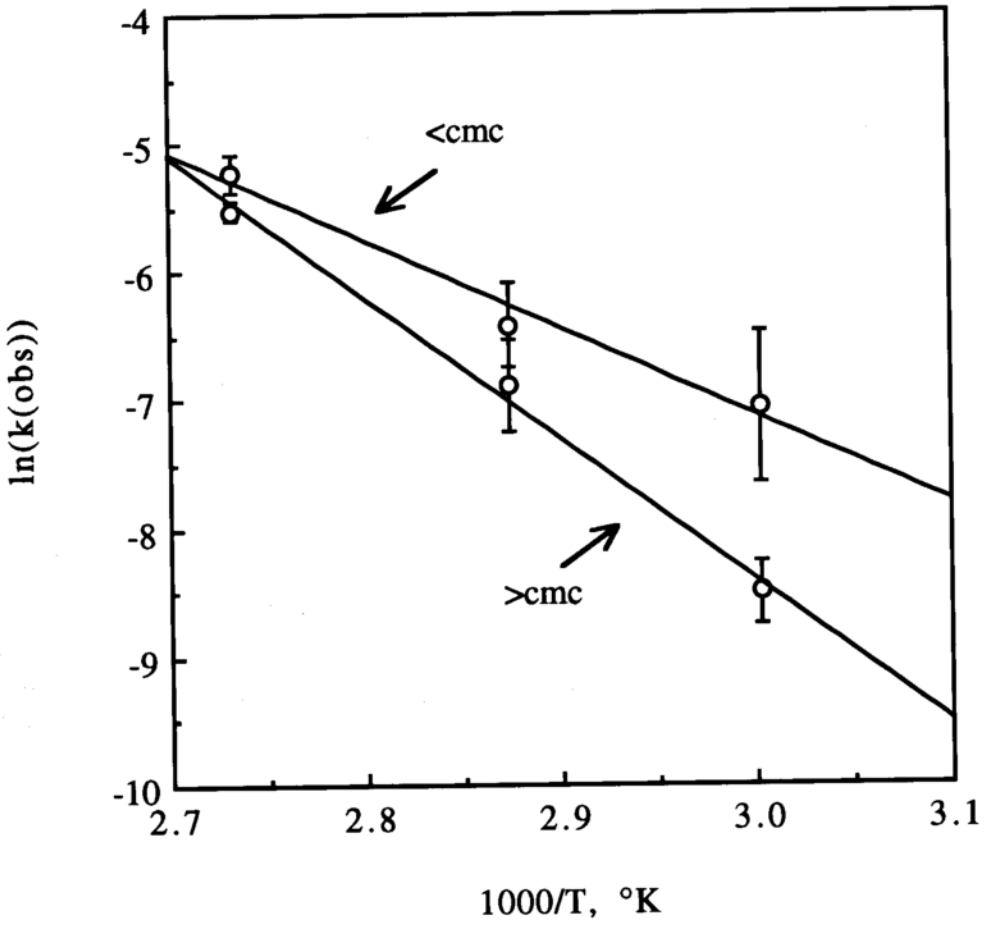

Figure IX-9 Arrhenius plot, argon sparge, for pooled data obtained in 0.1, 0.2, and 0.4 M pH 8 buffers. The E_a values are 21.3 kcal/mol and 13.9 kcal/mol at drug concentrations above and below the cmc, respectively. Data from Table VII-5 and Figures VII-7 and 8.

From Arrhenius and Van't Hoff:

$$\log k_o = -\frac{E_a}{RT} + Z_1 - \frac{\Delta H_{soln}}{RT} + Z_2 \qquad \text{(IX-45)}$$

$$\log k_o = \frac{(E_a + \Delta H_{soln})}{R}(\frac{1}{T}) - Z \qquad \text{(IX-46)}$$

In the case of the amphiphile herein studied, the higher energy of activation observed above the cmc may reflect contribution from the heat of micellization, that is the heat when a monomer is released from the micelle (Motsavage).

This analogy is not meant to imply that all surfactants will behave in this manner, only to show that in this case, it does. In many cases only a change in rate is observed, not a change in order because decomposition occurs simultaneously from the micelle and submicellar aggregates.

IX-F. Cautionary Remarks

There are some factors that may complicate the picture presented in Chapters VII, VIII, and IX. For example, the decomposition products B and C may form mixed micelles with A. It is also possible that EDTA.2Na may form mixed micelles with A (EDTA.2Na was present at a concentration of 5 mM, and the drug was present at a concentration of 0.1 mM (0.05 mg/mL) or 51 mM (25

mg/mL). However, in the presence of EDTA, the cmc was not much different from that in water, in fact, it was affected only to the extent that the counterion concentration was increased, due to the fact that the EDTA was present as the disodium salt. This would suggest that the effect of EDTA on micelle formation is minimal.

In addition, samples run in pH adjusted water vs pH adjusted 0.1% EDTA had nearly identical pseudo first-order rate constants, again suggesting that EDTA does not interfere with the micelle, that it only serves to sequester the metal ion, and may aid in solubilizing the degradation products by salting in (Master's Thesis).

The value of the present study with respect to the Master's Thesis is that herein one had a definite idea of what the cmc would be in a given system (given buffer concentration), and hence drug concentrations could be chosen high enough to guarantee virtual excess of micelles throughout the study, or at a concentration low enough so that micelles will not be present at any time during the study.

X. SUMMARY

The solution kinetics of an amphiphilic drug prone to oxidation have been shown to depend in a complicated way on temperature, drug concentration, and buffer concentration. Specifically:

1. In solution, the drug aggregates, and was found to have a cmc in H_20 of 8.8 mM. The cmc was found to be affected by buffer concentration, and, at high counterion concentrations, the amphiphilic behavior followed the Mukerjee and Chan extension of the Corrin-Harkins relation:

$$\log cmc = a - b*\log(C_S + cmc) - k_S(C_S + cmc)$$

2. In solution, in the presence of oxygen and trace metals, the drug decomposed to a sulfoxide by an autooxidative route which was trace metal catalyzed. This route competed with a non-oxidative *elimination reaction* from which the cinnamate analog was formed:

$$A + A \longleftrightarrow A_2$$

$$+ \text{ oxygen}$$

$$cinnamate \longleftrightarrow sulfoxide$$

3. In solution, and in the *absence* of trace metals: the drug decomposed by *zero order* kinetics at concentrations above the cmc and by *first order* kinetics at concentrations below the cmc. The explanation for this is sought in the view that a submicellar species, probably the dimer, decomposes, whereas the micelle and other n-mers do not. Analogous to decomposition from a suspension, whenever a dimer decomposes, it is replenished by the micellar pool, hence the decomposition appears zero order, because the concentration of the decomposing species remains constant.

4. The energies of activation for the thermal and oxidative routes were consistently higher at drug concentrations above the cmc than below the cmc at both pH 7 (no EDTA) and pH 8 (with EDTA). The difference may be due to the heat of micellization. This is analogous to suspensions, where the observed energy of activation from the Arrhenius plot is the sum of the energy of activation for the reaction plus the heat of solution.

XI. CONCLUSIONS

1. These findings suggest that reaction mechanisms for the decomposition of the drug in solution at pH 7 and 8 are concentration dependent, and different.

2. The autooxidation of the drug is marked by sigmoidally-shaped kinetic profiles, and the reaction order is different above and below the cmc. Therefore, one would expect very complicated kinetic profiles if, during the course of the autooxidation reaction, the drug concentration should drop below the cmc.

3. Therefore, care should be taken in the design of kinetic studies and interpretation of kinetic data generated for surface-active compounds, and, Arrhenius extrapolation from data on compounds prone to oxidation should be done with caution.

XII. SUGGESTIONS FOR FUTURE WORK

1. The scope of this thesis included investigation of the kinetics of the model compound at pH 7 and 8 with phosphate buffers, slightly above the second pK_a of the compound. Additional studies could be conducted with other buffer salts, and at other pH values. It is expected that below the pK_a, the solubility would be greatly reduced, and the aggregation state of the molecule would not be an issue.

2. Additional studies might be conducted in solvents, or mixed solvents, for example in methanol/H_2O with and without oxygen. In addition to affecting free radical formation, this would cause micellar inversion, which would be expected to affect the rate of reaction.

3. The determination of an aggregation number, for example by light scattering, may help elucidate the size and structure of the molecule, and confirm the result obtained by geometrical considerations. These studies would have to be conducted at low and high salt concentrations, that is, under the same experimental conditions as the kinetic studies. NMR and circular dichroism studies may also help in this regard.

4. Since the compound is amphiphilic, when the solid compound is in contact with limited amounts of moisture, a liquid crystalline gel would form. It would be of interest to determine the kinetics of decomposition from the gel at various temperatures, in an inert as well as in an oxygen atmosphere.

5. Partition coefficients at a variety of drug concentrations may provide interesting correlations regarding the association of the molecule in both aqueous and organic phases and the kinetics of decomposition in these phases. It may also show whether the drug could be delivered transdermally, since surfactants are known to be penetration enhancers.

APPENDIX A

ON THE NONLINEARITY OBSERVED IN THE CORRIN-HARKINS RELATION AT HIGH COUNTERION CONCENTRATIONS: A POSSIBLE MEANS OF ESTIMATING THE CMC IN H_20 WHEN LIMITED QUANTITIES OF SURFACTANT ARE AVAILABLE.

As mentioned above, critical micelle concentrations (cmc) plotted logarithmically against log(total counterion concentration) were found to deviate from linearity at high counterion concentration. These data could be fitted to a modification of the Corrin-Harkins relation as proposed by Chan (1993) and Mukerjee (1993) which is a derived relation consistent with the historical interpretation of micellization.

It is also noted that empirically the data can be shown to be linear when the logarithm of the cmc is plotted against the square root of ionic strength (μ) of added salt. Plotting the data in this manner gives reasonable estimates of the cmc in H_20 when extrapolated to zero μ, which could be useful for predicting the cmc values in H_20 of surfactants in limited supply, such as investigational new drugs. This should not replace the actual determination when sufficient surfactant is available, however, since this represents an extrapolation rather than an interpolation, and such estimates can be incorrect in some cases. It may also be possible to use this relationship to determine or confirm the ionic strength of an unknown solution.

The empirical relationship that was observed to linearize these data is

$$\log(cmc) = \log(cmc_o) + \sqrt{\mu} \qquad [A\text{-}1]$$

where μ represents ionic strength of the salt or buffer and cmc_o is the cmc in H_20. Note that any contribution by the surfactant to the ionic strength is not taken into account. It is stressed that this is an empirical observation, that is, there is no theoretical derivation for the relationship as shown below.

Plotting the three sets of data in Figure A-1 by Eq. [A-1] linearizes the data and predicts reasonably well the cmc in H_20 for SDS, LiPFO, and Compound A, as may be seen in Figures A-2, A-3 and Table A-1. From a practical standpoint therefore, such a plot may be useful in predicting the cmc in H_20 when limited amounts of surfactant are available (e.g. if the surfactant is, as in the case of Compound A, an investigational drug). Providing solubility is not an issue, by determining the cmc in 3 high concentrations of the same salt, e.g. 0.4, 0.6, and 0.8 M NaCl, which requires very little surfactant, one can extrapolate to zero salt to obtain a reasonable estimate of the cmc in H_20.

In order to probe the validity of this method, various sets of published data were plotted according to Eq. [A-1], and the plots are shown in Figures A-4, and A-6 through 9. The plots show the trends found in a homologous series, as well as the effect of counterion valence. As may be seen in Table A-1, most of the data give reasonably linear fits. It should be noted that these fits are not as

good as the fits obtained by plotting according to Eq. [VI-1], the double logarithmic Corrin-Harkins relation, which the reader may verify from the original publications. However, plotting in this manner does serve the purpose of providing an estimate of the cmc in H_20, as may be seen from Table A-1; estimates are difficult to obtain from Eq. [VI-1].

For a homologous series plotted according to Eq. [A-1], the slopes and intercepts become more negative as chain length is increased (Figure A-5). In each case, the plots are linear, and the intercept predicts the cmc in H_20 reasonably well (Table A-1).

When the cmc values of the same compound are determined in, e.g. 1:1 vs 1:2 or 2:1 electrolytes and the data plotted by Eq. [A-1], the slopes appear not to be very different in most cases (Table A-1), but the y-intercepts are shifted slightly upwards from that of the 1:1 electrolyte (Figures A-6 through 9) which appears to be the best predictor for the cmc in H_20. The differences observed with other electrolytes is most likely due to salting out and counterion effects, as explained by Eq. [VI-3], and it may be that this information is contained in the slope; it is also possible, of course, as pointed out by the tabulators that some of these data are erroneous (Mukerjee and Mysels). The original manuscript reported some scatter in the data, but overall, they were shown to fit Eq. [VI-1] very well.

As mentioned, there is no theoretical basis for the empirical relation described. On the surface, it may appear that Eq. [A-1] could be derived from the Debye-Huckel limiting law as follows

$$a=fc \tag{A-2}$$

where a is activity, f is activity coefficient, and c is concentration. Taking logs gives

$$\log a = \log f + \log c \tag{A-3}$$

or

$$\log c = - \log f + \log a \tag{A-4}$$

The Debye-Huckel limiting law predicts that

$$\log f = -QZ_AZ_B\sqrt{\mu} \tag{A-5}$$

where Z_A and Z_B are species charges, Q is $1.825 \times 10^6 \times (\rho/\varepsilon^3T^3)^{0.5}$, ρ is the density, ε the dielectric constant, and T the absolute temperature. From this it would follow that

$$\log c = QZ_AZ_B\sqrt{\mu} + \log a \tag{A-6}$$

so that a plot of log(cmc) vs $\sqrt{\mu}$ should be a straight line with a slope of $Q\ Z_AZ_B$, and an intercept of log a; at zero ionic strength, log c = log a, and the activity coefficient is assumed to be 1.

The flaw with this argument, of course, is that Eq. [A-5] was derived assuming μ to be very small, less than 0.01, allowing a simplifying approximation, and in the systems herein examined, the

ionic strengths are much higher. For example, for a twice negatively charged surfactant, $Z_A Z_B = -2$ and the slope should be ca. -1.0 (Carstensen, 1970) but it varies from 0.6 to 2.0 for sodium octylsulfate to sodium dodecyl sulfate (Table A-1), so that some other factor belongs in the equation perhaps related to the carbon length of the surfactant or a salting out coefficient.

In this light, the above argument is only presented here as a starting point for further consideration. It may be that the relationship predicted by Eq. [A-1], i.e. that the log(cmc) is linear in $\sqrt{\mu}$, may hold to higher ionic strengths than allowed by the theory from which it appears to be derived because the true meaning of the slope is yet undetermined. This has been suggested in other relationships involving ionic strength and counterions (Carstensen, 1970; Moelwyn Hughes; Odijk).

Table A-1 Estimates of cmc in H_2O by Eq. [A-1]

Data plotted by Eq. [A-1] are shown in Figures A-2 through 4 and A-6 through 9, and the results of regressing log(cmc) on $\sqrt{\mu}$ are shown below. The y-intercept represents the predicted log(cmc) in water; the $\log(cmc_{H2O})$ values were those experimentally determined in the references listed in the corresponding figures. As can be seen below, the two compare reasonably well where these data are available.

Surfactant/Salt	T(°C)	y-int.	slope	r^2	Log cmc_{H2O}	Fig.
A/pH 7 KH_2PO_4/KOH	22°C	-2.12	-1.33	0.992	-2.06	2
A/pH 7 KH_2PO_4/KOH	30°C	-2.09	-1.31	0.999	n.d.	3
A/pH 7 KH_2PO_4/KOH	40°C	-2.15	-1.20	0.961	n.d.	3
A/pH 7 KH_2PO_4/KOH	50°C	-2.03	-1.24	0.993	n.d.	3
A/pH 7 KH_2PO_4/KOH	60°C	-2.04	-1.23	0.980	n.d	3
A/pH 7 KH_2PO_4/KOH	75°C	-1.98	-1.15	0.984	n.d.	3
A/pH 10 K_2HPO_4/KOH	40°C	-1.82	-1.48	0.996	n.d.	3
A/pH 10 K_2HPO_4/KOH	75°C	-1.93	-1.12	0.995	n.d.	3
LiPFO/LiCl	25°C	-1.48	-1.08	0.996	-1.47	2
NaOctylSO_4/NaCl	21°C	-0.85	-0.60	0.980	-0.89	4
NaNonylSO_4/NaCl	21°C	-1.17	-0.74	0.986	-1.19	4
NaDecylSO_3/NaCl	26°C	-1.39	-0.62	0.972	-1.40	6
NaDecylSO_3/Na_2SO_4	26°C	-1.36	-0.64	0.996	-1.40	6
NaDecylSO_4/NaCl	25°C	-1.47	-1.18	0.985	-1.47	2
NaDecylSO_4/NaCl	21°C	-1.49	-1.21	0.990	-1.52	4
NaUndecylSO_4/NaCl	21°C	-1.83	-1.25	0.983	-1.85	4
NaDodecylSO_4/NaCl	21°C	-2.13	-1.98	0.975	-2.13	4
NaDodecylSO_4/NaCl	26°C	-2.28	-1.38	0.964	-2.22	8
NaDodecylSO_4/$Na_4P_2O_7$	26°C	-2.25	-0.99	0.979	-2.22	8
NaDodecylSO_4/Na_2SO_4	26°C	-2.30	-1.14	0.945	-2.22	8
K Laurate/NaCl	26°C	-1.66	-1.19	0.971	-1.64	7
K Laurate/K_2SO_4	26°C	-1.64	-1.02	0.989	-1.64	7
K Laurate/$Na_4P_2O_7$	26°C	-1.55	-1.08	0.987	-1.64	7
DTAB/NaCl	26°C	-1.17	-0.43	0.962	-1.20	9
DTAB/$BaCl_2$	26°C	-1.12	-0.43	0.992	-1.20	9
DOC/NaCl	26°C	-1.85	-1.39	0.962	-1.88	9
DOC/$BaCl_2$	26°C	-1.78	-1.38	0.993	-1.88	9
DOC/$LaCl_3$	26°C	-1.55	-1.93	0.990	-1.88	9

n.d. = not determined

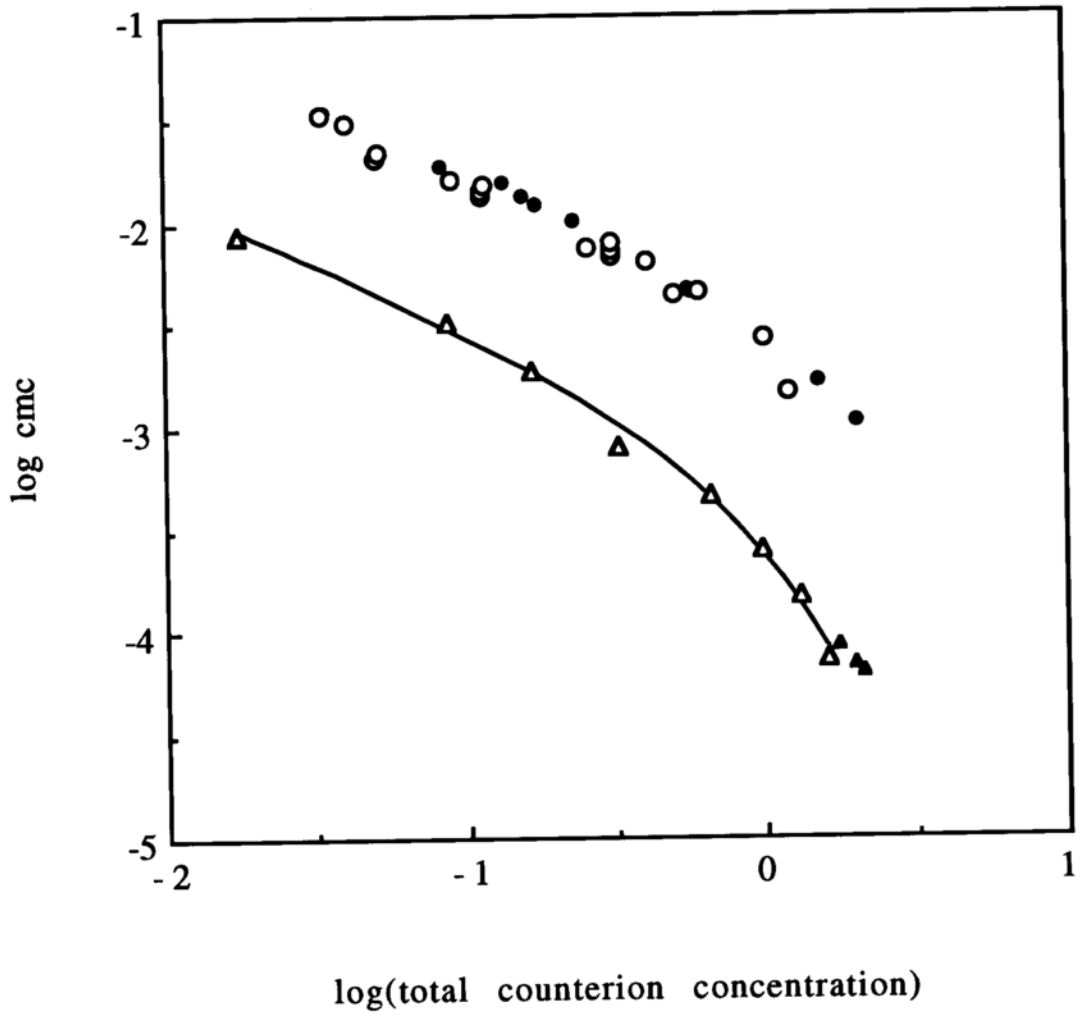

Figure A-1 Cmc as a function of total counterion concentration for a) o sodium decyl sulfate (NaDecS) in NaCl at 25°C (various methods; Mysels; and Chan, 1993); b) • lithium perfluorooctanoate (LiPFO) in LiCl at 25°C (UV spectroscopy, Chan, 1993) and d) Δ Compound A in pH 7 KH_2PO_4/KOH buffer at 22°C (surface tensiometry, Table VI-1). The fit shown for Compound A is to Eq. [VI-3].

The filled triangles represent cmc values of A determined in 0.2, 0.4, and 0.8 M buffers of the same ionic strength (2.23), hence similar $[K^+]$, as the 1.0 M buffer; these three buffers also contain KCl, whereas the other buffers used to determine the cmc values of Compound A contain only KH_2PO_4 and KOH.

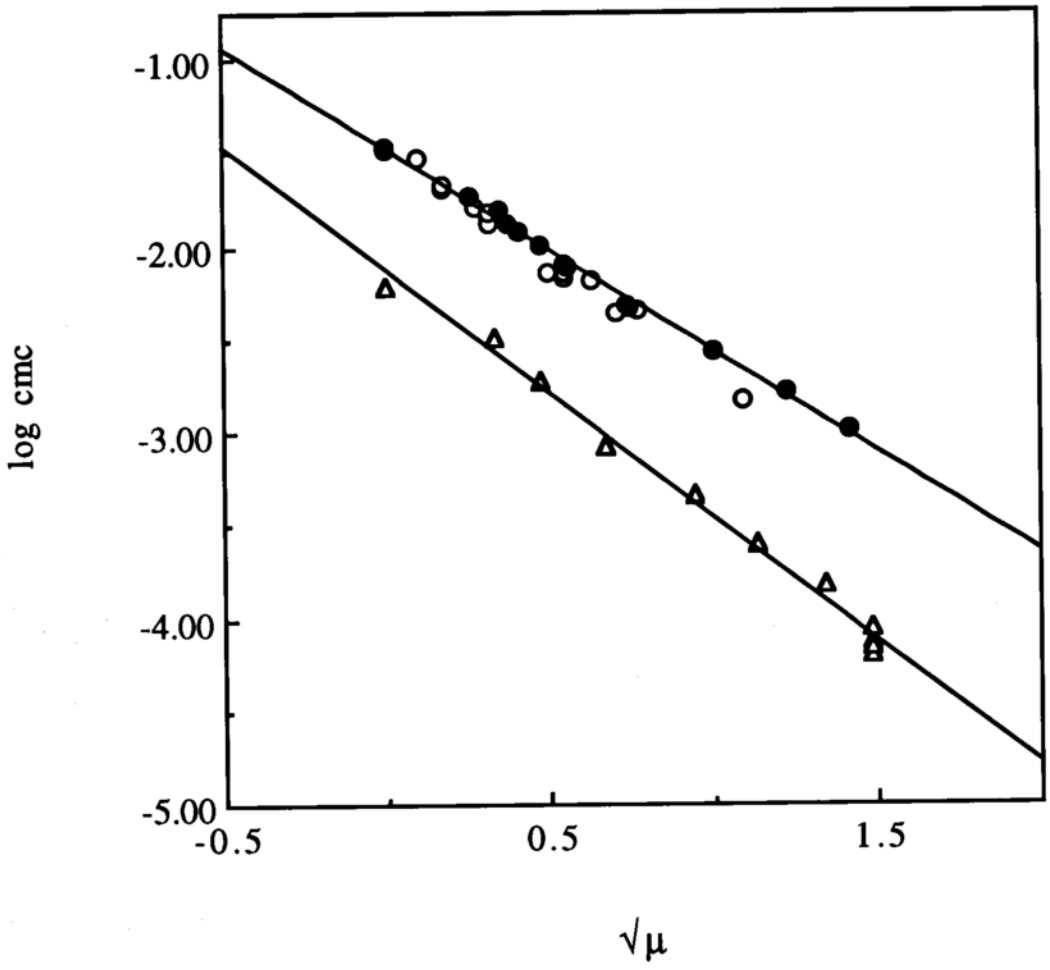

Figure A-2 Data in Figure A-1 plotted as log(cmc) vs square root of the ionic strength of NaCl, LiCl, or pH 7 KH_2PO_4/KOH. The linear regressions are shown for LiPFO and Compound A to guide the eye.

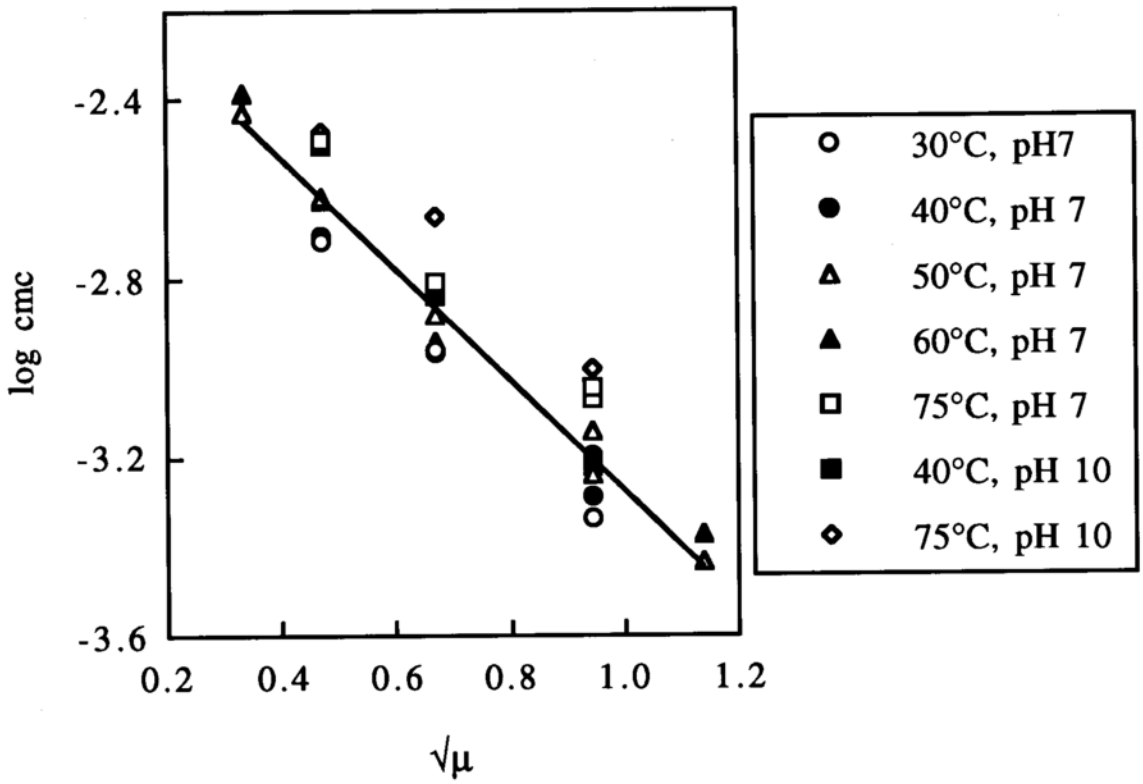

Figure A-3 Plot of log(cmc) vs square root of ionic strength for Compound A in pH 7 KH_2PO_4/KOH and pH 10 K_2HPO_4/KOH containing 0.2% EDTA disodium salt; the linear regression is drawn through the data at 50°C to guide the eye. Data from Table VI-1.

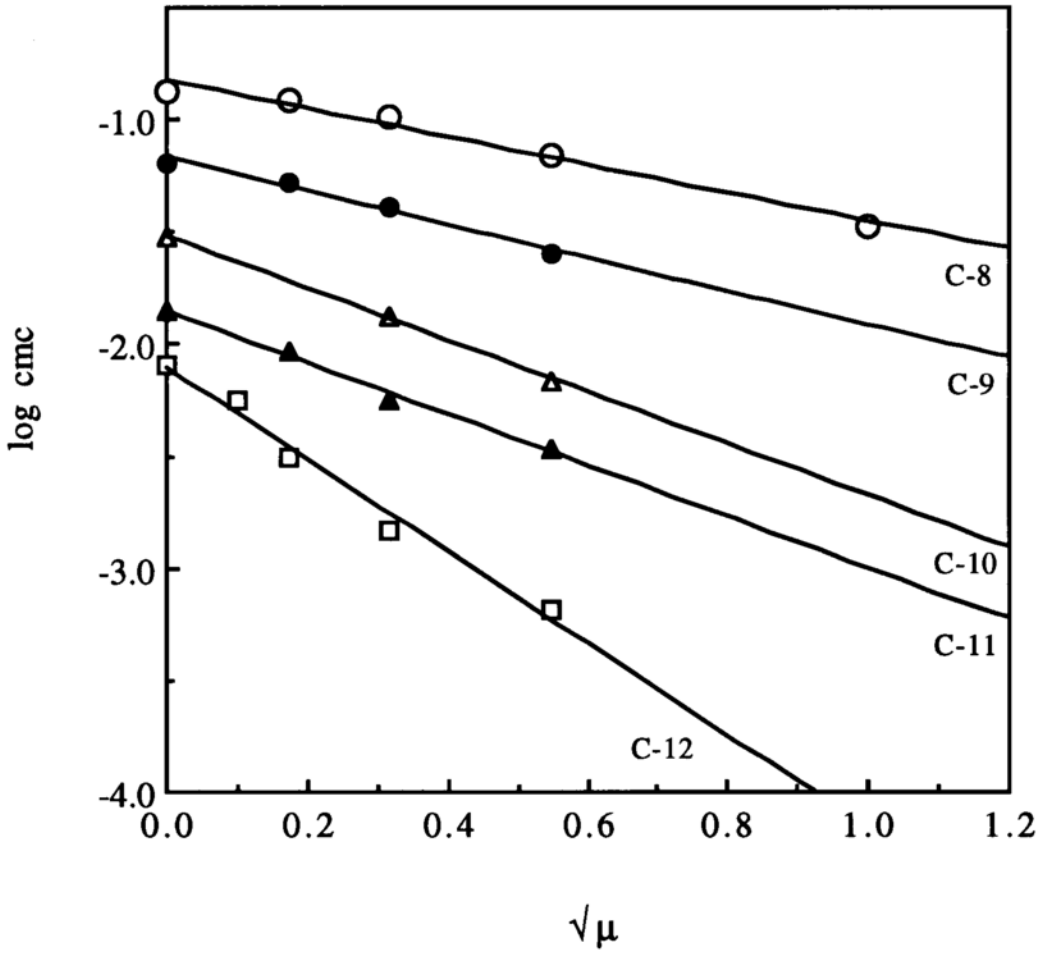

Figure A-4 Homologous series of sodium sulfates in NaCl. Data from Huisman (light scattering), plotted according to Eq. [A-1]; the cmc values have been converted to M/L.

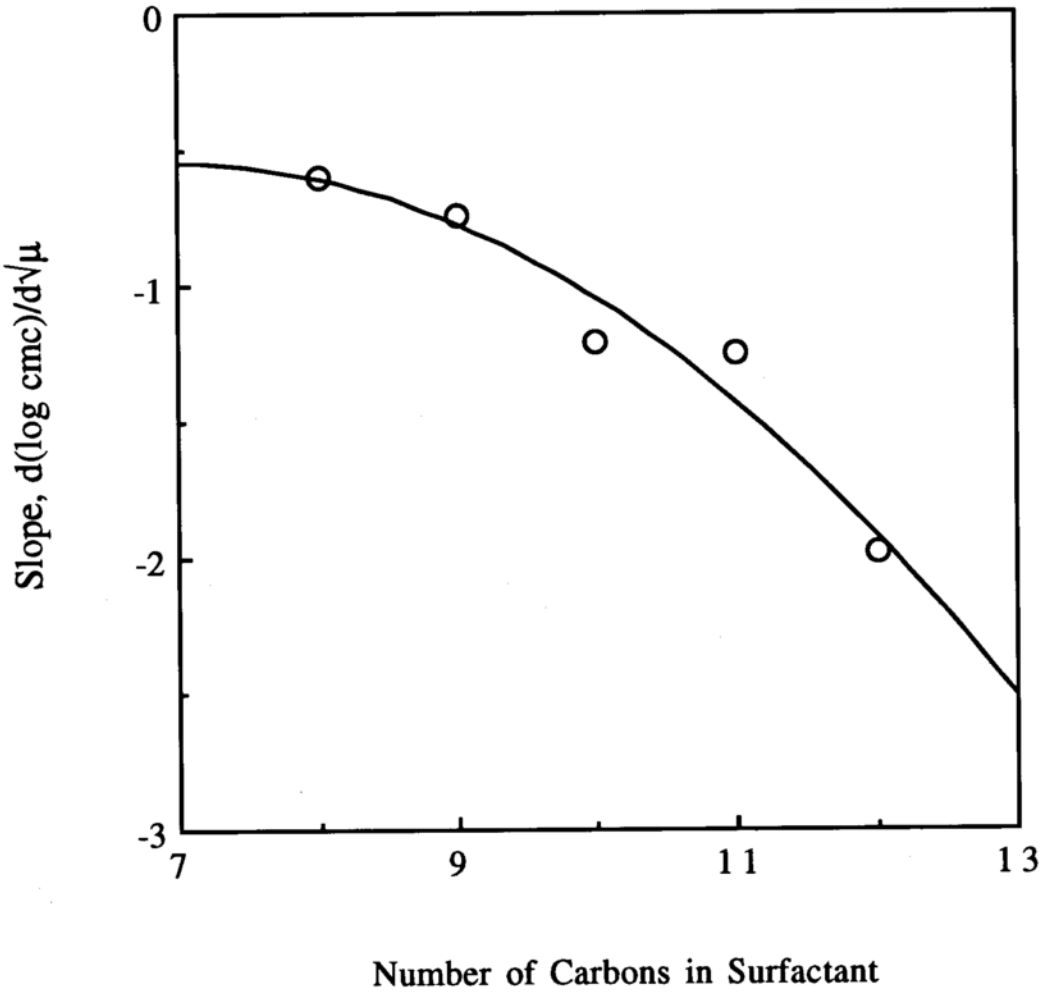

Figure A-5 Sensitivity of the cmc to ionic strength in a homologous series of surfactants; slopes from Figure A-4.

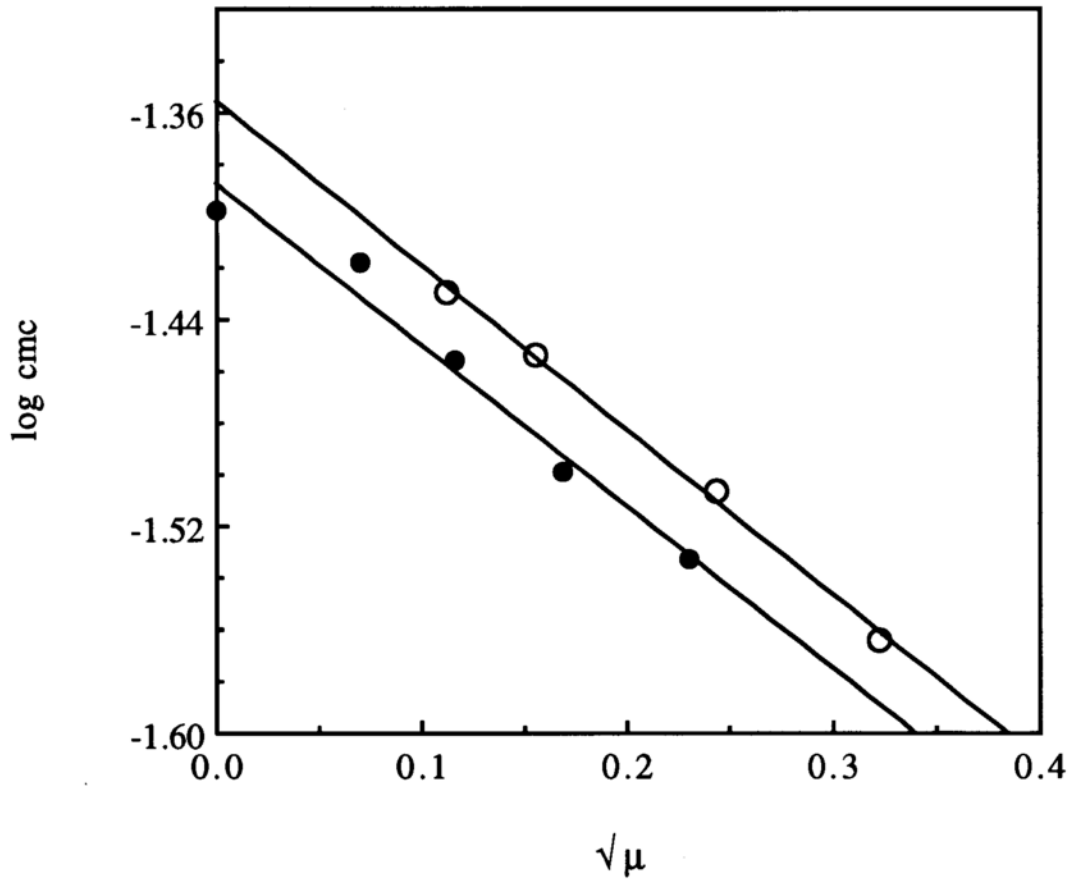

Figure A-6 Sodium decyl sulfonate data (visual spectral change) from Corrin and Harkins plotted according to Eq. [A-1]. NaCl, filled circle; Na_2SO_4, open circle.

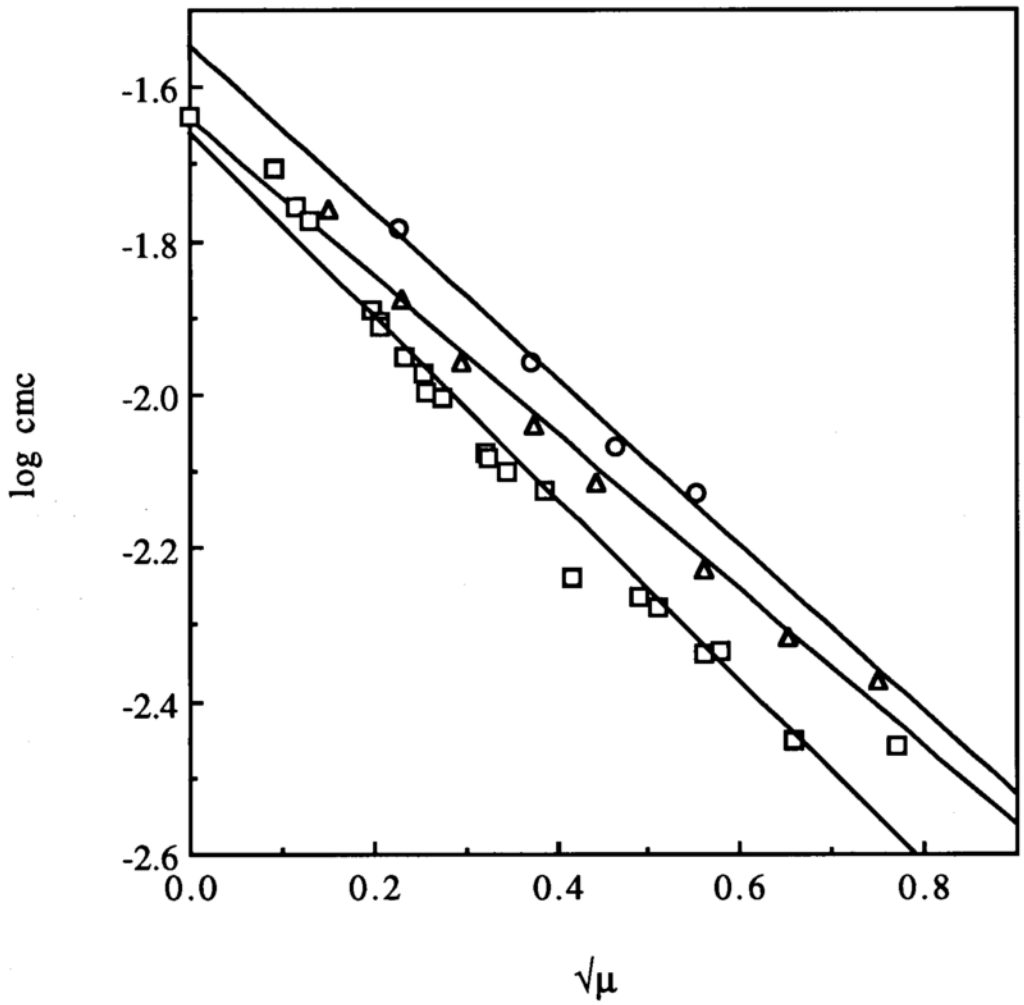

Figure A-7 Potassium laurate data (visual spectral change) from Corrin and Harkins plotted according to Eq. [A-1]. NaCl, squares; K_2SO_4, triangles; $Na_4P_2O_7$, circles.

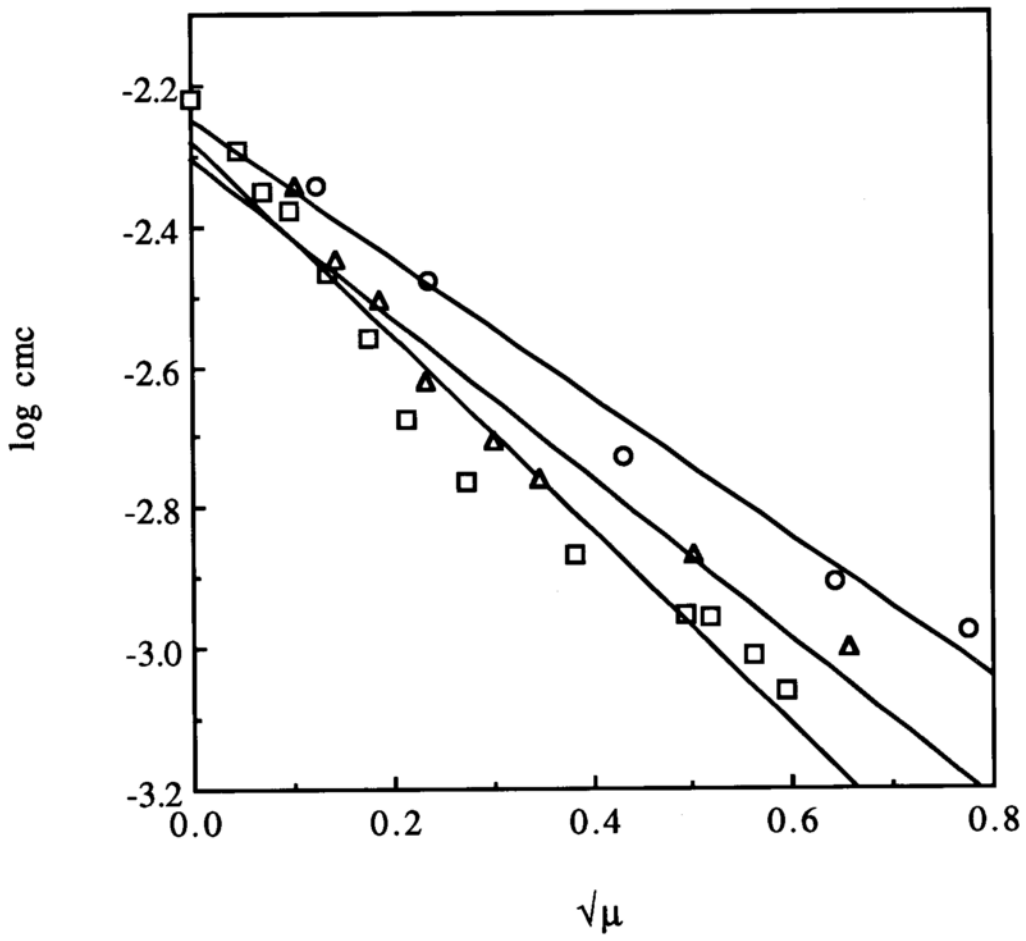

Figure A-8 Sodium dodecyl sulfate data (visual spectral change) from Corrin and Harkins plotted according to Eq. [A-1].
NaCl, squares; Na_2SO_4, triangles; $Na_4P_2O_7$, circles.

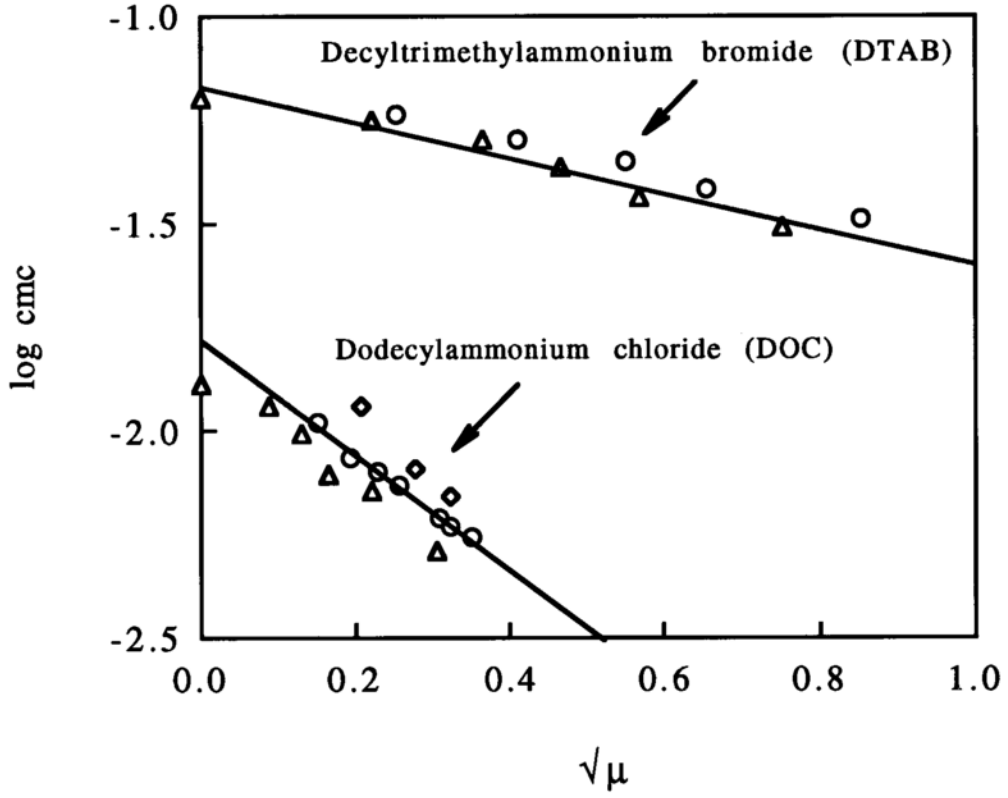

Figure A-9 Decyltrimethylammonium bromide (DTAB) and Dodecylammonium chloride (DOC) data from Corrin and Harkins (visual spectral change) plotted according to Eq. [A-1]. NaCl, triangles; $BaCl_2$, circles; $LaCl_3$, diamonds. Least squares fits are drawn through data obtained in NaCl (DTAB) and $BaCl_2$ (DOC).

APPENDIX B: RAW DATA, CMC

Data collected in indicated buffers and at indicated temperature for the determination of the cmc values of A using either the Cahn or Kruss surface tensiometer.

B-1. Determinations made with the Cahn instrument. Up to 45 minutes were allowed for equilibration for each measurement

B-1-a. 0.2 M pH 7 KH_2PO_4/KOH, 22°C, Cahn

Concentration, mM	dyn/cm
2.150	41.48
1.075	41.51
0.7166	41.99
0.5374	45.06
0.1792	51.42
0.1075	55.00
0.04070	61.47

B-1-b. 0.4 M pH 7 KH_2PO_4/KOH, 22°C, Cahn

Concentration, mM	dyn/cm
7.431	42.38
2.476	42.70
1.858	42.64
0.7431	42.70
0.5067	42.94
0.3539	44.14
0.2048	48.65
0.1238	50.51
0.03216	59.05
Buffer only	74.12

B-1-c. 0.2 M pH 7 KH_2PO_4/KOH, μ = 2.23 with KCl, 22°C, Cahn

Concentration, mM	dyn/cm
3.736	42.00
1.868	41.64
1.245	42.09
0.3675	41.97
0.1779	42.07
0.08896	41.91
0.05939	43.14
0.04741	43.22
0.03818	45.41
0.02826	49.08
0.02285	48.60

B-1-d. 0.8 M pH 7 KH_2PO_4/KOH, 22°C, Cahn

Concentration, mM	dyn/cm
1.477	42.32
0.4924	42.34
0.2954	42.43
0.1231	43.70
0.09232	45.37
0.05909	48.03
0.02686	53.22
0.01285	57.46
Buffer only	74.69

B-1-e. 0.8 M pH 7 KH_2PO_4/KOH, μ = 2.23 with KCl, 22°C, Cahn

Concentration, mM	dyn/cm
1.458	41.60
0.4861	41.82
0.2430	41.84
0.1326	41.84
0.07543	42.53
0.05833	43.68
0.04704	44.70, 44.00
0.03600	46.65
0.01944	47.86
Buffer only	74.56

B-1-f. 0.6 M pH 7 KH_2PO_4/KOH, 22°C, Cahn

Concentration, mM	dyn/cm
1.289	42.40
0.6445	42.47
0.4296	42.45
0.3222	42.50
0.1172	47.34
0.06138	51.61
0.05730	51.94
0.05321	52.14
0.02802	56.46

B-1-g. 0.2 M pH 7 KH_2PO_4/KOH, with 0.2% EDTA.2Na, 22°C, Cahn

Concentration, mM	dyn/cm
1.378	41.53
3.296	41.90
1.648	41.96
1.099	41.89
0.6893	43.11
0.4595	46.13
0.3446	48.34
0.1575	53.50
Buffer only	72.80

B-2. Determinations made with the Kruss instrument

B-2-a. Standardizing at 20°C with H_2O, Kruss

T, °C	CRC value	Experimental
20	72.75	72.8
30	71.20	71.2
40	69.60	69.6
50	67.94	67.6
60.7	66.10	66.5

Based on this experiment, for better accuracy, the instrument was recalibrated at the test temperature so that the readout agreed with the CRC value. Reading were taken after 4 minutes at 60°C, to minimize error from evaporation. A plastic sample holder cover also aided in this respect; after 10 minutes, sufficient sample evaporates to free the plate from the sample; equilibration is most rapid above the cmc, and the surface tension value is generally insensitive to changes in concentration above the cmc, so that the greatest error in measurement would be at readings below the cmc.

B-2-b. 1.0 M pH 7 KH_2PO_4/KOH, 22°C, Kruss

Readings taken after 10 minutes.

Concentration, mM	dyn/cm
1.272	41.6
0.6358	42.0
0.4239	42.0
0.3179	42.6
0.2119	42.6
0.1060	42.6
0.05299	46.1
0.03531	48.4
0.01767	54.4
0.01767	54.7
Buffer only	75.5

B-2-c. 0.05 M pH 7 KH_2PO_4/KOH, 22°C, Kruss

Readings taken after 10 minutes.

Concentration, mM	dyn/cm
12.63	41.6
8.418	41.6
6.313	41.4
4.209	41.4
3.156	40.5
2.104	44.1
1.052	49.7
0.5261	54.5
0.3507	57.2
Buffer only	72.6

B-2-d. 0.1 M pH 7 KH_2PO_4/KOH, 22°C, Kruss

Readings taken after 10 minutes.

Concentration, mM	dyn/cm
10.24	42.4
6.825	41.5
5.119	41.9
3.412	41.8
2.559	41.4
1.706	42.6
0.8531	46.5
0.4266	53.1
0.2844	55.8
Buffer only	73.3

B-2-e. 0.4 M pH 7 KH_2PO_4/KOH, μ=2.2 with KCl, 22°C, Kruss

Readings taken after10 minutes.

Concentration, mM	dyn/cm
1.369	41.4
0.9124	40.3
0.8364	41.6
0.6843	41.5
0.5703	41.6
0.4562	40.5
0.3422	40.9
0.2281	40.6
0.1140	41.1
0.05703	42.7
0.03802	44.6
0.03327	46.8
0.02851	48.2
Buffer only	74.8, 74.3

B-2-f. 0.4 M pH 7 KH_2PO_4/KOH, with 0.2% EDTA.2Na, 30°C, Kruss

Readings taken after 10 minutes.

Concentration, mM	dyn/cm
2.158	39.8
1.438	39.8
1.080	39.8
0.7193	40.0
0.5394	39.8
0.3596	41.6
0.1798	46.4
0.08974	51.4
0.05994	53.9
Buffer only	69.7

B-2-g. 0.2 M pH 7 KH_2PO_4/KOH, with 0.2% EDTA.2Na, 30°C, Kruss

Readings taken after 10 minutes.

Concentration, mM	dyn/cm
3.818	40.9
2.546	41.7
1.909	41.6
1.273	41.4
0.9546	42.7
0.6364	45.7
0.3182	50.9
0.1591	55.2
0.1061	57.9
Buffer only	71.0

B-2-h. 0.1 M pH 7 KH_2PO_4/KOH, with 0.2% EDTA.2Na, 30°C, Kruss

Readings taken after 10 minutes.

Concentration, mM	dyn/cm
7.904	42.2
5.269	41.3
3.952	41.8
2.635	41.6
1.976	41.4
1.317	43.9
0.6586	49.2
0.3293	53.9
0.2196	56.5
Buffer only	72.3

B-2-i. 0.4 M pH 10 K_2HPO_4/KOH, with 0.2% EDTA.2Na, 40°C, Kruss

Readings taken after 5 minutes.

Concentration, mM	dyn/cm
2.149	49.7
1.432	49.3
1.074	49.0
0.7163	48.4
0.5372	49.1
0.3581	50.8
0.1811	54.2
0.08953	57.2
0.05970	59.6
Buffer only	70.0, 70.2, 70.4, 71.2, 71.2, 71.5, 71.6

mean 70.9 ± 0.6 RSD = 0.85%

B-2-j. 0.2 M pH 10 K_2HPO_4/KOH, with 0.2% EDTA.2Na, 40°C, Kruss

Readings taken after 5 minutes.

Concentration, mM	dyn/cm
4.339	49.5
2.892	49.6
2.169	49.0
1.446	48.2
1.085	50.0
0.7230	52.3
0.3617	55.7
0.1808	58.7
0.1206	60.3
Buffer only	70.3

B-2-k. 0.1 M pH 10 K_2HPO_4/KOH, with 0.2% EDTA.2Na, 40°C, Kruss

Readings taken after 5 minutes.

Concentration, mM	dyn/cm
9.885	49.6
6.590	49.8
4.942	49.7
3.295	47.8
2.471	48.9
1.647	51.4
0.8237	55.7
0.4117	59.2
0.2747	60.7
Buffer only	69.8

B-2-l. 0.1 M pH 7 KH_2PO_4/KOH, with 0.2% EDTA.2Na, 40°C, Kruss

Readings taken after 5 minutes.

Concentration, mM	dyn/cm
8.284	41.0
5.523	41.7
4.142	41.4
2.761	41.0
2.071	41.3
1.381	43.7
0.6904	49.5
0.3452	53.8
0.2301	57.0
Buffer only	69.7

B-2-m. 0.2 M pH 7 KH_2PO_4/KOH, with 0.2% EDTA.2Na, 40°C, Kruss

Readings taken after 5 minutes.

Concentration, mM	dyn/cm
4.719	42.7
3.146	43.1
2.360	43.7
1.573	43.2
1.180	43.2
0.7865	45.5
0.3933	50.5
0.1966	55.8
0.1311	57.8
Buffer only	71.6

B-2-n. 0.4 M pH 7 KH_2PO_4/KOH, with 0.2% EDTA.2Na, 40°C, Kruss

Readings taken after 5 minutes.

Concentration, mM	dyn/cm
2.080	41.9
1.387	40.8
1.271	41.7
1.040	41.3
0.6935	41.7
0.5201	42.4
0.3468	45.7
0.1734	49.9
0.08669	53.9
0.05778	56.9

B-2-o. 0.1 M pH 7 KH_2PO_4/KOH, with 0.2% EDTA.2Na, μ=0.89 with KCl, 40°C, Kruss

Readings taken after 5 minutes.

Concentration, mM	dyn/cm
2.076	42.3
1.384	41.7, 41.7, 42.3, 41.4, 42.7, 42.3, 42.7, 41.6, 42.6, 41.5
1.038	42.1
0.6921	42.0
0.5191	41.7
0.3461	43.5
0.1730	48.6
0.08652	52.3
0.05768	55.8
Buffer only	71.3

1.384 mM, mean = 42.0 ± 0.5, RSD = 1.2%

B-2-p. 0.2 M pH 7 KH_2PO_4/KOH, with 0.2% EDTA.2Na, μ=0.89 with KCl, 40°C

after 45 minutes plate lifts off 43.5->42.5->41.9->39.5 at 5, 10, 13, 45 minutes

Concentration, mM	dyn/cm
2.155	41.9
1.437	42.4
1.078	42.4
0.7184	42.1
0.5388	41.9
0.3592	43.5
0.1796	48.0
0.08981	53.7
0.05987	55.6
Buffer only	71.3

B-2-q. 0.6 M pH 7 KH_2PO_4/KOH, with 0.2% EDTA.2Na, 50°C, Kruss

Readings taken after 5 minutes.

Concentration, mM	dyn/cm
1.547	42.1
1.031	42.1
0.7735	42.0
0.5157	42.0
0.3868	42.3
0.2578	44.6
0.1289	49.5
0.06446	54.2
0.04298	56.3
Buffer only	70.1

B-2-r. 0.2% pH 7 EDTA.2Na, 50°C, Kruss

Readings taken after 5 minutes.

Concentration, mM	dyn/cm
17.16	42.8
11.44	40.5
5.719	42.2
8.578	40.5
4.289	44.1
2.859	47.1
1.430	53.8
0.7148	58.2
0.4766	60.1
Buffer only	67.6

B-2-s. 0.05 M pH 7 KH_2PO_4/KOH with 0.2% EDTA.2Na, 50°C, Kruss

Readings taken after 5 minutes.

Concentration, mM	dyn/cm
13.11	42.0
8.741	41.2
6.556	41.0
4.370	40.5
3.278	41.0
2.185	44.4
1.093	48.9
0.5463	54.0
0.3641	56.5
Buffer only	67.8

B-2-t. 0.1 M pH 7 KH_2PO_4/KOH with 0.2% EDTA.2Na, μ=0.89 with KCl, 50°C, Kruss

Readings taken after 5 minutes.

Concentration, mM	dyn/cm
2.440	41.8
1.624	41.7
1.218	41.4
0.8119	41.7
0.6089	41.7
0.4059	43.9
0.2031	48.9
0.1015	53.6
0.6765	56.1
Buffer only	70.3

B-2-u. 0.1 M pH 7 KH_2PO_4/KOH, with 0.2% EDTA.2Na, 50°C, Kruss

Readings taken after 4.5 minutes.

Concentration, mM	dyn/cm
8.880	41.6
5.920	41.8
4.440	41.6
2.960	41.2
2.220	41.9
1.480	44.3
0.7398	48.6
0.3699	54.6
0.2466	56.8
Buffer only	68.4

B-2-v. 0.2 M pH 7 KH_2PO_4/KOH, with 0.2% EDTA.2Na, 50°C, Kruss

Readings taken after 4.5 minutes.

Concentration, mM	dyn/cm
4.169	41.7
2.780	41.7
2.085	41.4
1.390	41.4
1.042	43.2
0.6950	45.6
0.3473	51.1
0.1737	55.7
0.1158	57.4
Buffer only	67.9

B-2-w. 0.4 M pH 7 KH_2PO_4/KOH, with 0.2% EDTA.2Na, 50°C, Kruss

Readings taken after 4.5 minutes.

Concentration, mM	dyn/cm
2.106	41.9
1.404	42.0
1.287	41.5
1.053	41.9
0.7020	42.4
0.5265	43.3
0.3510	45.8
0.1755	51.0
0.08775	55.0
0.05850	56.7

B-2-x. 0.2 M pH 7 KH_2PO_4/KOH, with 0.2% EDTA.2Na, μ=0.89 with KCl, 50°C, Kruss

Readings taken after 5 minutes.

Concentration, mM	dyn/cm
2.112	41.3
1.408	41.2
1.056	41.4
0.7039	40.7
0.5279	41.9
0.3520	44.2
0.1760	49.3
0.08799	53.8
0.05867	55.8
Buffer only	69.5

B-2-y. 0.4 M pH 7 KH_2PO_4/KOH, with 0.2% EDTA.2Na, 60°C, Kruss

Readings taken after 4 minutes.

Concentration, mM	dyn/cm
1.707	41.2
1.138	41.2
0.8537	40.2
0.8237	40.6
0.6178	39.0
0.5691	40.4
0.4118	42.3
0.3089	44.6
0.1963	47.7
0.1074	50.8
0.04928	58.4
Buffer only	67.4

B-2-z. 0.2 M pH 7 KH_2PO_4/KOH, with 0.2% EDTA.2Na, 60°C, Kruss

Readings taken after 4 minutes.

Concentration, mM	dyn/cm
3.321	41.4
2.214	41.3
1.660	41.5
1.107	41.4
0.8302	44.4
0.5535	47.3
0.2768	50.7
0.1384	56.0
Buffer only	61.2

B-2-aa. 0.1 M pH 7 KH_2PO_4/KOH, with 0.2% EDTA.2Na, 60°C, Kruss

Readings taken after 4 minutes.

Concentration, mM	dyn/cm
7.714	41.0
5.143	41.1
4.629	39.1
2.572	39.7
1.929	38.2
1.286	44.6
0.6429	48.5
0.3214	54.8
0.1928	58.1
Buffer alone	67.5

-2-bb. 0.2 M pH 7 KH_2PO_4/KOH, with 0.2% EDTA.2Na, μ adj. to 0.89 with KCl, 60°C, Kruss

Readings taken after 4 minutes.

Concentration, mM	dyn/cm
1.760	41.1
1.173	40.8
0.8800	41.0
0.5866	41.5
0.4400	42.0
0.2933	45.9
0.1467	49.2
0.07333	54.2
0.04888	56.2
Buffer only	68.1

B-2-cc. 0.1 M pH 7 KH_2PO_4/KOH, with 0.2% EDTA.2Na, μ adj. to 0.89 with KCl, 60°C, Kruss

Readings taken after 4 minutes.

Concentration, mM	dyn/cm
1.698	40.8
1.132	40.9
0.8492	40.6
0.5661	40.4
0.4246	43.5
0.2830	46.3
0.1415	49.0
0.07076	54.6
0.04716	57.1
Buffer only	68.3

B-2-dd. 0.05 M pH 7 KH_2PO_4/KOH, with 0.2% EDTA.2Na, 60°C, Kruss

Readings taken after 4 minutes.

Concentration, mM	dyn/cm
12.14	41.5
8.096	41.1
6.072	40.5
4.048	40.1
3.036	42.4
2.024	44.7
1.012	49.6
0.5060	54.5
0.3373	56.2
Buffer only	67.1

B-2-ee. 0.6 M pH 7 KH_2PO_4/KOH, with 0.2% EDTA.2Na, 60°C, Kruss

Readings taken after 4 minutes.

Concentration, mM	dyn/cm
1.310	41.9
0.8730	41.6
0.6548	41.9
0.4365	41.9
0.3274	42.9
0.2182	45.7
0.1091	51.0
0.05456	54.9
0.03638	55.8
Buffer only	68.6

B-2-ff. 0.1 M pH 7 KH_2PO_4/KOH, with 0.2% EDTA.2Na, 75°C, Kruss

Readings taken after 2.5 minutes.

Concentration, mM	dyn/cm
7.924	41.5
5.283	41.1
3.962	40.3
2.642	41.4
1.981	43.5
1.321	46.1
0.6604	50.9
0.3302	55.3
0.2202	57.2
Buffer only	64.1

B-2-gg. 0.2 M pH 7 KH_2PO_4/KOH, with 0.2% EDTA.2Na, 75°C, Kruss

Readings taken after 2.5 minutes.

Concentration, mM	dyn/cm
3.705	41.0
2.470	40.5
2.264	39.9
1.852	40.2
1.235	41.6
0.9262	43.5
0.6175	47.7, 47.0
0.3087	51.8
0.1544	55.8
Buffer only	64.9

B-2-hh. 0.4 M pH 7 KH_2PO_4/KOH, with 0.2% EDTA.2Na, 75°C, Kruss

Readings taken after 2.5 minutes.

Concentration, mM	dyn/cm
2.075	40.6
1.383	39.6
1.268	40.2
1.037	39.8
0.6916	41.5
0.5187	43.2
0.3458	44.9
0.1729	49.7
0.08645	54.6
0.05764	56.4
Buffer only	64.9

B-2-ii. 0.1 M pH 7 KH_2PO_4/KOH, with 0.2% EDTA.2Na, μ=0.89 with KCl, 75°C, Kruss

Readings taken after 3 minutes.

Concentration, mM	dyn/cm
2.091	41.2
1.394	41.1
1.046	40.6
0.6971	41.6
0.5228	43.8
0.3485	46.2
0.1743	50.4
0.08714	55.2
0.05809	57.0
Buffer only	65.7

B-2-jj. 0.4 M pH 10 K_2HPO_4/KOH, with 0.2% EDTA.2Na, 75°C, Kruss

Readings taken after 3 minutes.

Concentration, mM	dyn/cm
2.066	46.1
1.378	45.7
1.033	44.6
0.6889	46.5
0.5166	47.7
0.3444	50.0
0.1722	52.8
0.08611	56.1
0.05740	57.5
Buffer only	65.4

B-2-kk. 0.2 M pH 10 K_2HPO_4/KOH, with 0.2% EDTA.2Na, 75°C, Kruss

Readings taken after 3 minutes.

Concentration, mM	dyn/cm
4.439	46.2
2.959	45.7
2.713	45.2
2.219	46.0
1.480	46.6
1.110	48.2
0.6771	50.5
0.3699	53.5
0.1850	57.1
0.1127	58.5
Buffer only	64.1

B-2-ll. 0.1 M pH 10 K_2HPO_4/KOH, with 0.2% EDTA.2Na, 75°C, Kruss

Readings taken after 3 minutes.

Concentration, mM	dyn/cm
9.608	46.5
6.405	45.8
4.804	45.5
3.203	45.6
2.402	46.6
1.601	48.9
0.8006	52.8
0.4003	56.7
0.2669	58.0
Buffer only	64.3

APPENDIX C: RAW DATA, KINETIC EXPERIMENTS

Table C-1 Initial assays of samples prepared with air headspace, or sparged with argon or oxygen. μ indicates the ionic strength of the buffer has been adjusted with KCl to that of the 0.4 M pH 8 buffer. Buffers also contain 0.2% EDTA.2Na.

a) Initial drug concentration above the cmc.

	mg/mL			
pH 8 buffer/Temp.	AIR	ARGON	OXYGEN	Mean±SD
0.1M/93°C	25.3	25.0	23.7	
	25.2		23.5	24.5±0.9
0.2M/93°C	24.4	26.1	24.8	
	24.8	25.8	24.7	25.1±0.7
0.4M/93°C	25.0	24.8	25.2	
	25.0	24.9	25.3	25.0±0.2
0.1Mμ/93°C	25.1	24.8	25.1	
	25.0	25.1	25.1	
			25.0	25.0±0.1
0.2Mμ/93°C	25.6	26.2	25.7	
	25.3	25.8	25.2	25.6±0.4
0.1M/75°C	26.5	25.3	25.0	
	25.8	25.1	25.0	25.4±0.6
0.2M/75°C	25.1	25.1	24.8	
	25.0	25.0	24.9	25.0±0.1
0.4M/75°C	24.8	24.9	25.0	
	25.0	25.2	25.0	25.0±0.1
0.1M/60°C	24.8	25.0	25.1	
	24.7	24.6	24.6	24.8±0.2
0.2M/60°C	25.0	25.0	24.9	
	24.9	25.0	24.8	24.9±0.1
0.4M/60°C	24.8	24.8	24.9	
	24.9	24.8		24.8±0.1
0.4Mμ/93°C pH 7	25.1	24.3	24.2	
	25.0	24.1	24.6	24.6±0.4
0.4M/93°C pH 8	24.8	25.0	24.8	
	24.8	24.8	24.8	24.8±0.1

Table C-1, continued

b) initial drug concentration below the cmc

mcg/mL

pH 8 buffer/Temp.	AIR	ARGON	OXYGEN	Mean±SD
0.1M/60°C	52.2	52.1	51.4	
	52.4	51.9	52.0	52.0±0.3
0.2M/60°C	52.4	51.6	50.7	
	52.7	51.7	52.4	51.9±0.7
0.4M/60°C	52.4	51.1	51.9	
	51.6	51.7	51.8	51.8±0.4
0.1M/93°C	52.8	50.8	52.5	
	53.0	51.3	52.2	52.1±0.9
0.2M/93°C	52.5	51.0	52.2	
	52.2	50.2	51.6	51.6±0.9
0.4M/93°C	52.4	52.2	52.5	
	52.0	47.9	52.0	51.5±1.8
0.1Mμ/93°C	52.3	50.3	44.5	
	52.6	52.0	49.3	50.2±3.0
0.2Mμ/93°C	52.8	48.0	45.6	
	52.3	47.2	46.6	48.8±3.0
0.4Mμ/93°C pH 7	56.8	55.2	57.3	
	57.0	54.2	56.9	56.2±1.2
0.4M/93°C pH 8	57.0	54.4	61.1	
	56.8	54.9	58.1	57.0±2.4

Table C-2 Statistical analysis of data in Table C-1 by the Wilcoxon rank test (Friedman)

	TREATMENT					
	AIR HEADSPACE		ARGON SPARGED		OXYGEN SPARGED	
pH8 Buffer/Temp.	mg/mL	Rank	mg/mL	Rank	mg/mL	Rank
0.1M/93°C	25.3	3	25.0	2	23.6	1
0.2M/93°C	24.6	1	26.0	3	24.8	2
0.4M/93°C	25.0	2	24.8	1	25.2	3
0.1Mμ/93°C	25.1	2.5	25.0	1	25.1	2.5
0.2Mμ/93°C	25.4	1.5	26.0	3	25.4	1.5
0.1M/75°C	26.1	3	25.2	2	25.0	1
0.2M/75°C	25.1	3	25.0	2	24.9	1
0.4M/75°C	24.9	1	25.0	2.5	25.0	2.5
0.1M/60°C	24.8	2	24.8	2	24.8	2
0.2M/60°C	25.0	2.5	25.0	2.5	24.9	1
0.4M/60°C	24.9	2.5	24.8	1	24.9	2.5
0.4Mμ/93°C pH 7	25.0	3	24.2	1	24.4	2
0.4M/93°C pH 8	24.8	1.5	24.9	3	24.8	1.5
	mcg/mL		mcg/mL		mcg/mL	
0.1M/60°C	52.3	3	52.0	2	51.7	1
0.2M/60°C	52.6	3	51.6	1.5	51.6	1.5
0.4M/60°C	52.0	3	51.4	1	51.8	2
0.1M/93°C	52.9	3	51.0	1	52.4	2
0.2M/93°C	52.4	3	50.6	1	51.9	2
0.4M/93°C	52.2	2	50.0	1	52.3	1
0.1Mμ/93°C	52.4	3	51.2	2	46.9	3
0.2Mμ/93°C	52.5	3	47.6	2	46.1	1
0.4Mμ/93°C pH 7	56.9	2	54.7	1	57.1	3
0.4M/93°C pH 8	56.9	2	54.7	1	59.6	3
Sum		55.5		39.5		43.0

p = number of treatments = 3
n = number of replicates = 23
DF = p-1 = 2; sum of ranks = 3 + 2 + 1 = 6

$$\chi_r^2 = \frac{12}{np(p+1)} \times \Sigma(ranktotal)^2 - 3n(p+1) = 6.2$$

For two degrees of freedom, $\alpha = 0.01$, $\chi_r^2 = 9.21$.

APPENDIX C, continued. Raw data from kinetic studies done at pH 7 and 8 at 60°, 75°, and 93°C. These tables do not include data generated fro the Master's Thesis.

Table C-3 Compound A Solution Kinetics at **93°C** in **0.1 M** pH 8 K_2HPO_4
Initial Drug Concentration **25.2** mg/mL (> cmc)

	AIR HEADSPACE				ARGON PURGED				OXYGEN PURGED			
Time (days)	Frac. A Retain.	Fraction as Cinn.	SUM	pH	Frac.A Retain.	Fraction as Cinn.	SUM	pH	Frac.A Retain.	Fraction as Cinn.	SUM	pH
0	1.000	0.000	1.000	8.0	1.000	0.000	1.000	8.0	1.000	0.000	1.000	8.0
0.5	1.000		1.000	8.0	0.992		0.992	8.0	1.010		1.010	7.9
1	0.992		0.992	8.0	0.980		0.980	8.0	1.000		1.000	8.0
1					0.960		0.960	8.0				
2	0.984		0.984	8.0	0.988		0.988	8.0	0.980		0.980	8.0
4	0.968	0.022	0.990	8.0	0.960	0.016	0.976	8.0	0.976	0.021	0.997	8.0
10	0.932	0.007	0.939	8.0					0.921	0.007	0.928	7.9
30	0.786	0.210	0.996	7.9	0.774	0.150	0.924	8.0	0.726	0.268	0.994	7.7
51	0.625	0.377	1.002	7.9	0.785	0.249	1.034	8.0	0.586	0.399	0.985	7.3
60									0.389	0.520	0.909	7.3
75	0.452	0.558	1.010	8.0	0.659	0.363	1.022	8.2	0.302	0.568	0.870	7.2
75									0.278	0.513	0.791	7.1
90	0.323	0.709	1.032	8.2	0.528	0.546	1.074	8.4	0.238	0.726	0.964	7.3
107	0.227	0.782	1.009	8.4								
112					0.504	0.571	1.075	8.4				
153					0.265	0.716	0.981	8.7	(0.014)	0.424	0.438	7.2
210					(0.222)	0.763	0.985	8.4				

Table C-4 Compound A Solution Kinetics at 93°C in 0.2 M pH 8 K_2HPO_4
Initial Drug Concentration 25.1 mg/mL (>cmc)

	AIR HEADSPACE				ARGON PURGED				OXYGEN PURGED			
Time (days)	Frac. A Retain.	Fraction as Cinn.	SUM	pH	Frac. A Retain.	Fraction as Cinn.	SUM	pH	Frac. A Retain.	Fraction as Cinn.	SUM	pH
0	1.000	0.000	1.000	8.0	1.000	0.000	1.000	8.0	1.000	0.000	1.000	8.0
10	0.948	0.037	0.985	8.0	0.944	0.022	0.966	8.0	0.936	0.016	0.952	7.9
20	0.912	0.078	0.990	8.0	0.904	0.064	0.968	8.0	0.852	0.118	0.970	7.9
30	0.865	0.148	1.013	8.0	(0.900)	0.107	1.007	8.0	(0.801)	0.215	1.016	7.7
30	0.817	0.180	0.997	7.9								
40	0.822	0.187	1.009	7.9	0.845	0.169	1.014	8.0	0.725	0.226	0.951	7.7
40					0.841	0.184	1.025	8.0				
50									0.622	0.383	1.005	7.5
60	0.677	0.310	0.987	7.8	0.764	0.271	1.035	8.0	(0.436)	0.364	0.800	7.4
60	0.720	0.283	1.003	7.8	0.810	0.224	1.034	8.0				
80	0.534	0.458	0.992	7.7	0.733	0.298	1.031	8.0				
80	0.598	0.372	0.970		0.673	0.394	1.067					
82									0.441	0.444	0.885	7.5
102	0.526	0.452	0.978	7.9	0.614	0.386	1.000	8.2				
122	(0.288)	0.783	1.071	8.2	(0.322)	0.441	0.763	8.0				
150									(0.080)	0.703	0.783	7.5
203	0.120	0.992	1.112	8.3	0.187	0.657	0.844	8.2	(0.039)	0.407	0.446	7.6
203	0.088	0.963	1.051	8.3					(0.034)	0.475	0.509	7.0
203	0.096	0.968	1.064	8.2								

Table C-5 Compound A Solution Kinetics at 93°C in **0.4 M** pH 8 K_2HPO_4
Initial Drug Concentration 25.0 mg/mL (> cmc)

	AIR HEADSPACE				ARGON PURGED				OXYGEN PURGED			
Time (days)	Frac. A Retain.	Fraction as Cinn.	SUM	pH	Frac.A Retain.	Fraction as Cinn.	SUM	pH	Frac.A Retain.	Fraction as Cinn.	SUM	pH
0	1.000	0.000	1.000	8.0	1.000	0.000	1.000	8.0	1.000	0.000	1.000	8.0
0.5	1.000		1.000	8.0	1.000		1.000	8.0	1.010		1.010	8.0
1	1.000		1.000	8.0	0.990		0.990	8.0	0.996		0.996	8.0
1					0.986		0.986	8.0				
2	0.984	0.008	0.992	8.0	0.988		0.988	8.0	0.980	0.012	0.992	8.0
2	0.992		0.992	8.0								
3	0.980	0.016	0.996	8.0	0.984		0.984	8.0	0.968	0.013	0.981	8.0
9	0.952	0.009	0.961	8.0	0.940	0.016	0.956	8.0	0.916	0.010	0.926	8.0
20	0.860	0.123	0.983	8.0	0.892	0.083	0.975	8.0	0.820	0.158	0.978	7.9
30									0.720	0.234	0.954	7.9
40	0.772	0.228	1.000	8.0					0.672	0.326	0.998	7.8
50									0.592	0.407	0.999	7.6
54					0.768	0.276	1.044	8.0				
60	0.632	0.359	0.991	7.8						0.359		
71									0.400	0.429	0.829	7.5
71									0.416	0.539	0.955	7.6
75	0.616	0.370	0.986	7.9	0.660	0.361	1.021	8.0				
82									(0.424)	0.538	0.962	7.7
93									(0.338)	0.583	0.921	7.7
91	0.492	0.587	1.079	7.9	0.620	0.530	1.150	8.0				
111					0.536	0.594	1.130	8.0				
123	(0.408)	0.616	1.024	7.8	0.324							
146	(0.304)	0.671	0.975	8.0								
209	(0.176)	0.918	1.094	7.9								

Table C-6 Compound A Solution Kinetics at 93°C in 0.1 M μ-adjusted pH 8 K_2HPO_4
Initial Drug Concentration 25.0 mg/mL (> cmc)

	AIR HEADSPACE				ARGON PURGED				OXYGEN PURGED			
Time (days)	Frac. A Retain.	Fraction as Cinn.	SUM	pH	Frac.A Retain.	Fraction as Cinn.	SUM	pH	Frac.A Retain.	Fraction as Cinn.	SUM	pH
0	1.000	0.000	1.000	7.9	1.000	0.000	1.000	8.0	1.000	0.000	1.000	7.9
0.5	1.000		1.000	7.9	0.960		0.960	8.0	0.992		0.992	7.9
0.5									1.010		1.010	7.9
1	1.000		1.000	7.9	0.980		0.980	8.0	0.988		0.988	7.9
1					0.992		0.992	8.0				
2	0.992		0.992	7.8	0.980		0.980	8.0	0.988	0.006	0.994	7.9
3	0.988	0.011	0.999	7.9	0.980	0.011	0.991	7.9	0.984	0.016	1.000	7.9
3	0.984	0.010	0.994	7.9								
5	0.984		0.984	7.9	0.968			8.0	0.928	0.004	0.932	7.9
9												
10	0.948	0.008	0.956	7.9	0.948	0.007	0.955	7.9	0.796	0.194	0.990	7.6
30	0.824	0.165	0.989	7.8	0.884	0.119	1.003	7.9	0.656	0.364	1.020	
50												
51	0.716	0.300	1.016	7.6	0.812	0.210	1.022	8.0	0.496	0.466	0.962	7.3
75	0.600	0.370	0.970	7.6	0.700	0.350	1.050	7.9				
75	0.588	0.411	0.999	7.6								
100	0.432	0.416	0.848	7.8	0.588	0.500	1.088	7.9	0.258	0.369	0.627	7.2
106												
124					0.536	0.550	1.086	8.0				

Table C-7 Compound A Solution Kinetics at 93°C in 0.2 M μ-adjusted pH 8 K_2HPO_4
Initial Drug Concentration 25.7 mg/mL (> cmc)

	AIR HEADSPACE				ARGON PURGED				OXYGEN PURGED			
Time (days)	Frac. A Retain.	Fraction as Cinn.	SUM	pH	Frac.A Retain.	Fraction as Cinn.	SUM	pH	Frac.A Retain.	Fraction as Cinn.	SUM	pH
0	1.000	0.000	1.000	8.0	1.000	0.000	1.000	8.0	1.000	0.000	1.000	8.0
10	0.946	0.046	0.992	8.0	0.953	0.034	0.987	8.0	0.914	0.014	0.928	7.9
20	0.868	0.104	0.972	8.0	0.903	0.083	0.986	8.0	0.836	0.150	0.986	7.8
20									0.856	0.130	0.986	7.8
30	0.813	0.205	1.018	7.9	0.883	0.130	1.013	8.0	0.766	0.231	0.997	7.6
40	0.794	0.235	1.029	7.8					0.650	0.312	0.962	7.6
50	0.700	0.305	1.005	7.8	0.798	0.247	1.045	8.0	0.630	0.392	1.022	7.5
50									(0.179)	0.454	(0.633)	7.2
57									0.540	0.439	0.979	7.4
70	0.572	0.409	0.981	7.6	0.724	0.303	1.027	8.0	0.261	0.404	0.665	7.3
70	0.576	0.405	0.981	7.7	0.735	0.288	1.023	8.0	0.362	0.423	0.785	7.4
91	0.444	0.613	1.057	7.7	0.634	0.466	1.100	7.9				
122	(0.388)	0.659	1.047	7.8	0.498	0.616	1.114	8.0	0.097	0.420	0.517	7.3
150	(0.196)	0.939	1.135	8.2								
203					(0.335)	0.847	1.182	8.0				

Table C-8 Compound A Solution Kinetics at 93°C in 0.1 M pH 8 K_2HPO_4
Initial Drug Concentration 0.0521 mg/mL (< cmc)

	AIR HEADSPACE				ARGON PURGED				OXYGEN PURGED			
Time (days)	Frac. A Retain.	Fraction as Cinn.	SUM	pH	Frac.A Retain.	Fraction as Cinn.	SUM	pH	Frac.A Retain.	Fraction as Cinn.	SUM	pH
0	1.000	0.000	1.000	8.0	1.000	0.000	1.000	8.0	1.000	0.000	1.000	8.0
15	0.862	0.177	1.039	8.0	0.923	0.090	1.013	8.0	0.764	0.207	0.971	7.8
30	0.758	0.247	1.005	7.9	0.831	0.175	1.006	8.0	0.597	0.342	0.939	7.4
30	0.737	0.252	0.989	7.9	0.810	0.193	1.003	8.0	0.572	0.384	0.956	7.4
35									0.566	0.361	0.927	7.4
40	0.718	0.287	1.005	7.8	0.798	0.212	1.010	8.0				
46									0.438	0.422	0.860	7.3
56	0.674	0.355	1.029	7.7	0.756	0.259	1.015	7.9	0.420	0.450	0.870	7.2
66	0.624	0.403	1.027	7.7	0.712	0.322	1.034	8.0	(0.672)*	0.351	1.023	8.0
80	0.597	0.456	1.053		0.681	0.372	1.053	7.9	0.364	0.484	0.848	7.2
101	0.537	0.516	1.053	7.7	0.601	0.450	1.051	8.0	0.313	0.502	0.815	7.4
108									0.271	0.528	0.799	7.2
139	0.426	0.578	1.004	7.6	0.507	0.529	1.036	8.0				
140									0.221	0.507	0.728	7.4
200	0.330	0.676	1.006	7.6	0.359	0.637	0.996	8.0	(0.179)	0.623	0.802	7.5
262	0.222	0.851	1.073	7.8	0.245	0.866	1.111	7.8				
262	0.236	0.917	1.153	7.7	0.293	0.878	1.171	7.8				

*no ppt before dilution ---> no change in pH, full mass balance

Table C-9 Compound A Solution Kinetics at 93°C in 0.2 M pH 8 K_2HPO_4
Initial Drug Concentration 0.0516 mg/mL (< cmc)

	AIR HEADSPACE				ARGON PURGED				OXYGEN PURGED			
Time (days)	Frac. A Retain.	Fraction as Cinn.	SUM	pH	Frac.A Retain.	Fraction as Cinn.	SUM	pH	Frac.A Retain.	Fraction as Cinn.	SUM	pH
0	1.000	0.000	1.000	8.0	1.000	0.000	1.000	8.0	1.000	0.000	1.000	8.0
15	0.899	0.102	1.001	8.0	0.841	0.072	0.913	8.0	0.818	0.190	1.008	7.9
30	0.773	0.257	1.030	7.9	0.828	0.204	1.032	8.0	0.587	0.372	0.959	7.6
35									0.539	0.352	0.891	7.5
35									0.568	0.399	0.967	7.5
40	0.748	0.299	1.047	7.8	0.800	0.232	1.032	8.0	0.560	0.432	0.992	7.5
40	0.736	0.301	1.037	7.9	0.756	0.200	0.956	8.0				
56	0.682	0.350	1.032	7.8	(0.620)	0.229	0.849	7.9	0.440	0.471	0.911	7.4
66	0.649	0.412	1.061	7.8	(0.581)	0.262	0.843	8.0	0.380	0.499	0.879	7.4
80	0.626	0.450	1.076	7.8	0.645	0.349	0.994	8.0	0.382	0.528	0.910	7.4
101	0.552	0.499	1.051	7.8	0.568	0.432	1.000	8.0	0.302	0.521	0.823	7.5
108									0.279	0.566	0.845	7.4
139	0.459	0.550	1.009	7.8	0.492	0.509	1.001	8.0				
140									0.227	0.600	0.827	7.4
200	0.356	0.694	1.050	8.0	0.420	0.644	1.064	8.1				
262	0.266	0.908	1.174	7.8	0.269	0.875	1.144	7.9				
262	0.236	0.945	1.181	7.8	0.277			7.9				

Table C-10 Compound A Solution Kinetics at 93°C in 0.4 M pH 8 K_2HPO_4
Initial Drug Concentration 0.0522 mg/mL (< cmc)

	AIR HEADSPACE				ARGON PURGED				OXYGEN PURGED			
Time (days)	Frac. A Retain.	Fraction as Cinn.	SUM	pH	Frac.A Retain.	Fraction as Cinn.	SUM	pH	Frac.A Retain.	Fraction as Cinn.	SUM	pH
0	1.000	0.000	1.000	8.0	1.000	0.000	1.000	8.0	1.000	0.000	1.000	8.0
15	0.874	0.148	1.022	8.0	0.784	0.090	0.874	8.0	0.697	0.177	0.874	8.0
30	0.766	0.265	1.031	8.0	0.718	0.181	0.899	8.0	0.561	0.398	0.959	7.8
30	0.745	0.256	1.001	8.0	0.787	0.183	0.970	8.0	0.624	0.372	0.996	7.7
35									0.542	0.414	0.956	7.7
40	0.728	0.307	1.035	7.9	0.736	0.200	0.936	8.0	0.557	0.435	0.992	7.7
46	0.701	0.312	1.013	8.0	0.711	0.244	0.955	8.0	(0.624)	0.371	0.995	7.8
56	0.665	0.353	1.018	7.9	0.586	0.235	0.821	8.0	(0.628)	0.411	1.039	
66	0.628	0.424	1.052	7.9	0.561	0.292	0.853	8.0	0.393	0.542	0.935	7.6
80	0.611	0.456	1.067	7.9	0.594	0.338	0.932	8.0	0.358	0.563	0.921	7.6
101	0.521	0.540	1.061	7.9	0.485	0.442	0.927	8.0	0.276	0.615	0.891	7.6
108									0.238	0.546	0.784	7.6
139	0.408	0.582	0.990	8.0	0.391	0.480	0.871	8.0				
140									0.216	0.585	0.801	7.6
200	0.305	0.724	1.029	8.1	0.287	0.694	0.981	8.2				
262	0.189	0.877	1.066	7.9	0.245	0.776	1.021					

Table C-11 Compound A Solution Kinetics at 93°C in 0.1 M μ-adjusted pH 8 K_2HPO_4
Initial Drug Concentration 0.0518 mg/mL (< cmc)

	AIR HEADSPACE				ARGON PURGED				OXYGEN PURGED			
Time (days)	Frac. A Retain.	Fraction as Cinn.	SUM	pH	Frac.A Retain.	Fraction as Cinn.	SUM	pH	Frac.A Retain.	Fraction as Cinn.	SUM	pH
0	1.000	0.000	1.000	7.9	1.000	0.000	1.000	7.9	1.000	0.000	1.000	7.9
15	0.890	0.111	1.001	7.9	0.880	0.079	0.959	8.0	0.815	0.199	1.014	7.7
30	0.764	0.268	1.032	7.7	0.701	0.176	0.877	7.9	0.548	0.366	0.914	7.2
35									0.585	0.392	0.977	7.2
35									0.454	0.290	0.744	7.2
40	0.764	0.296	1.060	7.6	0.772	0.225	0.997	7.9	0.521	0.452	0.973	7.1
40	0.743	0.301	1.044	7.7	0.788	0.226	1.014	7.9				
46	0.726	0.317	1.043	7.6	0.660	0.221	0.881	7.9	0.486	0.445	0.931	7.1
46	0.726	0.310	1.036	7.6	0.664	0.241	0.905	7.9	0.514	0.433	0.947	7.1
56	0.681	0.369	1.050	7.6	0.591	0.230	0.821	7.8	0.469	0.494	0.963	7.0
66	0.641	0.415	1.056	7.6	0.699	0.374	1.073	7.8	0.336	0.438	0.774	7.1
80	0.633	0.461	1.094	7.6	0.610	0.392	1.002	7.8	0.347	0.485	0.832	7.0
101	0.525	0.546	1.071	7.5	0.475	0.444	0.919	7.9	0.234	0.465	0.699	6.9
108									0.226	0.461	0.687	6.9
139	0.369	0.631	1.000	7.6	0.274	0.504	0.778	7.8				
200	0.309	0.710	1.019	7.7	0.293	0.643	0.936	8.0				

Table C-12 Compound A Solution Kinetics at **93°C** in **0.2 M** ***μ*-adjusted** pH 8 K_2HPO_4
Initial Drug Concentration **0.0487** mg/mL (< cmc)

	AIR HEADSPACE				ARGON PURGED				OXYGEN PURGED			
Time (days)	Frac. A Retain.	Fraction as Cinn.	SUM	pH	Frac.A Retain.	Fraction as Cinn.	SUM	pH	Frac.A Retain.	Fraction as Cinn.	SUM	pH
0	1.000	0.000	1.000	8.0	1.000	0.000	1.000	8.0	1.000	0.000	1.000	8.0
15	0.934	0.140	1.074	8.0	0.928	0.092	1.020	8.0	0.714	0.157	0.871	7.8
30	0.778	0.313	1.091	7.8	0.881	0.221	1.102	8.0	0.587	0.330	0.917	7.5
35									0.554	0.405	0.959	7.4
35									0.583	0.397	0.980	7.4
40	0.823	0.281	1.104	7.8	(0.544)	0.138	0.682	8.0	0.460	0.402	0.862	7.2
40	0.793	0.292	1.085	7.8	0.790	0.256	1.046	8.0				
46	0.778	0.314	1.092	7.9	0.747	0.230	0.977	8.0	0.530	0.455	0.985	7.4
46	0.786	0.326	1.112	7.8	0.714	0.232	0.946	8.0	0.546	0.481	1.027	7.4
56	0.721	0.379	1.100	7.7	0.708	0.291	0.999	7.9	0.530	0.513	1.043	7.3
66	0.686	0.428	1.114	7.8	0.714	0.353	1.067	8.0	0.433	0.506	0.939	7.3
80	0.661	0.505	1.166	7.7	0.694	0.418	1.112	7.9	0.406	0.572	0.978	7.3
101	0.575	0.575	1.150	7.7	0.569	0.502	1.071	7.9	0.257	0.500	0.757	7.3
108									0.230	0.480	0.710	7.4
139	0.437	0.639	1.076	7.8	0.456	0.603	1.059	8.0				
200	0.345	0.748	1.093	8.0	0.335	0.755	1.090	8.1				

Table C-13 Compound A Solution Kinetics at **93°C** in **0.4 M** μ-adjusted pH 7 KH_2PO_4
Initial Drug Concentration **24.5** mg/mL (> cmc)

	AIR HEADSPACE				ARGON PURGED				OXYGEN PURGED			
Time (days)	Frac. A Retain.	Fraction as Cinn.	SUM	pH	Frac.A Retain.	Fraction as Cinn.	SUM	pH	Frac.A Retain.	Fraction as Cinn.	SUM	pH
0	1.000	0.000	1.000	7.0	1.000	0.000	1.000	7.0	1.000	0.000	1.000	7.0
10	0.922	0.102	1.024	7.0	0.963	0.075	1.038	7.0	0.873	0.147	1.020	7.0
20	0.808	0.232	1.040	7.0	0.894	0.139	1.033	7.0	0.731	0.318	1.049	7.0
31	0.588	0.465	1.053	7.0					0.555	0.489	1.044	6.9
41	0.576	0.447	1.023	7.0	0.767	0.285	1.052	7.1	0.433	0.595	1.028	7.0
73	0.310	0.781	1.091	7.0	0.616	0.493	1.109	7.0	(0.171)	0.668	0.839	7.0
73	0.290	0.812	1.102	7.0	0.620	0.492	1.112	7.1	(0.208)	0.606	0.814	7.0
80									(0.204)	0.541	0.745	7.0
80									(0.143)	0.229	0.372	7.0
90	(0.200)	0.570	0.770	7.0					(0.114)	0.414	0.528	6.9
100	(0.167)	0.250	0.417	7.0	0.473	0.626	1.099	7.1	(0.082)	0.254	0.336	6.9
120	(0.094)	0.290	0.384	7.1								
133					0.339	0.758	1.097	7.0				
140	(0.040)	0.710	0.750	7.2								
162					(0.257)	0.049	0.306	7.1				
188					(0.155)	0.774	0.929	7.2				

Table C-14 Compound A Solution Kinetics at **93°C** in **0.4 M** pH 8 K_2HPO_4
Initial Drug Concentration **24.8** mg/mL (> cmc)

	AIR HEADSPACE				ARGON PURGED				OXYGEN PURGED			
Time (days)	Frac. A Retain.	Fraction as Cinn.	SUM	pH	Frac.A Retain.	Fraction as Cinn.	SUM	pH	Frac.A Retain.	Fraction as Cinn.	SUM	pH
0	1.000	0.000	1.000	8.0	1.000	0.000	1.000	8.0	1.000	0.000	1.000	8.0
10	0.960	0.055	1.015	8.0	0.976	0.032	1.008	8.0	0.911	0.095	1.006	
20	0.871	0.140	1.011	8.0	0.935	0.066	1.001	8.0	0.778	0.255	1.033	7.8
31									0.677	0.324	1.001	7.8
41	0.746	0.251	0.997	7.9	0.867	0.144	1.011	8.1	0.508	0.469	0.977	7.8
73	0.544	0.500	1.044	8.0	0.738	0.315	1.053	7.9	0.339	0.653	0.992	7.6
73	0.532	0.479	1.011	8.0	0.726	0.312	1.038	8.0	0.347	0.652	0.999	7.6
80									0.282	0.626	0.908	7.8
100	0.380	0.660	1.040	8.0	0.613	0.432	1.045	8.0	0.196	0.692	0.888	7.2
100									0.245	0.672	0.917	7.4
120	0.262	0.794	1.056	8.0					0.105	0.552	0.657	7.8
133					0.543	0.528	1.071	7.9				
140	0.171	0.913	1.084	8.2								
162					0.400	0.095	0.495	8.1				
188	(0.045)	0.908	0.953	7.9	0.310	0.813	1.123					
188	(0.048)	0.763	0.811	7.9								

Table C-15 Compound A Solution Kinetics at **93°C** in **0.4 M** μ**-adjusted** pH 7 KH_2PO_4
Initial Drug Concentration **0.0562** mg/mL (< cmc)

	AIR HEADSPACE				ARGON PURGED				OXYGEN PURGED			
Time (days)	Frac. A Retain.	Fraction as Cinn.	SUM	pH	Frac.A Retain.	Fraction as Cinn.	SUM	pH	Frac.A Retain.	Fraction as Cinn.	SUM	pH
0	1.000	0.000	1.000	7.0	1.000	0.000	1.000	7.0	1.000	0.000	1.000	7.1
10	0.792	0.062	0.854	7.0	0.870	0.030	0.900	7.1	0.703	0.148	0.851	7.1
20	0.721	0.159	0.880	7.0					0.626	0.304	0.930	7.0
31	0.655	0.220	0.875	7.0	0.765	0.151	0.916	7.0	0.456	0.396	0.852	7.0
41	0.559	0.277	0.836	7.2	0.683	0.106	0.789	7.2	0.329	0.314	0.643	7.1
73	0.384	0.375	0.759	7.0	0.550	0.259	0.809	7.1	0.164	0.434	0.598	7.0
73	0.425	0.244	0.669	7.0	0.502	0.109	0.611	7.1	0.149	0.383	0.532	7.1
80									(0.063)	0.213	0.276	6.9
100	0.313	0.449	0.762	6.8	0.489	0.240	0.729	7.0	(0.263)	0.364	0.627	7.1
111									0.049	0.262	0.311	6.6
120	0.232	0.370	0.602	7.1								
133					0.269	0.230	0.499	7.1				
154	0.196	0.415	0.611	6.9								
162					0.200	0.049	0.249	7.0				
188	0.146	0.590	0.736	7.0								

Table C-16 Compound A Solution Kinetics at 75°C in 0.1 M pH 8 K_2HPO_4
Initial Drug Concentration 25.4 mg/mL (> cmc)

	AIR HEADSPACE				ARGON PURGED				OXYGEN PURGED			
Time (days)	Frac. A Retain.	Fraction as Cinn.	SUM	pH	Frac.A Retain.	Fraction as Cinn.	SUM	pH	Frac.A Retain.	Fraction as Cinn.	SUM	pH
0	1.000	0.000	1.000	8.0	1.000	0.000	1.000	8.0	1.000	0.000	1.000	8.0
10	0.961		0.961	8.0	0.953		0.953	8.0	0.949		0.949	8.0
20	0.964	0.014	0.978	8.0	0.941	0.022	0.963	8.0	0.921	0.045	0.966	8.0
30	0.957	0.032	0.989	8.1	0.949	0.026	0.975	8.1	0.886	0.084	0.970	7.9
45	0.941	0.039	0.980	8.0	0.917	0.059	0.976	8.0	0.862	0.116	0.978	7.9
65	0.921	0.066	0.987	8.0	0.878	0.098	0.976	8.1	0.783	0.168	0.951	7.9
90	0.894	0.102	0.996	8.0	0.831	0.150	0.981	8.1	0.685	0.270	0.955	7.8
120									0.630	0.327	0.957	7.7
162	0.744	0.228	0.972	7.9	0.724	0.276	1.000	8.1	(0.098)	0.489	0.587	7.4
179	0.725	0.239	0.964	8.0	0.701	0.289	0.990	8.3	(0.034)	0.356	0.390	7.7
260	0.643	0.290	0.933	7.8	0.502	0.510	1.012	8.1	nd	0.404	0.404	7.2
315	0.611	0.341	0.952	7.9	(0.383)	0.645	1.028	8.5	nd	0.235	0.235	7.1
315	0.533	0.408	0.941	8.0	(0.248)	0.705	0.953	8.6	nd	0.329	0.329	7.1

Table C-17 Compound A Solution Kinetics at 75°C in 0.2 M pH 8 K_2HPO_4
Initial Drug Concentration 25.0 mg/mL (> cmc)

	AIR HEADSPACE				ARGON PURGED				OXYGEN PURGED			
Time (days)	Frac. A Retain.	Fraction as Cinn.	SUM	pH	Frac.A Retain.	Fraction as Cinn.	SUM	pH	Frac.A Retain.	Fraction as Cinn.	SUM	pH
0	1.000	0.000	1.000	8.0	1.000	0.000	1.000	8.0	1.000	0.000	1.000	8.0
10	0.976		0.976	8.0	0.968		0.968	8.0	0.960		0.960	8.0
20	0.972	0.018	0.990	8.0	0.956	0.026	0.982	8.0	0.932	0.052	0.984	8.0
30	0.996	0.016	1.012	8.0	0.960	0.040	1.000	8.1	0.928	0.073	1.001	8.0
45	0.956	0.052	1.008	8.0	0.920	0.083	1.003	8.1	0.864	0.142	1.006	8.0
65	0.924	0.057	0.981	8.0	0.896	0.098	0.994	8.1	0.792	0.174	0.966	7.9
90	0.904	0.105	1.009	8.0	0.860	0.154	1.014	8.1	0.776	0.232	1.008	7.8
120									0.732	0.262	0.994	7.8
162	0.776	0.228	1.004	7.9	0.704	0.342	1.046	8.1	(0.261)	0.563	0.824	7.5
179	0.752	0.213	0.965	8.0	0.757	0.183	0.940	8.2	(0.131)	0.596	0.727	7.8
260	0.640	0.268	0.908	7.7	(0.712)	0.232	0.944	7.9	(0.014)	0.414	0.428	7.1
315	0.631	0.360	0.991	7.9	(0.451)	0.623	1.074	8.3	nd	0.112	0.112	7.3
315	0.616	0.341	0.957	7.9	(0.406)	0.615	1.021	8.4	nd	0.458	0.458	7.3

Table C-18 Compound A Solution Kinetics at 75°C in 0.4 M pH 8 K_2HPO_4
Initial Drug Concentration 25.0 mg/mL (> cmc)

	AIR HEADSPACE				ARGON PURGED				OXYGEN PURGED			
Time (days)	Frac. A Retain.	Fraction as Cinn.	SUM	pH	Frac.A Retain.	Fraction as Cinn.	SUM	pH	Frac.A Retain.	Fraction as Cinn.	SUM	pH
0	1.000	0.000	1.000	8.0	1.000	0.000	1.000	8.0	1.000	0.000	1.000	8.0
10	0.972		0.972	8.0	0.968		0.968	8.0	0.960		0.960	8.0
20	0.972	0.017	0.989	8.0	0.964	0.020	0.984	8.0	0.948	0.041	0.989	8.0
30	0.976	0.022	0.998	8.0	0.968	0.023	0.991	8.1	0.968	0.054	1.022	8.0
45	0.944	0.049	0.993	8.0	0.932	0.063	0.995	8.0	0.900	0.109	1.009	8.0
65	0.932	0.067	0.999	8.0	0.924	0.074	0.998	8.1	0.872	0.116	0.988	8.0
90	0.920	0.084	1.004	8.0	0.920	0.076	0.996	8.0	0.820	0.192	1.012	7.9
120									0.824	0.177	1.001	7.9
162	0.832	0.155	0.987	7.9	(0.755)	0.268	1.023	8.0	0.708	0.291	0.999	7.8
179	0.801	0.185	0.986	8.1	(0.287)	0.122	0.409		0.724	0.283	1.007	8.0
260	0.791	0.171	0.962	7.8	0.780	0.194	0.974	7.9	0.608	0.299	0.907	7.7
315	0.677	0.288	0.965	7.9	(0.513)	0.540	1.053	8.1	(0.050)	0.510	0.560	7.6
315	0.695	0.261	0.956	7.9	(0.758)	0.207	0.965	8.0				

Table C-19 Compound A Solution Kinetics at 60 °C in 0.1 M pH 8 K_2HPO_4
Initial Drug Concentration 24.8 mg/mL (> cmc)

	AIR HEADSPACE				ARGON PURGED				OXYGEN PURGED			
Time (days)	Frac. A Retain.	Fraction as Cinn.	SUM	pH	Frac.A Retain.	Fraction as Cinn.	SUM	pH	Frac.A Retain.	Fraction as Cinn.	SUM	pH
0	1.000	0.000	1.000	8.0	1.000	0.000	1.000	8.0	1.000	0.000	1.000	8.0
12	0.992		0.992	8.0	0.984		0.984	8.0	0.988		0.988	8.0
25	0.972	0.006	0.978	8.0	0.968	0.004	0.972	8.0	0.964	0.006	0.970	8.0
50	0.976	0.019	0.986	8.0	0.972	0.008	0.980	8.1	0.944	0.045	0.989	8.0
75	0.968	0.023	0.991	8.0	0.952	0.011	0.963	8.0	0.927	0.057	0.984	8.0
125	0.944	0.030	0.974	8.0	0.952	0.018	0.970	8.0	0.895	0.103	0.998	7.9
200	0.956	0.048	1.004	8.0	0.948	0.035	0.983	8.0	0.847	0.141	0.988	7.8
300	0.919	0.084	1.003	8.0	0.919	0.058	0.977	8.1	0.806	0.257	1.063	7.8
300	0.910	0.076	0.986	8.0	0.899	0.069	0.968	8.0	0.782	0.210	0.992	7.8

Table C-20 Compound A Solution Kinetics at 60°C in 0.2 M pH 8 K_2HPO_4
Initial Drug Concentration 24.9 mg/mL (> cmc)

	AIR HEADSPACE				ARGON PURGED				OXYGEN PURGED			
Time (days)	Frac. A Retain.	Fraction as Cinn.	SUM	pH	Frac.A Retain.	Fraction as Cinn.	SUM	pH	Frac.A Retain.	Fraction as Cinn.	SUM	pH
0	1.000	0.000	1.000	8.0	1.000	0.000	1.000	8.0	1.000	0.000	1.000	8.0
12	0.996		0.996	8.0	0.992		0.992	8.0	0.988	0.007	0.995	8.0
25	0.980	0.006	0.986	8.0	0.980	0.002	0.982	8.0	0.972	0.020	0.992	8.0
50	0.980	0.012	0.992	8.0	0.980	0.011	0.991	8.1	0.968	0.033	1.001	8.0
75	0.968	0.021	0.989	8.0	0.984	0.012	0.996	8.0	0.948	0.045	0.993	8.0
125	0.960	0.019	0.979	8.0	0.972	0.019	0.991	8.0	0.908	0.073	0.981	8.0
200	0.948	0.048	0.996	7.9	(0.924)	0.032	0.956	8.0	0.876	0.123	0.999	7.9
300	0.932	0.073	1.005	8.0	0.932	0.048	0.980	8.0	0.831	0.165	0.996	7.8
300	0.928	0.075	1.003	8.0	0.924	0.052	0.976	8.1	0.831	0.168	0.999	7.8

Table C-21 Compound A Solution Kinetics at **60°C** in **0.4 M** pH 8 K_2HPO_4
Initial Drug Concentration **24.8** mg/mL (> cmc)

	AIR HEADSPACE				ARGON PURGED				OXYGEN PURGED			
Time (days)	Frac. A Retain.	Fraction as Cinn.	SUM	pH	Frac.A Retain.	Fraction as Cinn.	SUM	pH	Frac.A Retain.	Fraction as Cinn.	SUM	pH
0	1.000	0.000	1.000	8.0	1.000	0.000	1.000	8.0	1.000	0.000	1.000	8.0
12	0.992		0.992	8.0	0.996		0.996	8.0				
25	0.984	0.007	0.991	8.0	0.984	0.005	0.989	8.0	0.980	0.010	0.990	8.0
50	0.992	0.008	1.000	8.1	0.996	0.003	0.999	8.1	0.968	0.024	0.992	8.0
75	0.992	0.017	1.009	8.0	0.992	0.011	1.003	8.0	0.968	0.036	1.004	8.0
125	0.968	0.031	0.999	8.0	0.968	0.017	0.985	8.0	0.903	0.058	0.961	8.0
200	0.956	0.047	1.003	8.0	0.976	0.023	0.999	8.0	0.899	0.101	1.000	7.9
300	0.919	0.060	0.979	8.0	0.960	0.036	0.996	8.1	0.855	0.154	1.009	7.9
300	0.940	0.065	1.005	8.0	0.940	0.045	0.985	8.0	0.831	0.135	0.966	7.9

Table C-22 Compound A Solution Kinetics at **60°C** in **0.1 M** pH 8 K_2HPO_4
Initial Drug Concentration **0.0520** mg/mL (< cmc)

	AIR HEADSPACE				ARGON PURGED				OXYGEN PURGED			
Time (days)	Frac. A Retain.	Fraction as Cinn.	SUM	pH	Frac.A Retain.	Fraction as Cinn.	SUM	pH	Frac.A Retain.	Fraction as Cinn.	SUM	pH
0	1.000	0.000	1.000	8.0	1.000	0.000	1.000	8.0	1.000	0.000	1.000	8.0
10	1.001		1.001	8.0	1.001		1.001	8.0	0.990		0.990	8.0
25	0.983	0.006	0.989	8.0	0.962	0.016	0.978	8.0	0.983		0.983	8.0
50	0.969	0.015	0.984	8.0	0.983		0.983	8.0	0.929	0.040	0.969	8.0
80	0.948	0.043	0.991	8.0	1.010	0.014	1.024	8.0	0.921	0.083	1.004	8.0
125	0.933	0.055	0.988	8.0	0.979	0.007	0.986	8.0	0.902	0.125	1.027	8.0
200	0.879	0.068	0.947	8.1	0.983	0.024	1.007	8.2	0.769	0.177	0.946	8.0
262	0.862	0.160	1.022	8.0	0.975	0.058	1.033	8.1	0.733	0.260	0.993	8.2
262	0.871	0.143	1.014	8.0	0.977	0.034	1.011	8.1	0.692	0.257	0.949	8.2

Table C-23 Compound A Solution Kinetics at 60°C in 0.2 M pH 8 K_2HPO_4
Initial Drug Concentration 0.0519 mg/mL (< cmc)

	AIR HEADSPACE				ARGON PURGED				OXYGEN PURGED			
Time (days)	Frac. A Retain.	Fraction as Cinn.	SUM	pH	Frac.A Retain.	Fraction as Cinn.	SUM	pH	Frac.A Retain.	Fraction as Cinn.	SUM	pH
0	1.000	0.000	1.000	8.0	1.000	0.000	1.000	8.0	1.000	0.000	1.000	8.0
10	1.008		1.008	8.0	1.010		1.010	8.0	0.990		0.990	8.0
25	0.986	0.008	0.994	8.0	0.971	0.018	0.989	8.0	0.940		0.940	8.0
50	1.006	0.017	1.023	8.0	0.977		0.977	8.0	0.956	0.028	0.984	8.0
80	0.961	0.031	0.992	8.0	0.971	0.019	0.990	8.0	0.927	0.065	0.992	8.0
125	0.950	0.037	0.987	8.0	0.998	0.010	1.008	8.0	0.908	0.101	1.009	8.0
200	0.913	0.076	0.989	8.2	0.984	0.018	1.002	8.0	0.838	0.134	0.972	8.1
262	0.890	0.096	0.986	8.0	0.956	0.043	0.999	8.1	0.782	0.211	0.993	8.1
262	0.911	0.078	0.989	8.0	0.979	0.030	1.009	8.0	0.769	0.174	0.943	8.1

Table C-24 Compound A Solution Kinetics at 60°C in 0.4 M pH 8 K_2HPO_4
Initial Drug Concentration 0.0518 mg/mL (< cmc)

	AIR HEADSPACE				ARGON PURGED				OXYGEN PURGED			
Time (days)	Frac. A Retain.	Fraction as Cinn.	SUM	pH	Frac.A Retain.	Fraction as Cinn.	SUM	pH	Frac.A Retain.	Fraction as Cinn.	SUM	pH
0	1.000	0.000	1.000	8.0	1.000	0.000	1.000	8.0	1.000	0.000	1.000	8.0
10	1.021		1.021	8.0	0.942		0.942	8.0	0.990		0.990	8.0
25	0.994	0.006	1.000	8.0	0.990	0.015	1.005	8.0	0.988	0.008	0.996	8.0
50	0.994	0.015	1.009	8.0	0.967		0.967	8.0	0.979	0.035	1.014	8.0
80	0.973	0.035	1.008	8.0	0.909	0.016	0.925	8.0	0.930	0.058	0.988	8.0
125	0.967	0.038	1.005	8.0	0.946	0.013	0.959	8.0	0.919	0.079	0.998	8.0
200	0.946	0.073	1.019	8.2	0.882	0.017	0.899	8.2	0.872	0.114	0.986	8.2
262	0.909	0.088	0.997	8.1	0.872	0.034	0.906	8.1	0.822	0.154	0.976	8.0
262	0.925	0.107	1.032	8.1	0.959	0.027	0.986	8.0	0.815	0.201	1.016	8.1

REFERENCES

Advant, S.J., Braswell, E.H., Kumar, C.V., and Kalonia, D.S., "The effect of pH and temperature on the self-association of recombinant himan interleukin-2 as studied by equilibrium sedimentation." *Pharm. Res.* **12**:5(1995)637-41.

Amante, J.C., Scamehorn, J.F., and Harwell, J.H., "Precipitation of mixtures of anionic and cationic surfactants II. Effects of surfactant structure, temperature, pH." *J. Coll. Int. Sci.* 144:1(1991)243-253.

Anacker, E.W., "Electrolyte effect on micellization." in Solution Chemistry of Surfactants., V. 1, Mittal, K.L., ed., Plenum Press, New York, 1978.

Aniansson, E.A.G., Wall, S.N., Almgren, M., Hoffmann, H., Kielmann, I., Ulbricht, W., Zana, R., Lang, J., and Tondre, C., "Theory of the kinetics of micellar equilibria and quantitative interpretaion of chemical relaxation studies of micellar solutions of ionic surfactants." *J. Phys. Chem.* **80**:9(1976)905-922.

Asker, A.F., and Larose, M., "Influence of uric acid on the photostability of sulfathiazole sodium solutions." *Drug Dev. Ind. Pharm.* **13**(1987)2239-2248.

Asker, A.F., Canady, D., and Cobb, C., "Influence of DL-methionine on the photostability of ascorbic acid solutions." *Drug Dev. Ind. Pharm.* **11**(1985)2109-2125.

Atherton, S.J., and Dymond, C.M.G., "Formation of clusters between ionic species and sodium dodecyl sulfate below the critical micelle concentration. Ethidium ions and divalent metal ions." *J. Phys. Chem.* **93**(1989)6809-6813.

Atkins, P.W., *Physical Chemistry*, 4th ed., W.H. Freeman and Co., N.Y. 1990, pp. 785-8, 800-02, 829-30, 833-5.

Attwood, D., Florence, A.T., and Gillan, "Micellar properties of drugs: properties of micellar aggregates of phenothiazines and their aqueous solutions." *J. Pharm. Sci.* **63**:6(1974)988-993.

Attwood, D., Natarajan, R., "Micellar properties of chlorpromazine hydrochloride in concentrated electrolyte solutions." *J. Pharm. Pharmacol.* **35**(1983)317-319. Note: This is a compound which self-associates through stacking interactions.

Attwood, D., and Florence, A.T., Surfactant Systems: Their Chemistry, Pharmacy, and Biology. Chapman and Hall, London 1983.

Attwood, D., Doughty, D., Mosquera, V., and Villar, V.P., "Complex aggregation patterns for the self-association of phenothiazine drugs in aqueous solution." *J. Coll. Int. Sci.* **141**:2(1991)316-321.

Azaz, E., Donbrow, M., and Hamburger, R., "Incompatibility of non-ionic surfactants with oxidisable drugs." *The Pharmaceutical Journal* July 7, 1973, p.15.

Bamford, C.H., and Tipper, C.F.H., eds., Chemical Kinetics, V.16 Liquid-Phase Oxidation. Elsevier Scientific Publishing Co., Amsterdam, 1980, pp. 222-248.

Barry, B.W., and Russell, G.F.J., "Interaction of amaranth with some alkyltrimethylammonium salts: a coacervation phenomenon." *J. Pharm. Sci.* **61**:4(1972)502-17.

Belen'Kii, L.I., ed. Chemistry of Organosulfur Compounds, General Problems. Ellis Horwood, NY 1990.

Brown, M., and Leeson, L.,J., "Protection of oxygen-sensitive pharmaceuticals with nitrogen." *J. Pharm. Sci.* **58**(1969)242-245.

Carstensen, J.T., "Kinetic salt effect in pharmaceutical investigations." *J. Pharm. Sci.* **59**:8 (1970)1140-1143.

Carstensen, J.T., Drug Stability, Principles and Practices, Marcel Dekker, N.Y., 1990, ch. 2, section 12.

Chan, Chun Chiu "Counterion effects in micellar systems." M.S. Thesis, U. Wisconsin-Madison, 1985.

Chan, Chun Chiu, "Electrolyte and interfacial free energy effects on micelle stability and micellar solubilization: dissociation constants

and hydrophobic behavior of fluorocarbon acids." Ph.D. Thesis, U. Wisconsin-Madison, 1993; uv spectroscopy was used to determine the cmc's of lithium perfluorooctanoate, LiPFO, in the presence of 0.3-2.0 M LiCl. Thanks to Dr. Mukerjee for allowing the use of Dr. Chan's extended Corrin-Harkins relation.

Cher, M., and Davidson, N., "The kinetics of the oxygenation of ferrous iron in phosphoric acid solution." *J. Am. Chem. Soc.* 77(1955)793-798, through Li, 1993.

Connors, K.A., Mollica, J.A., "Inhibition of an ester hydrolysis by imidazole." *J. Am. Chem. Soc.* **87**(1965)123-124.

Connors, K.A., Mollica, J. A., "Theoretical analysis of comparative studies of complex formation." *J. Pharm. Sci.* **55**:8(1966)772-780.

Connors, K.A., Infeld, M.H., and Kline, B.J., "Interactant structure and complex stability for complexes of theophylline with cinnamate esters and related compounds in aqueous solution." *J. Am. Chem. Soc.* **91**:13(1969)3597-3603.

Connors, K.A., Amidon G.L., and Stella, V.J., Chemical Stability of Pharmaceuticals, a Handbook for Pharmacists. 2nd ed., Wiley, NY 1986, ch. 5.

Corrin, M.L., and Harkins, W.D., "The effect of salts on the critical concentration for the formation of micelles in colloidal electrolytes." *J. Am. Chem. Soc.* **69**(1947)683-688.

Corti, M., and Degiorgio, "Investigation of aggregation phenomena in aqueous sodium dodecyl sulfate solutions at high NaCl concentration by quasielastic light scattering." in Solution Chemistry of Surfactants, V. 1, Mittal, K.L., ed., Plenum Press, New York, 1978.

CRC Handbook of Chemistry and Physics, 1993-94.

Daabis, N., and El-Khawas, F., "The influence of non-ionic surfactants on the rate of degradation of menadione (vitamin K3)." *Die Pharmazie* **24**(1969)750-756.

Darrington, R.T., and Anderson, B.D., "The role of intramolecular nucleophilic catalysis and the effects of self-association on the

deamidation of human insulin at low pH." *Pharm. Res.* **11**:6(1994) 784-793. Note: Initial (<10% decomposition) or first-order (<50% decomposition) rates are reported.

Davio, S.R, Kienle, K.M., and Collins, B.E., "Interdomain interactions in the chimeric protein toxin sCD4(178)-PE40: a differential scanning calorimetry (DSC) study." *Pharm Res.* **12**:5(1995)642-648.

Dawson, J.E., Hajratwala, B.R., and Taylor, H., "Kinetics of indomethacin degradation II: presence of alkali plus surfactant." *J. Pharm. Sci.* **66**:9(1977)1259-63.

DeVijlder, M. ,"An empirical equation describing the variation of the c.m.c. of surfactants by added electrolytes." *Z. Phys. Chem. Neue Folge* **162**(1989)S.255-258.

DeVijlder, M., "Micelles in aqueous electrolyte solution: a graphical determination method for the second c.m.c." *Z. Phys. Chem. Neue Folge.* **168**(1990)S. 225-230.

DeVijlder, M., "On the specific effectiveness of added ions to induce changes in the structure of sodium dodecyl sulfate micelles." *Z. Phys. Chem.* **174**(1991)S.119-128.

Dixon, M. and Tunnicliffe, H.E., *Proc. R. Soc. (London), Ser. B* (1923) 266, through Bamford.

Donbrow, M., Azaz, E., Pillersdorf, A., "Autooxidation of polysorbates." *J. Pharm. Sci.* 67:12(1978)1676-1681.

Dupuis, L., Saunderson, C.L., Puigserver, A., and Brachet, P., "Oxidation of methionine and 2-hydroxy 4-methylthiobutanoic acid sterioisomers in chicken tissues," *Brit. J. Nutrition* **62**(1989)63-75.

Eriksen, S., and Stelmach, H., "Single-step stability studies." *J. Pharm. Sci.* **54**(1965)1029-1034.

Esch, J.H., Nolte, R.J.M., Ringsdorf, H., and Wildburg, G., "Monolayers of chiral imidazole amphiphiles: domain formation and metal complexation." *Langmuir* 10(1994)1955-1961.

Franchini, M., "Oxidation kinetics of a novel leukotriene antagonist." M. S. Thesis, University of Wisconsin-Madison, December, 1992.

Franchini, M., Unvala, H., Carstensen, J.T., "Effect of electrolytes on oxygen solubility in aqueous systems." *J. Pharm. Sci.* **82**:5(1993)550.

Franchini, M.K., and Carstensen, J.T., "Critical micelle concentrations of a dicarboxylic acid drug substance as a function of buffer concentration, temperature, ionic strength, and pH." Poster at ACS National Meeting, March, 1994, San Diego.*ACS Abstracts of Meetings*, Part II, PHYS 328, March, 1994, poster; and, part of the work was presented as a podium at the 2nd Upjohn-Enz award symposium in Kalamazoo, MI in September, 1994.

Franchini, M.K., Carstensen, J.T., "Failure of high temperature extrapolation of oxidative reactions in solution." *Int. J. Pharm.* **111**(1994)153-158, and present work. Please note that the molecular formula and chemical name, although different in this reference, refer to the same drug as in the present document. Parts of this communication were presented as a poster at the 8th annual AAPS meeting in Lake Buena Vista, Florida in November, 1993, as a podium at the 9th annual AAPS meeting in San Diego, CA in November, 1994, and as a podium at the 2nd Upjohn-Enz award symposium in Kalamazoo, MI in September, 1994.

Friedman, M., "The use of ranks to avoid the assumption of normality." *J. Amer. Stat. Assn.* **32**(1937)675-701, through Wilcoxon, F., "Some rapid approximate statistical procedures." American Cyanamid Co., NY, July 1949.

Garnett, C.J, Lambie, A.J., Beck, and W.H., Liler, M., "Kinetics of the acid-catalyzed hydrokysis of dodecylsulfate and dodecyldiethoxysulphate surfactants in concentrated micellar solutions. Part I. Effects of acid and surfactant concentrations and of the nature and concentrations of counterions." and "Part II. Effects of added electrolytes on the hydrolysis of sodium dodecylsulphate and sodium dodecyldiethoxysulphate." *J. Chem. Soc. Faraday Trans. I* **79**(1983)953-1000.

Gehrke, C.W., Rexroad, P.R., Schisla, R.M., Absheer, J.S., and Zumwalt, R.W., "Quantitative analysis of cystine, methionine, lysine, and nine

other amino acids by a single oxidation-4 hour hydrolysis method." *J. Assoc. Off. Anal. Chem.* 70:1(1987)171-174.

Gleason, J. G. et al, U.S. Patent 4,874,792A, 10/17/89.

Gurovich, B. M., Frolova, T. V., Mezheritskii, S. M., "Surface tension of aqueous solutions of K_2CO_3, KOH, $(NH_4)_2SO_4$ and NH_4NO_3." *J. Appl. Chem. USSR* **56**:11(1983)2429-2431.

Hamid, I.A., Parrott, E.L., "Effect of temperature on solubilization and hydrolytic degradation of solubilized benzocaine and homatropine." *J. Pharm. Sci.* **60**:6(1971)901-906.

Hiemenz, P., Principles of Colloid and Surface Chemistry. 2nd ed., Dekker, New York, 1986, ch. 8; p. 434, p. 457

Huisman, H.F., "Light scattering of solutions of ionic detergents." N.V. Noord-Hollandsche Uitgevers Maatschappij, Amsterdam, 1964.

Hunt, C.A., and Tsang, S., "a-tocopherol retards autooxidation and prolongs the shelf-life of liposomes." *Int.J.Pharm.* **8**(1981)101-110.

Ikeda, S., "Salt-induced sphere-rod transition of ionic micelles." in Surfactants in Solution. V. 2 Mittal, K.L., and Lindman, B., eds., Plenum Press, New York, 1984. p. 825-839.

Ikeda, S., "Stability of spherical and rod-like micelles of ionic surfactants, in relation to their counterion binding and modes of hydration." *Colloid Polym. Sci.* **269**(1991)49-61.

Israelachvili, J.N., Intermolecular and Surface Forces. 2nd ed. Academic Press, London, 1992, Chapters 16 and 17.

Jasper, J.J., "The surface tension of pure liquid compounds." *J. Phys. Chem. Ref. Data* **1**:4(1972)841-1009.

Jencks, W.P., Catalysis in Chemistry and Enzymology. Dover Publications, NY 1987, ch. 7.

Kassem, M.A., Kassem, A.A., and Ammar, H.O., "Studies on the stability of injectable l-ascorbic acid solutions II. Effect of metal ions

and oxygen content of solvent water." *Pharm. Acta Helv.*, **44** (1969)667-675.

Kharasch, N., ed. Organic Sulfur Compounds, V. I. Pergamon Press, NY 1961.

Khomutov, N.E., and Groisman, A.S., " Temperature dependence of the solubility of oxygen in aqueous solutions of electrolytes." *Russian J. Phys. Chem.* **58**:3(1984)433-434.

Khomutov, N.E., and Groisman, A.S., "Thermodynamics of dissolution of oxygen in aqueous solutions of sodium carbonate and trisodium phoshate." *Deposited Doc , VINITI* (1983)1641-83, (Russ., CA:101:29309x).

Khomutov, N.E., and Konnik, E.I., "Solubility of oxygen in aqueous electrolyte solutions." *Russian J. Phys. Chem.* **48**:3(1974)359-362.

Khomutov, N.E., Groisman, A., and Popova, Z.A., "Dependence of oxygen solubility on the temperature in aqueous electrolyte solutions." *M.Kh.-T.I.* **121**(1982)136-43, (Russ., CA:98:133041j).

Kurz, J.L., "Effects of micellization on the kinetics of the hydrolysis of monoalkyl sulfates." *J. Phys. Chem.* **66**(1962)2239-.

Labuza, T.P., "Oxidative changes in foods at low and intermediate moisture levels," in Water Relations of Foods, proceedings of an international symposium held in Glasgow, Sept. 1974, ed. by Duckworth, R.B., Academic Press, London, 1975.

Lamy-Freund, M.T., Ferreira, V.F.N., Faljoni-Alario, A., and Schreier, S., "Effect of aggregation on the kinetics of autooxidation of the polyene antibiotic amphotericin B." *J. Pharm.Sci.* **82**:2(1993)162-166. Note: Although the authors refer to autooxidation, the published kinetic profiles appears to be first order, indicative of simple oxidation rather than autooxidation, which would have resulted in a sigmoidally shaped curve.

Lee, T.K. and Notari, R.E., "Kinetics and mechanism of captopril oxidation in aqueous solution under controlled oxygen partial pressure." *Pharm Res.* **4**:2(1987)98-103.

Lewis, E.S., Investigation of Rates and Mechanisms of Reactions. Part I, 3rd ed., (Vol. VI of Techniques of Chemistry, A. Weissberger, ed.,) Wiley Interscience, 1974, pp. 370-482.

Li, S., Schoneich, C., Wilson, G.S., and Borchardt, R.T., "Chemical pathways of peptide degradation. V. Ascorbic acid promotes rather than inhibits the oxidation of methionine to methionine sulfoxide in small model peptides." *Pharm. Res.* **10**:11(1993)1572-79. Note: Although initial rates are used to calculate first-order rate constants, the published kinetic profiles suggest the reaction reaches equilibrium after 1.5 half-lives, perhaps indicating an inhibitory effect by product.

Li, S., Schoneich, C., and Borchardt, R., "Chemical pathways of peptide degradation. VIII. Oxidation of methionine in small model peptides by prooxidant/transition metal ion systems: influence of selective scavengers for reactive oxygen intermediates." *Pharm. Res.* **12**:3(1995)348-55. Note: Published kinetic curves show that some reactions reached an equilibrium, while others demonstrate autooxidation, although the authors treat the data as zero or first-order.

Lim, Y.Y., and Tan, E.H.L., "Rate enhancement of the autooxidation of 3,5-di-*tert*-butylcatechol in micellized copper (II) solutions." *J. Molecular Catalysis* **81**(1993)L1-.

Lundberg, W.O., Autooxidation and Antioxidants, v. II. Interscience Publishers div. of John Wiley and Sons, New York, 1962.

Martin, A., Swarbrick, J., and Cammarata, A., Physical Pharmacy. 3rd edition, Lea and Febiger, Philadelphia, 1983, p. 358-9.

Masterton, W. L., Lee, T.P., "Salting coefficients from scaled particle theory." *J. Phys. Chem.* **74**:8(1970)1776-1783.

McDevit, W. F., and Long, F. A.,"The activity coefficient of benzene in aqueous salt solutions." *J. Am. Chem. Soc.* **74**(1952)1773-1777.

Meakin, B.J., Stevens, J., and Davies, D.J.G., "The effect of drug concentration on the thermal (dark) degradation of promethazine

hydrochloride in aqueous solution." *J. Pharm. Pharmac.* **30**(1978)75-80.

MicroMath Scientific Software, Salt Lake City, Utah 84121, 1993.

Microsoft Corporation.

Mitchell, D.J., Tiddy, G.J.T., Waring, L., Bostock, T., and McDonald, M.P., "Phase behavior of polyoxyethylene surfactants with water."

Mittal, K.L., and Lindman, B., eds. Surfactants in Solution, v. 2 proceedings of an international symposium held in 1982 in Lund, Sweden, Plenum Press, New York, 1984.

Moelwyn Hughes, E.A., The Chemical Statics and Kinetics of Solutions. Academic Press, 1971 pp. 159-163; 172.

Mollica, J.A., Connors, K.A., "Modification of reaction rates by complex formation. II. Inhibition of the rate of alkaline hydrolysis of methyl trans-cinnamate by some heterocyclic compounds." *J. Am. Chem. Soc.* **89**:2(1967)308-317.

Monig, J., Goslich, R., and Smus, K.D., "Thermodynamics of S...S 2 $\sigma/1\sigma^*$ three-electron bonds and deprotonation kinetics of thioether radical cations in aqueous solution." *Ber. Bunsenges. Phys. Chem.* 90(1986)115-121.

Morrison, T. J., "The salting-out of non-electrolytes. Part I. The effect of ionic size, ionic charge, and temperature." *J. Chem. Soc.* (1952)3814-3818.

Motsavage, V.A., and Kostenbauder, H.B., "The influence of the state of aggregation on the specific acid-catalyzed hydrolysis of sodium dodecyl sulfate." *J. Coll. Sci.* 18(1963)603-615.

Mukerjee, P., "Salt effects on nonionic association colloids."*J. Phys. Chem.* **69**(1965)4038-4040.

Mukerjee, P., "Dimerisation and pre-c.m.c. association." Part 4 of "The nature of the association equilibria and hydrophobic bonding in aqueous solutions of association colloids." *Adv. Coll. Interf. Sci.*, **1**(1967)241-275.

Mukerjee, P., and Mysels, K.J., Critical Micelle Concentrations of Aqueous Surfactant Systems. U.S. National Bureau of Standards, Washington, 1971, Ref. 47010, Compounds #1, 38, 91, 95, 182.

Mukerjee, P., "Micellar properties of drugs: micellar and nonmicellar patterns of self-association of hydrophobic solutes of different molecular structures--monomer fraction, availability, and misuses of micellar hypothesis." *J. Pharm. Sci.* **63**:6(1974)972-981.

Mukerjee, P., "Size distribution of micelles: monomer-micelle equilibrium, treatment of experimental molecular weight data, the sphere-to-rod transition and a general association model." in Micellization, Solubilizattion, and Microemulsions. V.1, Mittal, K.L., ed., Plenum Press, 1977.

Mukerjee, P., and Chan, Chiu Chun, "Effects of high concentrations of electrolytes on micelle formation and micellar solubilization." *ACS Abstracts of Papers* Part 1, COLL, **206**(1993)164.

Muller, N., Pellerin, J.H., Chen, W.W., "Investigation of micelle structure by fluorine magnetic resonance. VI. Quaternary ammonium salts." *J.Phys. Chem.* **76**:21(1972)3012-3017.

Muller, R. "Kinetics of micellization." in Solution Chemistry of Surfactants, v. 1, Mittal, K.L., ed., Plenum Press, New York, 1978.

Mysels, E.K., and Mysels, K.J., "Conductimetric determination of the critical micelle concentration of surfactants in salt solutions."*J. Colloid Sci.* **20**(1965)3718, through Mukerjee, P., *Adv. Coll. Interf. Sci.* **1**(1967)241 and Chan, Chun Chiu, Ph. D. Thesis, U. Wisconsin-Madison, 1993; compiled from literature; various methods were used to determine the cmc of sodium decyl sulfate, SDS, in the presence of 0.3-1.0 M NaCl.

Nguyen, T.H., Burnier, J., and Meng, W., "The kinetics of relaxin oxidation by hydrogen peroxide." *Pharm. Res.* **10**:11(1993)1563- . Note: The published kinetic profile does not suggest autooxidation, but rather simple oxidation (first-order).

Nikolov, A., Martynov, G., and Exerowa, D. "Associative interactions and surface tension in ionic surfactant solutions at concentrations much lower than the cmc." *J. Coll. Int. Sci.* **81**:1(1981) 116-124.

Nogami, H., Awazu, S., Nakajima, N., and Kanakubo, Y., "Studies on decomposition and stabilization of drugs in solution. XIII. On sodium lauryl sulfate." *Chem. Pharm. Bull. (Japan)* 11(1963)13. Note: One kinetic profile published in this article which showed decomposition beyond one half-life suggests autocatalysis, although the authors simply comment on the deviation from linearity in the first order plot.

Odijk, T., "Ionic strength dependence of the length of charged linear micelles." *J. Phys. Chem.* **93**(1989)3888-3889.

Olatunji, M.A., and Ayoko, G. A., "Kinetics and mechanism of the oxidation of l-methionine by aqueous solution of chromium(VI)." *Polyhedron* 7:1(1988)11-15.

Oliviera, A.G., Cuccovia, I.M., and Chaimovich, H., "Micellar modification of drug stability: analysis of the effect of hexaddecyltrimethylammonium halides on the rate of degradation of cephaclor." *J. Pharm. Sci.* 79:1(1990)37-42.

Ong,. J.T.H., and Kostenbauder, H.B., "Effect of self-association on rate of penicillin G degradation in concentrated aqueous solutions." *J. Pharm. Sci.* **64**:8(1975)1378-1380.

Ozeki, S., Ikeda, S., "The adsorption of dodecyldimethylammonium chloride on aqueous surfaces od concentrated NaCl solutions." *Bull. Chem. Soc. Jpn.* **53**(1980)1832-1836.

Ozeki, S.; Ikeda, S. *J. Coll. Interf. Sci.* **77**(1981)219-231.

Ozeki, S., Ikeda, S., "The difference in solubilization power between spherical and rod-like micelles of dodecyl dimethyl ammonium chloride in aqueous solutions." *J. Phys. Chem.* **89**(1985)5088-5093.

Perrin, D.D., and Dempsey, B., Buffers for pH and Metal Ion Control. Chapman and Hall, London, 1983, ch 2.

Pnigrahi, G.P., and Mishra, S.K., "Micellar catalysis: effect of sodium lauryl sulphate in the oxidation of lactic acid by chromic acid." *J. Molecular Catalysis* **81**(1993)349-362.

Romsted, L.S., "Micellar efects on reaction rates and equilibria." in Surfactants in Solution, v. 2. ed. Mittal, K.L., and Lindman, B., Plenum Press, NY, 1984.

Rosen, M. J., Surfactants and Interfacial Phenomena. 2nd ed., Wiley, New York, 1989, ch. 2, 3, p. 81-83.

Savige, W.E., and Fontana, A., "Interconversion of methionine and methionine sulfoxide." *Methods Enzymol.* (Enzyme struct., Part E) 47(1977)453-9, Hirs, C.H.W., and Timasheff, S.N., eds., Academic Press, NY.

Schroeter, L., "Kinetics of air oxidation of sulfurous acid salts." *J. Pharm. Sci.* **52**(1963)559-563.

Schroeter, L., "Oxidation of sulfurous acid salts in pharmaceutical systems." *J. Pharm. Sci.* **52**(1963)888-892.

Segal, R., Azaz, E., Donbrow, M., "Peroxide removal from non-ionic surfactants." *J. Pharm. Pharmacol.* **31**(1979)39-40.

Seltzer, S.H., "The influence of the state of molecular aggregation on the decomposition of mono-n-decyl and mono-p-octylphenyl dihydrogen phosphates and of dilithium acetyl phosphate." Ph.D. Thesis, Temple University, Sept. 24, 1973.

Setchenow, A.S., *Z. Physik. Chem. Leipzig* **4**(1889)117, through Jencks.

Shechter, Y. "Selective oxidation and reduction of methionine residues in peptides and proteins by oxygen exchange between sulfoxide and sulfide." *J. Biol. Chem.* 261:1(1986)66-70.

SKB Pharmaceutical Analysis Test Method AW-106203Z2-B-02, "Degradation Product Profile Assay for 106203, 50 mg Tablets by High Performance Liquid Chromatography."

SKB Draft Product Reference Guide, June 11, 1990; pKa's obtained by titration of SK&F S-106203-Z2, Lot NH-16907-92 in 2:1 methanol-water with HCl.

Sokoloski, T.D., and Higuchi, T., "Kinetics of degradation in solution of epinephrine by molecular oxygen." *J. Pharm. Sci.* **51**:2(1962)172-177.

Stewart, R., Oxidation Mechanisms Applications to Organic Chemistry. Frontiers in Chemistry Series, Breslow, R. and Karplus, M., eds., W.A. Benjamin, Inc., New York 1964, p.121-3.

Tan, X., Meltzer, N., and Lindenbaum, S., "Determination of the kinetics of degradation of 13-cis-retinoic acid and all-trans-retinoic acid in solution." *J. Pharm. Biomed. Anal.* **11**:9(1993)817-.

Tanaka, A., Ikeda, S., "Adsorption of dodecyltrimethylammonium bromide on aqueous surfaces of sodium bromide solutions." *Colloids and Surfaces.* **56**(1991)217-228.

The Mathworks Inc., Prentice-Hall, Englewood Cliffs, NJ 07632, 1992.

Timmins, P., Jackson, I.M., and Wang, Y.J., "Factors affecting captopril stability in aqueous solution." *Int. J. Pharm.* **11**(1982)329-336.

Trost, B.M., ed. in chief, and Fleming, I. deputy ed. in chief, Comprehensive Organic Synthesis, v. 7, Oxidation. Ley, S.V., volume editor, Pergamon Press, Oxford 1991.

Turney, T.A., Oxidation Mechanisms, Butterworths, London 1965, ch 10.

Ventura, P., Parravicini, F., Simonotti, L., Colombo, R., and Pifferi, G., "Degradation of propildazine in water." *J. Pharm. Sci.* **70**(1981)334-336.

Wallace, T.J., Schriesheim, A., "Solvent effects in the base-catalyzed oxidation of mercaptans with molecular oxygen." *J. Org. Chem.* **27** (1962)1514-16.

Wallace, T.J., Schriesheim, A., and Bartok, W., "The base-catalyzed oxidation of mercaptans. III. Role of the solvent and effect of mercaptan structure on the rate determining step." *J. Org. Chem.* **28** (1963)1311-1314.

Waters, W.A., Mechanisms of Oxidation of Organic Compounds. John Wiley and Sons, New York, 1964, chs. 2, 8.

Yamamoto, K. Takahashi, M., and Niki, E., "Role of iron and ascorbic acid in the oxidation of methyl linoleate micelles." *Chem. Lett.* (1987)1149-1152.

Yasuhara, M., Sato, F., Kimura, M.T., Muranishi, S., and Sezaki, H., "Catalytic effect of cationic surfactants on degradation of cephalexin in aqueous solution." *J. Pharm. Pharmac.* **29**(1977)638-640.